

UNIVERSITEIT
STELLENBOSCH
UNIVERSITY

**STRUCTURAL GEOLOGY OF THE USAKOS DOME IN
THE DAMARA BELT, NAMIBIA**



by

Shannon D. Johnson

Thesis presented in partial fulfillment of the requirements for the degree of

Master of Science

at the University of Stellenbosch

Supervised by Prof. Alex Kisters

Dec. 2005

DECLARATION

I, the undersigned, hereby declare that the work presented in this thesis is my own original work and that I have not previously in its entirety or in part submitted it at any other university for a degree.

ABSTRACT

The northeast-trending south Central Zone (sCZ) of the Pan-African Damara belt in central Namibia is structurally characterized by kilometer-scale, northeast-trending dome structures developed in Neoproterozoic rocks of the Damara Sequence. A number of different structural models have been proposed for the formation of these domes in the literature. This study describes the structural geology of the Usakos dome. The study discusses the structural evolution of the dome within the regional framework of the cSZ that represents the high-grade metamorphic axis of the Damara Belt, characterized by voluminous Pan-African granitoids.

The northeastern part of the Usakos dome is developed as an upright- to northwest-verging anticlinorium containing a steep southeasterly-dipping axial planar foliation. The northeast fold trend persists into the southwestern parts of the Usakos dome. However, this southwestern core of the dome is inundated by synkinematic granitic sheets. Distinct marker horizons of the Damara Sequence outcrop as screens within the granite, preserving a ghost stratigraphy. These screens illustrate the position and orientation of second-order folds. Significantly, most of the stratigraphy of the Damara Sequence is overturned in these folds. For example, some second-order anticlines developed in the northeastern parts of the Usakos dome can be followed along their axial traces into the southwestern hinge of the dome, where they appear as synformal anticlines, i.e. synformal structures cored by older strata, plunging towards the northeast. The inverted stratigraphy and northeasterly fold plunges suggest the northeast-trending folds are refolded by second-generation, northwest-trending folds, thus, forming kilometer-scale Type-2 interference folds. The resulting fold geometries are strongly non-cylindrical, approaching southwest-closing sheath folds indicating a top-to-the-southwest material transport. Lower-order folds in this overturned domain show radial fold plunges, plunging away from the centre of the dome core, as well as a shallowly-dipping schistosity.

The close spatial and temporal relationship between granite intrusion and the formation of the southwest-vergent, sheath-type folds, radial distribution of fold plunges and the subhorizontal foliation confined to the southwestern hinge of the Usakos dome are interpreted to signify the rheological weakening and ensuing collapse of the developing first-order Usakos dome immediately above the synkinematic granite intrusions. Orogen-parallel, southwest-vergent sheath folds and top-to-the southwest extrusion of the southwestern parts of the Usakos dome and northwest-vergent folding and thrusting characterizing the northeastern extent of the Usakos dome are both responses to the northwest-southeast- directed contractional tectonics recorded during the main collisional phase in the Damara belt. On a regional scale, the Usakos dome represents the link between the foreland-vergent northeastern part of the sCZ and the southwest-vergent, high-grade southwestern parts of the sCZ.

The results of this study illustrate how dramatic variations in structural styles may be caused by the localized and transient rheological weakening of the crust during plutonic activity.

UITTREKSEL

Die noordoos-strekkende, suidelike Sentrale Sone (sSS) van die Pan-Afrikaanse Damara gordel in sentraal Namibië word karakteriseer deur kilometer-skaal, noordoos-strekkende koepel strukture, ontwikkel in die Neoproterozoïkum gesteentes van die Damara Opeenvolging. 'n Aantal verskillende struktuur modelle is voorgestel in die literatuur vir die vorming van hierdie koepels. Hierdie ondersoek beskryf die struktuur geologie van die Usakos koepel. Die ondersoek bespreek die strukturele ontwikkeling van die koepel in die regionale konteks van die sSS, wat die hoë graadse metamorfe magmatiese as van die Damara Gordel verteenwoordig, en karakteriseer word deur omvangryke Pan-Afrikaanse granitoïede.

Die noordoostelike gedeelte van die Usakos koepel is ontwikkel as 'n antiklinorium met 'n vertikale- tot noordwestelike kantelrigting, wat 'n steil hellende, suidoostelike asvlak planêre foliasie bevat. Die noordoos-strekkende plooïing kom voor tot in die suidwestelike kern van die Usakos wat ingedring is deur sinkinematiese granitiese plate. Die posisie en oriëntasie van tweede-orde plooïe is afgebeeld in die graniete deur 'n skimstratigrafie wat preserveer is deur duidelike merker horisonne van die Damara Opeenvolging. Die stratigrafie van die Damara Opeenvolging is opmerklik meestal omgekeer in hierdie plooïe. Byvoorbeeld, tweede-orde antikliene ontwikkel in die noordoostelike gedeelte van die Usakos koepel kan gevolg word langs hul asvlakspore tot in die suidwestelike skarnier van die koepel, waar dit voorkom as sinforme antikliene, d.w.s. sinforme strukture met ouer strata in die kern wat na die noordooste duik. Die omgekeerde stratigrafie en noordoostelike plooï duiking impliseer dat die noordoos-strekkende plooïe weer geplooï is deur tweede-generasie, noordwes-strekkende plooïe, wat dus aanleiding gegee het tot die vorming van kilometer-skaal, tipe-2 interferensie plooïe. Die gevolglike plooï geometrieë is uitdruklik nie-silindries, en toon 'n oorgang na skede plooïe met 'n sluiting na die suidweste, wat dui op 'n bokant-na-die-suidweste materiaal vervoer. Laer-orde plooïe in die omgekeerde domein vertoon radiale duiking van die plooïe, weg van die middelpunt van die koepel kern, sowel as 'n vlak hellende skistositeit.

Die noue ruimtelike en temporele verwantskap tussen graniet intrusie en die vorming van skede-tipe plooie met 'n kantelrigting na die suidweste, die radiale verspreiding van plooie duiking, en die subhorisontale foliasie wat beperk is tot die suidwestelike skarnier van die Usakos koepel, word interpreteer as 'n aanduiding van die reologiese verswakking en die gevolglike ineenstorting van die ontwikkelende eerste-orde Usakos koepel, onmiddellik aan die bokant van die sinkinematiese graniet intrusies. Die orogeen-parallele skede plooie met kantelrigting na die suidweste en bokant-na-die-suidweste ekstrusie van die suidwestelike gedeelte van die Usakos koepel, en plooiing met kantelrigting na die noordweste en stootverskuiwing wat kenmerkend is van die noordoostelike gedeelte van die Usakos koepel, is beide 'n reaksie op die noordwes-suidoos-gerigte vernouings tektoniek opgeteken gedurende die hoof botsings fase in die Damara gordel. Op 'n regionale skaal verteenwoordig die Usakos koepel die verbinding tussen die noordoostelike gedeelte van die sSS met 'n voorland kantelrigting, en die hoë graad suidwestelike gedeelte van die sSS met 'n kantelrigting na die suidweste.

Die resultate van hierdie ondersoek toon aan hoe dramatiese variasies in struktuur style veroorsaak kan word deur die gelokaliseerde en kortstondige reologiese verswakking van die kors gedurende plutoniese aktiwiteit.

ACKNOWLEDGEMENTS

- I would like to thank Professor Alex Kisters for supervising this project. His contagious enthusiasm, selfless support and encouragement were my inspiration. It was a privilege to have worked with such a dynamic scientist.
- Navachab Gold Mine, thanks for financially supporting and facilitating this research.

Frick and Juanita Badenhorst thanks for your friendly and homely hospitality while I was in Namibia.

Berti Roesener thanks for organizing everything I needed during my field work and for your help and patience with Arc View.

Moses and Sam, thanks for all your help in the field and at the camp.

Everyone at the 'camp', thanks for your friendliness and smiles.

- Johann, Janus and Richard, I am so glad you were writing while I was, at least I always had someone to gauge my insanity against...and thanks for all those coffees.
- Stephan Kruger, thanks for your help with the Afrikaans translation of the Abstract and with the printing of the thesis.
- To my friends in South Africa and in New Zealand thanks for all your support and good humour.
- Finally I am forever indebted to my family scattered all over the world. You have all been so positive and supportive when it was most required. Thanks for providing me the means and drive to learn.

CONTENTS

DECLARATION	ii
ABSTRACT (ENGLISH)	iii
UITTREKSEL (AFRIKAANS)	v
ACKNOWLEDGEMENTS	vii
CONTENTS	viii
LIST OF FIGURES	xi
LIST OF TABLES	xiv
CHAPTER 1 INTRODUCTION	1
1.1 The study area	3
1.2 Purpose of the study	3
1.3 Methodology	4
CHAPTER 2 GEOLOGICAL SETTING	5
2.1 The Damara Orogen	5
2.2 Tectonostratigraphic Evolution of the Central Zone in Damara belt	6
2.3 Dome structures	12
2.4 Granites within the CZ	14
2.5 The Karibib District	15
CHAPTER 3 LITHOSTRATIGRAPHY AND FIELD RELATIONS	17
3.1 Introduction	18
3.2 Pre-Damaran Basement	
3.2.1 <i>Abbabis Metamorphic Complex</i>	18
3.3 Damara Sequence	
3.3.1 <i>Etusis Formation</i>	19
3.3.2 <i>Chuos Formation</i>	19
3.3.3 <i>Spes Bona Formation</i>	22
3.3.4 <i>Okawayo Formation</i>	23
3.3.5 <i>Oberwasser Formation</i>	27
3.3.6 <i>Karibib Formation</i>	30
3.3.7 <i>Kuiseb Formation</i>	34
3.4 Intrusive Rocks	
3.4.1 <i>Granitic and pegmatitic intrusions</i>	34
3.4.2 <i>Dolerite dykes and sills</i>	34
CHAPTER 4 STRUCTURAL GEOLOGY	38
4.1 Introduction	39
4.2 Primary Bedding (S0)	39
4.3 Folding	41
4.4 Fabrics	
4.4.1 <i>Foliation (S1)</i>	43
4.4.2 <i>Foliation (S2)</i>	43
4.4.3 <i>Lineations (L2)</i>	45

4.5 Sub-domains of the Usakos dome	50
4.5.1 <i>Introduction</i>	50
4.5.2 <i>Domain A</i>	51
4.5.3 <i>Domain B</i>	59
4.5.4 <i>Domain C</i>	67
4.5.5 <i>Domain D</i>	70
4.5.6 <i>Domain E</i>	84
4.6 The Upper Contact of the Karibib Formation along the southeastern limb of the dome	86
4.7 The overall geometry of the southwestern portion of the Usakos dome	91
CHAPTER 5 GRANITE AND PEGMATITE INTRUSIONS	99
5.1 Introduction	99
5.2 Salem Granite	
5.2.1 <i>Occurrence and distribution</i>	100
5.2.2 <i>Petrography and macroscopic appearance</i>	101
5.2.3 <i>Intrusive Relationships</i>	102
5.2.4 <i>Fabrics</i>	107
5.3 Klein Aukas Granite	
5.3.1 <i>Occurrence and distribution</i>	114
5.3.2 <i>Petrography and macroscopic appearance</i>	114
5.3.3 <i>Intrusive Relationships</i>	115
5.3.4 <i>Fabrics</i>	122
5.4 Granite and pegmatites along the northwestern limb of the dome	
5.4.1 <i>Occurrence and distribution</i>	129
5.4.2 <i>Macroscopic appearance</i>	129
5.4.3 <i>Intrusive Relationships</i>	130
5.5 The Significance of Granitic Fabrics: A Discussion	
5.5.1 <i>Introduction</i>	131
5.5.2 <i>Interpretation of Fabrics within the Salem Granite</i>	131
5.5.3 <i>Interpretation of Fabrics within the Klein Aukas Granite</i>	136
5.5.4 <i>Interpretation of Fabrics within the sills and dykes along the northwestern limb of the dome</i>	138
5.6 Granite Emplacement	139
CHAPTER 6 DISCUSSION	140
6.1 Tectonic Evolution of the Usakos Dome	140
6.2 Conclusions	148
CHAPTER 7 CONCLUSIONS	148
REFERENCES	150

APPENDICES

- APPENDIX I Geological Map of the Southwestern Portion of the Usakos Dome, Damara Belt, Namibia
- APPENDIX II Form Line Map illustrating major fold structures within the Southwestern Portion of the Usakos Dome, Damara Belt, Namibia
- APPENDIX III Geological Cross Section between A and A1
- APPENDIX IV Geological Cross Section between B and B1
- APPENDIX V Geological Longitudinal Section between C and C1
- APPENDIX VI ArcView Files on Compact Disc

LIST OF FIGURES	<u>Page</u>
1.1: Landsat Image of the Usakos dome	1
2.1: Sketch of the Damara Orogen	5
2.2: Schematic Map of the southern Central Zone of the Damara belt	13
3.1: Geological map of the Usakos dome	17
3.2: Field photograph of part of the Damara Sequence	20
3.3: Photographs of the Chuos Formation	21
3.4: Photographs of the Spes Bona Formation	24
3.5: Stratigraphic section through the Okawayo Formation	25
3.6: Photographs of the Okawayo Formation	26
3.7: Stratigraphic section through the Oberwasser Formation	28
3.8: Photographs of typical units of Oberwasser Formation	29
3.9: Photographs of tremolite-rich units within the Oberwasser Formation	30
3.10: Photographs of banded calc-silicate felses of the Karibib Formation	32
3.11: Photographs of banded marbles of the Karibib Formation	33
3.12: Photographs of specific units within the Karibib Formation	35
3.13: Photograph of the Kuiseb Formation	36
3.14: Photograph of primary fabrics preserved within the Kuiseb Formation	37
4.1: Field photographs of folding within the Usakos dome	38
4.2: Schematic map of the Usakos dome showing axial traces of major folds	42
4.3: Photograph of schistosity within metapelitic rock types	44
4.4: Field photographs of transpositional fabrics within calc-silicate felses of the Karibib Formation	46
4.5: Photographs of linear fabrics observed within the Usakos dome	47
4.6: Photographs of mesoscale folds	48
4.7: Sketch illustrating intersection lineations between the early- and late-S2 Foliations	49

	<u>Page</u>
4.8: Schematic map showing designated sub domains of the Usakos dome	50
4.9: Structural map of Domain A	53
4.10: Sketches of Big Syn	54
4.11: Sketch of fold axial traces within Domain A	56
4.12: Sketch illustrating mesoscale fold hinge lineations within Domain A	57
4.13: Structural map of Domain B	60
4.14: Map showing fold axial traces within Domain B	62
4.15: Stereographic projections of data from Domain B	63
4.16: Field photographs from Domain B	64
4.17: Sketch showing a cross sectional view across the southwestern termination of the Usakos dome	66
4.18: Block diagram illustrating strain partitioning along the southwestern termination of the Usakos dome	67
4.19: Stereographic projection of foliations and fold hinge lineations along the southwest termination of the dome	67
4.20: Structural map and stereographic projections from Domain C	69
4.21: Field photographs of transpositional folding along Domain C	71
4.22: Sketch of strain partitioning along Domain C	72
4.23: Photographs of tectono-stratigraphic layering along Domain C	73
4.24: Photograph showing the curvilinear fold hinge lines of folds within Domain C	74
4.25: Structural map of Domain D	75
4.26: Sketch showing the cross-sectional structure across Domain D	77
4.27: Photographs of folding along Domain D	78
4.28: Field photographs of transposed folding within the marbles along the southeastern limb of the Usakos dome	79
4.29: Photographs of transpositional fabrics within Domain D	80
4.30: Photographs of refolded folds from Domain D	82

	<u>Page</u>
4.31: Boudinage of bedding within Domain D	83
4.32: Structural map of Domain E	85
4.33: Photographs of southeast-trending folds within Domain E	87
4.34: Stereographic projections of structural data from Domain E	88
4.35: Form line map of the Usakos dome with stereographic projections of all structural data	93
4.36: Form line map showing fold axial traces across the dome	94
4.37: Sketch showing inversion of fold structures	96
4.38: Block diagram of the Usakos dome showing the structure in longitudinal view	97
5.1: Photograph showing abundant Klein Aukas Granite within the core of the dome	98
5.2: Schematic map illustrating the distribution of granite within the study area	99
5.3: Field photographs of the Salem granite	103
5.4: Cross-sectional sketch through an exposure of Salem granite	105
5.5: Field photographs of the Salem granite	106
5.6: Photographs of magmatic layering within the Salem granite	108
5.7: Photomicrographs of the Salem granite	109
5.8: Sketch of biotite aggregates within the Salem granite	111
5.9: Photomicrographs of the Salem granite	112
5.10: Photomicrographs of the Salem granite	113
5.11: Field photographs of the Klein Aukas granite	116
5.12: Sketch of sheeted intrusions of the Klein Aukas granite	117
5.13: Field photographs of the Klein Aukas granite	118
5.14: Photograph of boudinaged intrusion of Klein Aukas granite	119
5.15: Photograph of ghost-stratigraphy preserved within the Klein Aukas granite	120
5.16: Field photographs showing the transition between subvertical sheeting along the limbs of the dome and gently-dipping sheet within the core of the dome	121

	<u>Page</u>
5.17: Field photographs and stereographic projection of the sheeted Klein Aukas granite	123
5.18: Field photographs showing the subhorizontal sheeted Klein Aukas granite characteristic of the core of the dome	124
5.19: Field photographs of fabrics within the Klein Aukas granite	126
5.20: Microphotographs of the Klein Aukas granite	127
5.21: Microphotographs of the Klein Aukas granite	128
5.22: Field photograph of linear fabrics along a Klein Aukas granite contact	129
5.23: Field photograph of a folded pegmatitic sheet along the northwestern limb of the Usakos dome	138
6.1: Sketch illustrating the locality of the Usakos dome with respect to the orthogonal vergence directions characterizing the sCZ	146
6.2: A schematic 3-D model illustrating the development of the Usakos dome during progressive deformation (D2)	147

LIST OF TABLES

2.1: Stratigraphy of the Damara Sequence within the sCZ (modified from Badenhorst, 1992; Hoffmann et al., 2004).	7
4.1: Summary of the main fabric elements observed within the study area	40

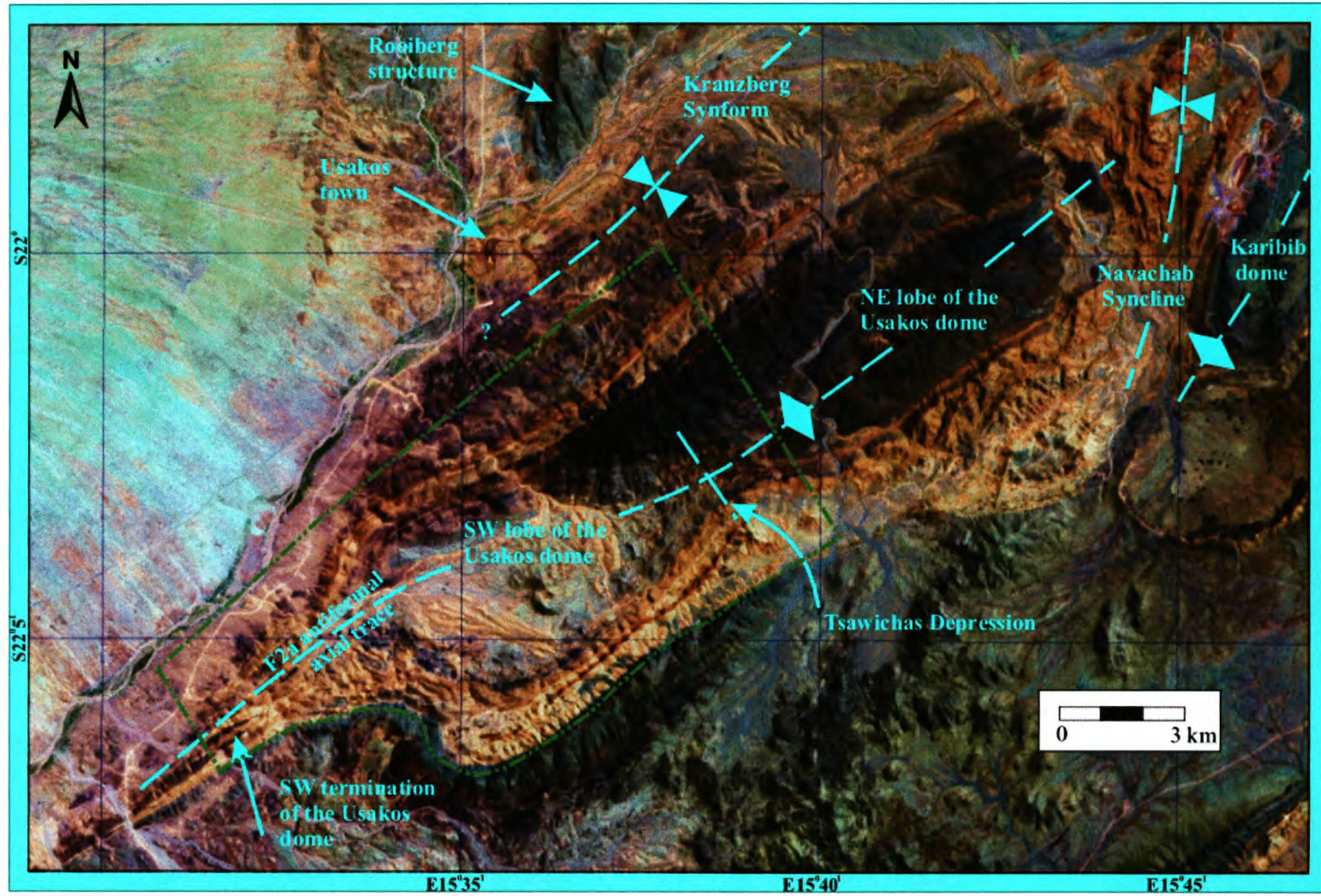


Fig. 1.1 Landsat image defining the Usakos dome structure. The dome is subdivided into a northeastern lobe and a southwestern lobe. The study area focuses on the southwestern lobe of the Usakos dome highlighted by the green dashed line.

CHAPTER 1 INTRODUCTION

Regional-scale dome structures are a common feature of many orogenic belts, particularly within high-grade metamorphic terrains. They occur in rocks of various ages, worldwide, and have intrigued geologists for many decades (Eskola, 1949 and references therein). In mid- to lower-crustal sections of orogenic belts, domes are typically cored by migmatites and/or granites which are structurally overlain by high-grade metasedimentary rocks (Eskola, 1949). In most parts of the world, the origin of these domes remains controversial where numerous models involving vertical and/or horizontal tectonics are described for both contractional and extensional settings. Some mechanisms proposed by workers range from diapirism of low-density middle crustal rocks or low-density magma (e.g. Teyssier and Whitney, 2002; Lee et al., 2004), to extensional exhumation of middle-crustal rocks below low-angle normal faults (e.g. Brun and Van Den Driessche, 1994; Holm and Lux, 1996) and cross folding (e.g. Blewett, 2002).

Kilometer-scale antiformal dome structures constitute the dominant structural feature within the deeply eroded Central Zone of the Pan-African Damara Orogen in central Namibia. Here, like elsewhere in the world, their formation is controversially discussed and numerous models of dome formation have been suggested over the past three decades (Smith, 1965; Downing and Coward, 1981; Coward, 1983; Sawyer, 1981; Jacob et al., 1983; Miller, 1983; Kröner, 1984; Oliver, 1994; Poli and Oliver, 2001; Kisters et al., 2004). Most of the previous work done on dome structures has focused within the granulite-facies, southwestern portion of the southern Central Zone. The presence of basement gneisses and/or intrusive granitoids within the cores of the domes led some workers to suggest the domes developed by diapirism of the low-density basement gneisses or magmatic ballooning of the intrusive granites (e.g. Sawyer, 1981; Kröner, 1984; Steven, 1993). Oliver (1994, 1995) proposed a metamorphic core complex model for the domes based on the highly strained basement/cover contact which was interpreted as a regional extensional detachment. Downing and Coward (1981) and Coward (1983) suggested the dome structures developed within a crustal-scale shear zone with a top-to-the southwest tectonic transport. Some areas of the Damara belt show evidence for polyphase folding and Jacob et al. (1983) propose the dome structures reflect regional-scale fold interference patterns. More recently, Poli and

Oliver (2001) postulated mid-crustal constrictional folding being responsible for the formation of the dome structures. Kisters et al. (2004) studied two domes located further northeast within mid-amphibolite facies metamorphic grades and interpreted these domes as large tip-line folds located above blind thrusts.

This project focuses on a dome structure, the Usakos dome (Fig. 1.1) located between the well-documented granulite-facies rocks exposed to the southwest and the mid-amphibolite facies rocks studied by Kisters et al (2004) to the northeast. It attempts to link the dome forming mechanisms described from the higher-grade southwestern parts of the sCZ with those from the lower-grade rocks to the northeast.

1.1 The study area

The Usakos dome is a 22 km long, 6 km wide antiformal structure cored by Pan-African granite, situated to the south and southeast of the town Usakos (22° 00'S ; 15° 35'E) (Fig. 1.1). It forms part of a large inlier of Damaran and Pre-Damaran lithologies partially overlain by more recent Tertiary to Quaternary calcrete and sand cover of the Kalahari Group. The dry, arid climate of the Namib Desert and associated sparse scrubby acacia vegetation provides an excellent setting for geological fieldwork. Much of the study area comprises well-exposed rocky slopes with deeply incised river valleys, ideal for a structural investigation of the dome structure.

1.2 Purpose of the study

The Exploration Division of the Navachab Gold Mine engaged on a regional mapping program in 2002 to gain a better understanding of the regional geology, specifically the structural geology of the area surrounding the mine. Structural maps of the Karibib dome and the northeastern part of the Usakos dome were produced by Kisters et al. (2004) and Neumaier (2002). This study is a continuation of this program focusing on the structural geology of the southwestern portion and termination of the Usakos dome. For the purpose of this study, a regional geological map of the 120 km² area was produced during 3 ½ months of field mapping with the aid of aerial photographs (1:8000 scale), Landsat images and a geographical positioning system (GPS). The field area covers parts of the farms Naob 69, Narubis 87, Klein Aukas 68 and Gross Aukas 68. Lithological and structural maps of the study area at a 1:10 000 scale with their

corresponding cross sections are provided in Appendices I to V. ArcView files are provided in Appendix V.

The main aims of the study can be summarized as follows:

- To develop a regional 1:10 000 scale structural and lithological map of the southwestern portion of the Usakos dome.
- To provide a detailed description and up-to-date interpretation of the overall structure of the Usakos dome and structures therein.
- During the initial field season it was noticed that the bulk of the core of the Usakos dome comprises sheeted granite. It soon became evident that these granites may play a major role in the tectonic evolution of the dome and were therefore studied in more detail.
- To investigate the tectonic evolution of the Usakos dome and compare it to other domes within the Central Zone of the Damara belt.

1.3 Methodology

During fieldwork, observations and descriptions were made of the main lithological units and structural features. Structural readings were taken using a Breithaupt structural compass. Mineral phases of the main lithological units were identified using petrographic studies and the Scanning Electron Microscope (SEM) at Stellenbosch University was used to identify mineral compositions listed in the thesis. Structural and lithological maps of the area were digitally reproduced using Geographical Information Systems (GIS), namely ArcView 3.3 and Corel Draw. Cross-sections, longitudinal sections and the maps produced during fieldwork provided the basis for the interpretation of the geometry and tectonic evolution of the Usakos dome. In the following, all planar readings are given as the dip azimuth and dip angles and all linear elements are given as the plunge direction and plunge.

CHAPTER 2 GEOLOGICAL SETTING

2.1 The Damara Orogen

The Damara Orogen in Namibia is one of several Pan-African orogenic belts exposed in Africa. It consists of reworked Mesoproterozoic basement and a pre- to syn-orogenic succession referred to as the Damara Sequence. The orogen is characterized by three main tectonostratigraphic branches, namely a coastal branch in the north, the Kaoko belt, a coastal branch to the south, the Gariep belt, and an inland branch trending northeast from Swakopmund, the Damara belt 'sensu stricto' (Miller, 1983; Porada, 1989) (Fig. 2.1a). These belts form a triple junction between the Rio De La Plata Craton, the Congo Craton and the Kalahari Craton (Prave, 1996).

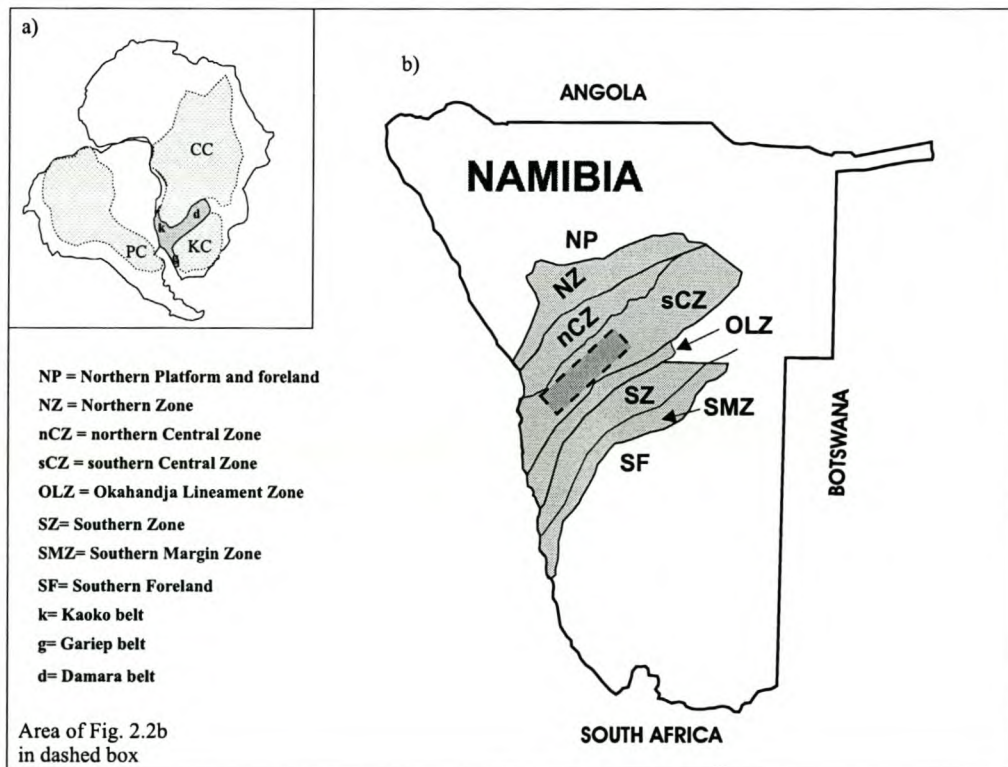


Fig. 2.1 (a) Reconstruction of part of Gondwana (after Maloof, 2000) showing the positions of the Kaoko belt, Gariep belt and Damara belt in relation to the Congo (CC), Rio de la Plata (PC) and Kalahari Cratons (KC). (b) Map of the present-day Damara belt showing its main tectonostratigraphic components (Martin and Porada, 1977).

For a compilation of some of the earlier works on the Damara Orogen, the reader is referred to the volume edited by Miller (1983). The area investigated in this study is located in the central parts of the northeast-trending Damara belt (Fig. 2.1b).

The Damara belt extends for >1000 km northeast from Swakopmund reaching ca. 400 km in width. It is subdivided into a number of tectonostratigraphic zones based on structure, stratigraphy, metamorphism, igneous intrusives, geochronology and aeromagnetic expression (Martin, 1965; Martin and Porada, 1977; Barnes and Sawyer, 1980; Miller and Hoffman, 1981; Corner, 1982, 2000; Anderson and Nash, 1997). These include the Northern Platform, the Northern Zone, the Central Zone, the Southern Zone, the Southern Marginal Zone and the Southern Foreland, separated from each other by major crustal lineaments. The CZ, within which the study area is located, is further subdivided into a northern Central Zone (nCZ) and a southern Central Zone (sCZ) (Fig. 2.1b). A summary of the evolution of the Damara belt, specifically the CZ is provided below.

2.2 Tectonostratigraphic Evolution of the Central Zone in the Damara belt

The Damara Sequence of the CZ consists of a several kilometer-thick meta-volcano sedimentary succession deposited prior to and/or during the Damaran orogeny. These metasediments are subdivided into a younger Swakop Group and an older Nosib Group (Smith, 1965). A simplified stratigraphic table of the Damara Sequence in the sCZ is shown in Table 2.1. For simplicity, the sequence of events leading to the development of the Damara Orogen is subdivided into five main phases. These are 1) rifting, 2) marine sedimentation, 3) convergence, 4) collision, and 5) post-collisional equilibration.

1) Rifting

The onset of rifting along a triple junction between the Congo, Kalahari and Rio de la Plato Cratons led to the formation of Neoproterozoic extensional basins.

Table 2.1 Stratigraphy of the Damara Sequence within the sCZ (modified from Badenhorst, 1992; Hoffmann et al., 2004).

Group	Formation	Description	Thickness	Age
Swakop	Kuiseb	Quartz-biotite-schist, interbedded calc-silicate felses and marble.	40 to >3300 m (Smith, 1965; Badenhorst, 1987).	
	Onguati (*)	Interbedded biotite-schist, quartzites, calc-silicate felses and marble.	0 to 800 m (Badenhorst, 1988a).	
	Karibib	Calcitic and dolomitic marbles and calc-silicate felses.	Up to 1500 m	
	Ghaub	Glaciomarine pelites, psammities and dropstone units.	0 to tens of meters	635.5±1.2 Ma (Hoffmann, 2004)
	Daheim member	Amphibolites	0 to 120 m (Badenhorst, 1992).	
	Oberwasser	Quartz-biotite-tremolite-cordierite schist.	50 to 700 m (Botha, 1978; Badenhorst, 1987).	
	Okawayo	Calcitic marbles and calc-silicate felses.	ca. 100 m thick	
	Spes Bona	Quartz-biotite schists and meta-psammities.	20 to >600 m (Badenhorst, 1992; Steven, 1993).	
	Chuoss	Glaciomarine diamictite.	0 to 700 m (Henry et al., 1986)	ca. 750-720 Ma (Kaufmann et al., 1997)
Rössing (*)	Calcitic and dolomitic marble and calc-silicate felses.	0 to 300 m (Steven, 1993).		
Nosib	Khan (*)	Pyribole calc-silicate felses, biotite schist, graphite schist and marble.	0 to 1500 m (Steven, 1993).	
	Etusis	Quartz-arenites.	0 to 3500 m (Smith, 1965; Miller, 1983; Lehtonen et al., 1996).	756±2 Ma to 746±2 Ma (Hoffman et al., 1996)

* not present in the study area

Based on facies variations, rifting along the inland branch of the Damara belt is interpreted by Henry et al., (1990) to have formed two, east-northeast-trending detachment systems separated by a topographic high. Accumulation of meta-arkoses and meta-volcanics into these basins form the lowermost units of the Nosib Group, the Etusis Formation. These rift-type sediments unconformably overlie Mesoproterozoic basement gneisses of the Congo Craton (Jacob et al., 1983). U-Pb zircon ages of some of these meta-volcanics place rifting between 746 ± 2 and 756 ± 2 Ma (Hoffman et al., 1996). These are overlain by calc-silicate felses and gneisses of the Khan Formation.

2) Progressive basin evolution and marine sedimentation

Progressive rifting led to the opening of two main oceans, the north-south-trending Adamastor Ocean and the northeast-trending Khomas Sea. Thermal subsidence in response to continued rifting initiated marine transgressions and the deposition of shelf sequences characteristic of the lower Swakop Group (Hartnady et al., 1985; Henry et al., 1988; Stanistreet et al., 1991; Hoffmann, 1990). These include mixed carbonates, quartz arenites and mudstone shelf sequences of the Rössing Formation. The Rössing Formation is overlain by the glaciomarine deposits of the Chuos Formation which is extensively developed throughout the Damara Orogen, providing an excellent marker horizon. They are interpreted as having formed during the Sturtian glacial event (between 750 and 720 Ma) (Hoffmann et al., 2004). Overlying the Chuos Formation is the Spes Bona Formation comprising dark-grey siliciclastic and psammitic units that resemble turbiditic sequences. With progressive widening of the marine basins, mature oceanic shelves developed on either side of the Khomas Sea. This resulted in a switch from deep-marine sedimentation to shelf-dominated sedimentation (Stanistreet et al., 1991). Carbonate sedimentation dominated the continental margin of Congo Craton, while predominantly terrigenous sedimentation dominated the Kalahari margin (Stanistreet et al., 1991). In the sCZ, a thin marble-dominated unit, the Okawayo Formation, overlies the Spes Bona

Formation. This, in turn, is overlain by quartz-biotite schists of the Oberwasser Formation. The upper portion of the Oberwasser Formation is interbedded with mafic volcanic rocks of the Daheim Member. These volcanics are interpreted to have erupted via deep-seated fractures in the basement along the basin margins (Steven, 1993). Associated with the volcanic rocks are glaciomarine sedimentary rocks of the Ghaub Formation, dated at 635.5 ± 1.2 Ma (Hoffmann et al., 2004). The Congo continental shelf was subsequently swamped by a thick succession of carbonate sedimentation giving rise to the Karibib Formation (Stanistreet et al., 1991).

3) Convergence of the Cratons

Carbonate sedimentation was succeeded by sediments related to the convergence and subsequent closure of the Khomas Sea and the Adamastor Ocean between 650 and 600 Ma (Miller, 1983). This phase is characterized by the deposition of immature siliciclastic sediments that form the Kuiseb Formation. The SZ of the Damara belt is interpreted by Kukla and Stanistreet (1991) as an accretionary prism formed during the northwesterly-directed subduction of the Kalahari Craton beneath the Congo Craton (Kasch, 1983b). The onset of convergence coincides with the generation of the first granitoids that intruded throughout and subsequent to the Damaran orogeny. Early, bedding-parallel structures described as D1 structures in many previous works (e.g. Miller, 1983; Sawyer, 1981; Coward, 1983; Kisters et al., 2004) may have developed during this convergent tectonic regime (Miller, 1983).

4) Collisional stage

Progressive convergence of the cratons ultimately led to their collision and the formation of the north-south-trending and northeast-trending orogenic belts between 540 and 550 Ma (Miller, 1983; Tack et al., 2002). The relative timing of the closure of the Adamastor and Khomas basins is debated extensively in the literature (e.g. Stanistreet et al., 1991; Prave, 1996; Frimmel and Frank, 1998; Goscombe et al., 2003). Continental collision is responsible for the prominent east-northeast-directed structural grain in the CZ of the Damara belt.

The regional and structural geology within the sCZ, is discussed by Smith (1965), Sawyer (1981), Martin (1983), Miller (1983), Jacob et al. (1983), Poli and Oliver (2001), Kröner et al. (1984), Bühn and Stanistreet (1992), Anderson and Nash (1997),

Nex et al. (2001), Kisters et al. (2004) and Basson and Greenway (2004). Between two and four deformational phases are described to have had an effect on the Damara Sequence within the sCZ. However, a correlation of these events over the entire sCZ has proven problematic. The heterogeneity of fold and/or dome and/or thrust vergence within the sCZ has previously led workers to explain the tectonic evolution using multiple deformation phases. More recently however, structural mapping of the Namibfontein and Khan Mine areas by Oliver (1994) and Poli and Oliver (2001) present evidence for only two deformational phases. These are referred to as D1 and D2. **D1** is responsible for the formation of the earliest structures, which are largely overprinted by D2, particularly in the southwest. D1 is expressed as a bedding-parallel foliation (S1), intrafolial and isoclinal folding (F1) and bedding-parallel mylonites (Kisters et al., 2004). **D2** is interpreted as the main deformational event, producing much of the mesoscale structures currently preserved within the sCZ such as the southwest-trending folds and dome structures, their associated structures as well as large-scale thrusts and/or detachments described by Oliver (1994; 1995), Poli and Oliver (2001) and Kisters et al. (2004). Zircon and titanite ages of syn-D2 Mon Repos granodiorites along the Karibib dome and the U-Pb ages of early, post-D2 granitoids along the Ida and Khan domes confine the D2 event between ca. 560 and 550 Ma (Jacob et al., 2000; Tack et al., 2002).

Oliver (1994, 1995) and Poli and Oliver (2001) propose that progressive convergence and collision led to significant thickening of the crustal sequences and the development of constrictional deformation at deep crustal levels. It is these crustal rocks that are exposed at the present-day erosional surface. During the late-stages of collision, gravitational collapse of the overthickened crust to the southwest resulted in orogen-parallel, southwest-directed extrusion (Poli and Oliver, 2001). Kisters et al. (2004) further developed this model, incorporating areas slightly to the northeast. They agree that constrictional tectonics and lateral extrusion were dominant processes at the deep crustal levels exposed to the southwest. However, at shallower levels, for example in the rocks exposed within the Karibib District, northwest-vergent fold-and-thrust tectonics dominates. Granitic intrusions exhibiting syn-tectonic characteristics commonly intrude into the cores of domes (Barnes and Downing, 1979; Poli and Oliver, 2001).

The sCZ is regarded as a typical high-temperature, low-pressure (HT-LP) metamorphic terrain. Metamorphic grade progressively increases from the northeast towards the southwest. Previous works have emphasized the polymetamorphic nature of the CZ and describe at least two main metamorphic events, namely M1 and M2. M1 refers to the initial HT-MP phase of metamorphism that occurred during collision ca. 550-540 Ma (Nex et al., 2001; Jung and Mezger, 2003).

5) Post-Collisional evolution

Decompression possibly related to extension and crustal thinning followed the main collisional event (Tack and Bowden, 1999; Jung and Mezger, 2003). This was accompanied by voluminous intrusion of granite, which is interpreted as having been responsible for a second phase of metamorphism referred to as M2 (Jung and Mezger, 2003). M2 is a post-tectonic HT-LP metamorphic phase characterized by a period of thermal peaks between 505 and 478 Ma (Bowden et al., 1995; Bowden et al., 1999; Jacob et al., 2000), the timing of which, coincides with the main phase of late-to-post-tectonic granite emplacement that occurred between 530 and 480 Ma within the Damara belt (Briqueu et al., 1980; Allsop et al., 1983; De Kock and Walraven, 1994; Bowden et al., 1995; Nex, 1997). Metasediments within the Karibib District in the northeast exhibit low-amphibolite facies metamorphism with temperatures estimated between 560 and 650° C and pressures of 3 ± 1 kbars (Puhan, 1983; Steven, 1993). Approximately 125 km further southwest, upper-amphibolite to granulite metamorphic conditions are evident. These high-grade rocks contain abundant migmatites and exhibit temperatures between 700 and 800° C and pressures of ca. 5 kbars (Masberg, 2000; Masberg et al., 1992; Nex et al., 2001). This prolonged thermal event is responsible for the annealing of fabrics and minerals within the Damara Sequence and the igneous rocks throughout the CZ. Post-Damara cooling occurred at ca. 465 ± 2 Ma (Tack and Bowden, 1999).

The sCZ contains considerable variation in metamorphic grade, abundance of granitoids and fold vergence along its northeast-southwest strike extent. The length of this zone is therefore thought to expose an oblique crustal section with progressively deeper levels exposed towards the southwest (Hoffer, 1978; Barnes and Downing 1979; Hoernes and Hoffer, 1979; Kasch, 1983a).

2.3 Dome structures

The dominant regional structural feature within the sCZ is the presence of kilometer-scale dome structures easily identifiable on aerial photographs and satellite imagery (Fig. 2.2b). Domes are made up of rocks of the Damara Sequence forming large antiformal structures which are often cored either by Mesoproterozoic Abbabis basement gneisses and/or Pan-African granite. They are elongate, ovoid-shaped structures, trending northeast-southwest varying between 10 and 40 km in length and 4 to 18 km in width. Domes are separated from each other by keel-shaped, tight and structurally complex synforms of infolded rocks of the Damara Sequence.

Domes to the southwest of the Usakos dome are southwest-vergent, contain large quantities of Pan-African granite (up to 70% total volume) and are typically developed as pervasive L-tectonites (Barnes and Downing, 1979; Poli and Oliver, 2001). In contrast, domes to the northeast of the Usakos dome are northwest-vergent, contain little if any Pan-African granite and are dominated by S-tectonites (Kisters et al., 2004). Despite numerous studies on the dome structures, their mechanism of formation remains highly controversial.

To date eight theories for dome formation have been proposed which are briefly summarized below:

- 1) The buoyant rise of older basement within the cores of domes led Eskola (1949) and Barnes (1981) to consider that density driven diapirism of these lower, less dense units into the upper, denser metasedimentary cover may have led to the development of a basin and dome outcrop pattern.
- 2) Magmatic deformation caused by the diapiric rise of magma or magmatic ballooning has been suggested by Sawyer (1981), Coward (1981), Barnes and Downing (1979) and Kröner (1984). Kröner (1984) suggests that the buoyant rise of granitic melt into antiforms was hindered by an impermeable horizon. Continued melt production led to balloon-like expansion of the granite causing 'doming' of the overlying Damara Sequence.
- 3) Polyphase folding by more than one deformational event creating superposed fold interference patterns giving rise to a dome and basin terrain (Smith, 1965; Jacob et al., 1983).

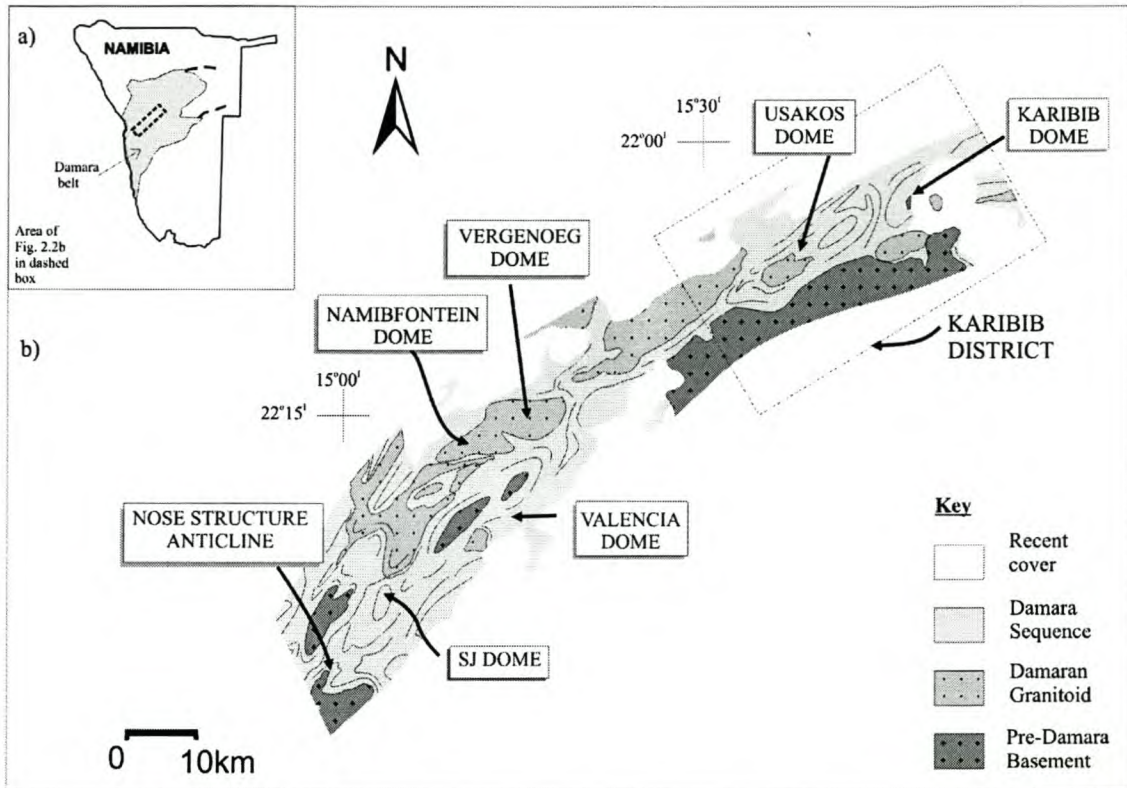


Fig. 2.2 a) Simplified map showing the locality of Fig. 2.2b) within the Damara belt. (b) Schematic geological map of parts of the southern Central Zone of the Damara belt showing the localities of various dome structures with respect to the Karibib District (after Miller, 1988; Kisters et al., 2004).

- 4) Coward (1983) suggests that a large, low-angle shear zone with an overthrust sense to the southwest produced the kilometer-scale sheath folds (dome structures) within the CZ. He suggests that the significantly higher strain zones along the underlying antiformal limb of the sheath folds supported this model.
- 5) Oliver (1994) suggests that the Damara belt could represent a deeper seated equivalent to the North American metamorphic core complex. The cover sequence was detached from the basement along a ductile extensional shear zone, developed as the Khan River Detachment (Oliver, 1994; 1995).
- 6) Poli and Oliver (2001) discuss the possibility of progressive polyphase folding of the middle crust during constriction. They suggest, the sCZ was exposed to a single deformational event, however, oversteepening during the oblique collision between the Congo and Kalahari Cratons caused the Damara Sequence to extrude laterally towards the southwest resulting in a basin and dome terrain.

- 7) More recent structural analysis by Kisters et al. (2004) led to the development of a model relating the domes within the Karibib District to tip-line folds above blind thrusts within a fold-and-thrust belt.

These contrasting models for dome formation were proposed by various geologists, many of whom studied domes at different localities within the sCZ. When faced with the structural heterogeneity of the sCZ, it is no wonder so many models for dome formation have been proposed. Barnes and Downing (1979) pointed out that present day erosional surfaces within the sCZ may expose an oblique section through the crust with progressively deeper levels to the southwest. Kisters et al. (2004) show that this is a fundamental aspect to consider when interpreting the dome forming mechanisms across the sCZ. They propose that domes at higher crustal levels in the northeast resulted from fold-and-thrust-tectonics while domes exposed further southwest developed as a result of constrictional tectonics at deeper crustal levels (as described by Poli and Oliver, 2001).

2.4 Granites within the CZ

One of the characteristic features of the sCZ is the abundance of Pan-African igneous intrusive rocks. Granite is by far the most common igneous rock type in the Damara belt making up 96% of all igneous intrusions. The remaining 4% comprises equal proportions of gabbro/diorite and tonalite/granodiorite (Miller, 1983). Miller (1983) classified the granites within the Damara belt into three main types, firstly the red, medium- to fine-grained granites, secondly the coarsely-porphyritic, biotite monzogranites and associated dioritic rock types, collectively referred to as the 'Salem Granite Suite' and, finally, the fine- to coarse-grained leucogranites, pegmatitic alaskites and pegmatites.

Rocks of the Salem Granite Suite include granites, granodiorites, diorites and tonalites of variable textures (Allsopp et al., 1983; Miller, 1983). Tentative dates for these rocks include U-Pb zircon ages of ca. 580 ± 30 Ma and 535 ± 8 Ma to 720 ± 77 Ma Rb-Sr whole-rock ages (Allsopp et al., 1983). The Salem Granite Suite almost exclusively occurs above the Karibib Formation, particularly within synforms of the Kuiseb Formation. It forms large, concordant plutons often exhibiting marginal phases with gradational relationships and a strong, penetrative foliation which decreases in intensity towards the

centre of the plutons (Miller, 1983). Syn-, late- and post-tectonic intrusions of Salem-type granite are described from the Damara belt (Smith, 1965; Jacob, 1974; Miller, 1983).

2.5 The Karibib District

The current study focuses on the Usakos dome situated within the southeastern part of the Karibib District in Central Namibia. The Karibib District, as defined for the purpose of this study, covers the area surrounding the towns of Karibib and Usakos (Fig. 2.2). Domes within the Karibib District include the Rooiberg structure (northeast of the town Usakos), and the Karibib and Usakos domes which are separated by the Navachab Syncline (Fig. 1.1). Structural maps of the Karibib dome and the northern portion of the Usakos dome were produced for Navachab Mine by Kisters et al. (2004) and Neumaier (2002) respectively and the information therein is documented in Kisters et al. (2004).

Domes within the Karibib District comprise metasediments of the Damara Sequence, underlain by the AMC. The Damara Sequence within the Karibib District follows the stratigraphy documented by Badenhorst (1992), illustrated in Table 2.1.

The Karibib dome and northeastern parts of the Usakos dome are northeast-trending, northwest-verging, doubly-plunging antiformal structures. They range between 9 and 12 km in length with half-wavelengths of approximately 4 km. The Karibib dome contains a complete stratigraphic sequence from the AMC in the core of the dome to the Karibib Formation and parts of the Kuiseb Formation along the limb. Both domes preserve an early D1 fabric, expressed as a bedding-parallel foliation recorded in the Chuos and Spes Bona Formations (S1), isoclinal folding within the Okawayo Formation (F1) and mylonites between the Chuos and Etusis Formations. D2 is interpreted to have formed the mesoscale domes and their associated small-scale structures. The southeastern limb of the Karibib dome is truncated by the syn-tectonic Mon Repos diorites and granodiorites dated between 564 ± 5 Ma and 539 ± 6 Ma (Jacob et al., 2000). The southeastern limb of the Usakos dome is truncated by a large, northwest-verging thrust, known as the Mon Repos Thrust Zone (MRTZ) (Kisters et al., 2004). This thrust forms the northeastern boundary of a large, >16 km long and 11 km wide structural window exposing Pre-Damaran basement referred to as the Abbabis Inlier (Brandt, 1987).

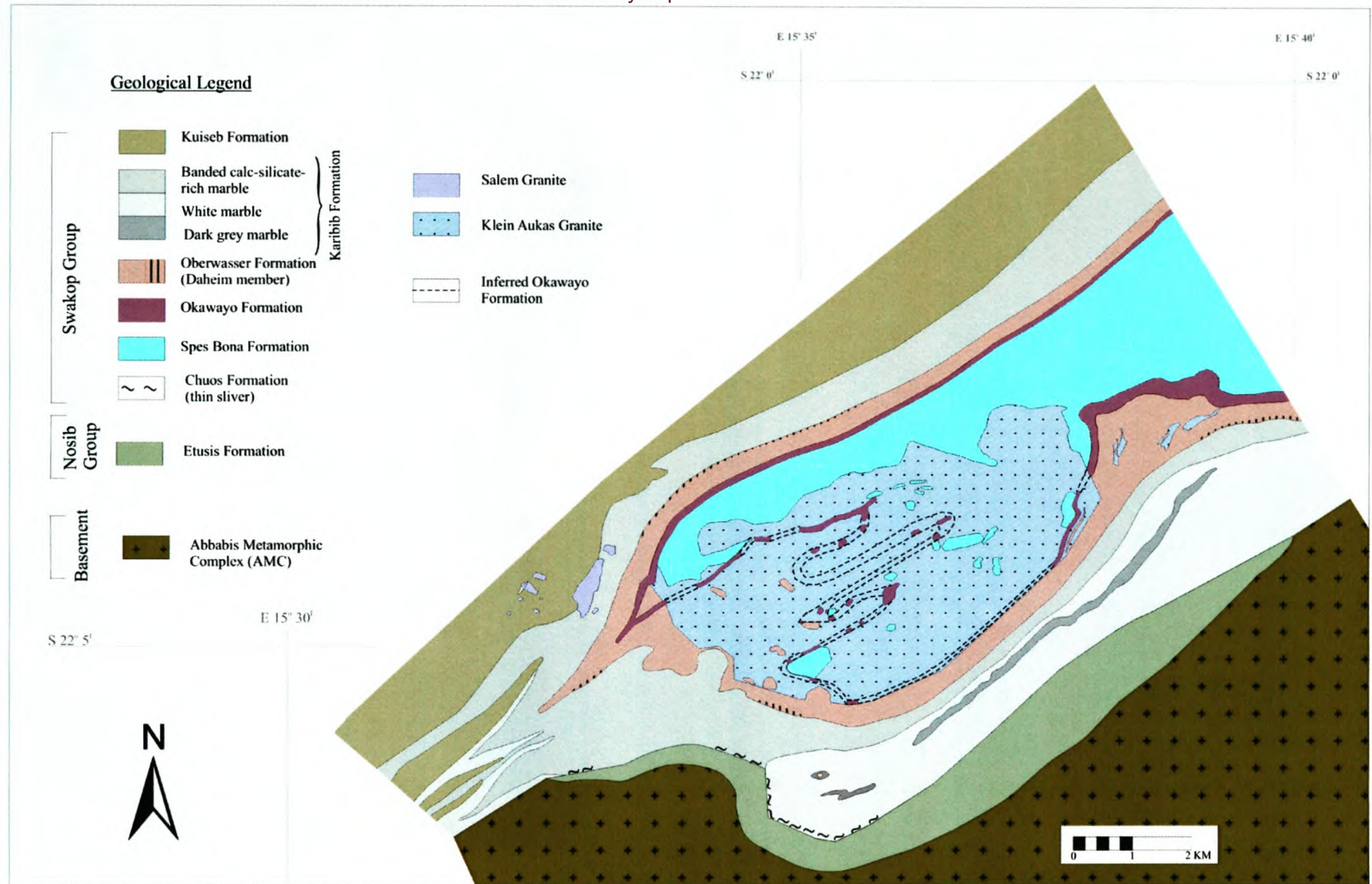


Figure 3.1 Schematic geological map showing the main lithological units exposed within the southwestern part of the Usakos dome.

CHAPTER 3 LITHOSTRATIGRAPHY AND FIELD RELATIONS

3.1 Introduction

This study follows the stratigraphy of the Damara Sequence detailed by Badenhorst (1992) for the Karibib District outlined in Table 2.1. Within the study area, however, the Khan and Rössing Formations are not developed. They are only exposed to the southwest of the Usakos dome and to the north of the study area in the Rooiberg structure (Badenhorst, pers. comm.). The Onguati Formation represents a transition between the calcareous lithotypes of the Karibib Formation and the schistose metapelites of the Kuiseb Formation. The contact between the Karibib and Kuiseb Formations in the study area is relatively sharp. It was therefore decided to omit the transitional Onguati Formation from the stratigraphy of the area.

The Usakos dome exposes the upper stratigraphic formations of the Damara Sequence. The Spes Bona Formation outcrops within the core of the dome and is progressively surrounded by the younger Okawayo, Oberwasser, Karibib and Kuiseb Formations towards the dome margins.

Basement rocks of the Abbabis Metamorphic Complex (AMC) and formations forming the lowermost portion of the Damara Sequence, including the Etusis and Chuos Formations bound the southeastern part of the Usakos dome (Fig. 3.1).

3.2 Pre-Damaran Basement

3.2.1 *Abbabis Metamorphic Complex (AMC)*

On a regional scale, the Damara Sequence is underlain by Pre-Damaran basement referred to as the AMC (Brandt, 1987). These basement rocks are characterized by pink and grey gneisses with minor amphibolites and schists. They are intruded by 1.7-2.0 Ga (U-Pb age) pegmatites (Jacob et al., 1978). A kilometer-scale 'inlier' of the AMC bounds the Usakos dome to the southeast (Smith, 1965; Brandt, 1987). The contact between the AMC and Karibib Formation forms part of the southeastern boundary to the study area. The AMC is not discussed in further detail in this study. For detailed descriptions of the AMC, the reader is referred to Brandt (1987).

3.3 Damara Sequence

3.3.1 *Etusis Formation*

Rocks of the Etusis Formation are exposed as a wedge between the Karibib Formation and the AMC along the southeastern limb of the Usakos dome (Fig. 3.1). These metasediments form the striking reddish-brown ridge known as Gamgamichabberg that trends northeast-southwest for ca. 7.5 km (Fig. 3.2). The contact between the Etusis Formation and the Karibib Formation forms part of the southeastern boundary of the study area. The Etusis Formation reaches a maximum outcrop thickness of ca. 1.2 km, although it pinches out to the northeast and southwest along its strike extent.

This formation predominantly comprises dark, reddish-brown arkosic metasediments and thin interbedded metapelitic and metaconglomeratic units. The meta-arkoses preserve massive bedding, particularly cross-bedding, where individual cross-bedded units reach up to 3 m in thickness. It is intruded by numerous dark-reddish-brown Pan-African pegmatites, that trend north-northeast.

The meta-arkoses predominantly consist of anhedral to polygonal grains of quartz (60-80%), microcline and orthoclase feldspar (15-35%) and muscovite (5%). Accessory minerals include magnetite, apatite and zircon. The quartz and feldspar grains range between 0.25 and 0.5 mm in diameter. Muscovite tends to form anhedral, randomly oriented grains averaging ca. 0.1-0.25 mm in diameter, often interstitial between quartz and feldspar.

3.3.2 *Chuos Formation*

A thin horizon of grey metapelites outcropping along part of the Karibib/ Etusis contact is interpreted as a sliver of the Chuos Formation. The horizon ranges in thickness between 0.5 and 10 m and extends for up to 1.5 km along strike between positions S22° 06' 10"; E15°

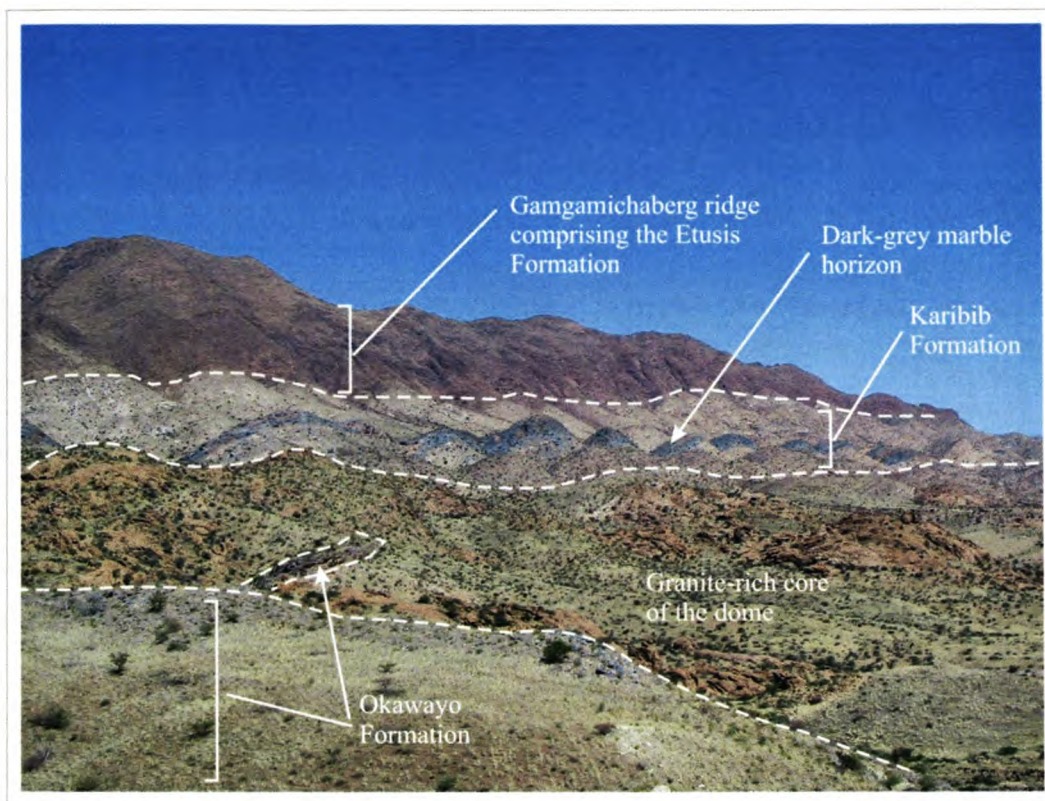


Figure 3.2 Photograph taken from the northern extent of the study area facing south, showing the prominent red meta-arkoses of the Etusis Formation, forming the Ganggamichaberg ridge in the background and the white and grey marbles of the Karibib Formation extending along the southeastern limb of the dome. The central portion of the picture shows the granite-rich core of the dome containing screens of the Okawayo Formation.

35° 25" and S22° 06' 00"; E15° 36' 20". The metapelites are characterized by dark-grey, well-foliated, quartz-biotite±muscovite schists (Fig. 3.3a). In places, fine-grained quartzite clasts and cordierite porphyroblasts are present (Fig. 3.3b and c). These field observations suggest that these schists may correlate with the lowermost portion of the Chuos Formation, described as the N¹ Unit by Badenhorst (1988b).

The metapelites comprise equigranular quartz, biotite, muscovite, K-feldspar, plagioclase (An₂₀) and cordierite with grain sizes averaging ca. 0.2 mm.

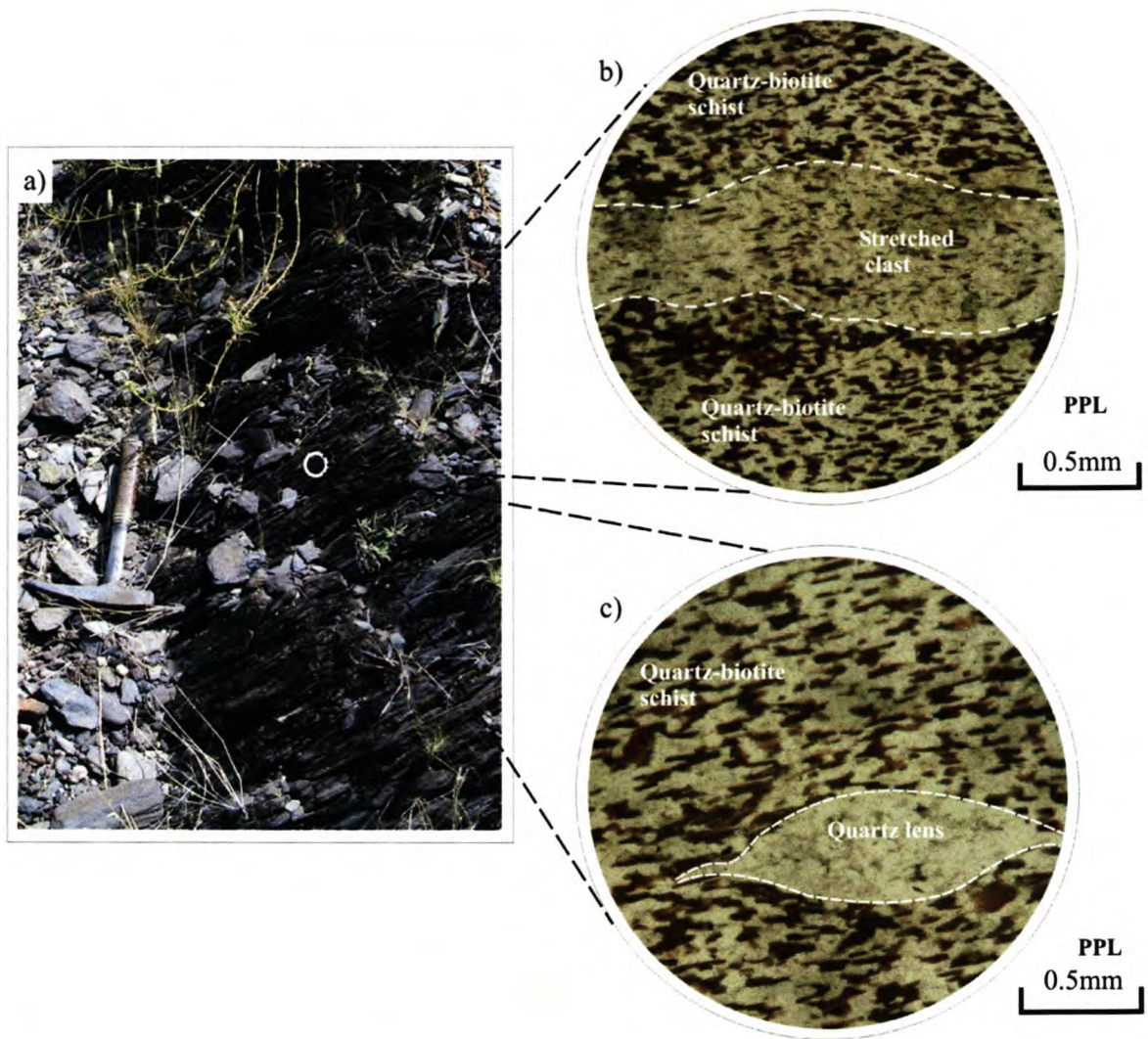


Figure 3.3 a) Photograph showing well-foliated quartz-biotite±muscovite schist outcropping along the Etusis-Karibib contact. It is interpreted as the Chuos Formation. (b) Photomicrograph taken parallel to the lineation and perpendicular to the foliation direction of the schist showing a stretched polymineralic clast within a quartz-biotite-rich matrix. Minerals within the clast include quartz, muscovite, biotite and clinzoisite. (c) Photomicrograph showing quartz-biotite-schist within the Chuos Formation containing a lens-shaped structure comprising annealed quartz. Photomicrographs are taken parallel to the lineation and perpendicular to the foliation direction.

Accessory minerals include apatite, garnet and tourmaline. Biotite comprises 20-40% of the matrix occurring as euhedral, unstrained laths. Two generations of biotite growth are evident, producing two distinct foliations that intersect at low angles

($\leq 20^\circ$). However, one foliation direction predominates. Muscovite is not always present, but may comprise up to 30% of the rock, also defining the dominant foliation.

Quartz, comprising ca. 50% of the mineralogy, may occur as polygonal grains, or as slightly elongate grains with pinned-grain boundaries. Thus, many of the quartz grains exhibit slight grain-elongation, oriented parallel to the foliation defined by the micas. Feldspar forms anhedral grains that contributes to ca. 10% of the mineralogy. Poikilitic, porphyroblastic cordierite is often present, averaging between 1.5 to 2 mm in diameter and containing rounded inclusions of muscovite, biotite and quartz.

Pale-grey clasts within the schists are observed in places (Fig. 3.3b). They often appear stretched, reaching up to several centimeters in length, comprising polymineralic aggregates incorporating minerals such as poikilitic muscovite (≤ 1.5 mm in diameter) (20% of the clast), randomly oriented biotite (0.2 mm in length) (20% of the clast), round to polygonal quartz (0.2 mm in diameter) (30% of the clast), and poikilitic clinozoisite (15% of the clast). Lens-shaped structures comprising annealed quartz are also common within these schists (Fig. 3.3c). They range between 0.4 and 3 mm in length, defining a weak lineation.

3.3.3 *Spes Bona Formation*

The Spes Bona Formation outcrops over a large area within the core of the Usakos dome. Its lower contact is not exposed, but a minimum thickness of ca. 600 m can be estimated from the construction of cross-sections. Lithologically, it is highly heterogeneous and consists mainly of dark-grey to black biotite schists, pale-grey meta-psammites and minor interbedded calc-silicate felses. It is intensely folded and intruded by granite, making the correlation of units within the formation difficult. It is clear, however, that the upper part of the Spes Bona Formation consists predominantly of banded meta-psammites and calc-silicate felses with occasional interbedded schistose units (Fig. 3.4a), while lower down in the sequence, quartz-biotite-cordierite schists predominate.

The quartz-rich units of the Spes Bona Formation often preserve primary textures, particularly cross-bedding. Individual cross beds range between 2 mm and 1 cm in thickness, recognized by changes in colour and/or grain sizes.

The units rich in meta-psammites, often show resistance to weathering by forming high topographic features, such as, for example, Nubbeberg, locally known as Kranzberg Mountain that reaches 700 m above the surrounding peneplain. They are pale-green to light-grey in colour on fresh surfaces but tend to develop dark-grey or black weathered surfaces. The meta-psammites comprise well-annealed quartz and minor amounts of tourmaline, biotite and K-feldspar. The calc-silicate felses are also equigranular, medium-grained rocks containing anhedral to polygonal quartz (ca. 40%), poikilitic diopside/hedenbergite (ca. 25%), anorthite (An_{90-100}) (ca. 20%), epidote (5-10%), sphene (up to 7%) and accessory calcite and opaque minerals. The lower, schistose metapelitic units of the Spes Bona Formation comprise massive quartz-biotite schists with variable amounts of cordierite, hornblende, K-feldspar, plagioclase (An_{50}) and tourmaline (Fig. 3.4b). Accessory minerals include calcite, chlorite, apatite, zircon and opaque minerals. The average grain size within these schists is ca. 0.3 mm, though hornblende and cordierite may form poikilitic porphyroblasts, where hornblende laths reach 0.7 mm in length and cordierite averages between 0.5 and 1.0 cm in diameter. The quartz and K-feldspar occur as polygonal grains, often exhibiting pinned-grain boundaries. Two generations of biotite growth are evident, defining slightly offset foliation planes.

3.3.4 Okawayo Formation

The Okawayo Formation is a thin, marble-rich unit separating the darker schistose lithologies of the Spes Bona and Oberwasser Formations. It is exposed along the length of the northeastern and parts of the southwestern limbs of the Usakos dome and infolded

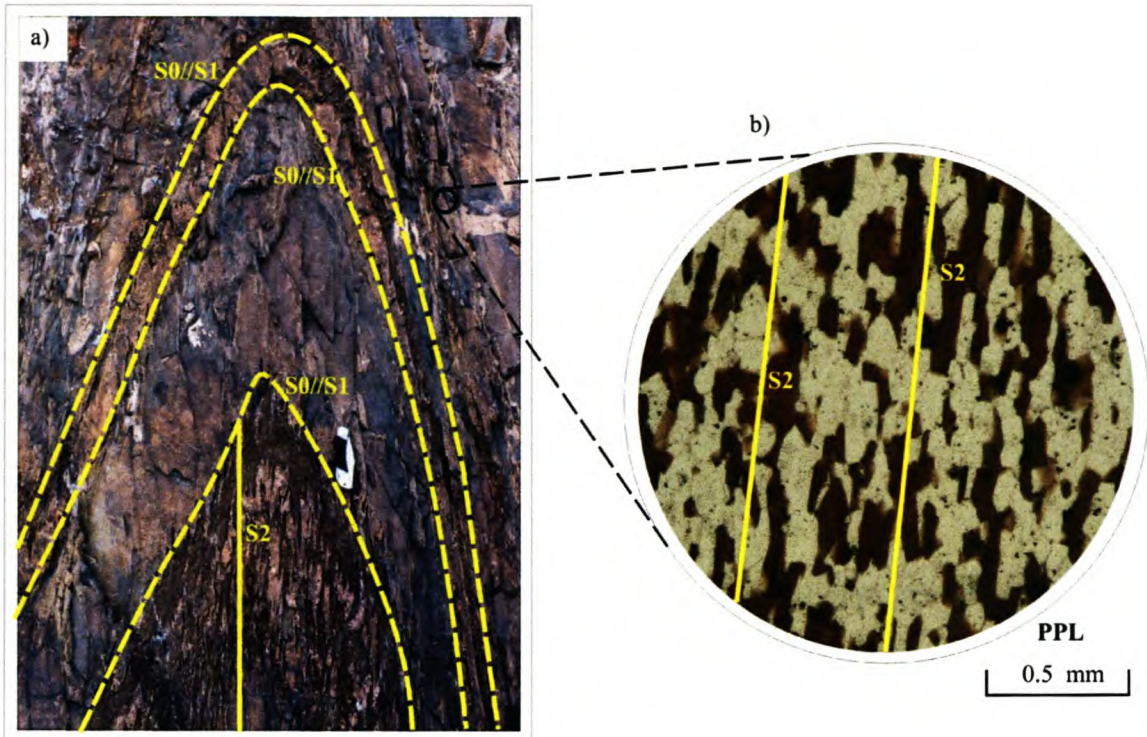


Figure 3.4 a) Photograph showing a typical outcrop of folded Spes Bona Formation. Biotite-rich layers (bottom centre) preserve a relatively strong schistose fabric (S2) compared to the more quartz-rich layers (centre). S0 refers to bedding. (b) Photomicrograph showing a typical quartz-biotite-feldspar schist of the Spes Bona Formation. Note the dominant schistosity defined by well-oriented, reddish-brown biotite laths. Transparent quartz and feldspar with pinned-grain boundaries also define the dominant schistosity.

within the core of the dome (Fig. 3.1). The formation varies in thickness between ca. 40 m within the core of the dome and ca. 115 m along the limbs of the dome. These thickness variations are likely to be the result of deformation rather than a primary depositional feature.

The upper- and lowermost portions of the Okawayo Formation are dominated by banded, pale-grey marble with interbedded calc-silicate-bearing units, while the central and bulk of the formation comprises banded, white and grey marbles (Fig. 3.5).

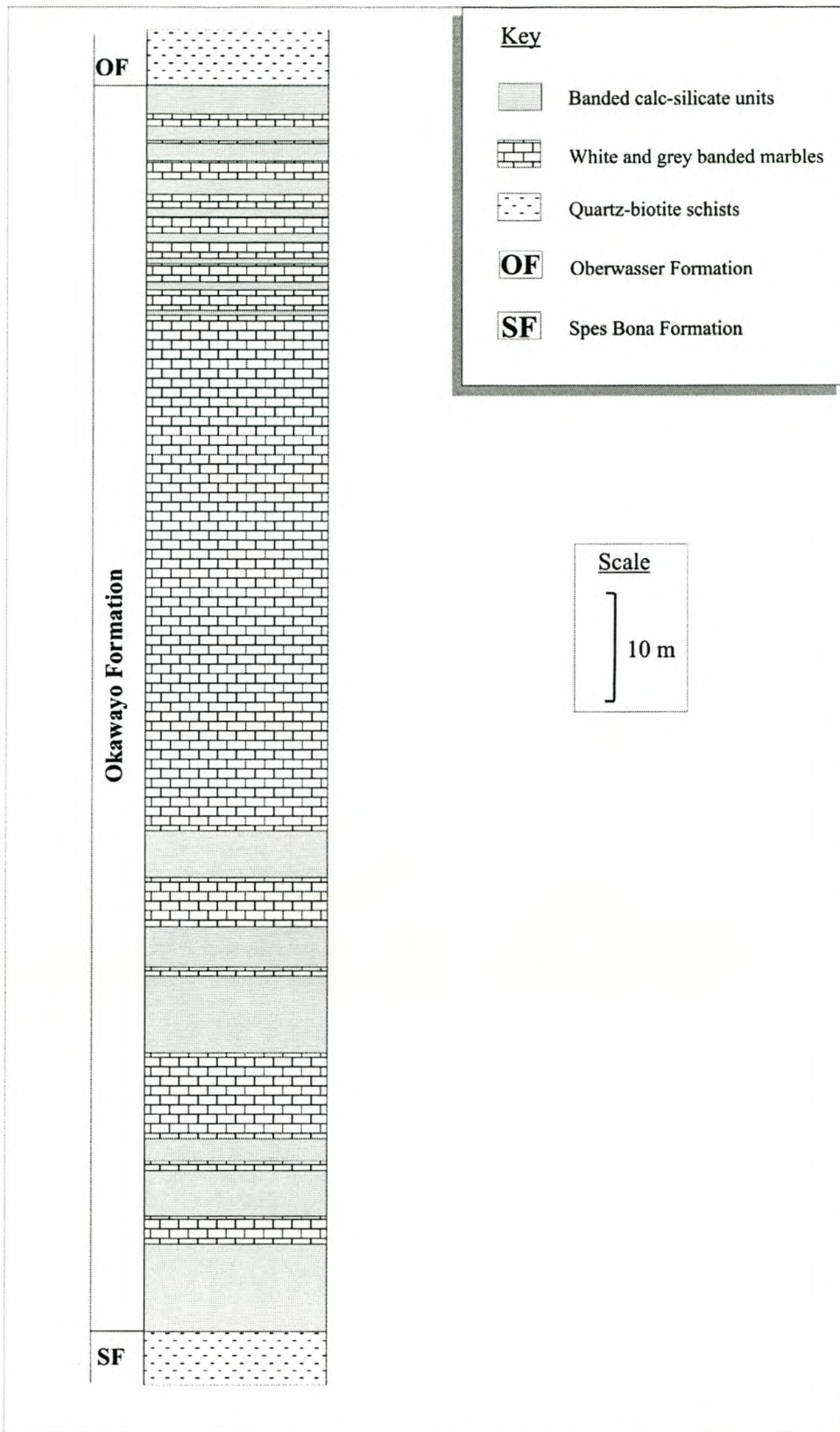


Figure 3.5 Synoptic stratigraphic section showing the main lithological units forming the Okawayo Formation along the southwestern limb of the Usakos dome.

The reddish-brown calc-silicate layers range between 1 and 10 cm in thickness and consist of fine-grained biotite, plagioclase, clinopyroxene, calcite and minor amounts of pyrite (Fig. 3.6a, b). The marble layers are slightly thicker, between 1 and 30 cm in thickness, predominantly comprising polygonal calcite. The banding within the light-grey and white calcitic marbles within the central portion of the Okawayo Formation ranges between 1 cm and a few meters in thickness. Generally, the contacts between bands are gradual. In places, dark-grey, laminated marble horizons (ca. 40 cm in thickness) are observed.

In places where the Okawayo Formation is in contact with granitic or pegmatitic intrusions, the rocks develop a <1 cm to 1 m wide contact aureole. Here the calc-silicate felses contain abundant vesuvianite.

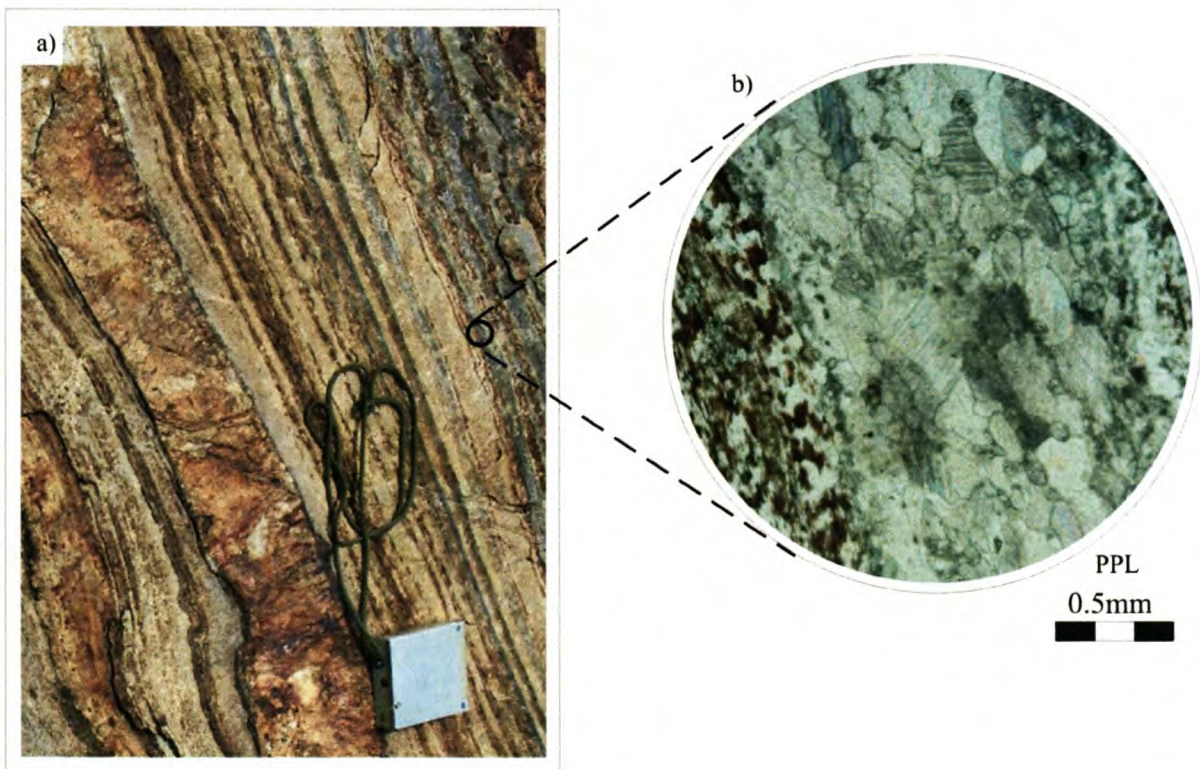


Figure 3.6 a) Banded calcitic marble (pale-grey and white) and layers of calc-silicate felses (reddish-brown) from the Okawayo Formation. Geological compass for scale. (b) Photomicrograph taken from the Okawayo Formation showing a calc-silicate-rich layer on the far left and a marble layer in the centre and right of the picture. The calc-silicates include fine-grained biotite, plagioclase, clinopyroxene, calcite and pyrite.

3.3.5 Oberwasser Formation

The Oberwasser Formation is a 130-300 m thick metapelitic unit comprising biotite-schists, biotite-cordierite schists and biotite-tremolite schists with minor marble breccia horizons, meta-psammites, calc-silicate felses and amphibolites (Fig. 3.7). This formation occurs along both limbs and within the southwestern closure of the dome (Fig. 3.1). Quartz-biotite-schists forming the most common rock-type of the Oberwasser Formation are pale- to dark-grey in colour and often spotted in appearance due to the presence of cordierite porphyroblasts (Fig. 3.8a, b). Bedding is, in many cases, difficult to ascertain in the field as the biotite-rich units tend to develop a pervasive schistosity (see Chapter 4). However, in general, variations in colour, texture and mineral abundance within the schists indicate the original bedding (Fig. 3.8a and 3.9a).

The base of the Oberwasser Formation, dominated by quartz-biotite-schist, contains several centimeter-thick horizons of calc-silicate felses. These gradually thin, and give way to the more massive, commonly porphyroblastic quartz-biotite-cordierite schists forming the bulk of the Oberwasser Formation higher up in the succession (Fig. 3.7). These schists consist mainly of quartz (20-50%), biotite (30-50%), plagioclase (ca. 10%) and cordierite with some tremolite, muscovite, microcline and accessory apatite, allanite and sphene. Quartz, plagioclase and microcline often form polygonal grains, averaging 0.2 mm in diameter. Biotite laths are well-oriented, defining two schistositities, one significantly stronger than the other. Cordierite occurs as small grains (<0.05 mm) or as large, ovoid, poikilitic porphyroblasts up to 1.5 cm in diameter.

Centimeter-thick tremolite-rich units, often provide good marker horizons within the Oberwasser Formation. They are easily recognized by their pale-grey colour, weakly-developed schistosity and mottled texture (Fig. 3.9a). Tremolite, contributes up to 60% of their mineralogy, often forming acicular, radiating crystal aggregates, 0.5-2 mm in length (Fig. 3.9b). The preferred alignment of tremolite defines a schistosity, in places.

In the upper parts of the Oberwasser Formation, the schists show a marked increase in interbedded quartzitic and tremolite-rich units.

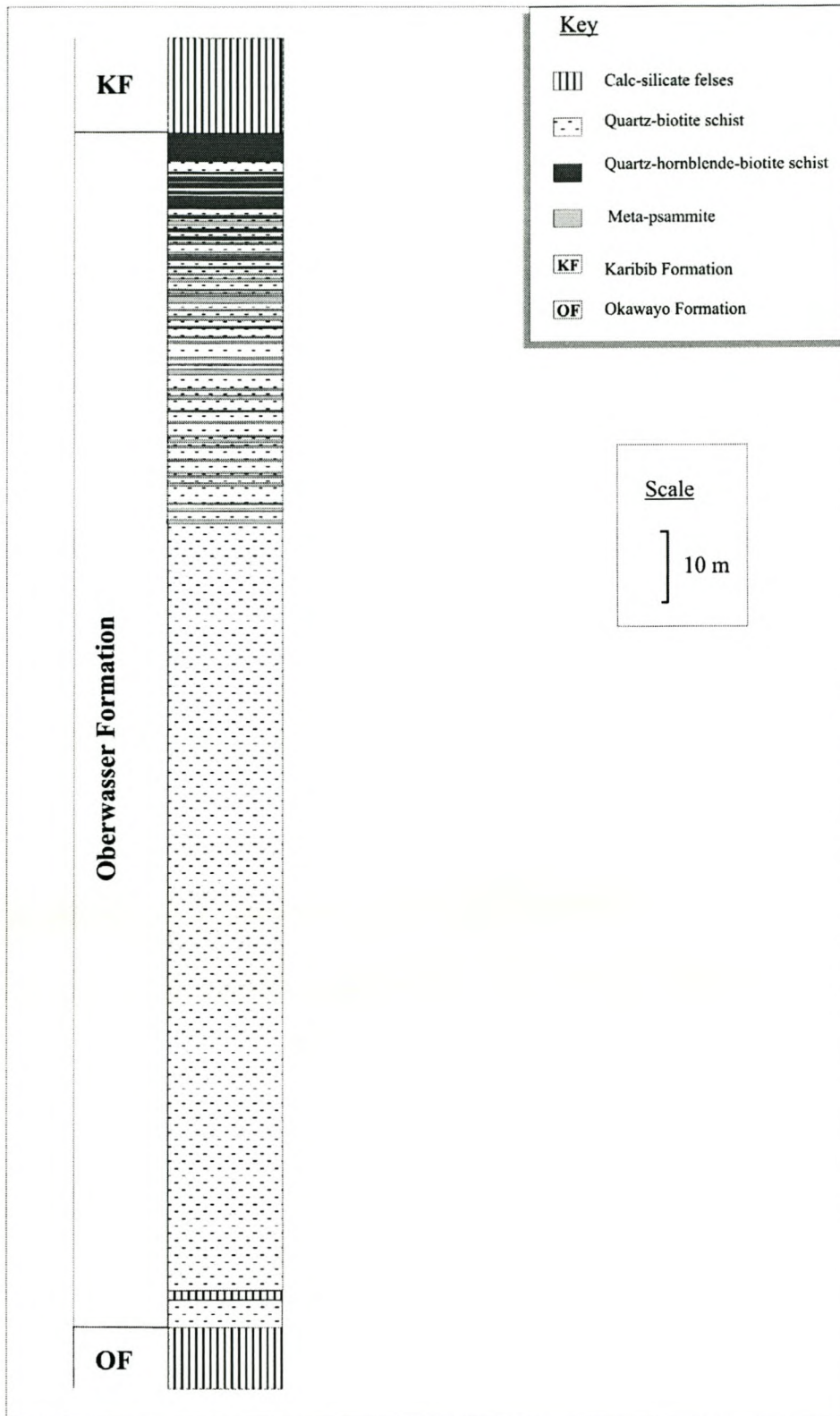


Figure 3.7 Synoptic stratigraphic section taken from the southeastern limb of the Usakos dome showing the main units comprising the Oberwasser Formation.

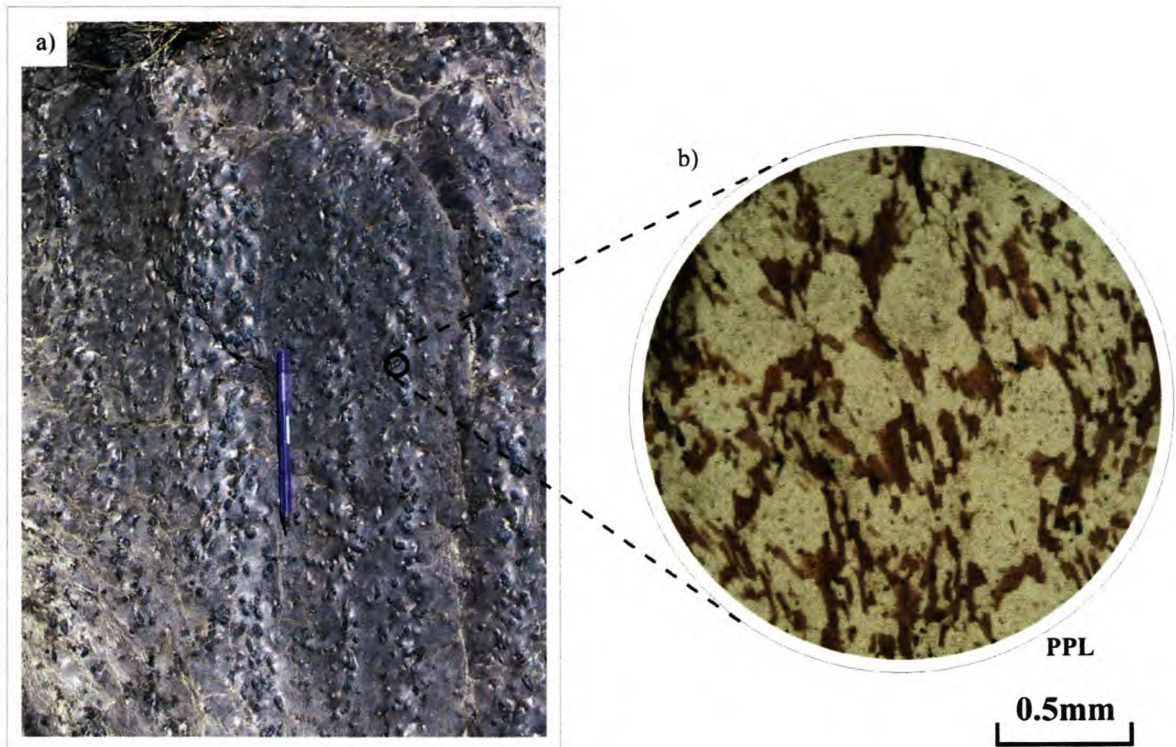


Figure 3.8 a) Quartz-biotite-cordierite schist from the Oberwasser Formation containing large, centimeter-sized cordierite porphyroblasts giving the rock a spotted appearance. The photograph is taken along the southwestern limb of the dome. The pen is aligned with bedding (and S1), which is defined by variable concentrations of cordierite. (b) Photomicrograph of a typical quartz-biotite-cordierite schist from the Oberwasser Formation. The large rounded and transparent grains are cordierite (ca. 0.4 mm), while the smaller brown and transparent minerals are biotite and quartz (\pm plagioclase) respectively. The biotite and quartz are preferentially aligned defining the schistosity.

An intermittent dark-green to black horizon, dominated by amphibole and often marked with white flecks, forms the Daheim member (Badenhorst, 1992). This reaches up to 40 m in thickness but may also be absent.

The hanging-wall contact of the Oberwasser Formation with the overlying Karibib Formation along the northwestern limb of the Usakos dome, is locally, developed as a 1-10 m thick breccia horizon. The breccia consists of biotite- and muscovite-rich clasts (ca. 2 cm in diameter) within a calcareous matrix. The discontinuity and appearance of this breccia renders its origin uncertain. Its relative position between the Karibib and Oberwasser Formations correlates with the Daheim member where it could represent a primary volcanic

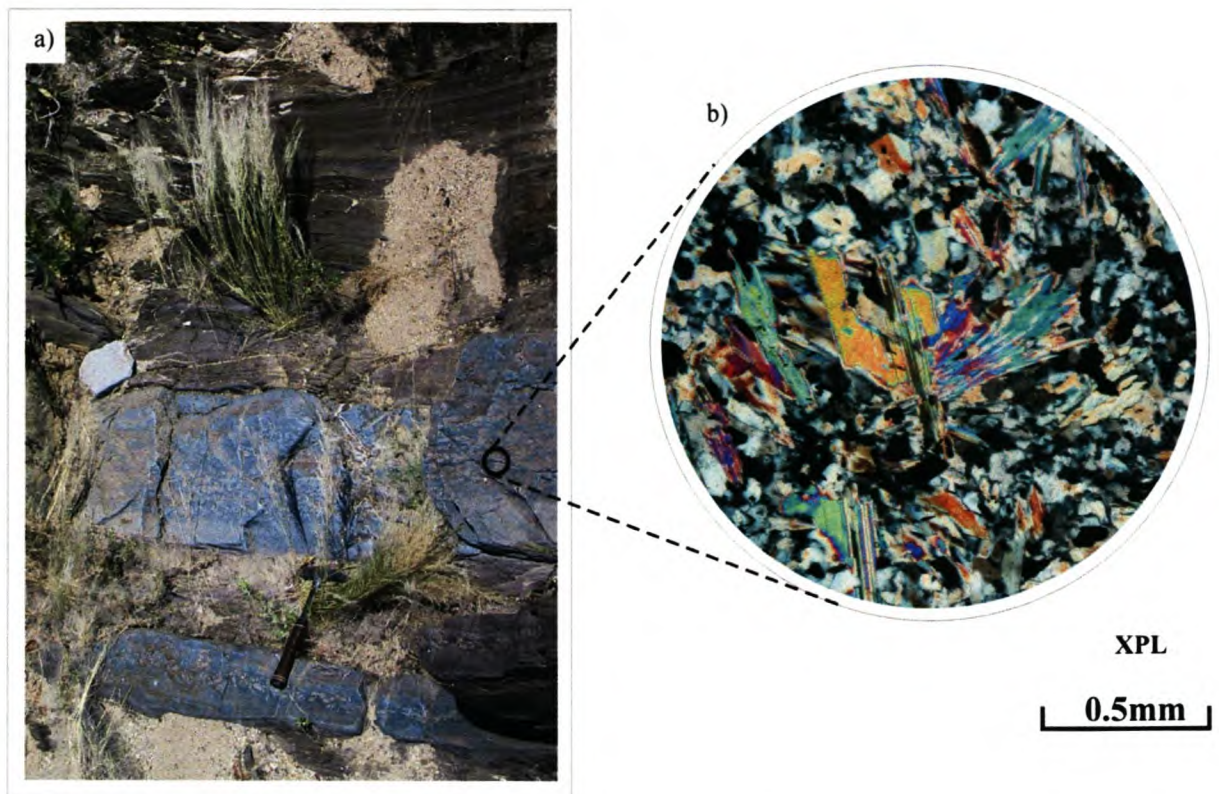


Figure 3.9 a) Photograph showing the contrasting dark-grey quartz-biotite schists (top) and the interbedded, pale-grey tremolite-rich horizons (center) of the Oberwasser Formation. The photograph is taken from the southeastern limb of the dome, facing southwest with a geological hammer for scale. (b) Photomicrograph from a tremolite-rich horizon, showing radial tremolite and quartz grains dominating the mineralogy.

breccia. However it may also correlate with the diamictites of the Ghaub Formation (Hoffmann et al., 2004).

3.3.6 Karibib Formation

The Karibib Formation is a thick, marble-dominated unit. It consists predominantly of calcitic and dolomitic marbles and banded, reddish-brown, calc-silicate-rich units and minor cordierite-biotite schists. The formation is exposed around the whole circumference of the Usakos dome, where it ranges in thickness between 0.5 km along the northwestern limb and 2 km along portions of the southeastern limb of the dome. These thickness variations are interpreted as a result of duplication through intense folding and deformation, discussed further in Chapter 4.

Deformation has obliterated primary features throughout much of the Karibib Formation, so that a correlation of marker beds throughout the Usakos dome is not possible. However, a few distinct tectono-stratigraphic horizons are recognized through most parts of the Usakos dome.

The most prominent horizons include:

- banded calc-silicate units;
- banded white and pale-grey calcitic marble units;
- white or cream-coloured dolomitic marble units;
- dark-grey marble units and;
- marble breccias.

A large proportion of the Karibib Formation is banded, comprising alternating layers of marble and calc-silicate felses (Fig. 3.10a, b). Individual layers in these units range between a few millimeters and 10 cm in width. The calc-silicate layers are brick-red in colour on weathered surfaces but vary between pale-green, light-grey and medium-grey on fresh surfaces. They comprise fine-grained diopside, quartz, K-feldspar, calcite, hornblende, actinolite, sphene, biotite and accessory tourmaline, pyrite, apatite and \pm magnetite. The pale-coloured layers within these banded rocks comprise medium- to coarse-grained calcitic marble.

Pale-grey, banded marbles are common, forming up to 900 m thick units within the Karibib Formation. The banding is defined by gradual variations in colour between white and light-grey calcitic marble. In places, the banding is closely-spaced (millimeters), giving the marbles a laminated texture (Fig. 3.11). These marbles contain minor muscovite, tremolite and dolomite.

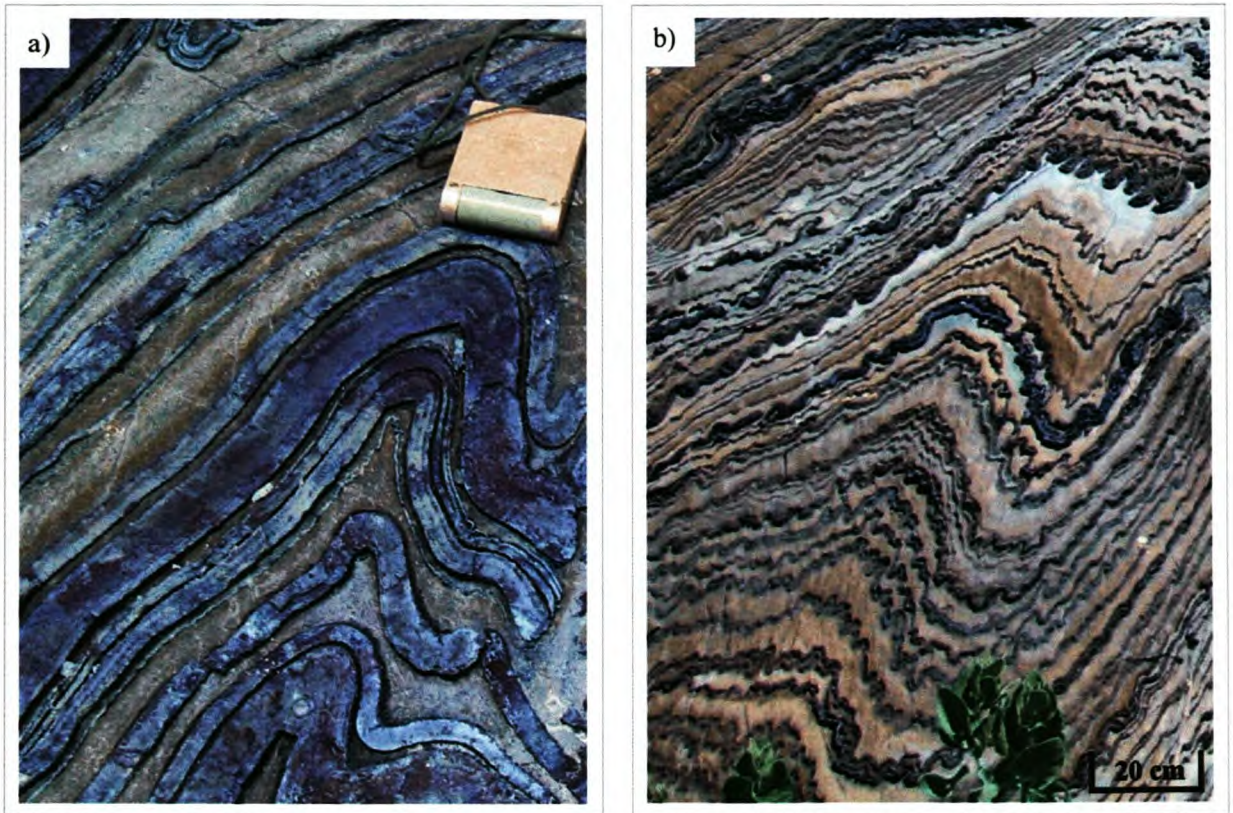


Figure 3.10 Banded unit of the Karibib Formation, (a) abundant in reddish-brown calc-silicate fels-rich layers and (b) rich in grey marble-rich layers with thin, interbedded calc-silicate felses.

Dolomitic marble, recognized by its cream-coloured weathered surfaces and its white, ‘sugary’-textured fresh surfaces occurs throughout the Karibib Formation, particularly in zones showing evidence of intense deformation (Fig. 3.1 and Fig. 3.12). Although dolomitic marbles may appear very similar to the white calcitic marble, the former is distinguished by the presence of quartz-tremolite veining and its relative insolubility in dilute hydrochloric acid. It is significantly harder and resistant to weathering than calcitic marble, and thus, commonly forms 0.5 to 5 m high ridges. The grain size is variable, from medium- to coarse-grained, and well-annealed, polygonal grains are distinctive of these marbles.

Quartz-tremolite veining within dolomite stains the surface of the dolomite brown, giving it a rough and pitted appearance (Fig. 3.12a, b).

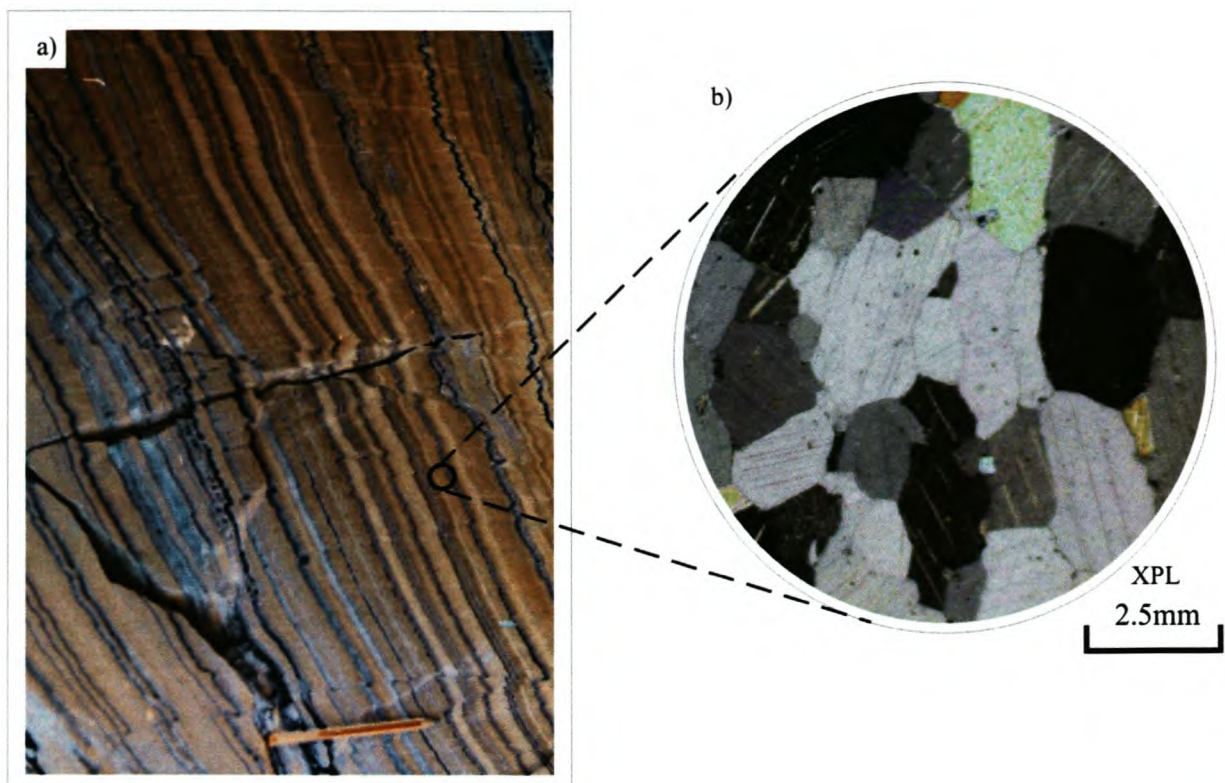


Figure 3.11 a) Banded white and grey calcitic marble from the Karibib Formation, pen for scale. (b) Photomicrograph of the calcitic marble. Note the polygonal, well-annealed grain shape of the calcite.

Dark-grey marbles form prominent marker horizons within the Karibib Formation (Fig. 3.1 and 3.2). They range in thickness from a few centimeters, for example along the northwestern limb of the dome, up to 130 m, for example along the southeastern limb of the dome, consisting mostly of calcite, interstitial dolomite and muscovite. The grey colour of the marble is attributed to microscopic grains of graphite scattered within and around the calcite grains.

Sedimentary marble breccias, 0.5-3 m in thickness, occur interbedded within the banded white and grey marbles. White or grey marble forms angular and commonly flattened clasts (Fig 3.12c), with aspect ratios ranging from 1:1 up to >20:1. In some highly strained areas, for example along the northwestern limb of the Usakos dome, the breccia horizons are not obvious and are interpreted as having been attenuated in to finely banded ribbon marbles.

3.3.7 *Kuiseb Formation*

The Kuiseb Formation is exposed along the northwestern limb and infolded within the southwestern termination of the Usakos dome. It is dominated by quartz-biotite-muscovite±cordierite schists (Fig. 3.13) with interbedded calc-silicate felses, marbles and psammitic units. Its thickness is uncertain as the upper contact is not exposed.

The base of the Kuiseb Formation comprises a ca. 15 m thick unit of brownish-purple, calc-silicate felses. These are overlain by a very thick succession (>200 m) of predominantly quartz-biotite-muscovite±cordierite schist. The fine- to medium-grained schists often preserve primary features such as bedding, lamination and cross-lamination, typical of a turbiditic depositional environment (Figs. 3.13a and 3.14) and, in places, cordierite porphyroblasts give the unit a spotted appearance. Four prominent grey calcitic marble horizons, ranging between 1 and 4 m in thickness are interbedded within the schists. Numerous meta-psammitic horizons (0.2-1 m thick) locally containing garnet porphyroblasts are also common. Progressively higher up the sequence (ca. 1 km), the schists increase in grain size becoming medium- to coarse-grained. Here, large, ovoid cordierite porphyroblasts (0.5-3 cm in diameter) are common. The preferred alignment of muscovite and biotite defines a schistsity within the Kuiseb schists, (Fig. 3.13b). The Kuiseb Formation is intruded by abundant granite and pegmatite dykes and sills. The pegmatites are locally mined for gemstone-quality tourmaline.

3.4 Intrusive Rocks

3.4.1 *Granitic and pegmatitic intrusions*

The Damara Sequence within the study area has been intruded by numerous granitic and pegmatitic intrusions. These are described separately in Chapter 5.

3.4.2 *Dolerite dykes and sills*

The Damara Sequence is transected by mainly northeast-trending Karoo-age dykes (Steven, 1983). These form 0.5 to 7 m wide, dark-brown to black ridges reaching up to several kilometers in length. Dolerite dykes post-date the Damaran Orogeny and are thus not discussed in any further detail.

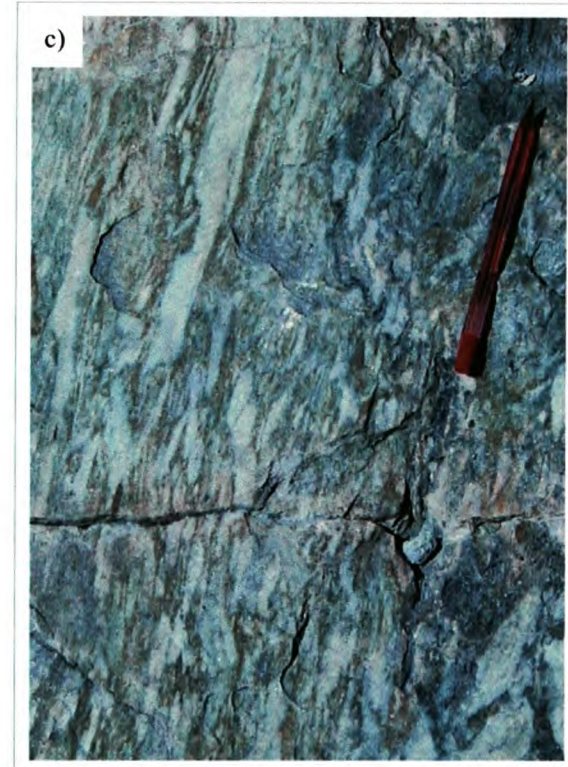
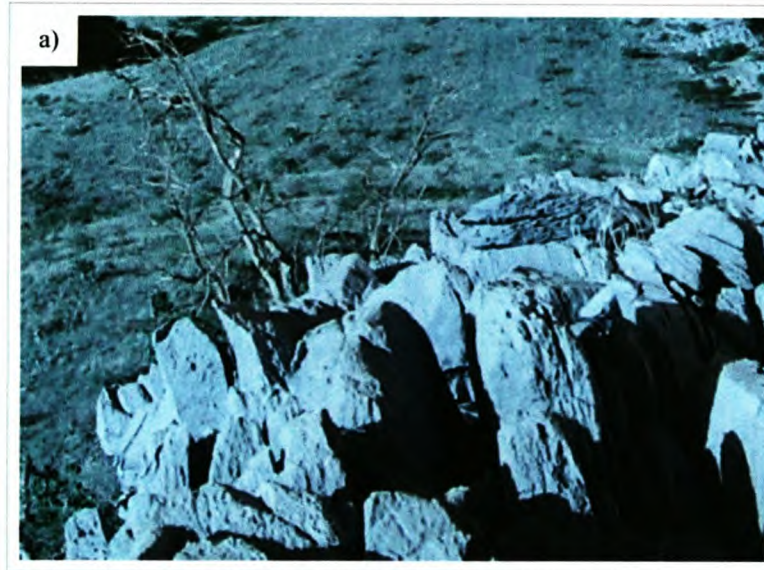


Figure 3.12 a) Photograph showing an outcrop of dolomitic marble from the Karibib Formation taken along the northwestern limb of the Usakos dome. The marble has a creamish-brown colour on weathered surfaces but appears bright white on a fresh surface. (b) Quartz+tremolite veining is common within the dolomitic marble, where tremolite laths may reach several centimeters in length often developed as radial aggregates. Taken facing vein surface (c) Marble breccia horizon of the Karibib Formation. Both the matrix and the clasts within these breccias comprise calcitic marble. The marble breccia horizons are best preserved within the low stain domain, along the southwestern closure of the Usakos dome.

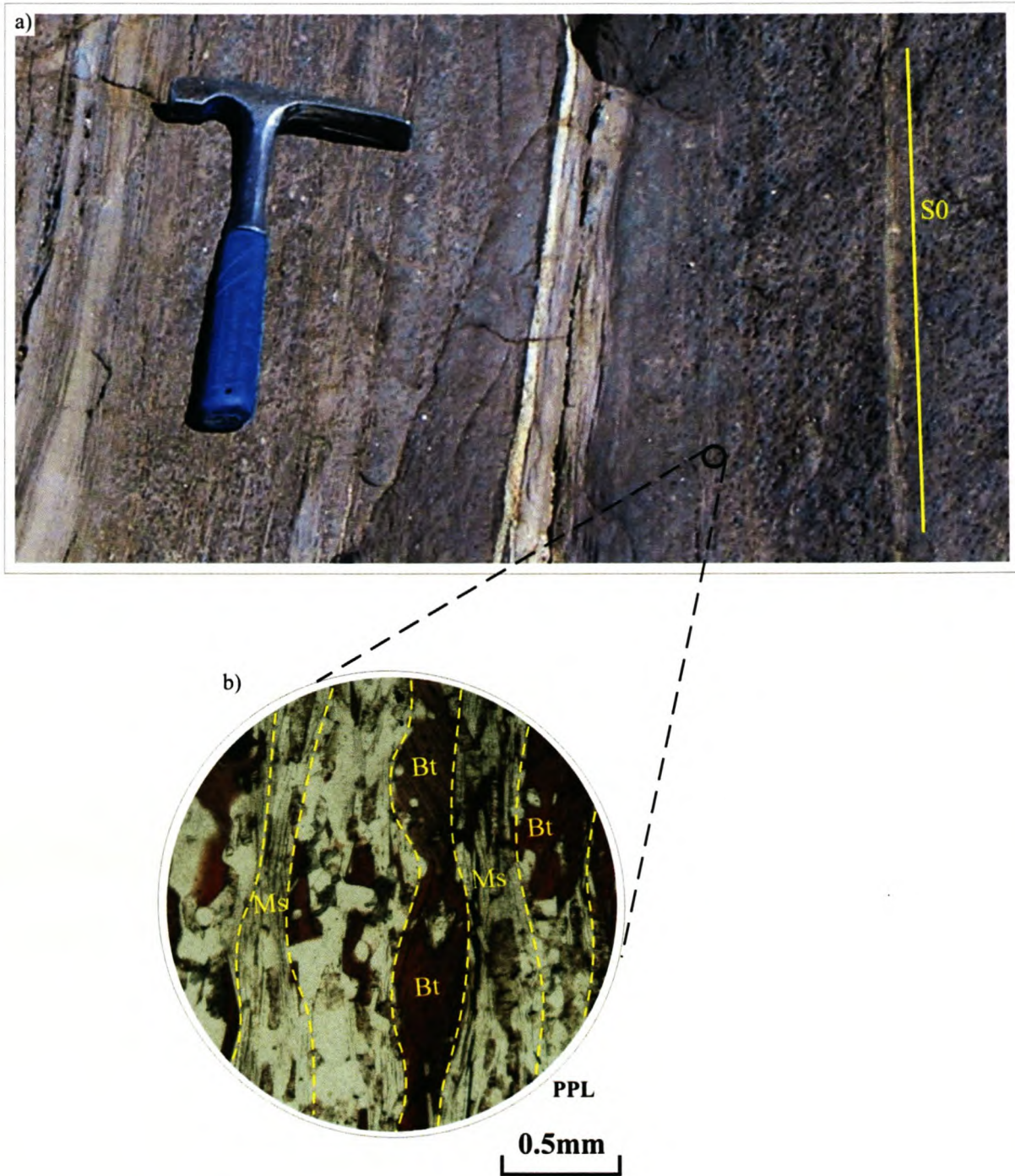


Figure 3.13 a) Quartz-biotite-muscovite-cordierite schist of the Kuiseb Formation. Cordierite porphyroblasts give the schist a spotted texture, for example on the right-hand-side of the picture. (b) Photomicrograph of a quartz-biotite-muscovite schist from the Kuiseb Formation. The preferred orientation of muscovite (Ms) and biotite define a foliation (dashed line).

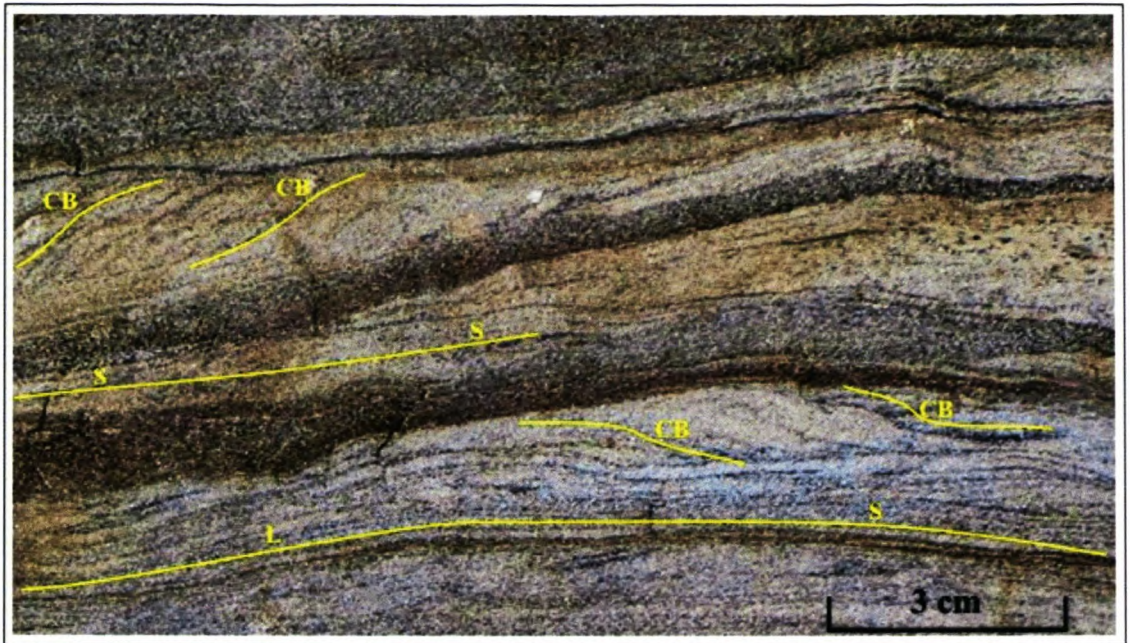
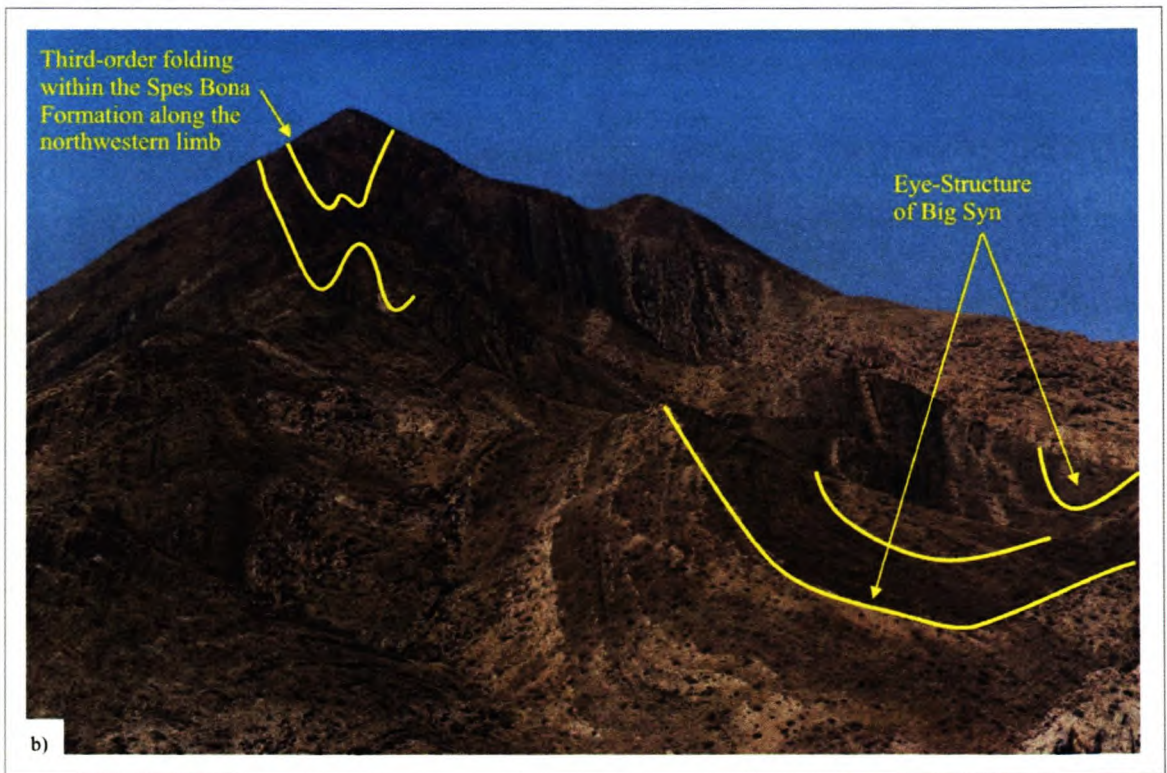


Figure 3.14 Fine-grained turbiditic units within the Kuiseb Formation exhibiting laminated bedding (S) and cross-bedding (CB). Photo is taken along the northwestern limb of the Usakos dome.



CHAPTER 4: STRUCTURAL GEOLOGY

4.1 Introduction

The Usakos dome is a 22 km long and 6 km wide, northeast-trending antiformal structure (F2a) situated some 2 km east and southeast of the town Usakos (Fig. 1.1). It can be divided into two northeast-trending lobes separated by a northwest-trending axial depression here referred to as the 'Tsawichas depression'. For structural maps and interpretation of the 'northeastern lobe of the Usakos dome' the reader is referred to Kisters et al. (2004) and references therein. This chapter focuses on the structural geology of the southwestern lobe of the dome. The main structural elements referred to in the following are summarized in Table 4.1 and discussed briefly below.

Based on cross-cutting and relative age relationships between the main fabric elements within the Damaran sequence, two main deformation phases, D1 and D2, could be identified. The structures formed during D2 display a progressive deformational event, and can thus be differentiated into early-D2 and late-D2 deformation. Structural elements with the prefix 'early', developed during the initial phase of D2 deformation (early-D2), while those with the prefix 'late', developed during the final D2 deformation phase (late-D2).

4.2 Primary Bedding (S0)

Formations of the Damara Sequence within the Usakos dome show definite lithological variations enabling easy recognition of the major stratigraphic units in the field, as well as on aerial photographs and LANDSAT images (Fig. 1.1). The Okawayo, Oberwasser and Karibib Formations can be followed with particular ease along the limbs of the dome where they show a consistent northeast-southwest strike extent.

Figure 4.1 a) Disharmonic meter-scale folding (F2d, Table 1) observed within the banded marbles and calc-silicate felses of the Karibib Formation along the southeastern limb of the dome. (b) Hundred meter-scale folding (F2b) developed within the Spes Bona Formation within the core of the dome. The large fold covering the right-hand-portion of the photograph defines an 'eye-structure' in plan view, forming the northeastern exposure of Big Syn. Bedding-parallel sheets of leucocratic granite (pale-brown in picture) are folded together with the metasedimentary rocks. The steep-sided ridge (Kransberg mountain) on the left-hand-side of the photo comprises Spes Bona Formation exhibiting tens-of-meter scale folding. Yellow line represents bedding (S0).

Table 4.1. Summary of the main fabric elements observed within the study area.

Deformation Phase	Fabric	Field expression, occurrence and orientation of fabric
Primary	S0	Primary bedding. Identified by variations in composition, grain size and colour of the rock. Defines the form of the dome structure. Orientation varies from place to place.
D1: early low angle shearing	S1	Bedding-parallel schistosity evident within metapelitic units.
D2: northwest-southeast-directed contraction during the collision of the Congo and Kalahari cratons (ca. 550-540 Ma)	Early-S2	Sub-vertical, northeast-trending foliation defined by steep, southeast dipping schistosity within metapelites and S0/S2 transposition domains within marble-rich units.
	Late-S2	Subhorizontal foliation observed within metapelitic and granitic units. This fabric is confined to the core of the dome.
	<u>Early-F2 folds</u>	Northwest-verging, doubly-plunging folds.
	Early-F2a	First-order antiformal structure of the Usakos dome. Measuring kilometers in half wavelength.
	Early-F2b	Second-order fold structures. Half wavelengths measure between 50 m and 1 km.
	Early-F2c and d	Parasitic folds within and parallel to lower-order fold structures. F2c folds are characterized by half wavelengths between 5 and 50 m, while F2d folds contain half wavelengths of < 5 m.
	<u>Late-F2 folds</u>	Northwest-trending folds.
	L2a	Mineral preferred orientation. For example hornblende, and/or cordierite and/or quartz. Common throughout the dome particularly developed along S2 surfaces within metapelitic-rich units. These lineations predominantly plunge $\pm 60^\circ$ towards the northeast, east and southwest.
	L2b	Plunge of the fold hinges of F2c and d folds. Predominantly towards the northeast or southwest (except parts of Domain E).
	L2c	Intersection lineation between S0, S1 and S2

Towards the southwest, the formations are folded around the southwestern closure of the dome. Within the individual formations, preservation of internal bedding is highly variable, depending on the rock type and strain intensity.

Folding, boudinage and transposition of bedding within the formations is common, particularly along the limbs and southwestern termination of the dome. Bedding within the interior of the dome is largely dismembered by voluminous intrusive granitic sheets. However, isolated, in-situ screens of the Damaran Sequence occur between these sheets, preserving a 'ghost stratigraphy'.

4.3 Folding

Folding is one of the most characteristic and spectacular features of the Usakos dome (Fig. 4.1). Two main fold trends occur within the Usakos dome. Firstly, there are northwest-verging, non-cylindrical folds (early-F2). Secondly, there are northwest-trending folds with shallow axial planes (late-F2). The former predominate the overall structural grain of the area. Folding occurs at all scales, with structures ranging from millimeter to kilometer-scales (Fig. 4.1). The Usakos dome itself forms a large antiformal structure (F2a), containing numerous second-, third- and fourth-order folds (F2b, c and d) commonly trending parallel to and verging in the direction of the higher-order folds along which they occur (Fig. 4.2 and refer to Appendices II and III). F2b folds range between 50 m and 1 km in wavelength and are often accompanied by smaller, F2c (50 m to 5 m in half wavelength) and F2d folds (<5 m in half wavelength). The amplitude and wavelength of early-F2 folds largely depend on the rock type and strain intensity. Marble-rich units along the limbs of the dome generally form tight folds with high amplitudes in comparison to the siliciclastic-rich core of the dome where folds tend to be more open.

Relying on the well established stratigraphy of the Karibib District (e.g. Smith, 1966; Badenhorst, 1992; Kisters et al., 2004), assisted in easy recognition of the main rock formations. From this stratigraphy it became evident that the younging direction of

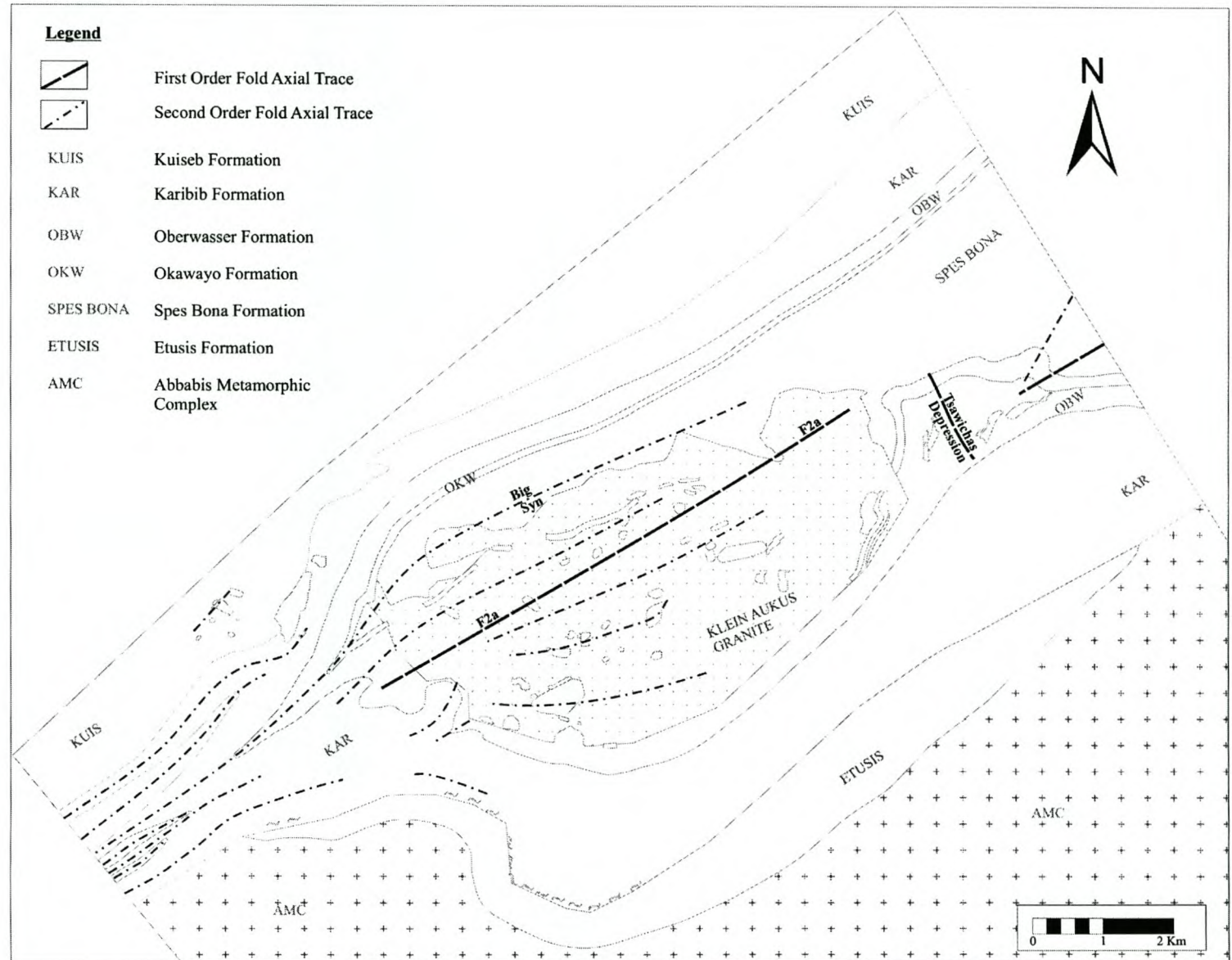


Figure 4.2 Simplified map of the Usakos dome showing the axial traces of the main first- and second-order folds.

bedding, particularly within the southwestern closure of the dome, is largely overturned, resulting in large areas of inverted stratigraphy. To describe and envisage fold geometries within these overturned domains, the following nomenclature is adhered to:

- An ‘anticline’ is a fold closing in any direction in which the oldest rocks occupy the core of the fold, whereas a ‘syncline’ is a fold where younger rocks occupy the core.
- A fold that is convex upwards is referred to as an ‘antiform’, and a convex-down fold is a ‘synform’.
- ‘Fold facing’ is the direction, normal to the fold hinge, along the fold axial plane, and towards the younger beds (Holdsworth, 1988).
- A ‘sheath fold’ is a fold with a hinge line variation of more than 90° (Ramsay and Huber, 1987).

4.4 Fabrics

Individual fabrics vary considerably in orientation and intensity across the Usakos dome. For that reason, while brief descriptions are provided below, more detail is included in the descriptions of specific areas later in the text.

.4.1 Foliation (S1)

Several types of planar fabrics can be distinguished within the Usakos dome. Based on cross-cutting relationships, there is evidence for an early-developed S1 foliation. This fabric is inconspicuous, but recognized within metapelitic units such as the Spes Bona, Oberwasser and Kuiseb Formations by a preferred orientation of bedding-parallel micas, mainly biotite but also muscovite. This fabric is particularly apparent within fold hinges where it can be easily distinguished from the more pronounced early-S2 foliation which cross-cuts the folded layer.

4.4.2 Foliation (S2)

Depending on the orientation and relative timing of formation, foliation (S2) fabrics have been sub-divided into early-S2 and late-S2. Early-S2 refers to the northeast-southwest-

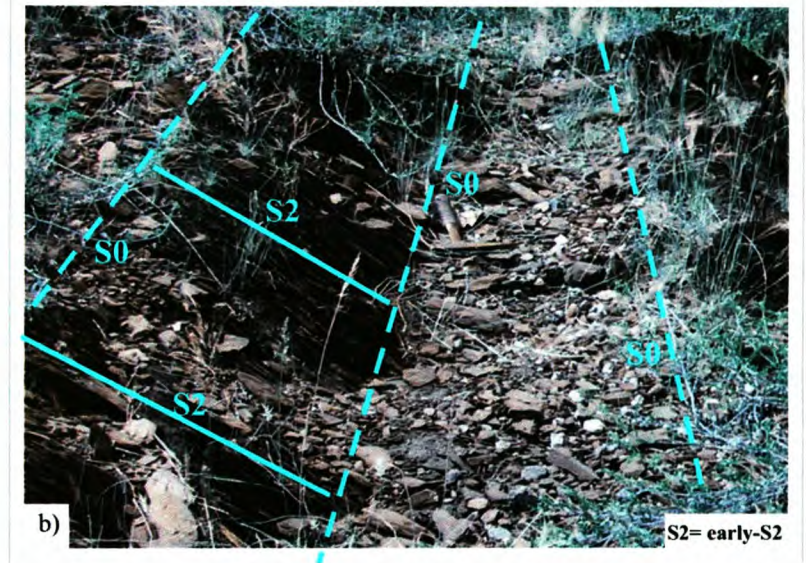
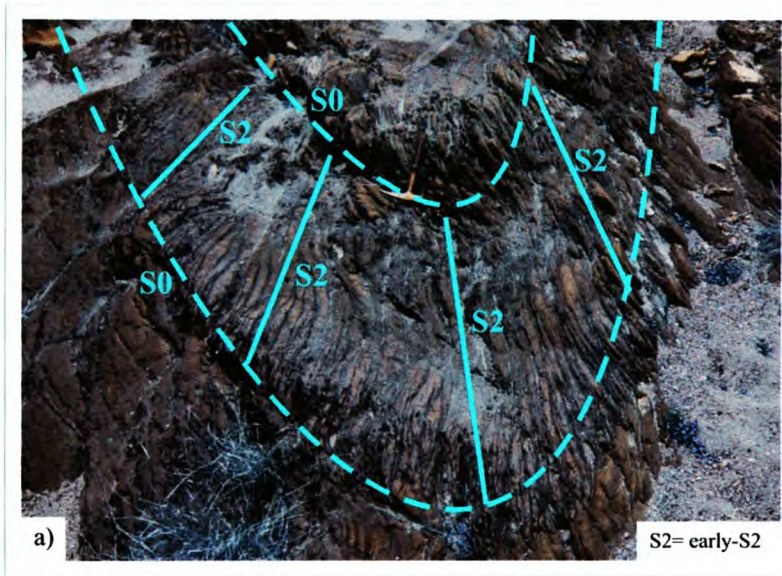


Figure 4.3 a) A fold hinge within the metapelitic units of the Kuiseb Formation exhibiting a prominent axial planar schistosity (early-S2), trending northeast-southwest. The picture is taken along the northwestern limb of the dome, facing northeast.

(b) Metapelitic unit of the Oberwasser Formation within the Tsawichas depression facing southeast along the northwestern limb of the dome. The metapelitic-rich units illustrate a well-developed schistose fabric (early-S2) at high angles to bedding (S0) within fold hinges.

(c) Gently southwesterly-dipping schistosity (late-S2) observed in the metapelitic units of the Obwerwasser Formation within the core of the dome.

trending, steep, often southeasterly-dipping foliation, oriented axial-planar to the first- and lower-order fold structures (early-F2) (Fig. 4.3a and b). Early-S2 fabrics are particularly prominent along the limbs of the Usakos dome. The late-S2 fabric refers to a less pronounced, gently-dipping to subhorizontal foliation that is particularly apparent within the central portion of the dome (Fig. 4.3c).

The majority of rock types within the Usakos dome contain a penetrative S2 foliation. Within metapelitic units of the Chuos, Spes Bona, Oberwasser and Kuiseb Formations, S2 is defined by a strong preferred orientation of either biotite, muscovite, tremolite, flattened quartz grains or a combination of these. The spacing of this planar fabric within the metapelitic units is largely dependent on rock composition, where mica-rich lithologies contain a stronger, closer spaced schistosity compared to the more massive siliceous units (Fig. 3.4a). Within the marble-rich units of the Karibib, Okawayo and Kuiseb Formations, S2, like bedding, is defined by colour and grain size variations in the marble-rich and calc-silicate-rich units (Fig. 4.4). Along high strain zones, clasts of primary breccia horizons appear highly attenuated and/or feathered. These horizons along high strain zones often appear as finely banded/ribbon marbles. Transposition of original bedding (S0) into a schistosity (S0/early-S2) is common, particularly within the marble-rich units along high strain domains (Fig. 4.4a and b). Orientation diagrams of these fabrics are presented for specific subareas of the study area, later in this chapter.

4.4.3 Lineations (L2)

Mineral lineations (L2a) observed along foliation and bedding planes are defined by rod-shaped cordierite, elongate quartz or biotite aggregates (Fig. 4.5). Generally, these lineations plunge parallel to the plunge of early-F2 folds, i.e. towards the northeast, east and southwest.

Hinge lines of centimeter- to meter-scale folds form crenulations, defining a lineation (L2b), particularly within calc-silicate-rich units within the Okawayo, Karibib and Kuiseb Formations (Fig. 4.6). These L2b lineations plunge generally parallel to higher-order fold hinges along which they occur. Due to the doubly-plunging nature of many of the early-

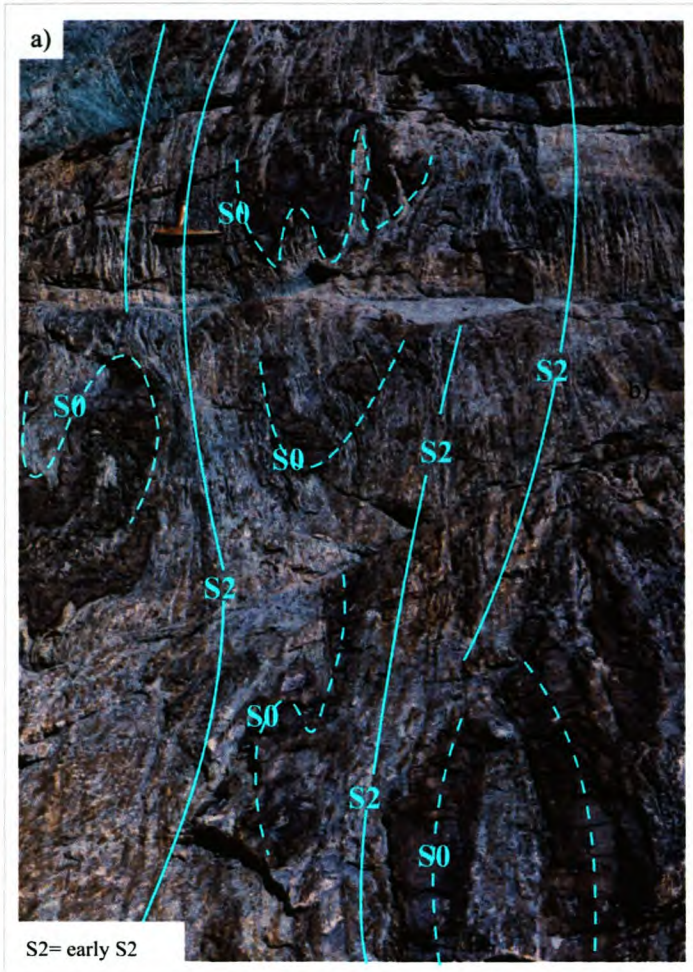


Figure 4.4 a) Typical transposition fabric (S0/S2) developed within the Karibib Formation. Relict bedding (S0) is only distinguished by the dismembered folding of the dark calc-silicate felses. The high strain S2 domains form the dominant fabric within these rocks. This photograph shows a plan view along the southwestern termination of the dome. (b) Photograph showing both bedding (S0) and early-S2 (S2) developed within the Karibib Formation. Bedding (S0) is preserved by the alternating marble and calc-silicate layers, while early-S2 forms the dominant fabric within the white marble-rich units. Bedding (S0) and early-S2 intersect at low angles. This picture is from a vertical section facing southwest, along the northwestern limb of the dome.



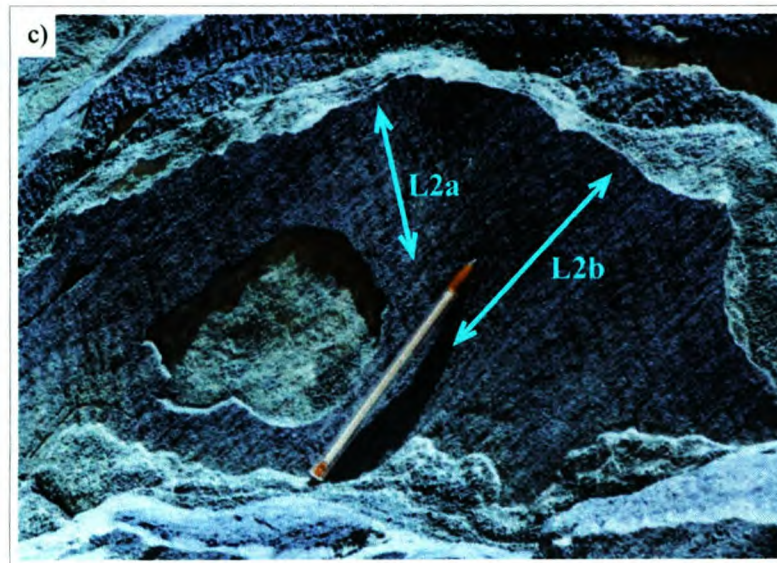
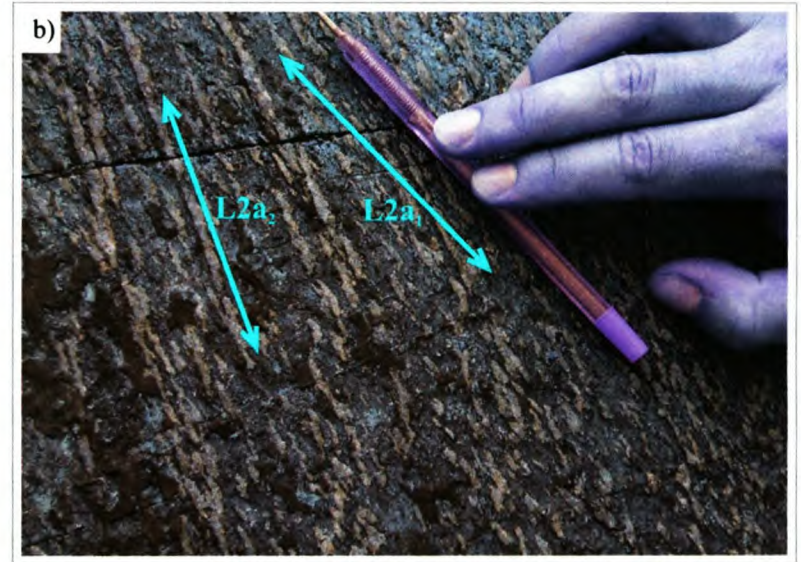


Figure 4.5 a) Stretched biotite aggregates observed on bedding/foliation surfaces within the Kuiseb Formation show a preferred orientation, thus defining a mineral lineation (L2a). (b) Photograph showing a contact surface between a sill of the Klein Aukas granite and the Oberwasser Formation from within the Tsawichas depression. The surface exhibits two quartz stretching lineations, labelled L2a1 and L2a2 (c) Photograph taken of a southerly-dipping bedding plane from the Okawayo Formation within the Tsawichas depression. Two sets of lineations are evident along the bedding surface, one crenulation lineation (L2b) plunging southeast, parallel to the pen, and a quartz stretching lineation (L2a) plunging down dip towards the south.

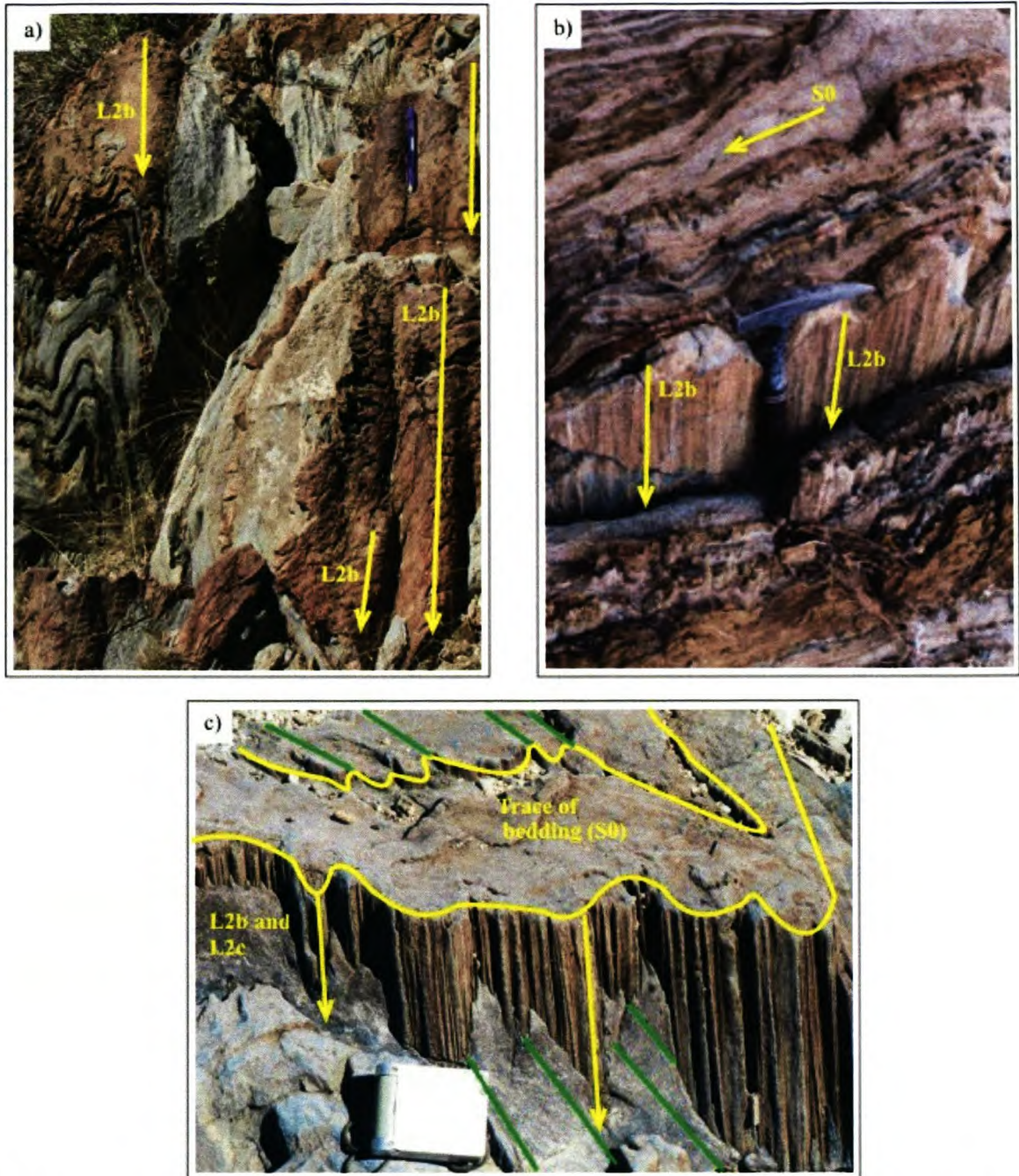


Figure 4.6 a) Mesoscale folds within the calc-silicate-rich units of the Karibib Formation show fold hinge lineations (L2b). The fold hinge lines (L2b) shown in this picture are undulating along strike, but generally plunge towards the southwest. (b) Centimeter-scale, steeply plunging L2b lineations observed within the Okawayo Formation taken from along the Tsawichas Depression. (c) Photograph showing an oblique view of a hinge zone of a northeast-southwest-trending, steeply-plunging fold within the Kuiseb Formation along the termination of the dome. The foreground shows a sub-vertical bedding plane containing a strong linear fabric. The fabric defines two parallel lineations, both a crenulation (L2b) and an intersection (S0/early-S2) lineation (L2c), steeply plunging towards the northeast. A trace of the early-S2 fabric is shown in green.

F2b and early-F2c folds, the L2b lineations plunge variably towards the northeast and southwest.

Intersections between S0 and/or S1 planes with S2 planes, define an intersection lineation (L2c). These lineations are particularly well developed within fold closures in siliciclastic-rich units of the Kuiseb, Oberwasser and Spes Bona Formations. They commonly plunge parallel to the F2b lineations towards the northeast or southwest.

Some northeast-trending, steeply-dipping metapelitic units, may present evidence for an intersection lineation between early-S2 and late-S2 foliation planes (L2c). These lineations are manifest on the better developed, early-S2 planes and are defined by biotite and/or muscovite laths, plunging moderately towards the northeast and east (Fig. 4.7).

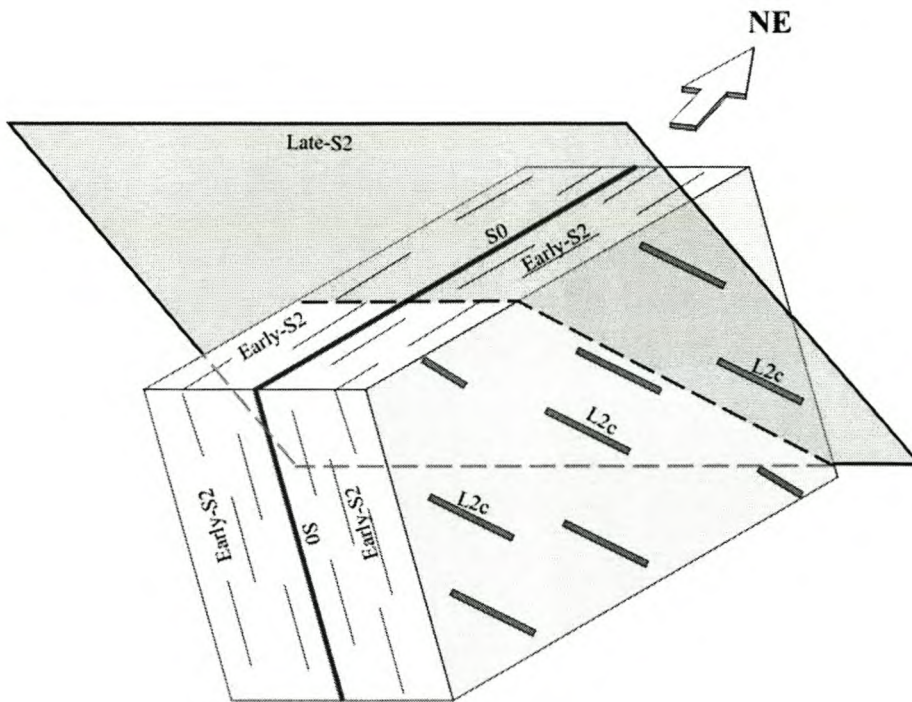


Figure 4.7 Schematic diagram illustrating the intersection lineation (L2c) formed at the junction between the steep, northeast-trending early-S2 fabric, and the shallow, northeast-dipping late-S2 fabric.

4.5 Sub-domains of the Usakos dome

4.5.1 Introduction

Given the variable strain intensities and orientation of structural elements within the southwestern lobe of the Usakos dome, a description in its entirety is difficult. As a result, the study area is divided into five sub-domains (Fig. 4.8) and the structural data obtained during fieldwork is analyzed for each.

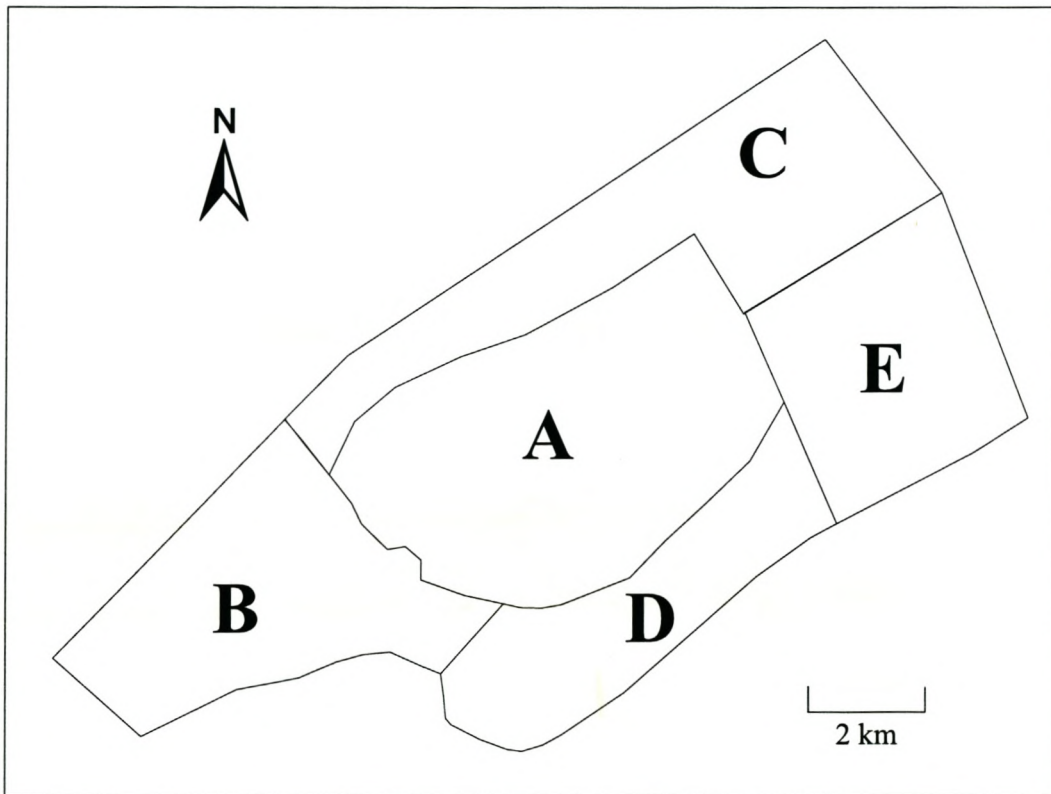


Figure 4.8 Map showing the selected domains of the field area.

The subareas are summarized as follows:

1. **Domain A:** The core of the dome.
2. **Domain B:** The southwestern termination of the Usakos dome.
3. **Domain C:** The northwestern limb of the dome, bounded to the northwest by the Kuiseb Formation and the Kranzberg Synform.
4. **Domain D:** The southeastern limb of the dome, bounded to the southeast by the Etusis Formation.
5. **Domain E:** The northeastern and southwestern lobes of the Usakos dome incorporating the “Tsawichas depression”.

4.5.2 Domain A

This central domain constitutes the core of the southwestern lobe of the Usakos dome. It is set within a topographically low-lying area, surrounded by ridges that correspond to the limbs of the dome. A significant proportion of this domain is covered by recent alluvial material, such as calcrete terrace deposits and unconsolidated sands and gravels. However, exposures of Damaran rocks indicate that ca. 70% of the dome core comprises leucocratic granite and pegmatites (Fig. 4.9). These intrusives form branching and coalescing sheets described in further detail in Chapter 5. In places screens of the Damara Sequence occur between neighbouring granitic sheets, forming the remaining 30% of Damaran rocks exposed within the dome core. These screens comprising marbles, meta-psammities and metapelites vary from a few meters to hundreds of meters in length and contain sharp contacts with the granite. Despite being enclosed by granite, the screens appear in-situ, following the structural trend of the surrounding Damara Sequence. This allows for the original metasedimentary sequence to be traced within the granite, preserving a ‘ghost stratigraphy’ (Pitcher, 1970).

The Okawayo Formation provides a particularly good marker horizon within the granite-rich core of the dome, defining various second-order fold structures (Fig. 4.9). Along the northwestern limb of the Usakos dome, bedding of the Okawayo Formation dips between 80 and 85 ° to the southeast showing an extremely linear strike extent, which is seemingly unaffected by second- and third-order folding. Towards the

southwest, however, the Okawayo Formation closes around the hinge of a large second-order fold structure, named 'Big Syn' (Fig. 4.9).

Big Syn is a northeast-trending fold cored by the Spes Bona Formation and rimmed by progressively younging lithologies (Fig. 4.9). It extends for ca. 8 km along strike, reaching 1.5 km in half wavelength. Although bedding (S0) is, in places, obscured by sheeted granite and a pervasive schistosity (early-S2), variations in fold shape are evident along the strike extent of Big Syn (Fig. 4.10a). In the northeast, Big Syn is manifest as an 'eye-structure' (Fig. 4.10). This eye-structure is bisected along strike by the late-F2 axial plane (Fig. 4.10b). On the northeastern limb of the late-F2 fold, Big Syn is manifest as an anticline, whereas along the southwestern limb, Big Syn displays a synformal fold geometry which is cored by the oldest lithologies, thus portraying a synformal anticline (Fig. 4.10). Along the southwestern hinge of Big Syn, bedding (S0) dips 60-80° towards the northeast, indicating a moderate- to steep, northeasterly fold plunge (Fig. 4.12a), and intersection lineations (L2c) between S0 and S2 similarly plunge towards the northeast/east. Parasitic second- and third-order folds within Big Syn range from 10's to 100's of meters in half wavelength. These form northeast-trending, northwest-vergent, tight-to isoclinal folds with undulating hinge lines (Fig. 4.1b).

Further into the core of the dome, the metapelites of the Spes Bona and Oberwasser Formations are pervasively inundated by granite. In places, only thin slivers of siliciclastic rocks (1 cm to 2 m wide) are exposed between granite sheets. Discrimination between the lithologically similar units of the Spes Bona and Oberwasser Formations is therefore often difficult. The calcitic marbles and calc-silicate felses of the Okawayo Formation, however, form a particularly good marker horizon within the granitic core of the dome, where they seem to form relatively unfavorable horizons for the intrusion of granites. The thickness of the Okawayo Formation reaches up to 40 m within the core, but is largely dependent on the outcrop conditions. Exposures of the Okawayo Formation interpolated within the core of

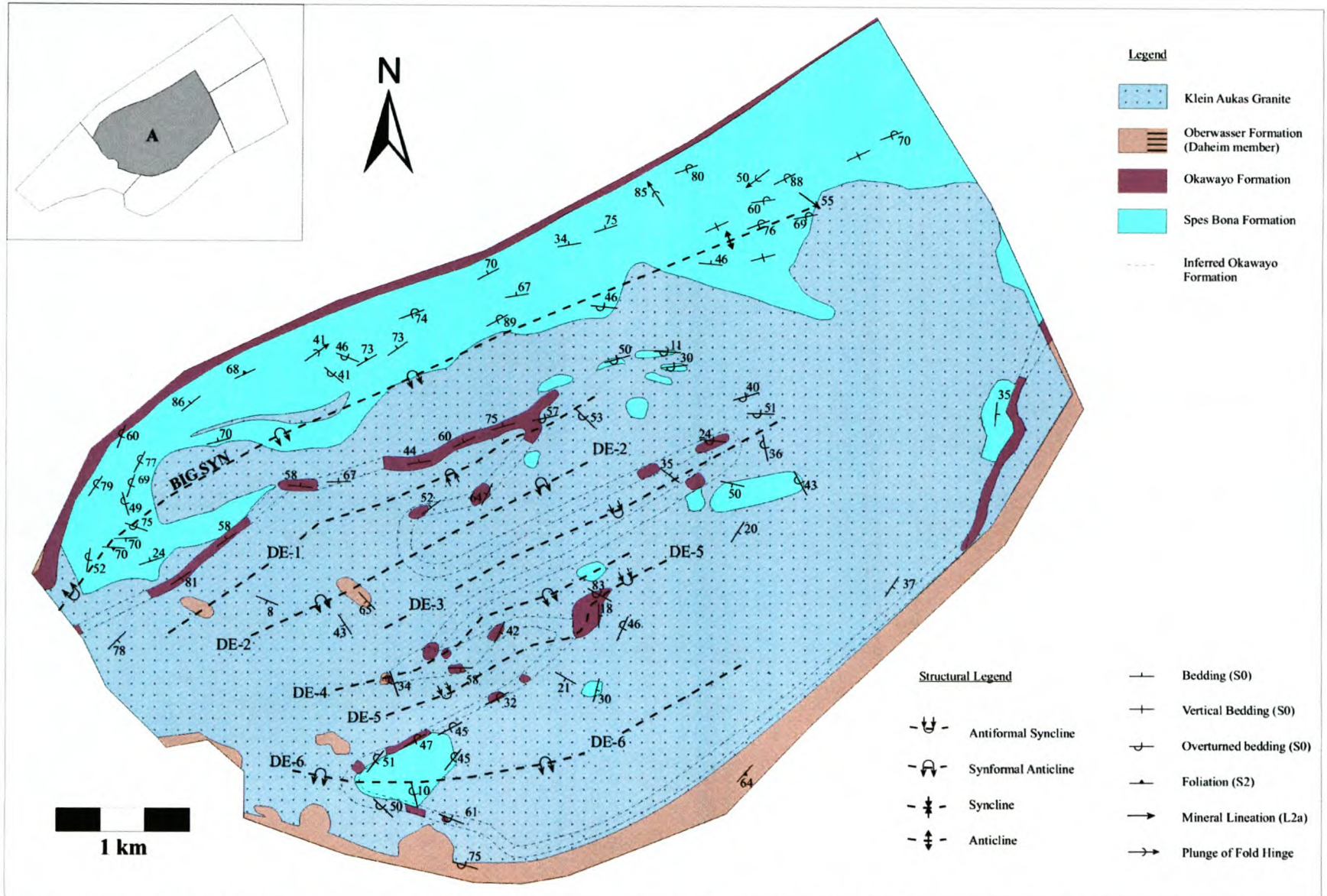


Figure 4.9 Structural Map of Domain A. (Note: bedding readings appearing within the Granite were taken from small screens of the Damara Sequence that have been omitted from the map for clarity).

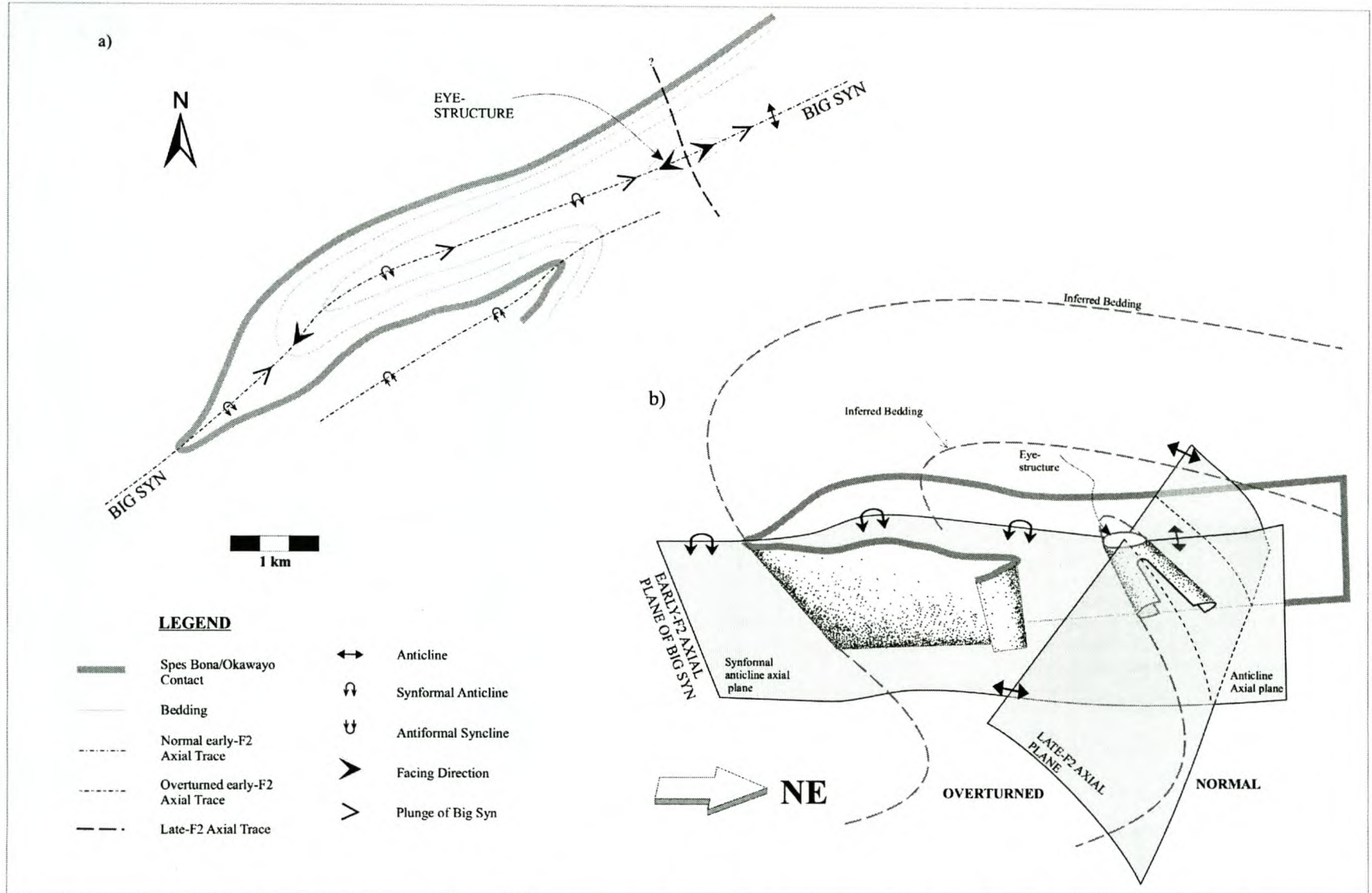


Figure 4.10 a) Schematic sketch of Big Syn in map view, showing the along-strike variations in fold shape, facing and plunge directions supported by lithological contacts and bedding (S0). See Appendices II and Fig. 4.9 for the locality of Big Syn with respect to the rest of the Usakos dome. (b) Schematic 3-D representation of Big Syn showing both the early-F2 and the late-F2 axial planes. Bedding and fold geometries on the southwestern limb of the late-F2 fold appear overturned, while those on the northeastern limb appear normal.

the dome delineate at least six second-order fold hinges. The folds trend northeast with open- to tight interlimb angles and northeasterly-plunging fold hinge lines. They are referred to, from northwest to southeast, as DE-1 to DE-6 (Fig. 4.9).

Consistent dips and strikes of bedding within screens of the Damara Sequence define a northeast-trending fold situated southeast of Big Syn which is referred to as DE-1. The antiformal fold shape and southwesterly fold facing of DE-1 indicates that it forms the corresponding antiformal syncline to Big Syn (Fig. 4.11). Bedding and lineation readings recorded from within the fold hinge are illustrated on equal area stereographic projections in Fig. 4.12b. Poles to bedding planes plot along a great circle indicating a shallow, northwesterly-plunging fold axis. Bedding planes measured along the limbs of fold DE-1 dip moderate- to steeply towards the northwest and west, while bedding planes measured along the fold closure dip towards the north and northeast. Additionally, on a meter-scale, bedding planes also appear buckled about several north- and northwest-plunging fold hinge lines (Fig. 4.12b).

Folds DE-2 and DE-4 are poorly exposed and thus, only inferred from the scattered outcrops. Both folds are interpreted to represent synformal anticlines (Fig. 4.11).

DE-3 and DE-5 represent antiformal synclines (Fig. 4.11). When illustrated on an equal area stereographic projection, poles to bedding planes recorded along these folds plot along small circles with cone axes plunging moderately towards the east (Fig. 4.12c, d). This distribution of poles along the small circles illustrates non-cylindrical fold shapes and northeasterly plunge directions for these folds. Fold hinge lineations of parasitic folds recorded from DE-3 and DE-5 plunge shallow- to moderately towards the east-southeast and south-southwest respectively (Fig. 4.12).

DE-6 forms yet another overturned fold structure developed within Domain A showing marked similarities to Big Syn (Fig. 4.11). It is a synformal anticline that faces southwest and plunges ca. 50 ° towards the northeast.

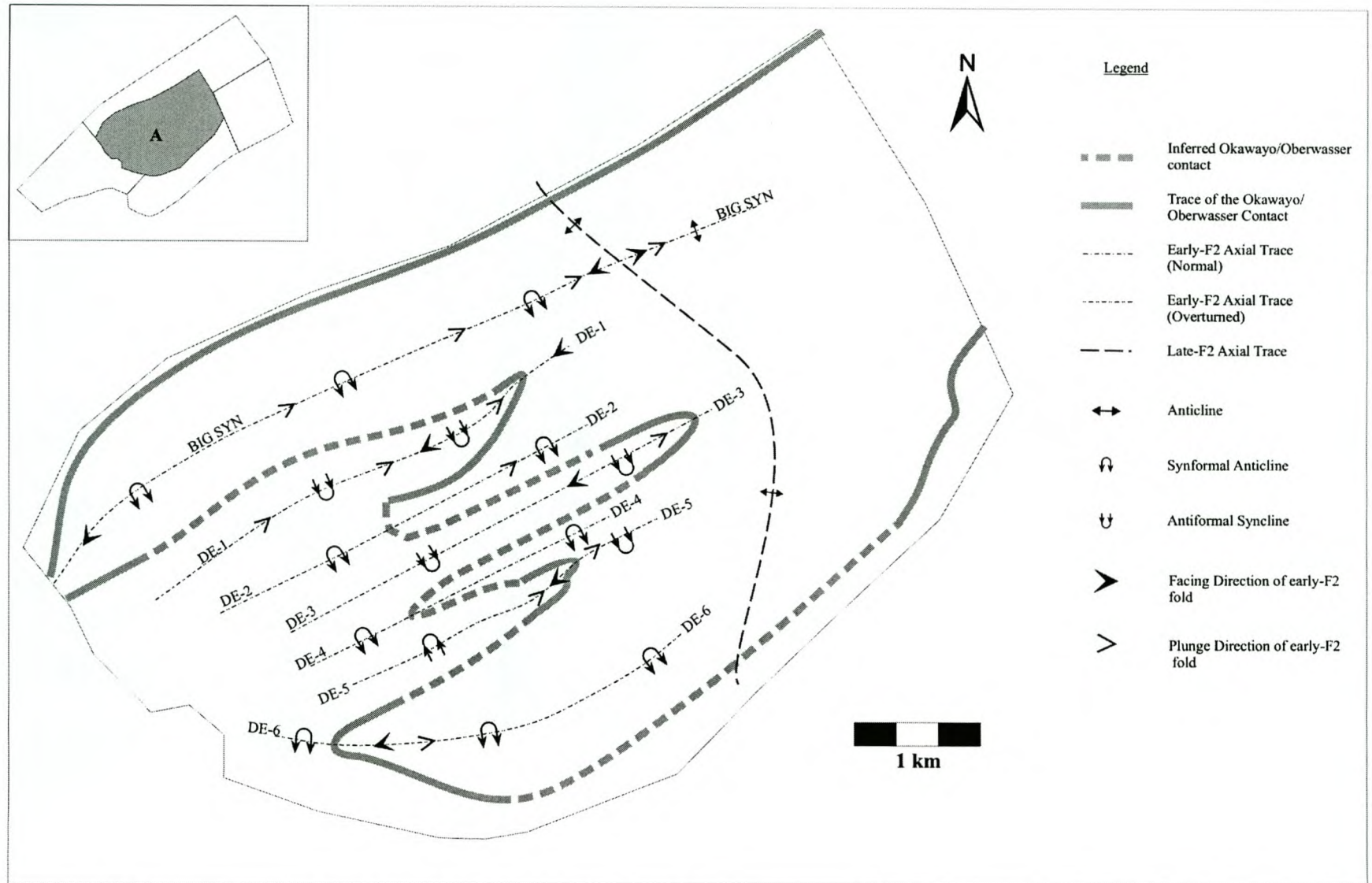


Figure 4.11 Schematic map of Domain A sketching the main fold axial traces, facing directions and plunge directions of early-F2 and late-F2 folds identified in the field.

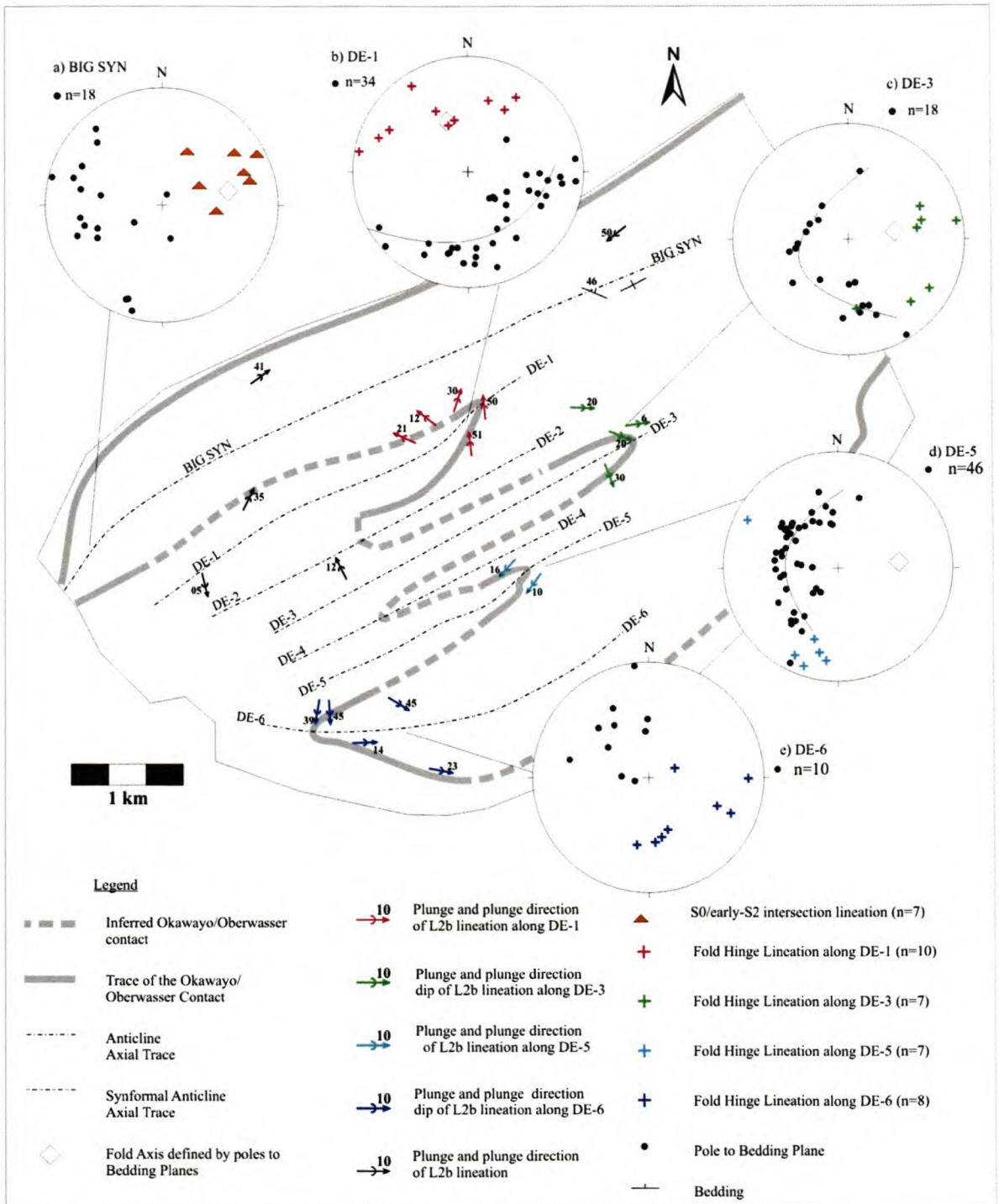


Figure 4.12 Schematic sketch of Domain A showing the orientation of structural data obtained from within screens of Damara Sequence within the granite-rich core of the dome. Equal area, lower hemisphere stereographic projections representing the orientation of bedding and L2b lineations are shown for the fold hinges of a) Big Syn, b) DE-1, c) DE-3, d) DE-5 and e) DE-6. The solid line within the stereographic projection represents the best-fit circle, a distribution described by poles to bedding. The distribution of poles along the small circles in c) and d) illustrates the non-cylindrical fold shapes and easterly plunge directions for these folds.

The schistosity (S2) (Chapter 4.4.2) within the metapelitic and granitic units in this central portion of the dome varies significantly. Foliation planes range from being steep northwesterly- or southeasterly-dipping (early-S2) to shallow, northeasterly- or southwesterly-dipping (late-S2).

Foliation planes, defined solely by the strong preferred orientation of mica in the metapelites, are shown on a stereographic projection in Fig. 4.13b. Generally, the steeply-dipping, early-S2 fabric predominates closer to the limbs of the dome, while the shallow-dipping late-S2 fabric predominates within the central portions of the dome. Notably, early-S2 and late-S2 fabrics are developed at approximately right angles to one another.

When plotted on an equal area stereographic projection, it is evident that the majority of fold hinge lineations (L2b) within Domain A plunge shallowly towards the dome margins defining a radial pattern (Fig. 4.13a).

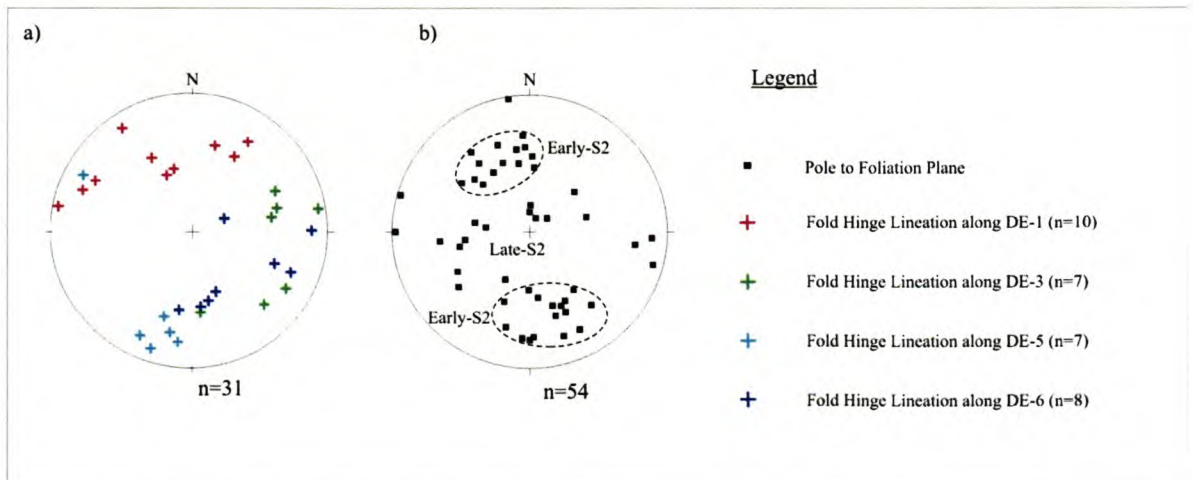


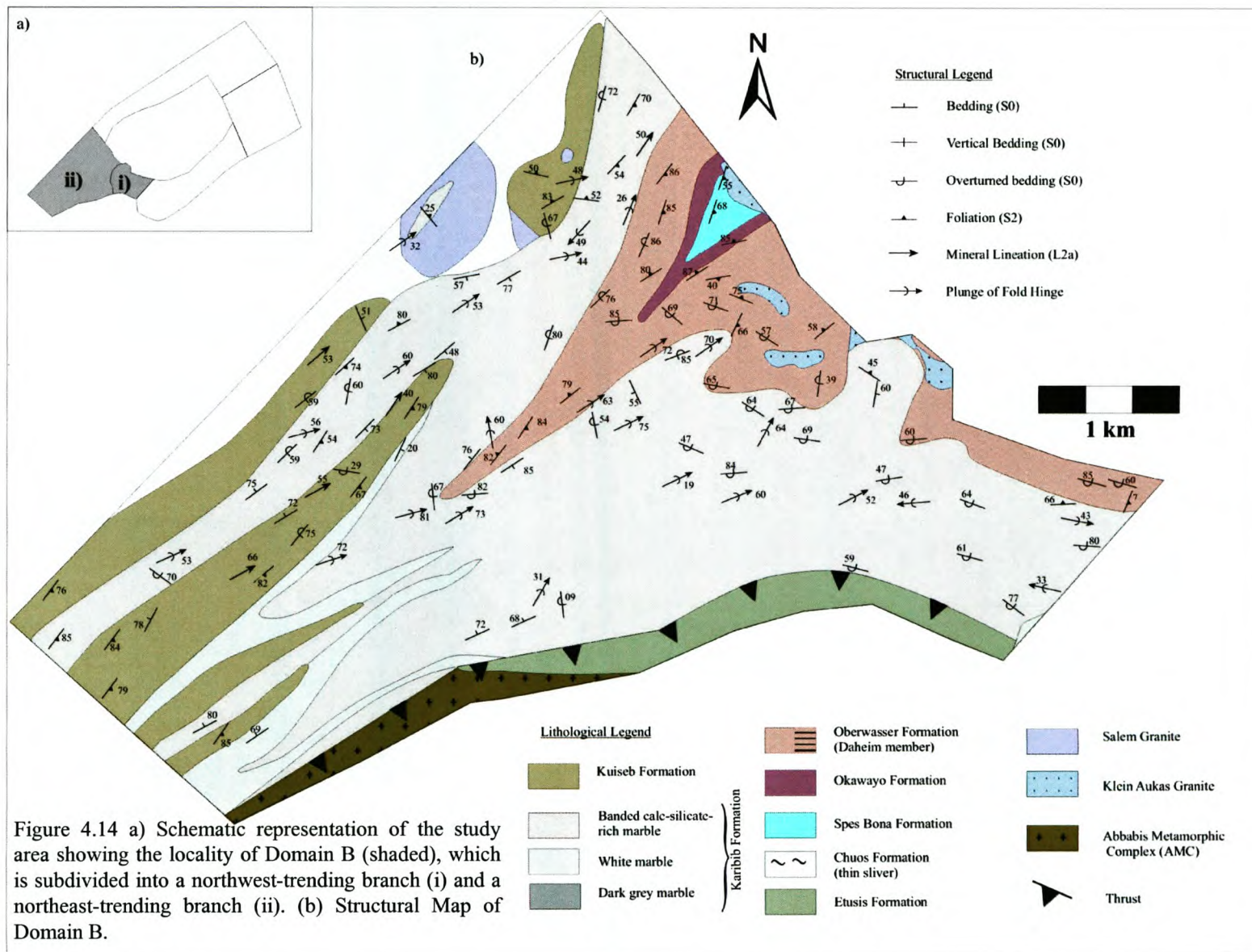
Figure 4.13 Equal-area, lower-hemisphere stereographic projections showing a) the radial pattern of fold hinge lineations (L2b) observed within the core of the dome, and (b) the variability in the orientation of foliation planes (Early-S2 and Late-S2) within the core of the dome. The closed dashed lines delineate the steeper northeast-trending Early-S2 fabric from the shallowly-dipping foliation (Late-S2) which is only observed within the core of the dome.

4.5.3 Domain B

Domain B incorporates the southwestern closure and termination of the Usakos dome. It can be subdivided into two sections based on significant variations in the orientation of structural elements such as bedding, foliation and linear fabrics. Firstly, a branch to the east is characterized by a northwesterly- and westerly-trending structural grain (see (i) in Fig. 4.14a). A second branch, trending northeast, is dominated by a northeasterly-trending structural grain (see (ii) in Fig. 4.14b).

Along the northwesterly-trending branch (i), bedding of the Karibib and Oberwasser Formations dips between 50 ° and 80 ° towards the north or northeast (Fig. 4.14b). As a result, the older rocks of the Oberwasser Formation overlie the relatively younger rocks of the Karibib Formation, so that the sequence is overturned. Much of the Karibib Formation along this northwest-trending branch comprises banded calcitic marbles and calc-silicate felses with interbedded marble breccia horizons (Fig. 3.12c).

Marbles within the northwest-trending branch of Domain B are folded into open, third- and fourth-order fold structures (F2c and F2d). These folds have axial traces that follow the closure of the dome (i.e. the basement-cover contact), assuming northwesterly and westerly trends, and plunge moderately towards the east or west (Fig. 4.15, 4.16a and c and 4.17a). Two foliations (early/late-S2), defined by the preferred orientation of biotite are described from metapelitic units (e.g. Oberwasser and Chuos Formations) along this branch of Domain B. Firstly, there is a closely-spaced, steep northwesterly- and southeasterly-dipping foliation oriented axial planar to the F2a dome structure, which is interpreted as an early-S2 fabric. Secondly, there is a faint, shallow southwesterly- and northeasterly-dipping schistosity, interpreted as a late-S2 fabric (Fig. 4.16b). The early-S2 fabric is particularly prominent close to the limbs of the dome, while late-S2 becomes particularly pronounced towards the core of the dome.



Along the northeast-trending branch of Domain B (see (ii) in Fig. 4.14) bedding and foliation fabrics resume a steep dip and a northeast-southwesterly trend (Fig. 4.14b). Likewise, the Etusis-Karibib Formation contact is northeast-trending, however, along strike towards the southwest, the Etusis Formation pinches out, resulting in the juxtaposition of the Karibib Formation and the AMC.

Lithological units along the northeast-trending branch of Domain B are tightly folded into northeast-trending, second-order folds (Fig. 4.15). These folds have upright- to steeply-dipping limbs and subvertical to steep northeasterly-plunging fold hinge lines (Fig. 4.14 to 4.16). They define tight to isoclinal fold shapes, between 250 m and 500 m in half wavelength with interlimb angles of 5 to 20°. One of the largest of these folds, Big Syn, is previously described as a synformal anticline (ie. an overturned anticline) in Domain A. This overturned fold geometry persists into Domain B, and at least four similar second-order synformal anticlines are exposed along the northeast-trending branch of Domain B (ii) (Fig. 4.15). These synformal anticlines have hinges closing towards the southwest and are cored by older lithologies (mainly the Karibib and Oberwasser Formations).

In between these synformal anticlines are corresponding antiformal synclines. These are also tight, upright folds with steep northeasterly-plunging fold axes. However, their hinges close towards the northeast and they are cored by younger lithologies (Fig. 4.15). The poor preservation of marker horizons in the Karibib Formation does not allow for a reliable correlation between folds along the northwest- and northeast-trending branches.

River valleys oriented perpendicular to the northeast-trending structural grain expose excellent vertical sections of these folds along the southwestern termination of the dome. These sections reveal dramatic variations in strain intensity due to significant competency contrasts between the marble-rich and siliciclastic-rich units. High strain intensities dominate the marble-rich units, which are characterized by a penetrative transposition of bedding (S₀) into a subvertical, northeast-trending foliation (early-S₂) (Fig. 4.18 and 4.19).

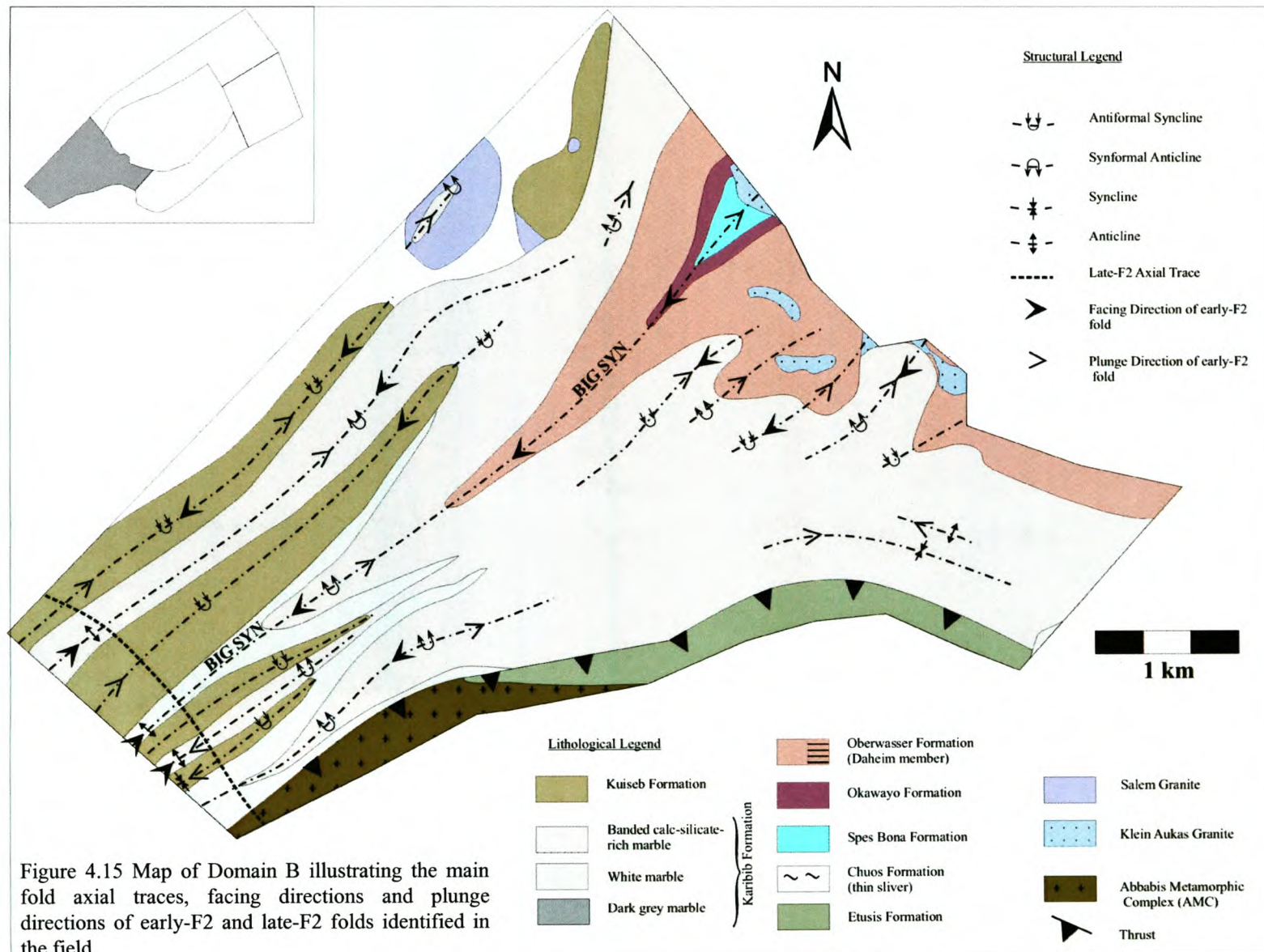


Figure 4.15 Map of Domain B illustrating the main fold axial traces, facing directions and plunge directions of early-F2 and late-F2 folds identified in the field.

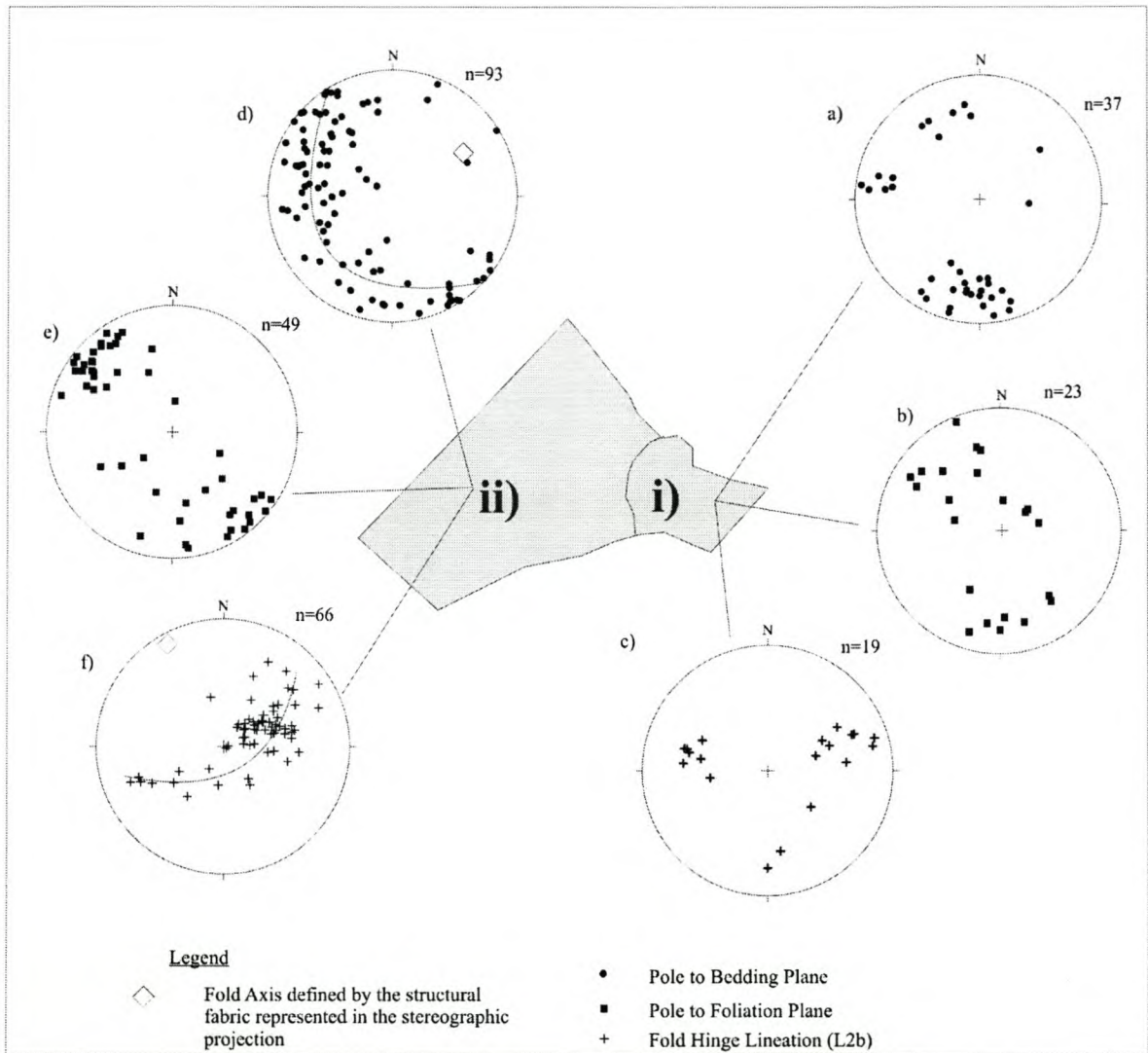


Figure 4.16 Outline of Domain B showing its northwest- and northeast-trending branches (i and ii respectively) and their relevant equal-area, lower-hemisphere stereographic projections of bedding (a and d), foliation (b and e) and linear fabrics (c and f). Bedding within i) predominantly dips towards the north (see a) indicating an overturned stratigraphy, but bedding is also folded by east and west plunging folds (see c). Bedding within ii) lies along a great circle (shown by the solid line in d) indicating folding about a northeast-plunging fold axis. When fold hinge lineations from ii) are plotted on a stereograph, although they predominantly plunge towards the northeast, they plot along a small circle (shown by the solid line in f) suggesting they have been refolded about a northwest-trending fold axis. Foliation planes in both i) and ii) trend northeast-southwest (see b and e).

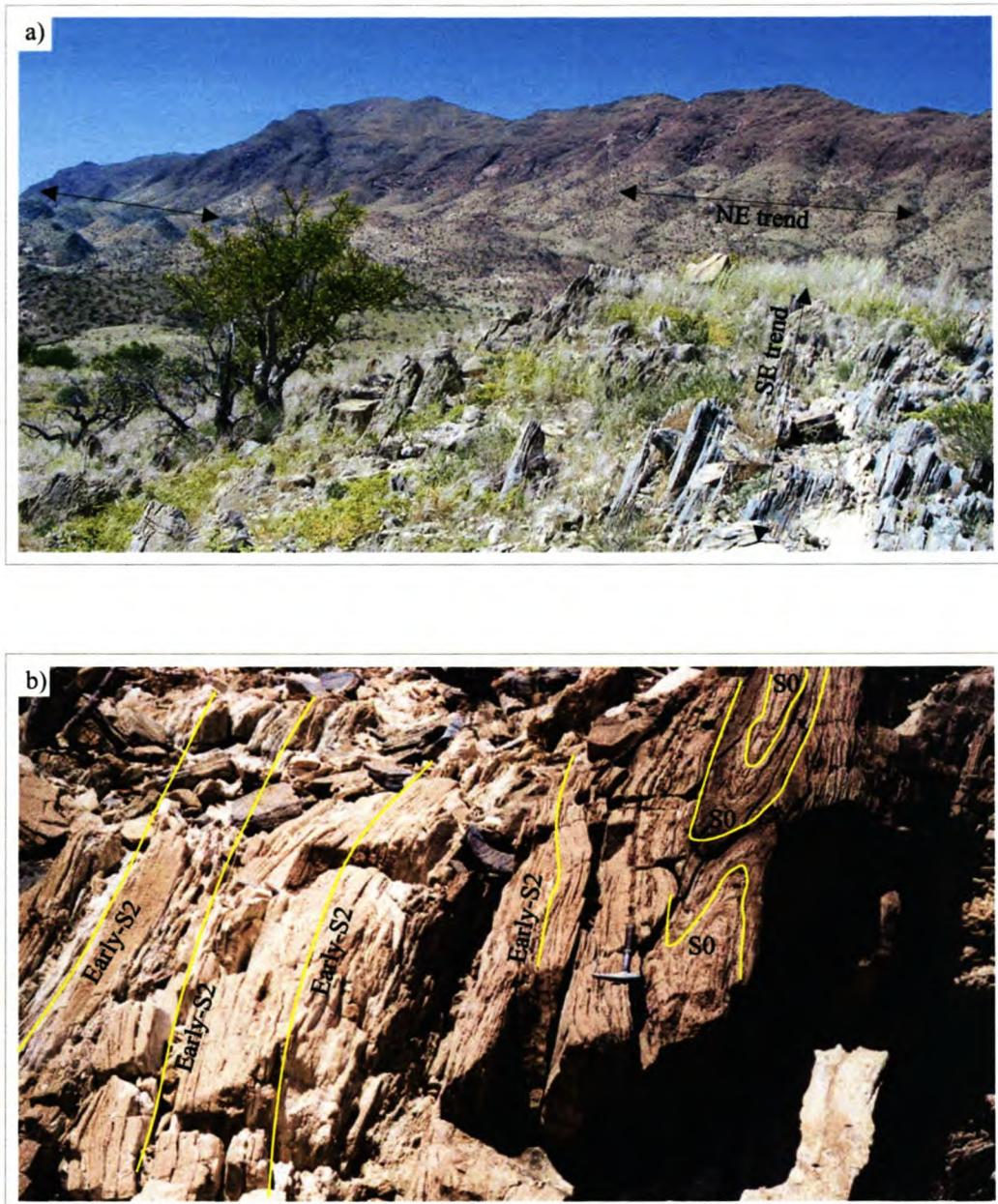


Figure 4.17 a) Photograph showing the southeast-trending bedding of the Karibib Formation in the foreground, contrasting with the northeast-trending bedding and/or S2 of the lithologies observed in the background (Domain D). The picture is taken facing southeast. (b) Photograph showing a cross-sectional view through highly-strained marbles along the southwestern termination of the dome. Isoclinal folds are preserved within the relatively calc-silicate-rich units to the right of the picture. However, any evidence of folding is completely obliterated by a strong, subvertical foliation (early-S2) in the purer marbles to the left of the picture.

These straight, highly strained domains may easily be mistaken for a primary layering (S0). However, they often bifurcate and dismember fold hinges developed within significantly competent units such as the siliciclastic and calc-silicate-rich layers (Fig. 4.4a and 4.17b). On an outcrop-scale, where the Karibib and Kuseb Formations are interbedded, the marbles of the Karibib Formation preserve only limited evidence of original bedding, forming high strain early-S2 domains between more competent, bedded siliciclastic domains of the Kuseb Formation. Thus, field evidence for the second-order folding shown in Figure 4.15 is best preserved within the more competent, siliciclastic units of the Kuseb Formation, rather than in the Karibib Formation (Fig. 4.19).

Mesoscale fold hinge lines (L2b) in Domain B plunge predominantly towards the northeast, however, when plotted on a stereographic projection, they define a small-circle, suggesting they have been refolded about a northwest-trending fold axis (Fig. 4.16 f).

Significantly, in the extreme southwestern extent of the mapping area, facing directions switch towards the northeast, showing a normal younging direction again. Lineations (L2b) also switch towards shallow southwesterly-plunges as opposed to the moderate- to steep northeasterly plunges observed elsewhere within this domain (Fig. 4.20). These plunge directions also indicate a normal younging direction within the extreme southwestern termination of the dome.

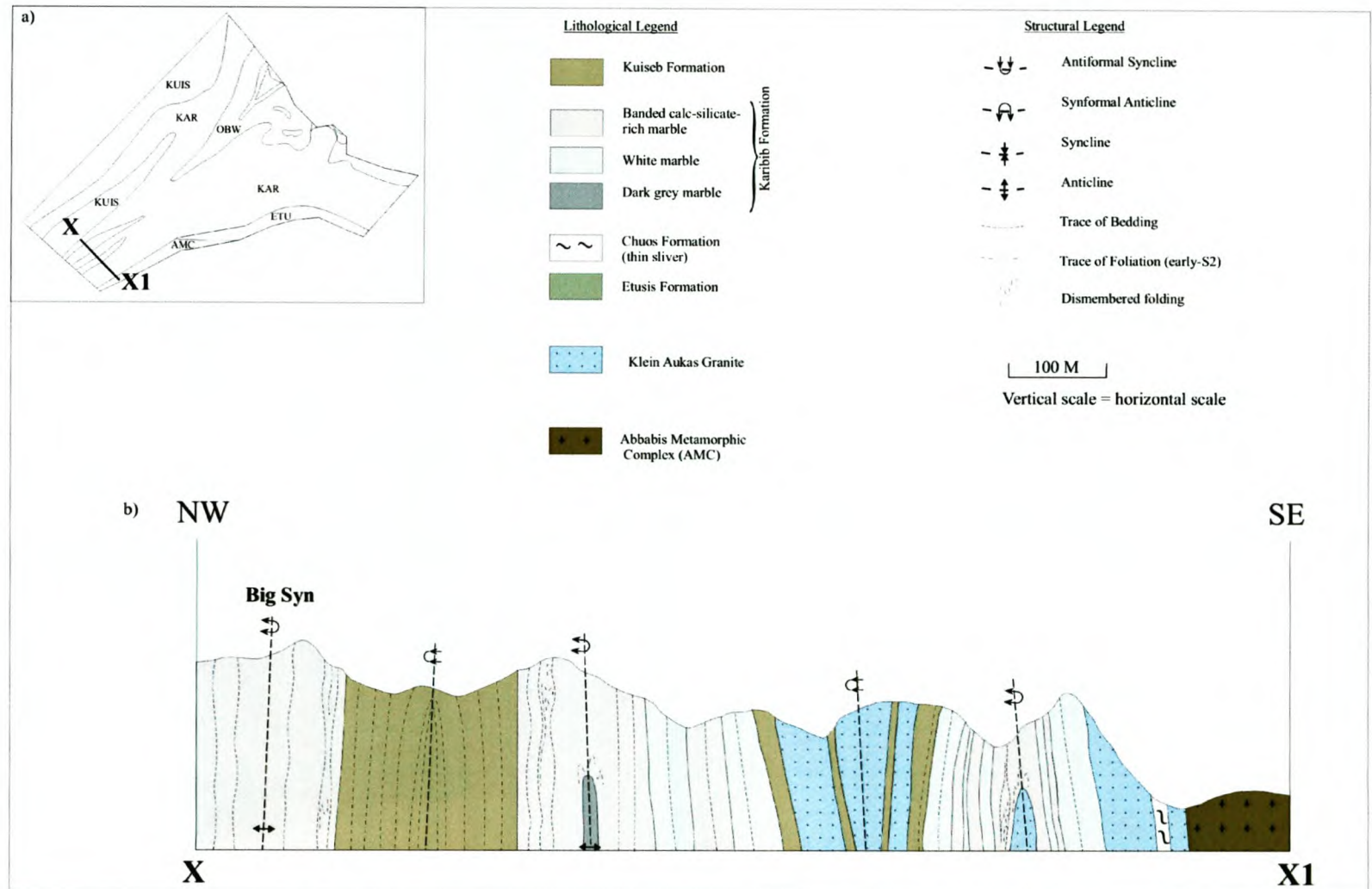


Figure 4.18 a) Schematic map of Domain B showing the locality of the cross section in b). (b) Cross-sectional view of the southwestern termination of the dome as exposed in river valleys. Second-order folds developed within the younger Kuiseb Formation appear as antiforms while those developed within the Karibib Formation appear mainly as synforms but also as antiforms towards the base of the section. As the youngest rocks form the cores of anticlines and the oldest rocks form the cores of synclines, these folds are overturned, forming the southwestern extent of the overturned first-order fold (F2a). Where synforms within the Karibib Formation become antiforms towards the base of this section marks the position where the F2b folds and F2a folds resumes a normal orientation again.

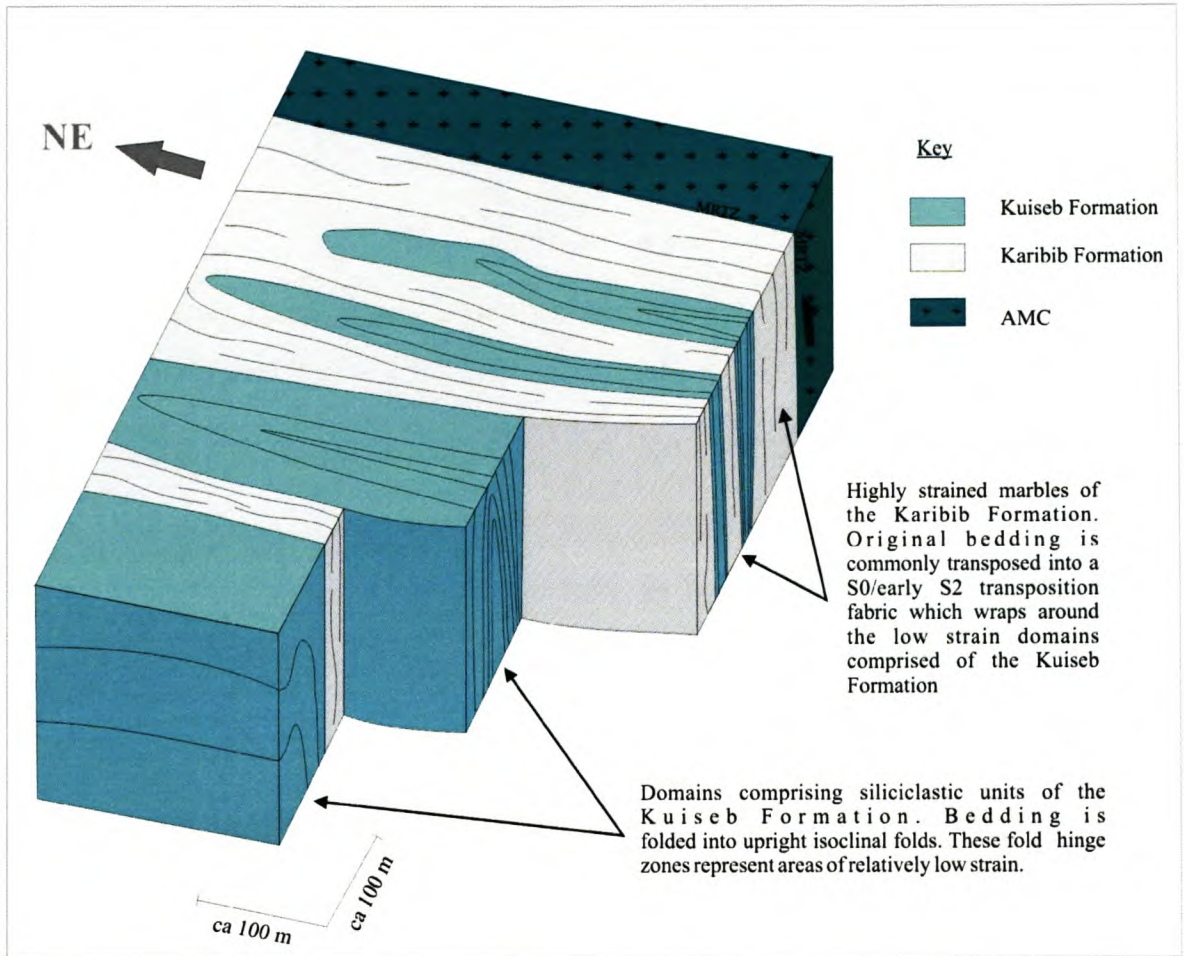


Figure 4.19 Block diagram illustrating the partitioning of strain between the ductile marbles of the Karibib Formation and the siliciclastic units of the Kuseb Formation along the southwestern termination of the Usakos dome. The highly strained marbles preserving limited bedding, wrap around the relatively lower strain fold hinge domains defined by the Kuseb Formation.

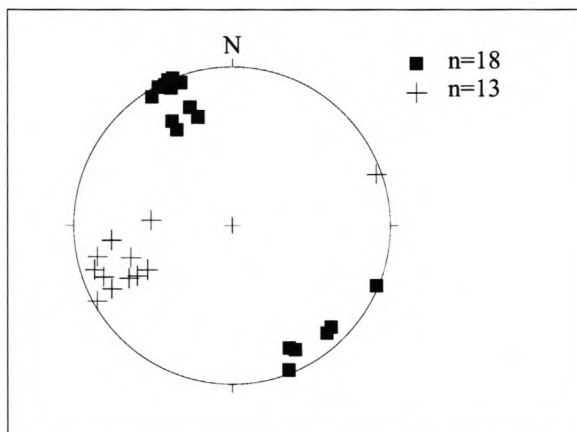


Figure 4.20 Equal-area, lower-hemisphere stereographic projection showing the steep, northeast-trending early-S2 foliation (boxes) and the shallow, southwest-plunging fold hinge lineations (crosses) (F2b/c/d) recorded from the extreme southwestern extent of the dome termination (i.e. southwest of positions X and X1 shown in Fig. 4.18).

4.5.4 Domain C

Domain C incorporates the northwestern limb of the Usakos dome (Fig. 4.21). The Kuiseb, Karibib and Oberwasser Formations exposed along this limb, trend northeast-southwest, dipping between 60 and 90° towards the southeast and northwest (Fig.4.21a). The northwestern limb of the dome is, thus largely upright.

The Oberwasser Formation forms a remarkably linear strike extent, where it appears unaffected by second- or third order folding. Bedding (S₀) within the Oberwasser Formation is often obliterated by a strong, predominantly steep southeasterly-dipping, but also northwesterly-dipping early-S₂ schistosity (Fig. 4.21b).

Along parts of the Oberwasser-Karibib contact there is a breccia horizon (described in Chapter 3) that may represent the Ghaub Formation (Hoffmann et al., 2004). Similar breccias are not observed elsewhere in the study area.

Northwest of the Oberwasser Formation are the highly deformed marble-rich units of the Karibib Formation. These units are tightly folded into northeast-trending, third- and fourth order, isoclinal folds (Fig. 4.22b). However, much of the folding within the Karibib Formation is dismembered by high strain, early-S₂ domains (Fig. 4.22a,b). Folded bedding (S₀) is best preserved by the more competent layers, such as calc-silicate felses, particularly within the low strain sites of fold hinge zones (Fig. 4.22). Bedding of less competent, marble-dominated units and along the high strain zones of fold limbs, is, on the other hand, commonly overprinted by an intense early-S₂ fabric (Fig. 4.4b). It is therefore, common to find fold hinge zones of competent calc-silicate felses completely dismembered from one another in both the vertical and horizontal plane by highly strained, marble-rich domains. These rootless fold hinges are observed at all scales, forming centimeter- to several hundred meter-wide pockets surrounded by early-S₂ transpositional domains (Fig. 4.22a, 4.23a and 4.24a). Some prominent northeast-trending transpositional domains (S₀/early-S₂) can be followed for >8 km along the northwestern limb, forming linear strike extents (Fig. 4.24b). They vary between 5 and 60 m in width and contain a well-defined early-S₂ fabric.

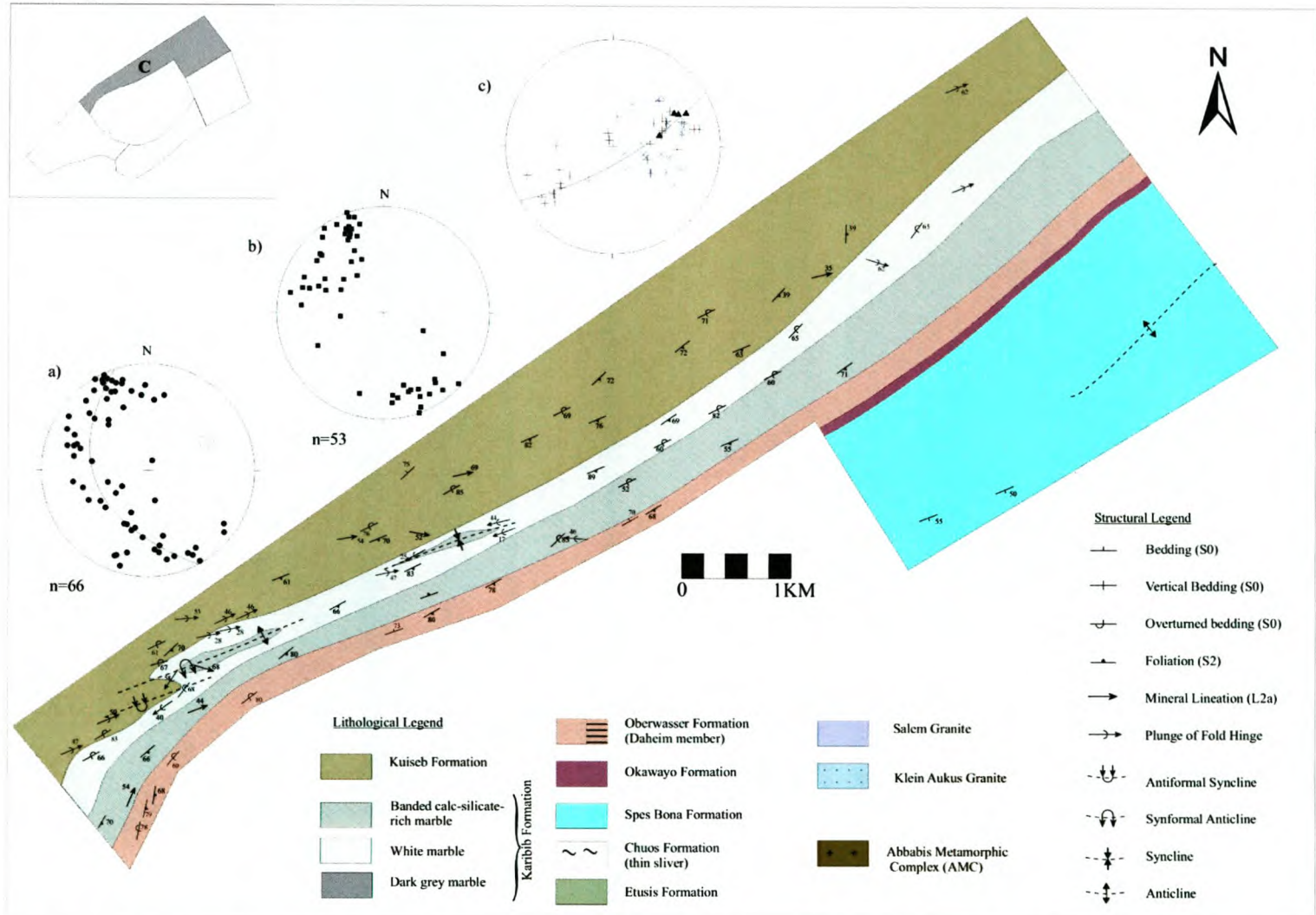


Figure 4.21 Structural map of Domain C and equal-area, lower-hemisphere stereographic projections showing (a) poles to bedding planes (circles), (b) poles to foliation planes (squares), and (c) linear data including fold hinge lineations (black crosses, n=36), mineral lineations (red crosses, n=16) and intersection lineations (black triangles, n=4). The solid line in a) indicates the best -fit circle described by poles to bedding. This great circle shows bedding folded about a northeast-plunging axis (F2a). Foliations are shown in b) to dip steeply, mainly towards the southeast but also towards the northwest. The solid line in c) indicates the best-fit circle described by fold hinge lineations. This shows refolding about a northeast-trending great circle ie. defining a shallow northwest-trending rotation axis (Late-F2).

Chocolate-tablet-boudinage of calc-silicate-rich units is also a common feature. This type of boudinage indicates northwest-southeast-directed shortening of the sequence.

Parasitic folds (F2c,d) exhibit highly variable degrees of fold hinge curvatures. These centimeter- to meter-scale folds may show hinge-line curvatures of 90-120° exhibiting sheath-like fold geometries, while adjacent folds may only show gently-undulating fold hinge lines (Fig. 4.25). This results in a scatter of fold hinges that plunge variably towards the northeast and southwest along much of this domain (Fig. 4.21c). The combined effects of variable fold plunges along strike and the dismemberment of the original sedimentary succession causes unusual outcrop patterns within the marbles that render a correlation of thin individual units impossible (e.g. Fig. 4.23).

4.5.5 Domain D

The Oberwasser and Karibib Formations form a linear northeasterly strike extent that defines the steep southeasterly-dipping, southeastern limb of the dome. Structures along this limb are described under Domain D, sharing several similarities to Domain C (Fig. 4.26), the opposite northwestern limb of the Usakos dome.

The Oberwasser Formation forms a 150-200 m thick, dark-grey siliciclastic unit. It preserves evidence of primary bedding (S₀), dipping steeply towards the southeast. However, the dominant fabric within these units is the early-S₂ foliation dipping between 40 and 80° towards the southeast. Numerous intrusive sheets of leucocratic granite inundate these rocks, oriented parallel to the S₀ and early-S₂ fabrics.

The Karibib Formation along this limb of the dome can be subdivided into three main tectonostratigraphic units, based on its composition and appearance. The lowermost unit of the Karibib Formation, in contact with the Oberwasser Formation, comprises banded marble and calc-silicate felses. This banded unit reaches ca. 220 m in thickness, dipping between 55 and 90° towards the north, southeast and south (Fig. 4.26a).

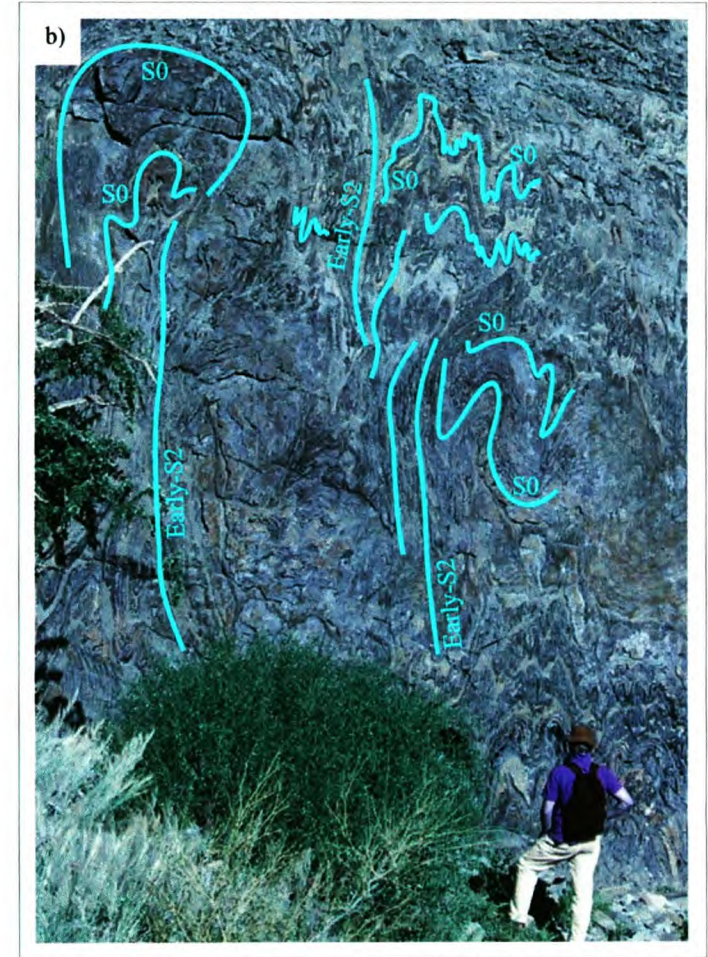


Figure 4.22 a) Typical exposure of the Karibib Formation along the northwestern limb of the Usakos dome. Fold hinges are separated from one another by high strain domains characterized by steeply-dipping, northeast-trending early-F2 fabric. Width of outcrop ca. 20 m (b) Dismembered folds are a common feature within calc-silicate-rich units along the northwestern limb of the dome. Both pictures are taken facing southwest.

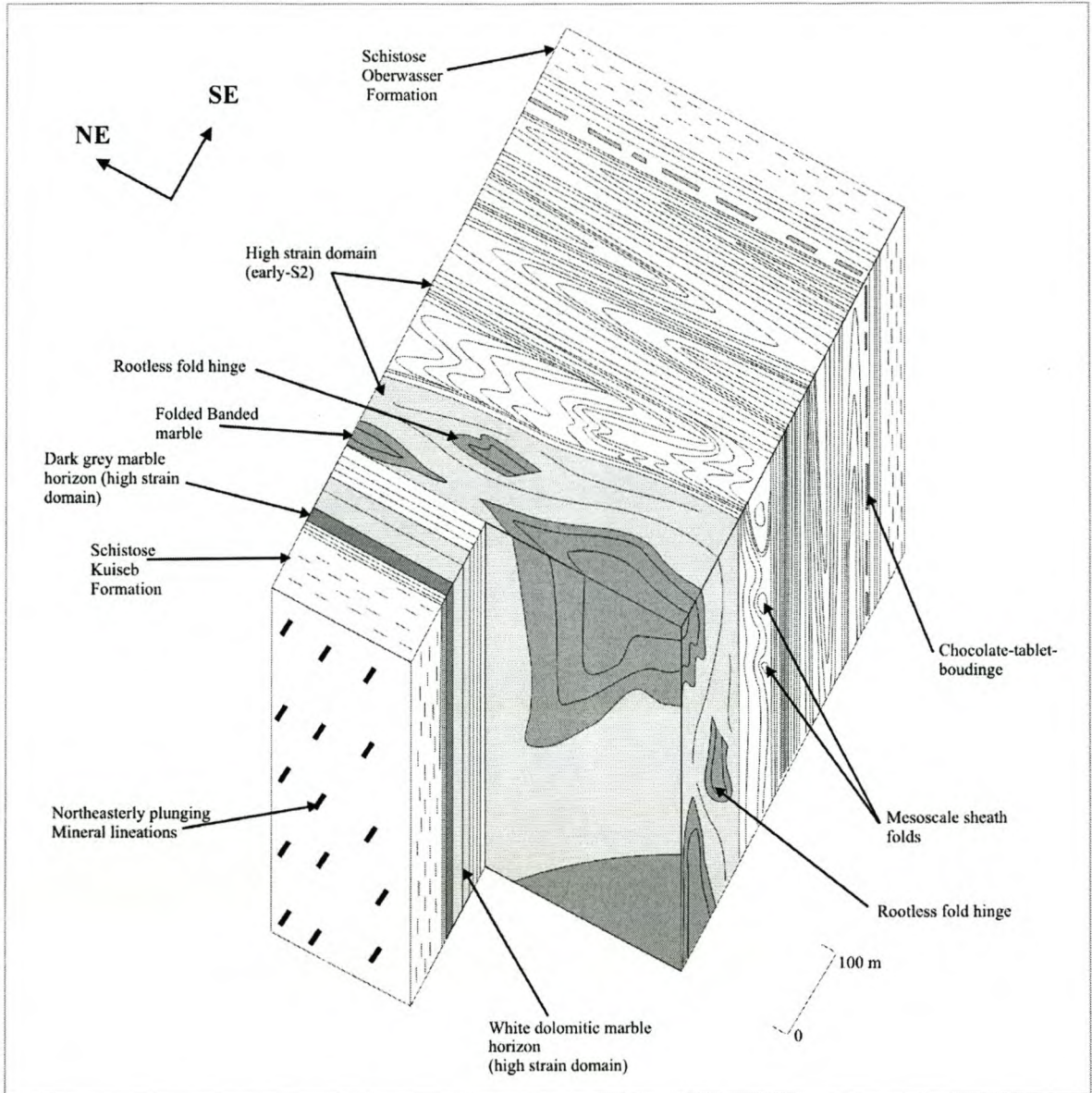


Figure 4.23 a) Schematic block diagram illustrating the contrasting styles of deformation across the width of the Karibib Formation forming the northwestern limb of the dome. Much of the primary bedding is tightly folded or transposed into an early-S2 foliation.

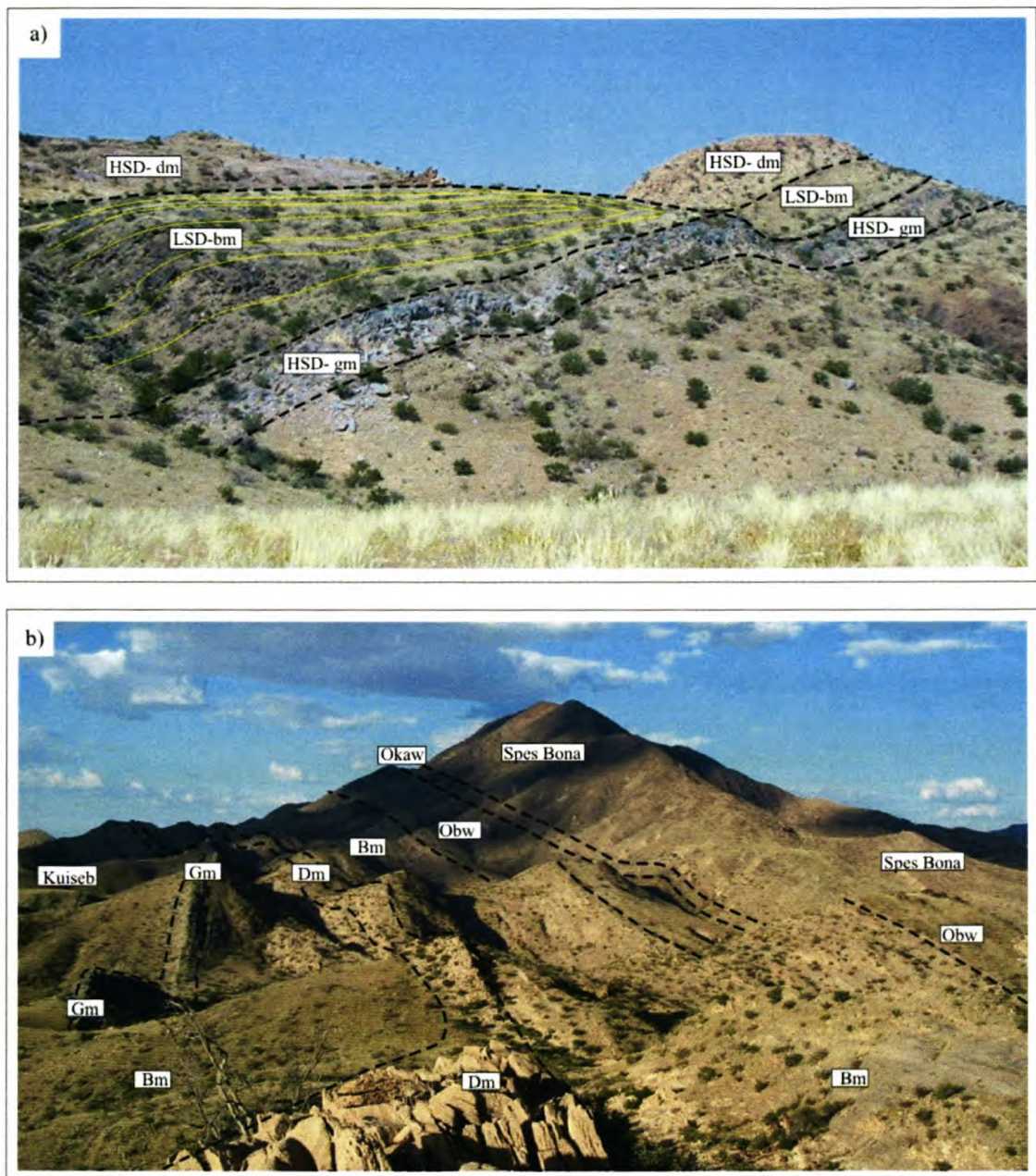


Figure 4.24 a) Photograph of kilometer-scale, alternating low strain domains (LSD) and high strain domains (HSD) along the northwestern limb of the Usakos dome. The LSD comprises banded calcisilicate felses (bm) folded into an isolated, northeast-trending fold hinge (bedding shown in yellow), bounded by undulating, northeast-trending high strain domains (HSD). The high strain domains form ridges of grey marble (gm) and cream-coloured dolomitic marble (dm) that contain a strong, subvertical northeast-trending early-S2 fabric, but no original bedding (S0). (b) Panoramic view of the northwestern limb of the Usakos dome showing the linear strike extent of all the major lithological units. (Kuisseb= Kuisseb Formation; Gm=grey marble; Bm=banded marble; Dm= dolomitic marble; Obw= Oberwasser Formation; Okaw= Okawayo Formation; Spes Bona= Spes Bona Formation). Picture is taken facing northeast.

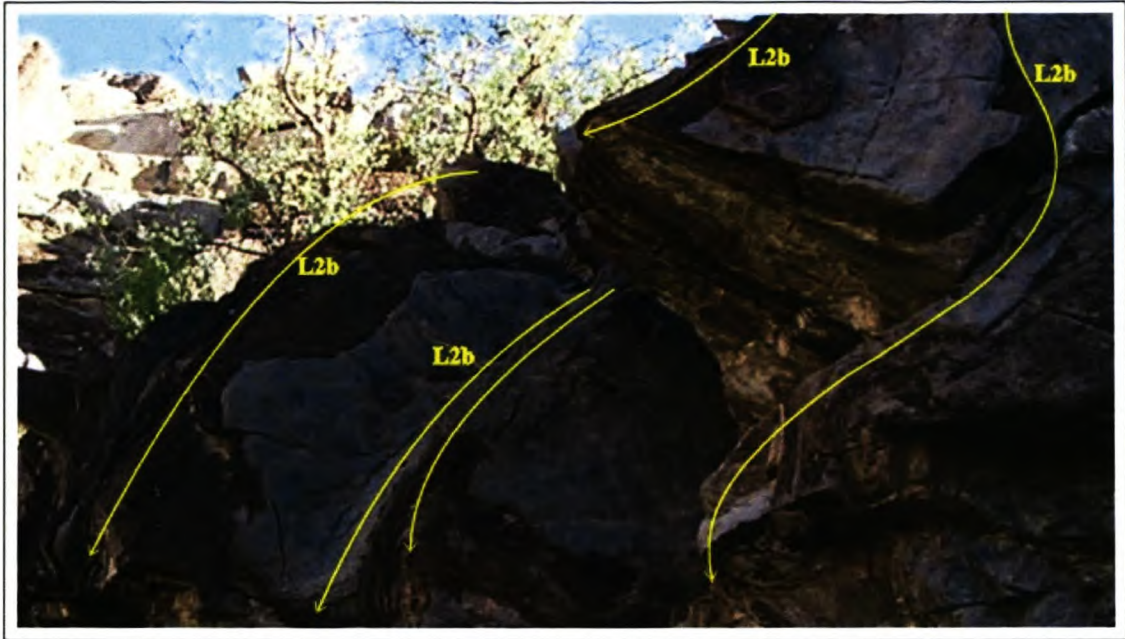


Figure 4.25 Photograph showing significant curvatures of fold hinge lines (L2b lineations shown in yellow) within calc-silicate felses of the Karibib Formation along the northwestern limb of the Usakos dome. Photograph is taken facing north.

Above the banded marbles are homogeneous, bright white calcitic and dolomitic marbles which are exposed up to the upper contact of the Karibib Formation. Their lack of obvious bedding prevents an accurate determination of thickness. However, the entire unit has an apparent thickness of up to 2 km. The third tectonostratigraphic unit of the Karibib Formation is a dark-grey marble horizon that is contained within the bright white marbles. It has an apparent thickness of between 50 and 250 m and is exposed over a strikelength of >6 km, forming a prominent northeast-trending ridge within the Karibib Formation.

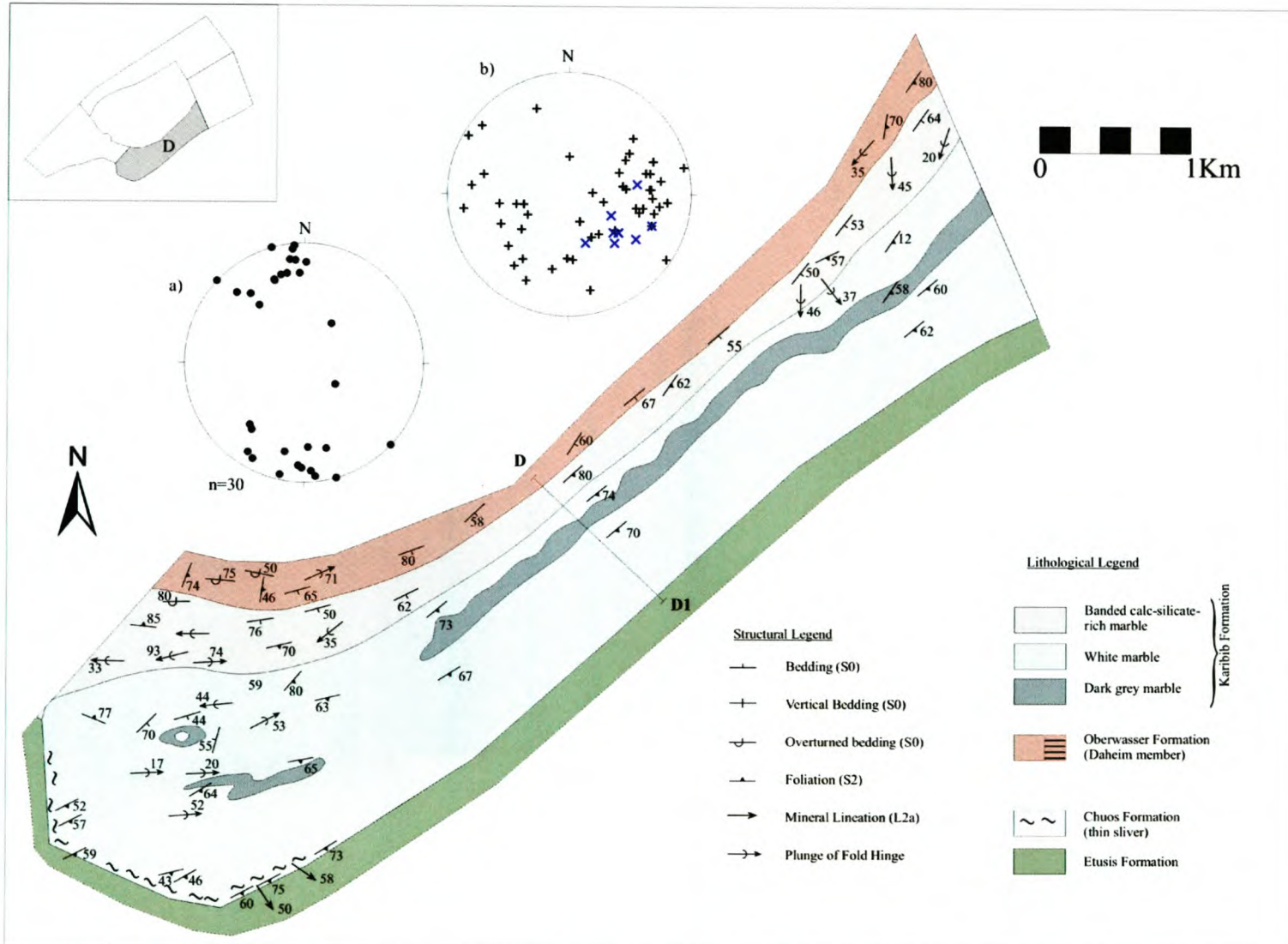


Figure 4.26 Structural and lithological map of Domain D with equal-area, lower-hemisphere stereographic projections of (a) poles to bedding planes (dots), (b) linear fabrics (+ = mesoscale fold hinge lineations, n=56) and (X = mineral lineations, n=9, taken from along the Karibib/Etusis contact). See Figure 4.27 for a cross section across D to D1. Poles to bedding planes shown in a) dip steeply towards the northwest and southeast reflecting a S0/early-S2 transpositional fabric. Fold hinge lineations in b) show a wide scatter, reflecting the northeast-trending folding parallel to the MRTZ and re-folding by a shallow, northwest-trending fold axis (late-F2). Southeast-plunging mineral lineations shown in b) reflect a top-to-the-northwest sense of movement along the MRTZ.

Variations in structure and appearance of the three units of the Karibib Formation record a significant increase in strain intensity from the lower contact with the Oberwasser Formation towards the upper contact with the Etusis Formation (Fig. 4.27). The lowermost 40 m of the Karibib Formation comprises the banded marbles and calc-silicate felses dipping uniformly between 60° and 85° towards the north and southeast. This banding is interpreted as primary bedding (S₀). Higher up in the formation, towards the southeast, these banded marbles appear folded into northeast-trending, open- to tight F_{2c} folds with interlimb angles between 25 and 60° (Fig. 4.28a and b). However, strain increases significantly towards the southeast where folds develop into upright, isoclinal folds (Fig. 4.29a). Further southeast, these isoclinal folds become highly dismembered (Fig. 4.29b) resulting in rootless fold hinges, separated by subvertical high-strain domains that represent former fold limbs (Fig. 4.27 and 4.30a,b). These high-strain domains comprise finely banded marbles, where the banding defines a subvertical, northeast-trending axial-planar foliation (early-S₂) so that S₀ is completely transposed into an early-S₂ fabric. The high-strain domains separating areas of lower-strain intensity, truncate bedding (S₀) suggesting they accommodated significant vertical and/or lateral shear slip during progressive shortening.

Along the width of the Karibib Formation there is a gradational transition from calc-silicate-rich units into a region of predominantly white marbles (Fig. 4.26). This transition coincides with the dismemberment of folding. Isolated fold hinges representing relatively low-strain domains become fewer and far between further southeast, while the marble-rich, highly strained transpositional domains (S₀/early-S₂) increase, so that the Karibib Formation within ca. 1 km of the Karibib/Etusis contact consists almost exclusively of highly-strained, white marble.

The white marbles, although relatively homogeneous, contain a steep southeasterly-dipping foliation (early-S₂), which wraps around isolated fold hinges (Fig. 4.27). Despite being highly transposed and homogenized, the white marble does, however, contain the dark-grey marble as a marker horizon. This horizon describes a linear, northeastern strike extent.

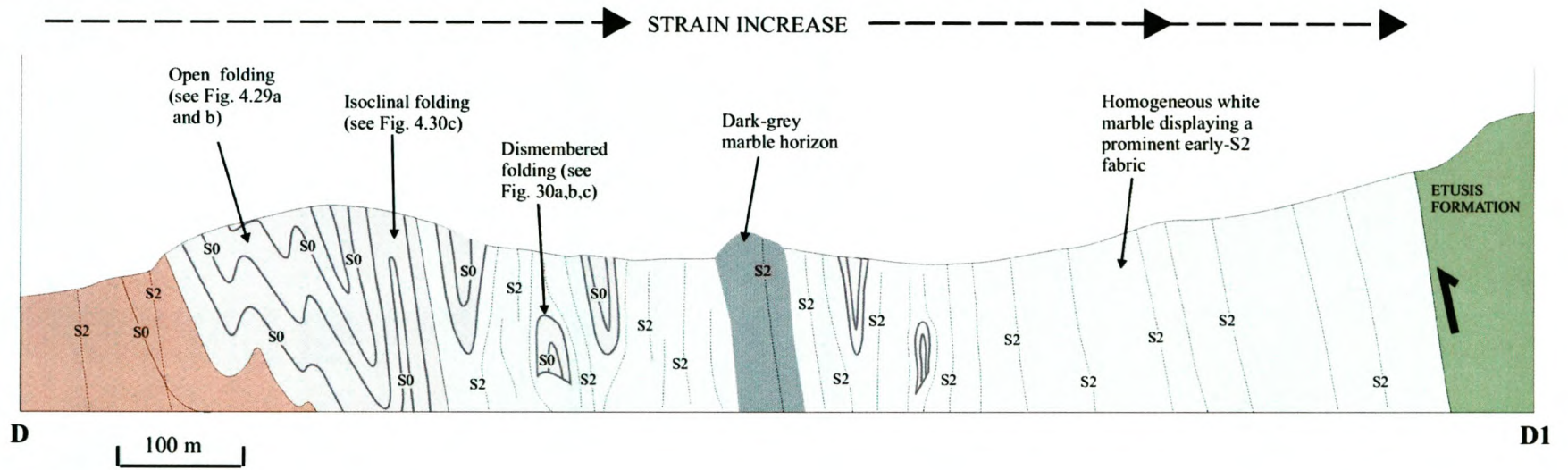


Figure 4.27 Cross section taken through the southeastern limb of the Usakos dome. Strain increases progressively from the southwest to the southeast towards the upper contact of the Karibib Formation (S2= early-S2). Legend as in Fig. 4.27.



Figure 4.28 a) and b) Photographs showing northwest-vergent folding preserved within the lowermost calc-silicate-rich units of the Karibib Formation along the southeastern limb of the dome. Facing southwest.

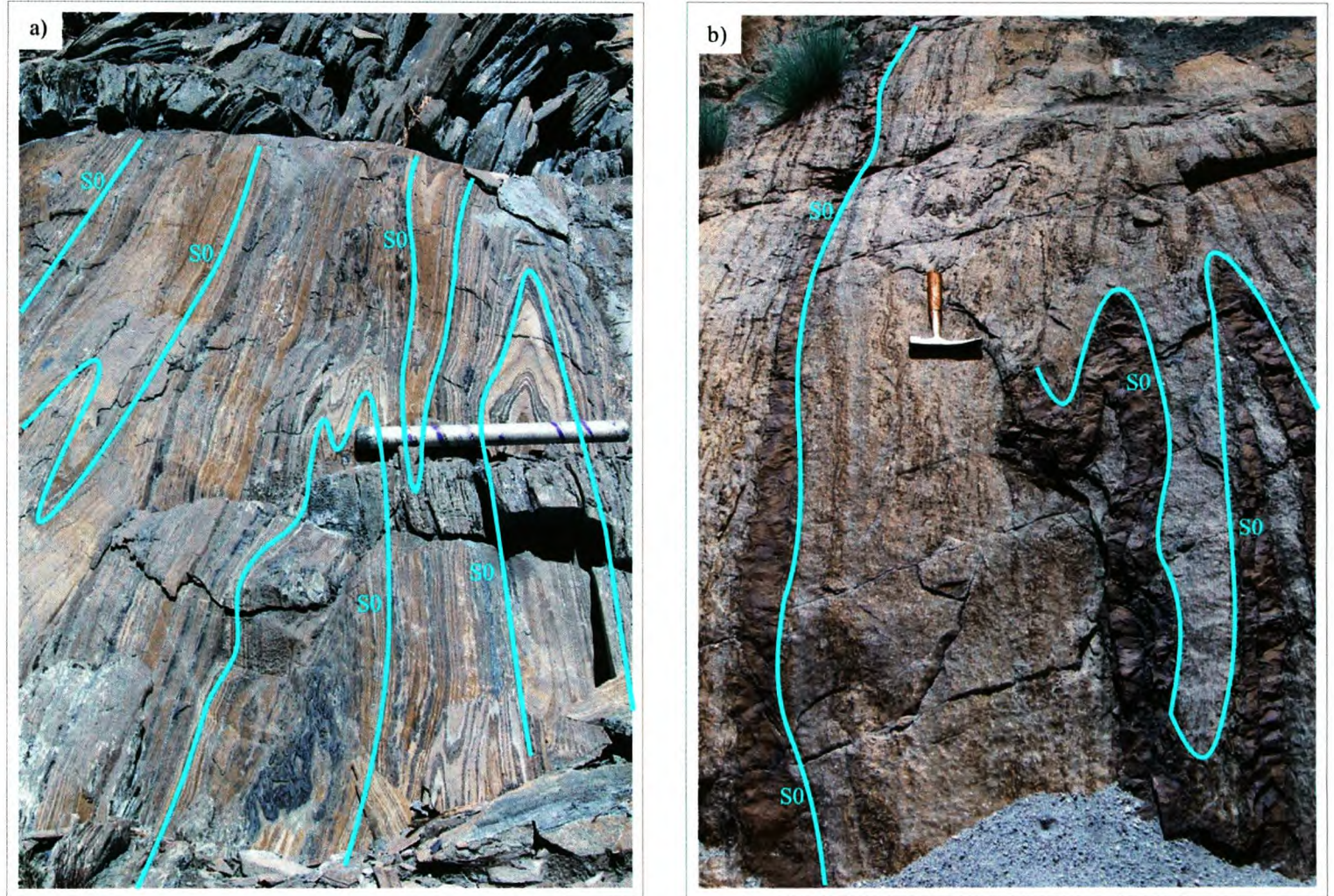


Figure 4.29 a) Nearer to the Etusis Formation than Fig. 4.29, folds within the marbles of the Karibib Formation become more isoclinal. (b) Progressively nearer the Etusis Formation, calc-silicate-felses within the Karibib Formation become increasingly dismembered.

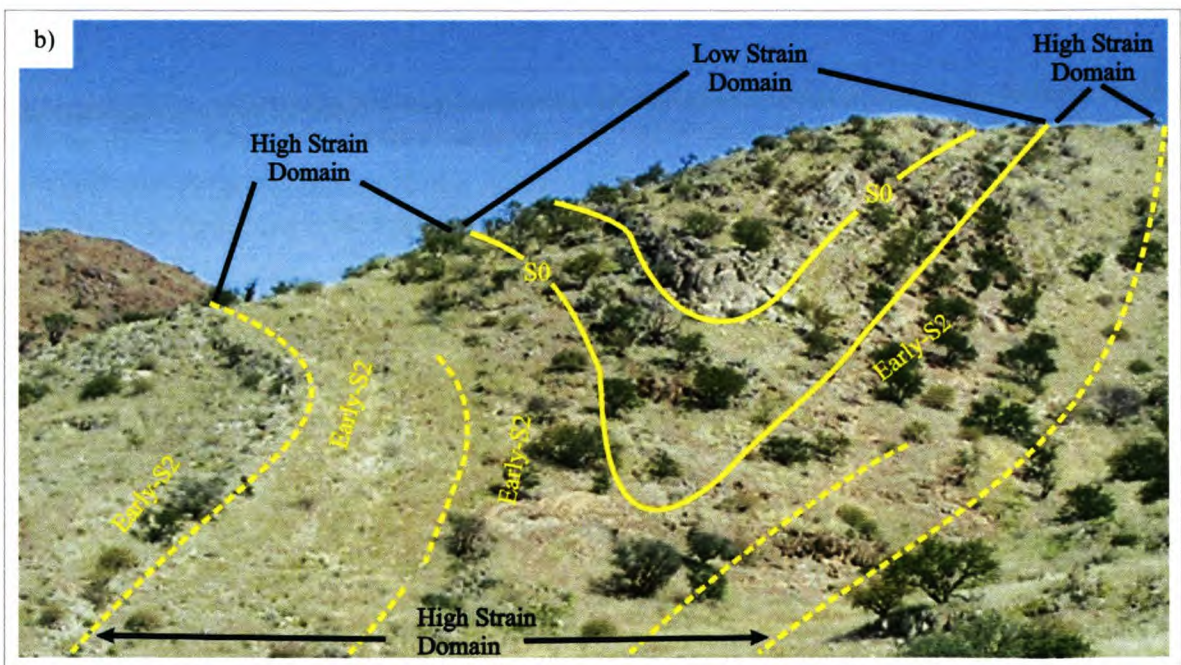
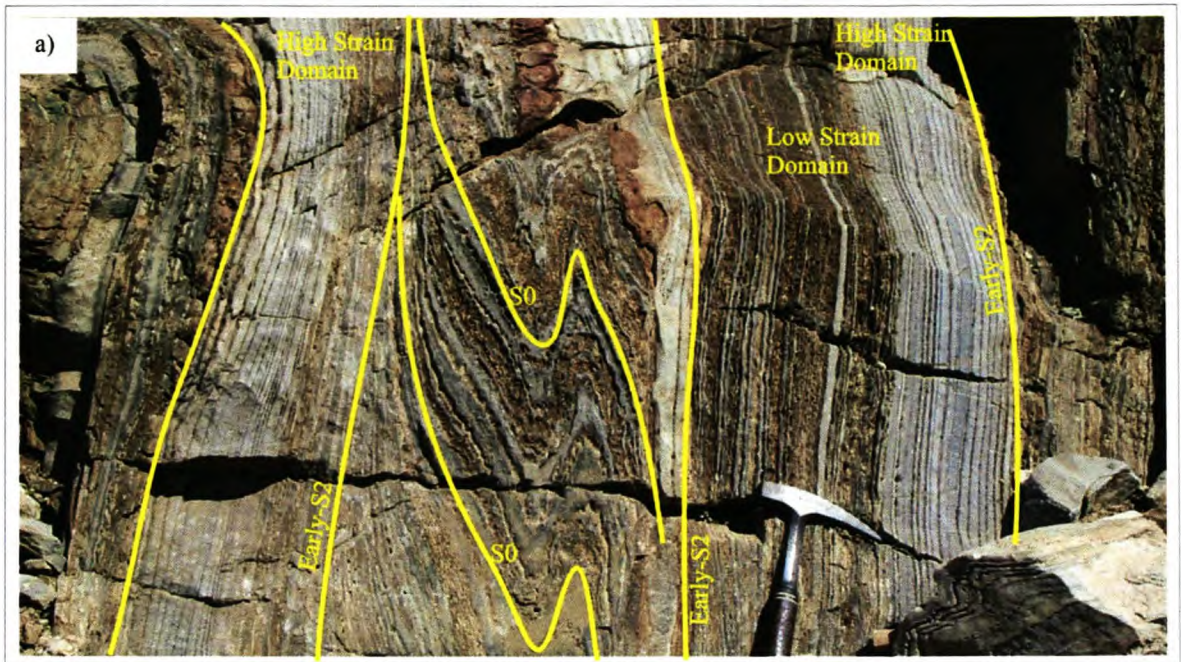


Figure 4.30 a) Photograph showing a decimeter-scale fold hinge, dismembered along its limbs by high strain domains (early-S2 transpositional domain). The high strain domains exhibit a strong early-S2 foliation represented by banding, very similar in appearance to primary bedding. (B) Tens of meter wide fold hinge within the Karibib Formation along the southeastern limb of the dome. The hinge is bound by anastomosing, predominantly northeast-trending high strain domains exhibiting a strong early-S2 fabric.

In map view, the horizon pinches and swells along its length and, in the far southwest, it is boudinaged and folded. Two fold structures with half-wavelengths of ca. 100 m are present within the dark-grey marble to the southwest. One of these folds displays a Z-shaped symmetry in plan view, plunging moderately towards the northeast. The other fold describes a northeast-trending, strongly periclinal, synformal geometry resembling a sheath fold. Centimeter- to meter-scale fold hinges within this synform are also doubly-plunging towards the east and west.

Along the northeastern portion of the limb, folding is characterized by undulating hinge lines that plunge between 25° and 55° towards the south, southeast and southwest. Along the southwestern portion of the limb, centimeter- to meter-scale folds exhibit doubly-plunging hinge lines, plunging between 15° and 50° to the west-southwest and between 20° and 75 ° to the east-northeast, with the majority of fold hinges plunging towards the east-northeast (Fig. 4.26b). This strongly doubly-plunging nature of the fold hinge lines and the predominance of northeast-plunging lineations (L2b) in the southwest suggests the folds (early-F2) may have been refolded about shallow-northwesterly plunging fold axes (late-F2). The presence of centimeter-scale, superposed folds (type-2 and type-3; Ramsay, 1967) in the southwestern extent of this domain supports this model of superimposition (Fig. 4.31a,b).

Throughout the banded marble and calc-silicate-rich unit of the Karibib Formation, the relatively competent calc-silicate-rich layers are extensively boudinaged. Boudinage occurs in both the vertical and horizontal planes, thus defining a 'chocolate-tablet-type' boudinage. In places, some boudins, when viewed in plan view, appear juxtaposed against one another, or folded, suggesting layer-normal shortening followed by northeast-southwest-directed, layer-parallel shortening (Fig. 4.32 a, b and c).

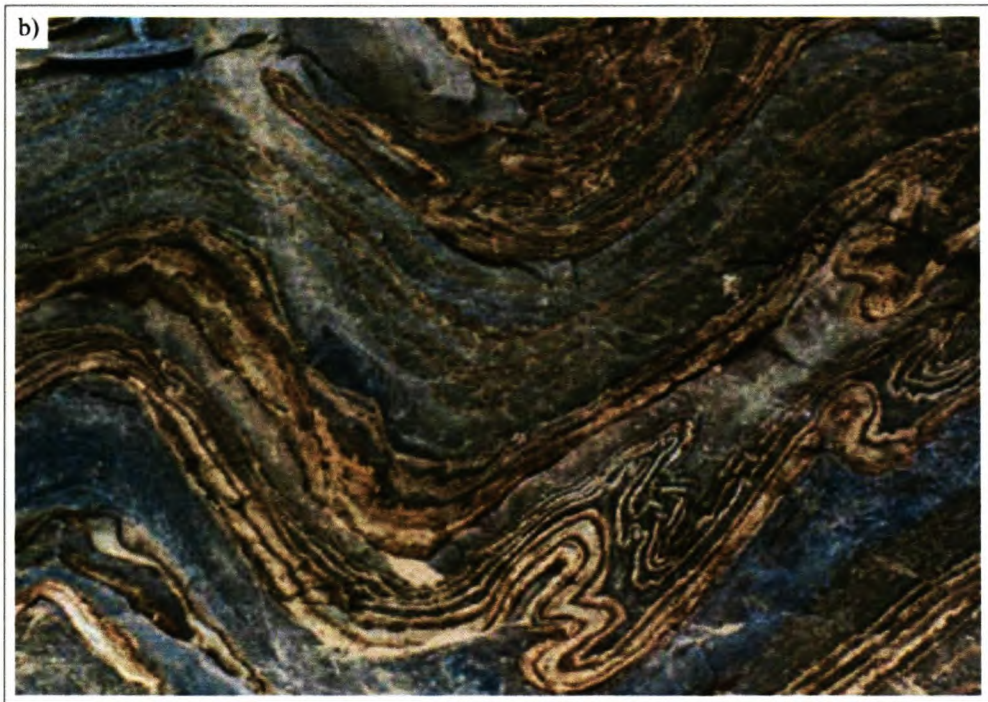


Figure 4.31 a) and b) Mesoscale refolded fold structures within calc-silicate-rich units of the Karibib Formation. These folds are observed along the southeastern limb of the Usakos dome, near the closure of the dome.

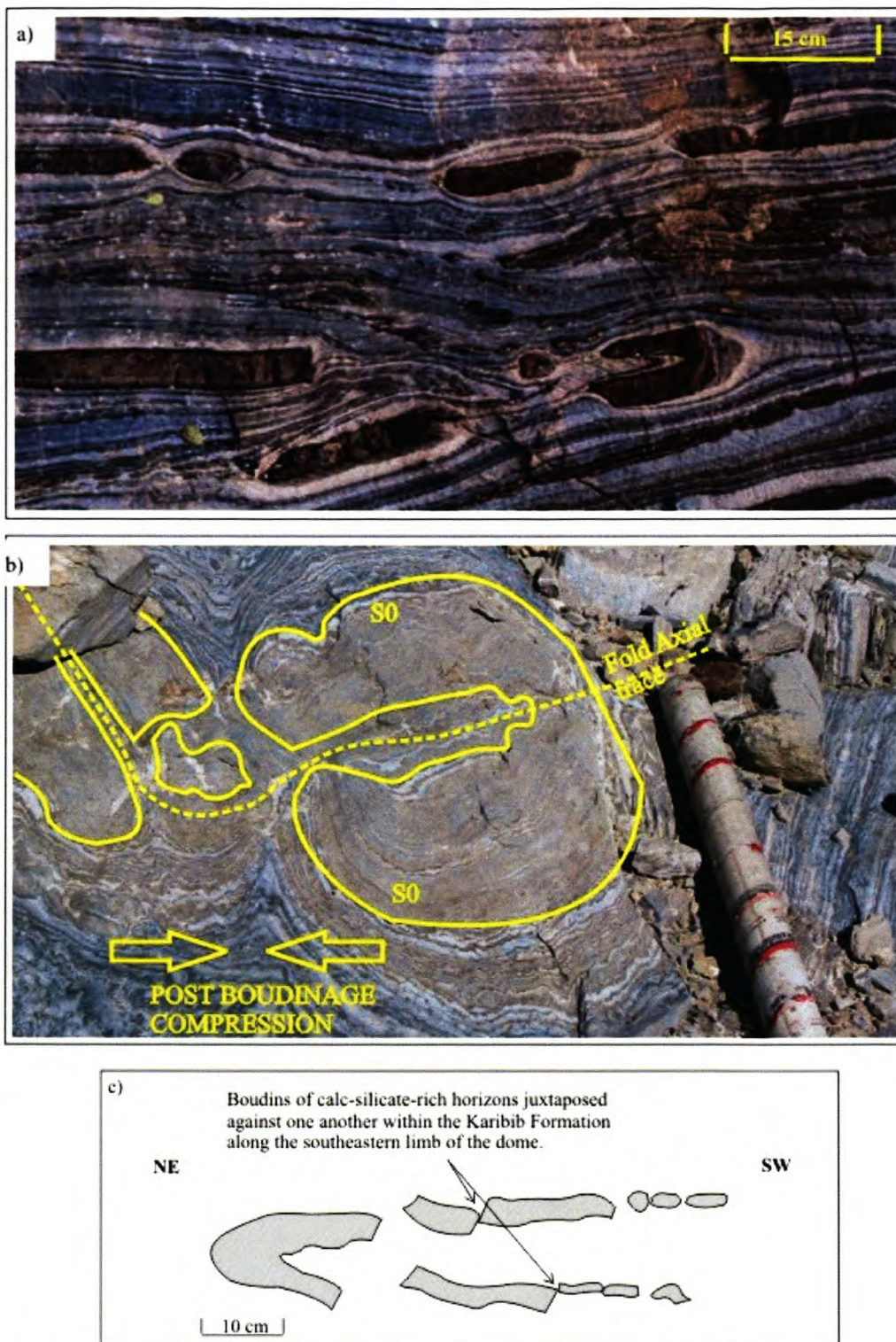


Figure 4.32 a) Photograph showing boudins within calc-silicate-rich units of the Karibib Formation along the southeastern limb of the dome (plan view). (b) Photograph showing folded bedding (S₀) that has undergone boudinage. The boudins appear to have subsequently undergone layer-parallel shortening from the NE and SW. Taken facing south, (c) Sketch showing the juxtaposition of boudins, in plan view, suggesting post-boudinage NE-SW-directed shortening.

4.5.6 Domain E

Domain E represents the northeastern extent of the mapping area incorporating the Tsawichas Depression (Fig. 4.33). Two major structures dominate this domain.

Firstly, in the northeast the Spes Bona Formation is folded into a southwesterly-plunging antiformal closure (see A in Fig. 4.33). This fold extends towards the northeast where it develops into a first-order fold that defines the domal geometry of the northeastern portion of the Usakos Dome (Neumaier, 2002). Along its southwestern closure, bedding dips between 30° and 40° towards the southwest. This fold is northwesterly-verging with bedding along the limbs dipping between 25° and 40° towards the southeast. Within the closure of this fold, fold hinge lineations (L2b) plunge shallowly towards the southwest, parallel to the hinge of the F2a fold.

Secondly, towards the centre of the Domain E, bedding of the Okawayo and Oberwasser Formations is folded into a southeasterly-plunging synformal structure. This synform, referred to as the Tsawichas Depression (Fig. 4.33) trends approximately perpendicular to the regional, northeastern structural trend and marks an axial depression within the F2a fold hinge line between the northeastern and southwestern portions of the Usakos dome (Fig. 1.1). The extent of the depression is only obvious within the Oberwasser and Okawayo Formations, as it dies out towards the northwest and southeast within the Spes Bona and Karibib Formations respectively. It can be traced for ca. 2 km along its southeasterly plunge and measures ca. 2.5 km in half wavelength. The plunge of the synform is steepest in the northwest near the Okawayo-Oberwasser contact (ca. 60°), becoming shallower towards the southeast (ca. 30°).

A well-developed schistosity (S2-early) is developed within the metapelites of the Spes Bona and Oberwasser Formations. This schistosity is steep, southeasterly-dipping and is clearly axial-planar to the northeast-trending, northwest-verging, early-F2 folds (Fig. 4.33). The foliation within the marbles of the Karibib Formation is similarly orientated. Within parts of the core of the Tsawichas Depression, a steep northeasterly-dipping schistosity is locally-developed, trending parallel to the axial plane of the Tsawichas Depression.

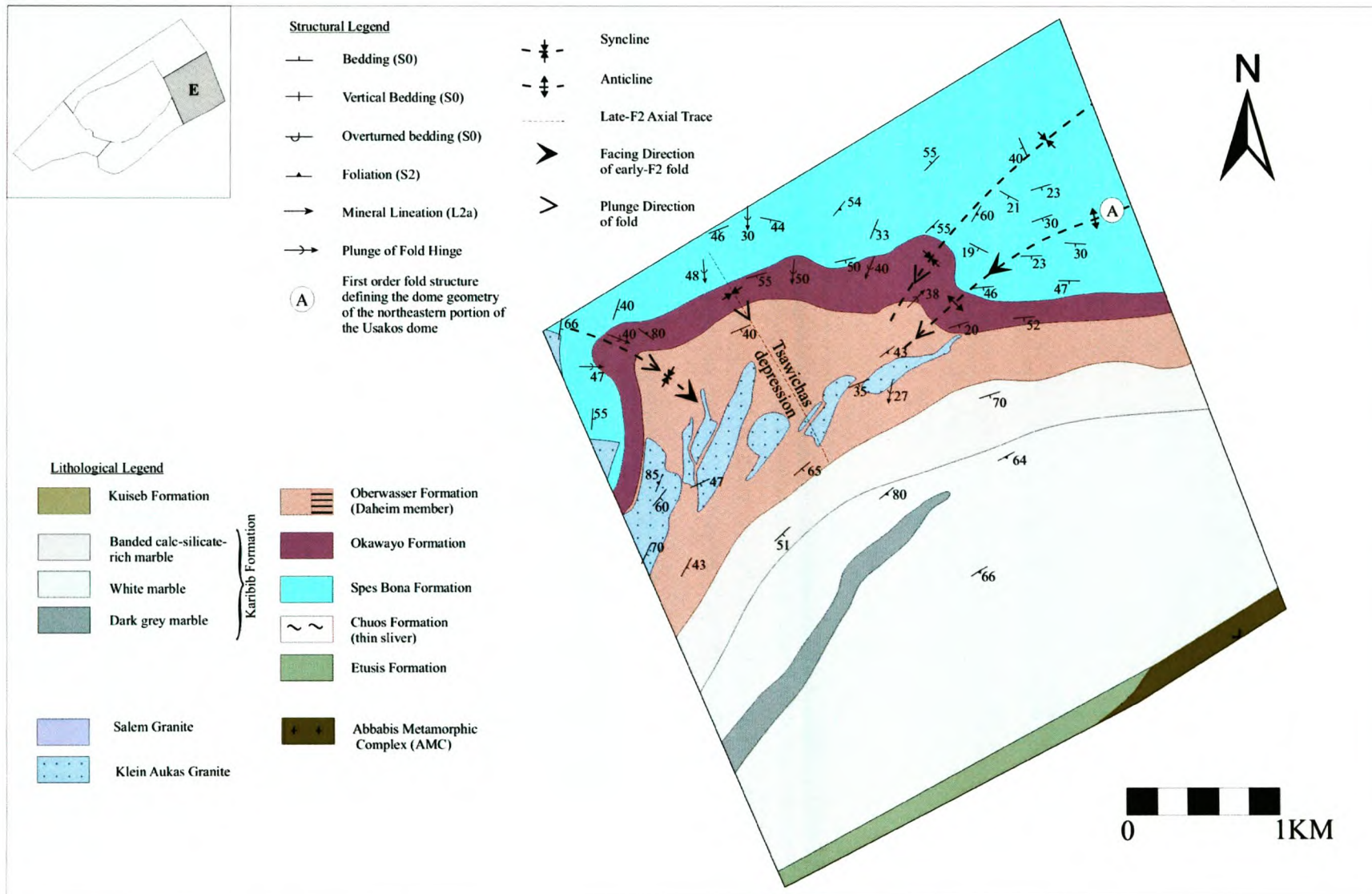


Figure 4.33 Structural map of Domain E.

The banded marbles of the Okawayo Formation within the Tsawichas Depression display two sets of mesoscale folds. Firstly, there are centimeter-scale folds (early-F2) with variable fold orientations that appear refolded by a later generation of folding (late-F2). (Fig. 4.34a,b).

The late-F2 folds are open folds that plunge moderately towards the east, southeast and south (Fig. 4.35). They have half wavelengths of 1-5 m and trend parallel to the fold hinge line of the Tsawichas Depression. They are therefore interpreted as parasitic folds formed during the formation of the Tsawichas Depression (late-F2d).

Quartz aggregate lineations occur along the contact surfaces between concordant granitic sills and the Oberwasser Formation. These lineations vary in plunge between 20 and 60° towards the south, oriented approximately parallel to the fold hinge line of the Tsawichas Depression (Fig 4.33 and 4.35a).

4.6 The Upper Contact of the Karibib Formation along the southeastern limb of the Usakos Dome

For the most part, the Etusis Formation forms the hanging wall with the Karibib Formation along the southeastern limb of the dome. This indicates that a large portion of the Damara Sequence, i.e. the Chuos Formation, the Spes Bona Formation, the Okawayo Formation and the Oberwasser Formation are missing or not developed along the contact. Along its northeastern and southwestern strike extents, the Etusis Formation pinches out, thus exposing the AMC adjacent to the Karibib Formation (Fig. 4.2). The upper contact of the Karibib Formation is easily recognized by the sharp contrast between the reddish-brown quartzites of the Etusis Formation or pink gneisses of the AMC and the white marbles of the Karibib Formation. For the most part, the contact shows a consistent northeast-southwest strike extent along the length of the southeastern limb of the Usakos dome.



Figure 4.34 a) Panoramic photograph facing northeast, parallel to the trend of the Okawayo Formation within the Tsawichas Depression. Meter-scale, late-stage folds are shown in yellow. The fold hinges plunge moderately towards the southeast. These folds are orthogonal to the dominant northeast-trending structural grain of the area. (b) Photograph facing northwest, on to the steeply southeast-dipping bedding plane of the Okawayo Formation within the Tsawichas Depression. Along the bedding surface are numerous refolded centimeter-scale folds. The yellow dashed line represents the axial trace of the late generation of folds.

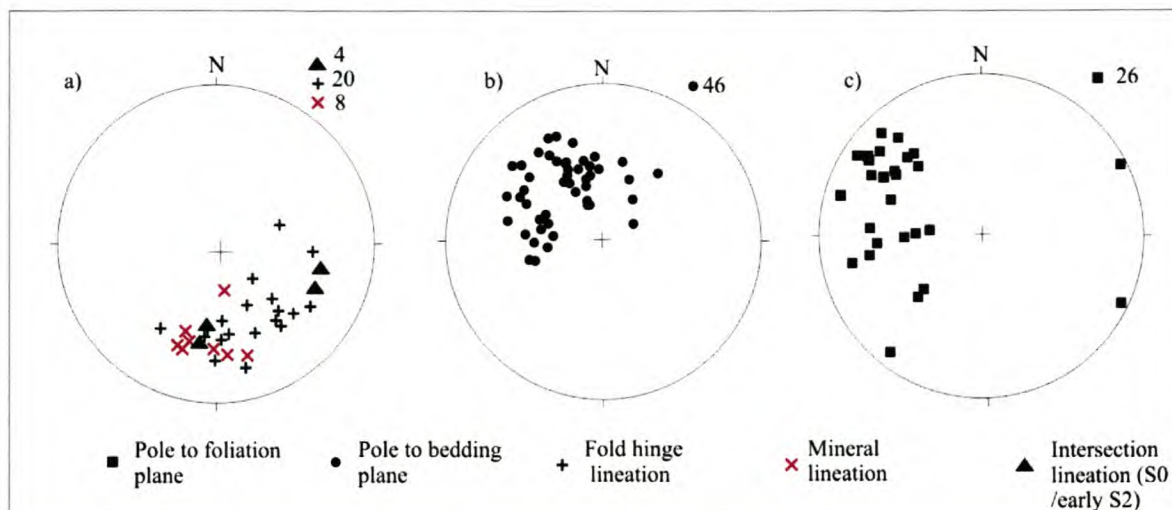


Figure 4.35 Equal-area, lower-hemisphere stereographic projections showing (a) lineations, (b) poles to bedding planes, and (c) poles to foliation planes from within the Tsawichas Depression (Domain E). Fold hinge lineations and mineral lineations shown in a) plunge moderately towards the southeast and south, parallel to the fold hinge of the Tsawichas Depression. Bedding within Domain E as shown in b) predominantly dips towards the southeast reflecting its position on the southeasterly-dipping southeastern limb of the F2a structure. Foliation within Domain E shown in c) dips towards the east and southeast. The easterly-dipping foliation is oriented axial planar to the Tsawichas Depression, while the southeasterly-dipping foliation is oriented axial planar to the dome (F2a).

Towards the southwestern closure of the dome (i.e. in Domain B), however, the contact describes a sharp 90 degree bend towards a more northwesterly trend for 2.5 km, before resuming its northeasterly trend again in the southwest (Fig. 4.2). The early-S2 schistosity prominent within the highly strained marbles of the Karibib Formation along this limb, is truncated by the Etusis Formation as it changes direction towards the northwest (Fig. 4.36).

A thin (ca. 10 m) sliver of metapelites, interpreted as being part of the Chuos Formation, can be traced for ≥ 1.5 km along the contact between the Karibib and Etusis Formation (Appendices I). These metapelites contain mineral and/or clast stretching lineations and a strong early-S2 foliation. The lineations are defined by stretched cordierite and fine-grained lithic clasts, plunging towards the east and southeast at angles between 35° and 60° (Fig. 4.26b). The schistosity dips between 40° and 80° towards the southeast, concordant with the regional early-S2 fabric and

parallel to the contact between the Karibib and Etusis Formations. No shear sense indicators could be identified in the field.

The upper contact of the Karibib Formation along the southeastern limb of the dome corresponds to the strike continuation of a large thrust referred to as the Mon Repos Thrust Zone (MRTZ) described by Kisters et al. (2004) from the farm Mon Repos, located ≥ 25 km northeast of the study area. Several other lines of evidence collected during this study suggest the contact represents a tectonic boundary that may be correlated with the Mon Repos Thrust Zone.

These include:

- The contact represents a significant gap in the stratigraphic succession, where the Spes Bona, Okawayo, Oberwasser and a large proportion of the Chuos Formations are missing between the younger Karibib Formation and the older Etusis Formation and/or the basement gneisses of the AMC. The presence of a thrust between the Karibib Formation and the older rock units may explain the gap in the stratigraphy.
- The ca. 1 km thick Etusis Formation pinches out along strike in the northeast and in the southwest. Rather than representing primary facies changes, the rapid-along strike thinning of the Etusis Formation may indicate truncation of the Etusis Formation by a thrust.
- The meta-arkoses of the Etusis Formation exhibit well-preserved, cross-bedded surfaces and appear much less deformed than the marbles of the adjacent Karibib Formation. A traverse through the Karibib Formation along the southeastern limb of the dome illustrates a significant increase in strain intensity towards the upper contact of the Karibib Formation (Fig. 4.27). This suggests the Etusis Formation was thrust on top of the Karibib Formation along the length of the southeastern limb of the dome and the majority of strain was accommodated by the rheologically weak marbles of the Karibib Formation. Thus, the Karibib Formation acted as a shear zone.
- The thin horizon of metapelites between the Karibib and Etusis Formations is interpreted as a wedge of the Chuos Formation. It is likely that the wedge was locally dismembered from the bulk of the formation during thrusting and

transported along the thrust where it became embedded. Similar allochthonous, kilometer-scale 'horse structures' of the Chuos Formation are described by Kisters et al. (2004) from the MRTZ type locality, on the farm Mon Repos.

- Stretching lineations defined by cordierite and biotite aggregates in the Chuos Formation plunge towards the east and southeast. Kisters et al. (2004) described similar east- and southeasterly-plunging lineations from the footwall and from within the Mon Repos Thrust Zone. If these lineations developed during thrusting their plunge may be used to indicate the transport direction along the thrust. Their easterly and southeasterly plunge suggests either a top-to-the-northwest/west or a top-to-the-southeast transport direction. Considering older rocks of the Etusis Formation overlie the younger rocks of the Karibib and Chuos Formations, a top-to-the northwest/west transport direction along a thrust, is suggested. This top-to-the-(north)west sense of movement along the MRTZ is compatible with the regional, northwest-directed fold vergence formed during northwest-southeast-directed compression.
- The abrupt termination of the bright white and dark-grey marbles of the Karibib Formation along the 90 degree bend in the upper contact of the Karibib Formation clearly points to truncation along a tectonic contact.

There is therefore sufficient evidence to conclude that the upper contact of the Karibib Formation along the length of the southeastern limb of the Usakos dome is, in fact, a thrust and it is regarded henceforth as part of the Mon Repos Thrust Zone (MRTZ).

Given the high-grades of metamorphism ie. mid-amphibolite grades (Masberg, 2000; Steven, 1993) during deformation, the marbles of the Karibib Formation are significantly less competent than the meta-arkoses of the adjacent Etusis Formation. As a result, the majority of strain during thrusting was preferentially partitioned into the marbles. Late recrystallization of these marbles is likely to have obliterated most, if not all of the small-scale, tell-tale structures indicative of thrusting, for example S-C fabrics and other kinematic indicators. The Karibib Formation along the southeastern limb of the dome reaches 2 km in thickness, almost double the thickness exposed along the northwestern limb. This significant variation in thickness is likely to be the

result of the intense folding, transposition and duplication the marbles experienced along the footwall of the MRTZ during thrusting.

The dip of the thrust within the study area is uncertain. However, it is generally accepted that a cleavage developed within a shear or fault zone is typically aligned parallel to those high strain domains (e.g. Ramsay, 1980; Davis and Reynolds, 1996). Foliation readings taken from within the Karibib and Chuos Formations adjacent to the MRTZ are northeast-southwest-trending, dipping between 60° and 80° towards the southeast, with steeper readings taken progressively southwest. These readings are used to infer the dip of the MRTZ, which is otherwise difficult to determine from the contact.

4.7 The overall geometry of the southwestern portion of the Usakos dome: a synopsis

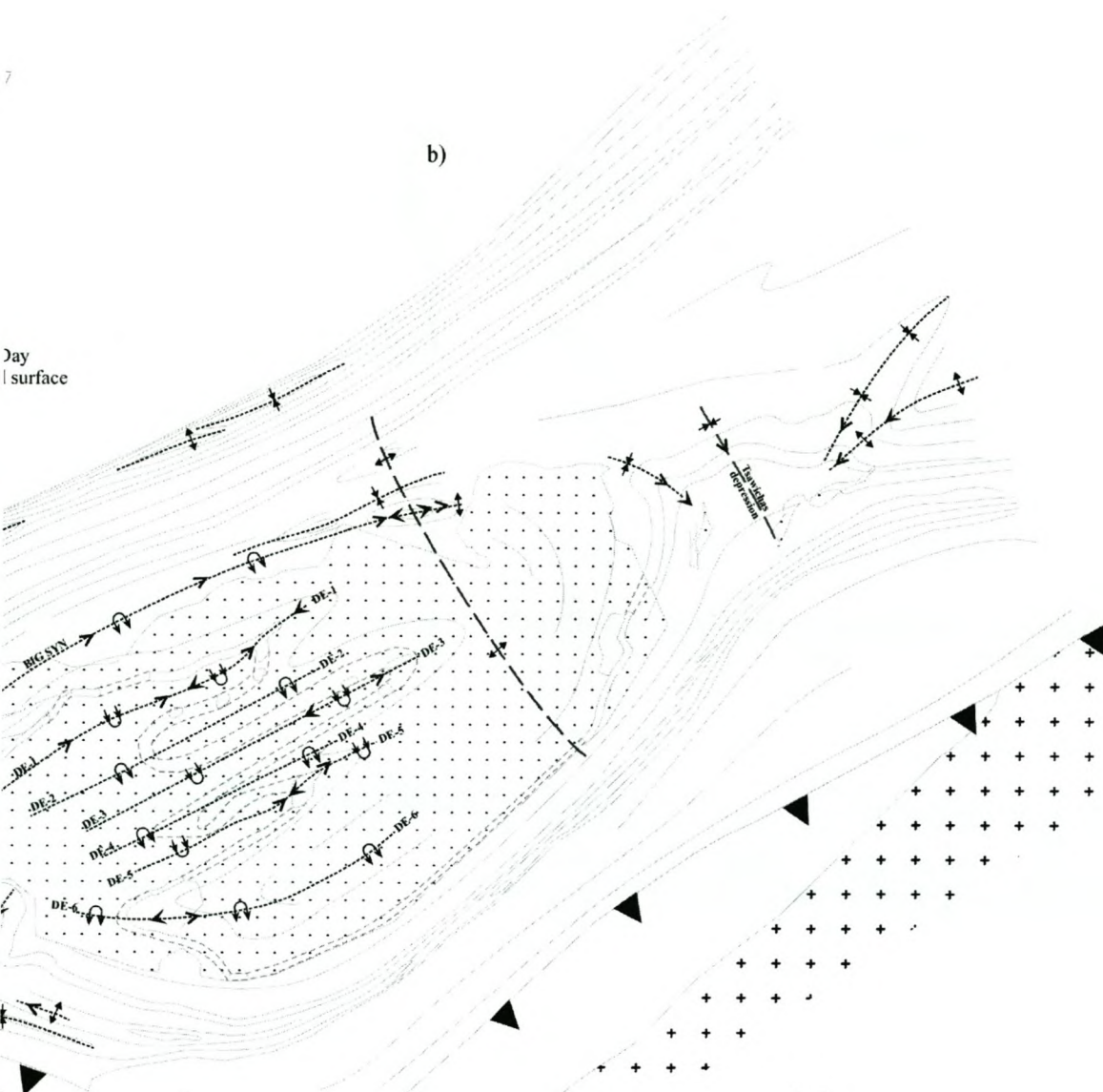
The southwestern lobe of the Usakos dome mapped during this study can be conceptualized as a kilometer-scale anticline bound by two northeast-trending limbs, terminating towards the southwest and cored by a central folded portion intruded by granites (Fig. 4.36 and 4.37).

Fold types, as well as their orientation, amplitude, wavelength, vergence and facing directions vary significantly throughout the dome (Fig. 4.37b). Fold amplitude and wavelength is largely dependent on lithology where the carbonate-rich units deform in a highly ductile manner, forming folds of significantly higher amplitude and lower wavelength compared to the less ductile siliciclastic-rich units. Along the strike length of the dome, there is a significant variation in the plunges of the predominantly northeasterly-trending folds. Folds located in the northeast are northeast-southwest-trending, northwesterly-verging and contain undulating fold hinge lines. Towards the southwest, the northeasterly fold trend persists, but facing directions indicate an overturned stratigraphy within the folds (Fig.4.37). For example, Big Syn, developed as a second-order anticline (100-500 m in half wavelength) in the northeast, can be followed for more than 8 km along its axial trace towards the southwestern hinge of the dome, where it appears as a synformal anticline, i.e. a synformal structure cored by older strata (Fig. 4.10). Fold plunges within these overturned sequences vary between 30° and 70° to the northeast. Along strike, towards the southwestern

boundary of the study area, fold plunges become shallower and folds show a normal younging direction again (Fig. 4.14 and 4.15). This suggests that the northeast-trending folds, referred as F2-early, were subsequently refolded by a gently dipping fold axial plane trending at high angles to the original folding (Fig. 4.38). Evidence for this late-F2 refolding is only apparent within the granite-rich, central portion of the Usakos dome, and not for example within the peripheral Kuiseb Formation.

Several other lines of evidence also point to refolding within the Usakos dome. For example:

1. The presence of northwest-trending folds within an area dominated by a northeast-trending fabric. The Tsawichas depression located in Domain E is an open, northwest-trending fold responsible for rotating centimeter- to meter-scale folds shown in Fig. 4.33. Bedding (S₀) along limbs of folds in Domain A is buckled along northwest-trending hinge lines.
2. The orientation of fold hinge lineations measured from the northeast-trending termination of the dome, when plotted on an equal area stereographic projection, lie along a small circle, plunging towards the northwest (Fig. 4.16f). This suggests the lineations (L_{2b}) were refolded about a northwest-trending fold hinge.
3. The MRTZ along the much of its length forms a linear northeast-southwest strike extent, dipping moderately (ca. 60°) to the southeast. However, along the 90 degree bend in the MRTZ towards the southwestern closure of the dome, the stratigraphy is overturned, and rocks of the Damara Sequence dip to the north, overlying rocks of the AMC. The abrupt 90 degree bend, as well as the northerly dips and overturned stratigraphy are consistent with the refolding of an initially inclined, southwesterly-dipping thrust contact by a northwesterly-trending subhorizontal late-F2 fold. Inclined, northeast-trending surfaces, when refolded about a northwest-trending fold axis (late-F2) will produce curved outcrop patterns while initially subvertical planes, in contrast will show little if any evidence of this refolding. These stratigraphic and geometric relationships suggest that the southeasterly-dipping contact inbetween the Etusis and Karibib Formations was in place prior to the late-D2 refolding event. The linear,



STRUCTURES

- Strike of form line (early-S2 and S0)
- - - - - Inferred Okawayo Formation
- ▼ Mon Repos Thrust Zone
- - - - - Late-F2 Axial Trace
- ∩ Antiformal Syncline
- ∪ Synformal Anticline
- ∓ Syncline
- ± Anticline
- Facing Direction of early-F2 fold
- > Plunge Direction of early-F2 fold

seemingly undisturbed, strike extent of the northwestern limb of the dome therefore reflects its subvertical orientation prior to refolding (late-F2).

These geometric constraints point to late-F2 folding, occurred after the development of the northwest-vergent, early-F2 folds and the MRTZ in map view therefore defines the mushroom-shape of the southwestern portion of the dome, a typical pattern for type-2 interference folding.

Significantly, the resulting overall geometry of the F2a dome structure is interpreted as a kilometer-scale sheath-type fold formed by type-2 (mushroom-type) interference folding. The overturned stratigraphy in the southwest form the overturned limb of the recumbent sheath fold and the southwestern termination of the Usakos dome represents the 'nose' of the southwest-vergent sheath fold (Fig. 4.36a and Fig. 4.39).

The highly strained, northeast-southwest striking limbs (Domains C and D), characterized by a pervasive, steep southeasterly-dipping foliation (early-S2) and layer-normal flattening, are here termed 'straightening zones'. These straightening zones largely comprise marble-rich units of the Karibib Formation where bedding is tightly folded and largely transposed into a subvertical, northeast-trending S0/early-S2 transposition fabric.

In contrast, rocks in the intervening zone between the straightening zones (Domain A) are characterized by a variably trending and significantly shallower-dipping foliation (late-S2) and, in places, improved preservation of primary bedding such as marble breccia horizons (branch i of Domain B). Due to its shallow dip, the late-S2 fabric dominating the intervening zone is oriented approximately normal to the steeply-dipping early-S2 fabric prevalent in the straightening zones.

Metasedimentary rocks, particularly some outcrops of the Okawayo Formation within this central core of the dome are preserved as a 'ghost stratigraphy' within the sheeted granites and are folded into several second-order, open- to tight, northeast-trending folds. The southwestern extent of the dome shows the closure of the first-order fold defining the dome. This closure is sub-divided into an east-west-trending, low-strain domain and a northeast-trending, high-strain domain. The former comprises overturned sequences of the Oberwasser and Karibib Formations dipping towards the

north-northeast, while the latter is characterized by upright, subvertical folds incorporating both the marble-rich units of the Karibib Formation and siliciclastic-rich units of the Kuiseb Formation. Bedding (S_0) along the northeast-trending termination of the dome is often transposed into a steep, northeast-trending S_0 /early- S_2 transposition fabric.

The dome is bound to the southeast by a major thrust, the MRTZ. This thrust predominantly trends northeast-southwest, but describes a prominent 90 degree bend along its southwestern strike extent (Fig. 4.36). Regional considerations, the placement of older on younger rocks and lineation patterns point to a top-to-the-northwest directed sense of displacement.

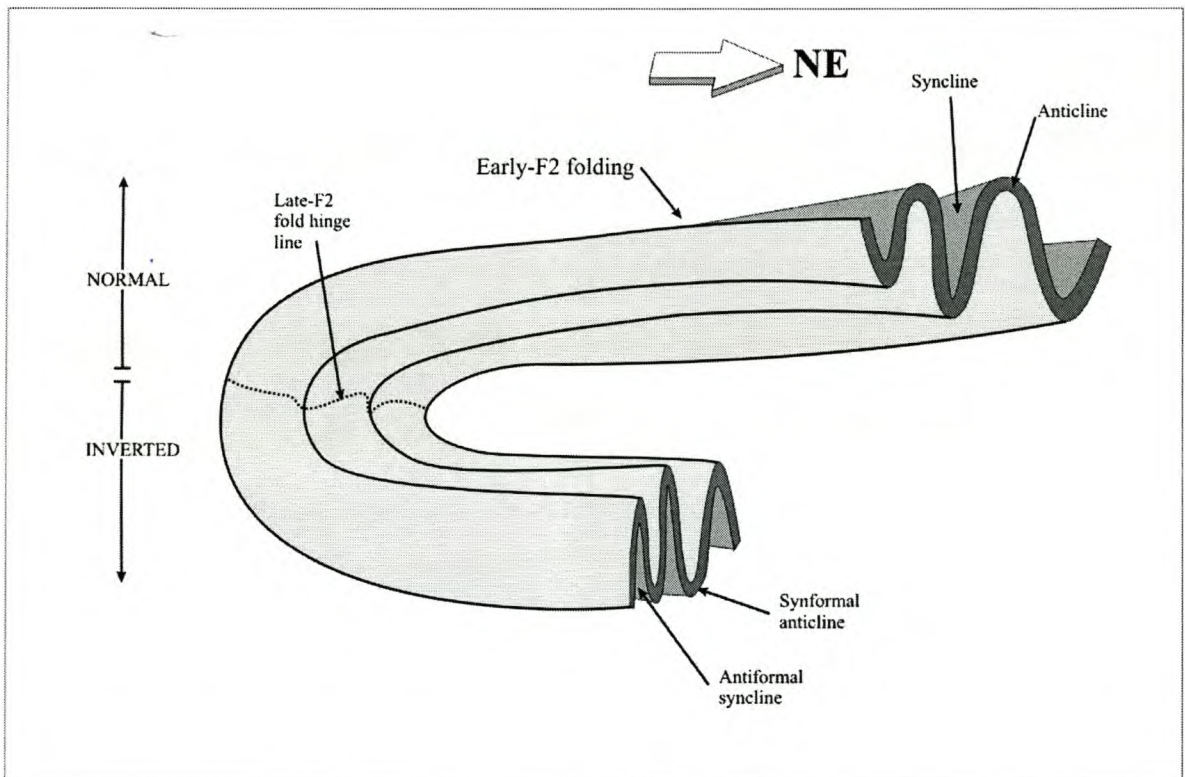


Figure 4.38 Sketch illustrating initially northeast-trending folds (Early-F2) refolded about a gentle northeasterly-dipping fold axis (Late-F2). Lithologies and fold structures along the under-riding limb of the late-F2 fold are overturned. Anticlines when inverted become synformal anticlines and synclines become antiformal synclines.

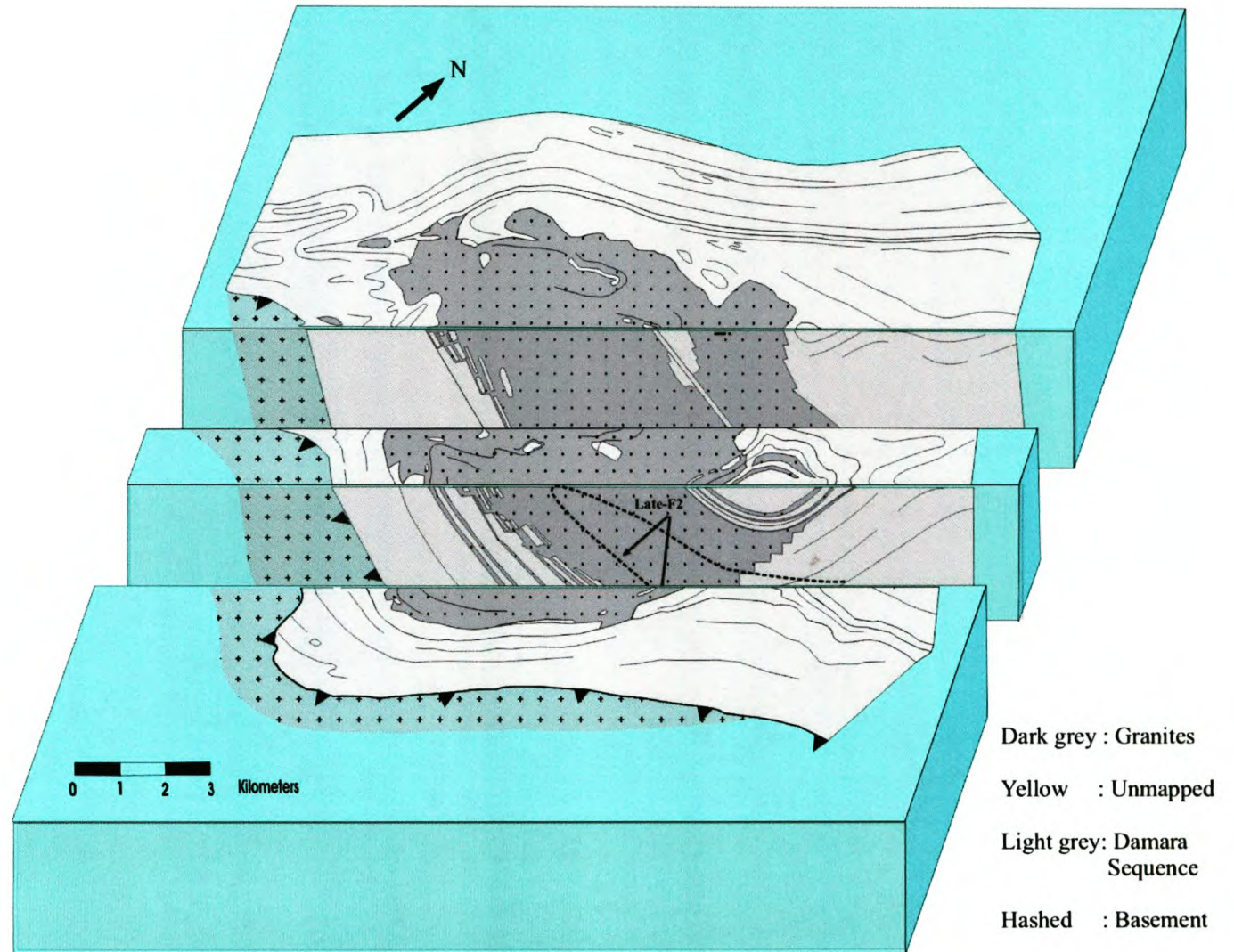


Figure 4.39 Three-dimensional block diagram with longitudinal sections through the Usakos dome, illustrating the southwest-vergent, late-F2 folding of the Damara Sequence within the southwestern portion of the Usakos dome.

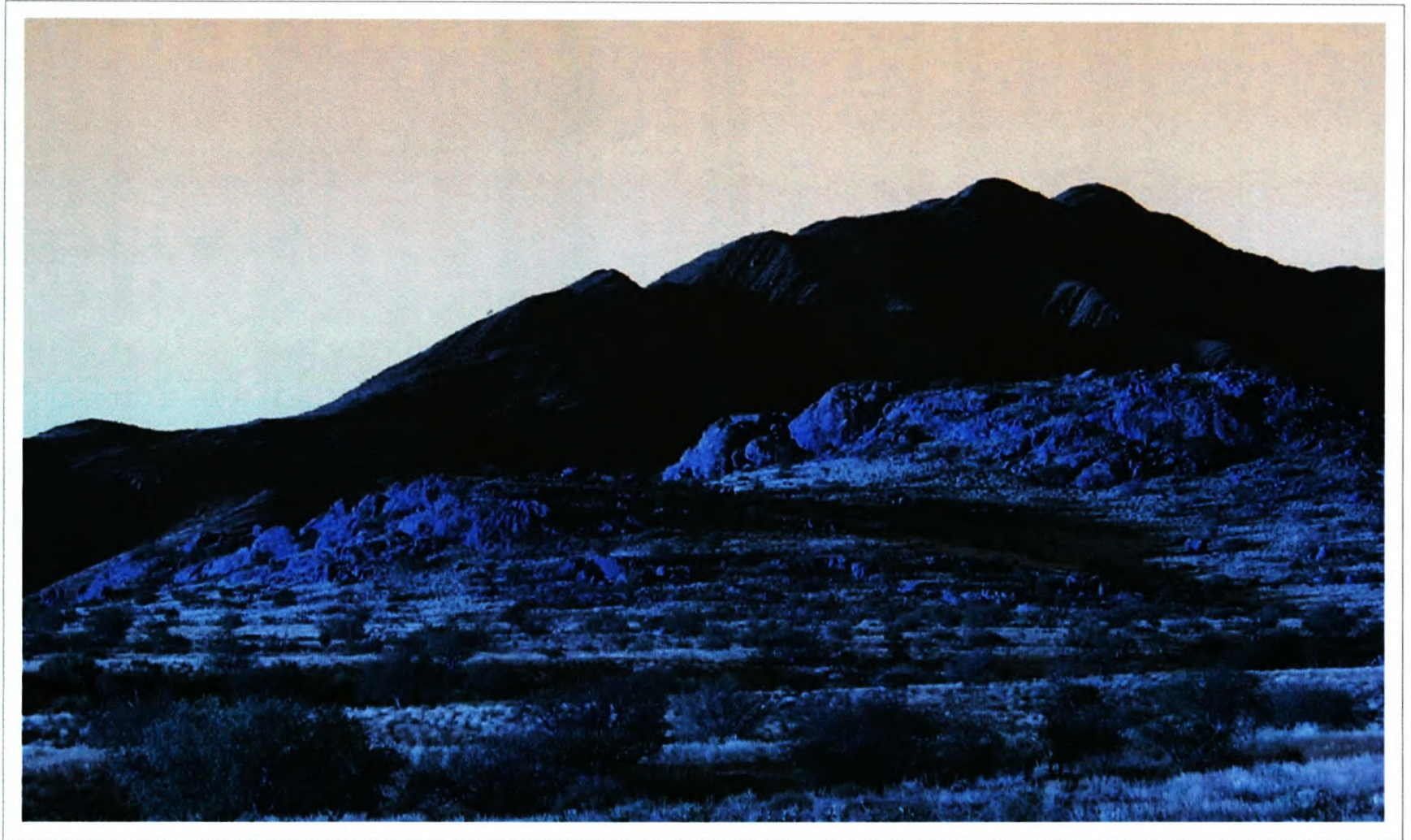


Figure 5.1 Panoramic photograph facing north, showing the granite-rich core of the dome in the foreground (Klein Aukas Granite) and the dark, folded units of the Spes Bona Formation forming the Kranzberg Mountain in the background.

CHAPTER 5 GRANITE AND PEGMATITE INTRUSIONS

5.1 Introduction

The Usakos dome contains numerous Pan-African granitic and/or pegmatitic intrusions which cross-cut and inundate the rocks of the Damara Sequence (Miller, 1985)(e.g. Fig. 5.1). The granites are divided into three types based mainly on mineralogy, geometry and location with respect to the Usakos dome. These are:

- 1) the Klein Aukas granite and pegmatites within the core of the dome,
- 2) the Salem granite, and
- 3) granite sills and dykes along the northwestern limb of the dome (Fig. 5.2).

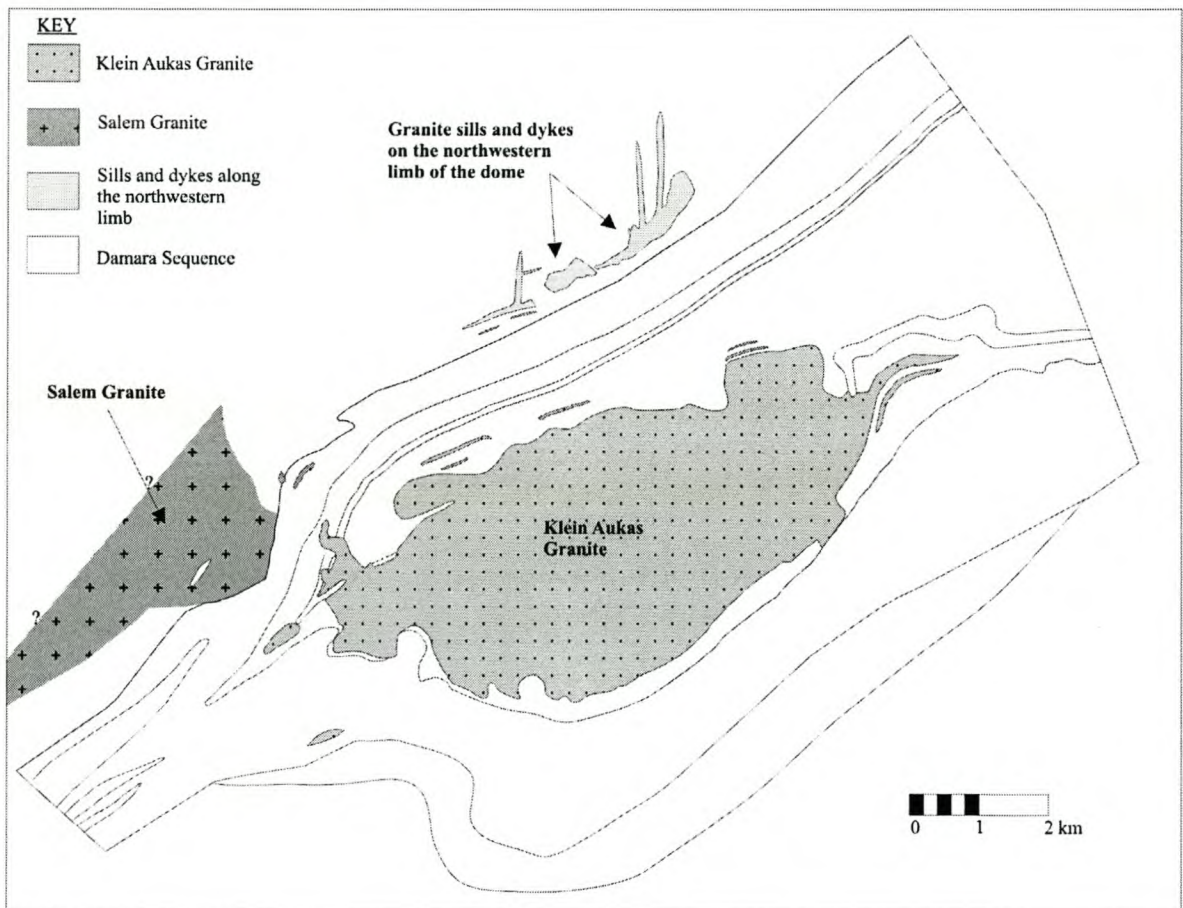


Figure 5.2 Distribution of the three main granite types within the study area of the Usakos dome. For simplicity, small granite sills and dykes are not shown on this map (refer to Appendix I).

The three granites are geometrically distinct. The Klein Aukas granite comprises a large central, sheeted granitic mass with a somewhat diffuse contact, along which leucocratic sills and dykes inundate the country-rock sequence. A detailed map showing the distribution of the Klein Aukas Granite is presented in Appendix I. The Salem granite also forms a large, sheeted igneous body, but with sharp wallrock contacts. Pegmatites along the northwestern limb of the dome form relatively small, sometimes interconnected dykes, sills and pods, rather than a large coherent body.

The spatial association, geometry and relative timing of all three granitoid types suggest a close genetic relationship between granite emplacement and the deformational style exhibited by the Usakos dome. The significance of these intrusives for the formation of the Usakos dome is discussed in Chapter 6.

For the purpose of this study a ‘dyke’ refers to a tabular igneous body which cross-cuts the layering of the country rocks irrespective of its orientation, whereas a ‘sill’ intrudes concordant to the layering of the host rock.

5.2 Salem Granite

A large number of granitic intrusions within the Damara orogen are collectively referred to as the ‘Salem Granitic Suite’ (Miller, 1983). Generally, the Salem Granitic Suite incorporates coarsely porphyritic, biotite-rich monzogranitic and granodioritic rocks containing large, euhedral microcline phenocrysts. The suite also includes coarse-grained, non-porphyritic diorites or tonalites that form the apparently earliest intrusive phases of the granite suite or that appear as marginal phases to the granites (Miller, 1983).

5.2.1 Occurrence and distribution

The Salem granite in the study area is restricted to the southwestern parts of the northwestern limb of the Usakos dome. Miller (1983) described the Salem granite as being confined exclusively to synclines occupied by the Kuiseb Formation. This more or less holds true within the current mapping area, where the Kuiseb Formation, occupying much of the core of the Kranzberg synform northwest of the Usakos dome, is intruded by the Salem granite. However, occasional thin, concordant, subvertical sheets of Salem granite are also observed within the Karibib Formation.

The Salem granite occurs near the boundaries of the study area, and regional maps (Smith, 1965; Miller, 1988) indicate that these outcrops represent the periphery of a much larger pluton exposed to the northwest. Thus, many of the descriptions provided below are likely to be features characteristic of the marginal zones of the pluton and may not necessarily represent the pluton as a whole. The Salem granites within the study area are likely to form part of the southeastern extent of the Stinkbank Granites described by Marlow (1983).

5.2.2 Petrography and macroscopic appearance

The Salem granite exposed within the study area is extremely heterogeneous. A large component of this heterogeneity can be attributed to the fact that the marginal zones of the pluton comprise a number of granitic sheets (see Chapter 5.2.3). Alternating sheets show dramatic variations in composition from dark-grey, biotite-rich units to white, leucocratic granite consisting almost exclusively of quartz and feldspar. Grain sizes are also highly between sheets ranging from porphyritic to equigranular and from medium-grained to pegmatitic. Two distinct phases, however, predominate the Salem granite. These include, firstly, an equigranular biotite-rich granite which is common along the margins of the pluton and, secondly, a porphyritic granitic phase that becomes the predominant granite-type towards the pluton interior.

The biotite-rich granite contains a solid-state pervasive foliation defined by biotite aggregates and flattened quartz grains. It forms a dark-grey, well-foliated, equigranular granite, containing quartz (30%), plagioclase (30%), biotite (25%) and K-feldspar (10%) with accessory sphene, apatite, zircon and garnet and can be mistaken, for example, with schists of the Damara Sequence. However, sharp, angular intrusive contacts with the Damara Sequence identify this unit as being igneous in origin. The porphyritic phase of the Salem granite usually cross-cuts and contains enclaves of the biotite-rich Salem granite, thus representing a relatively later intrusive phase (Fig. 5.3a). The granite consists of 3% to 40% of large, white, euhedral microcline phenocrysts reaching 3 cm in length, within a medium-grained groundmass consisting of quartz (20-30%), biotite (5-15%), K-feldspar (ca. 15%), plagioclase (An₅₀₋₆₀)(ca. 40%) and hornblende (ca. 5%) with accessory sphene, apatite and zircon. It is more abundant and regarded as the diagnostic phase of the Salem

granite, commonly being pale-to medium-grey in colour (Fig. 5.3b). The microcline phenocrysts occur as optically zoned, tabular crystals containing randomly oriented biotite and plagioclase inclusions. Quartz and feldspar in the matrix occur as equant to irregularly-shaped grains 0.5 to 1 mm in diameter. Both plagioclase and microcline are often altered to fine-grained, white mica. Biotite within the matrix is light- to dark-brown, strongly pleochroic reaching, on average, 0.5 mm in length. Biotite exhibits a moderate- to strong preferred orientation, imparting a solid state foliation to the rock. Biotite commonly forms aggregates and is observed in places to concentrate around feldspar phenocrysts. It is partially altered to chlorite. Anhedral hornblende occurs as randomly oriented grains reaching 0.8 mm in length.

The Salem granite contains a distinct layering, not only delineated by alternating intrusive sheets, but also within sheet layering. This within sheet layering is defined by variations in mineral abundances, grain sizes and magmatic fabrics seen on centimeter- to tens of centimeter-scales, and is further discussed in Chapter 5.2.4.

5.2.3 Intrusive Relationships

The Salem granite within the study area forms the southeastern marginal zone of a large pluton extending for several kilometers towards the north and northwest. Generally, the contact between the Salem granite and the Damara Sequence is sharp and, for the most part, concordant with the contact between the Kuiseb and Karibib Formations. Towards the southwest, however, where the Kuiseb Formation is infolded with the Karibib Formation, intrusive relationships are more complex. Some of these relationships are particularly well-exposed within a river valley between S22°04'55" E15°32'30" and S22°04'30" E15°32'15" along the northwestern limb of the Usakos dome, some of which are illustrated in Fig. 5.4. Within this river valley, rocks of the Salem granite truncate meter-scale fold structures developed in calc-silicate felses of the Karibib

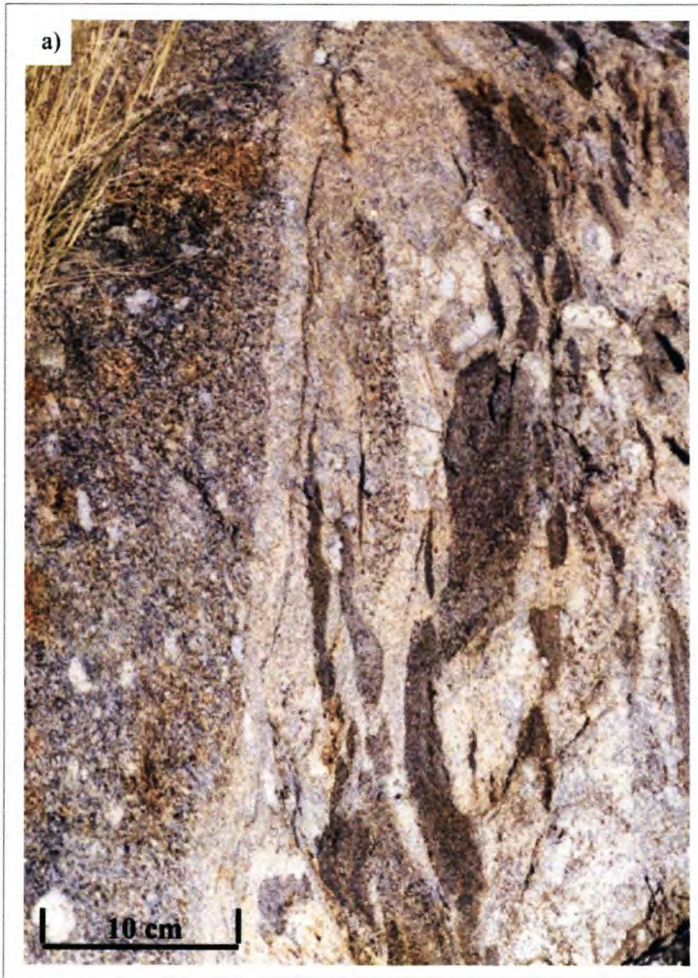


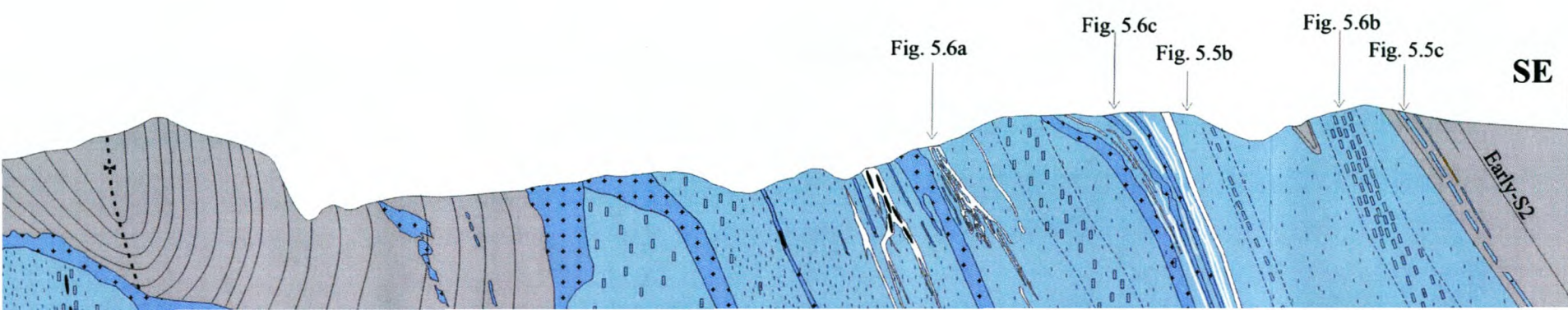
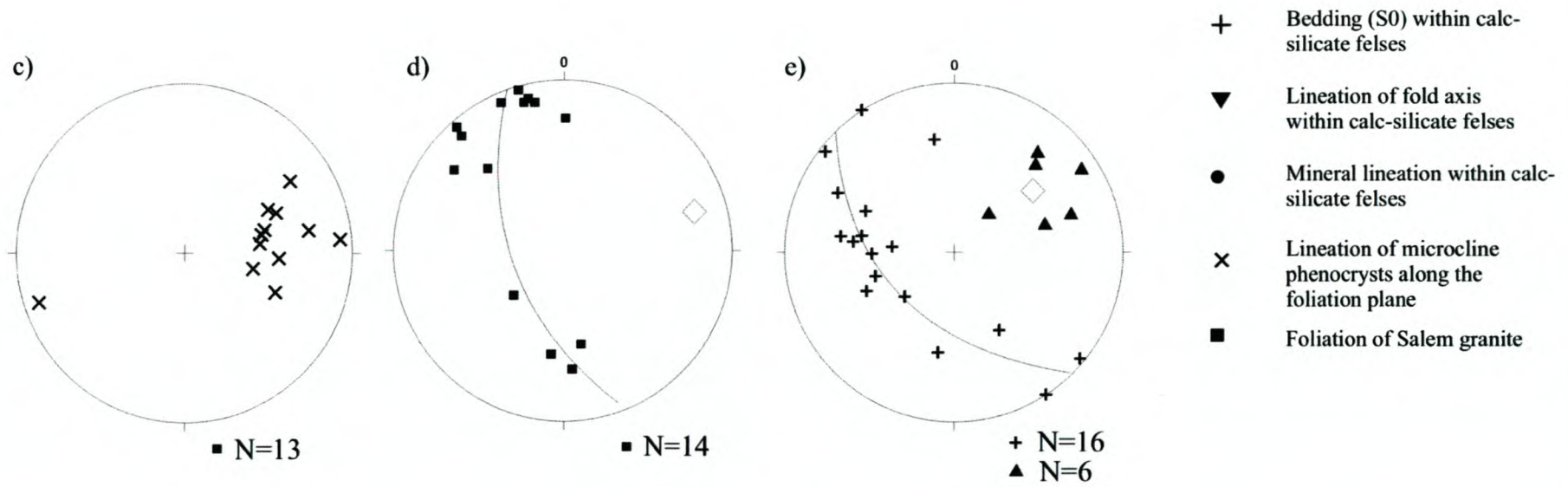
Figure 5.3 a) Contact between two contrasting sheets of the Salem granite. The sheet to the far left comprises porphyritic granite containing few, centimeter-scale mafic enclaves and numerous microcline phenocrysts (white). The sheet to the right is more leucocratic in composition, packed with numerous enclaves and containing relatively fewer microcline phenocrysts. The enclaves occur on a decimeter-scale and have an intermediate to mafic composition, comparable to the early biotite-rich phase of the Salem granite. Within both sheets, the preferred orientation of the enclaves and microcline phenocrysts is parallel to the sheet contacts. The photograph is taken in plan view, top to the southwest. (b) A typical outcrop of the porphyritic-type of the Salem granite with the large, white microcline phenocrysts and the

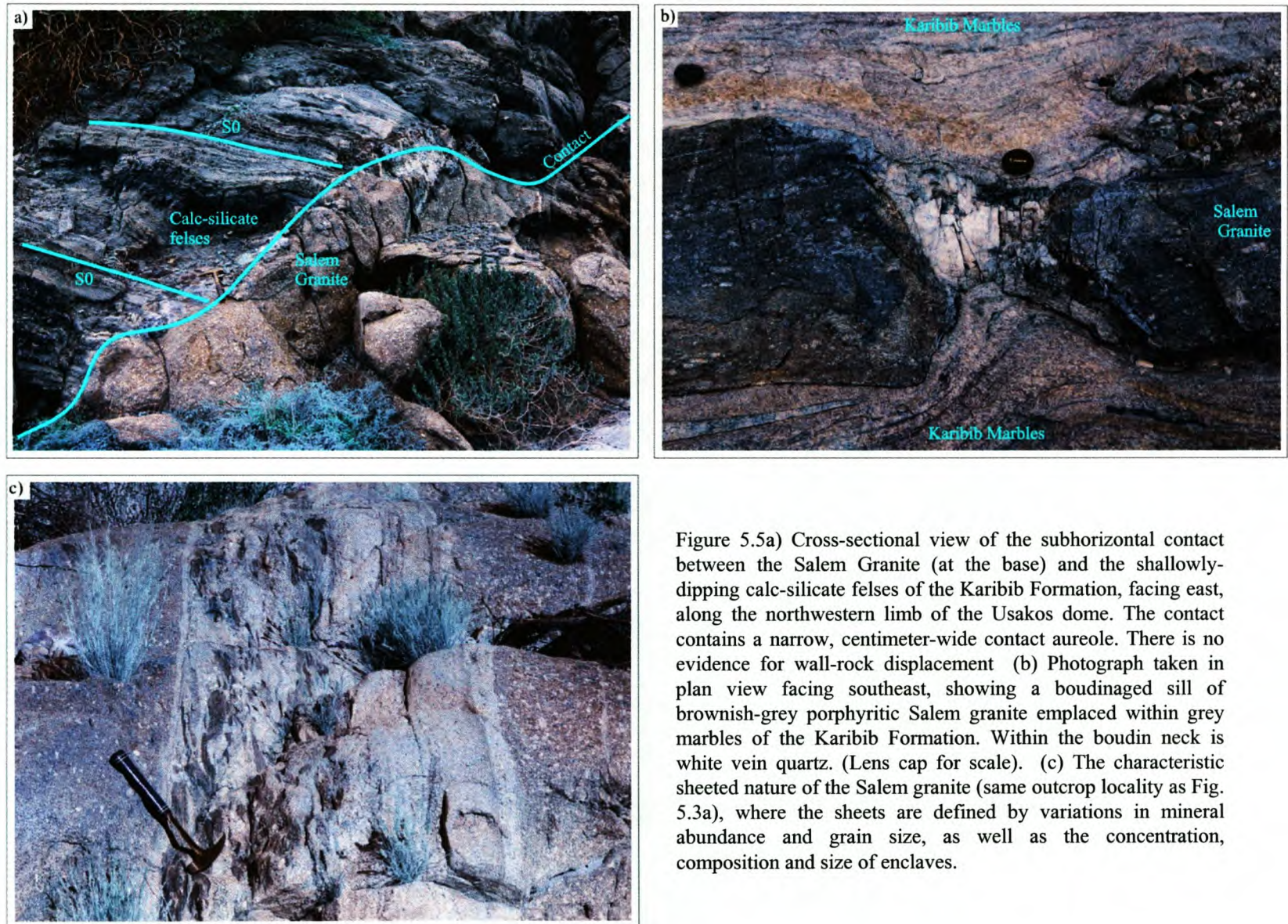


Formation along a slightly undulating, subhorizontal upper contact that can be followed for several hundred meters (Fig. 5.4 and 5.5a). This particular contact suggests the Salem granite intrudes the Damara Sequence as a large, subhorizontal sheet, of which only the upper contact and marginal zones are exposed. A few meters from the contact between the Salem granite and the Karibib Formation, occasional subvertical, northeast-trending sills of porphyritic Salem granite intrude the marbles of the Karibib Formation. These sills are ca. 50 cm wide, exposed over minimum strike lengths of 20 m and are boudinaged along strike (Fig. 5.5b).

The 700 m wide, southeastern marginal phase of the Salem granite is characteristically built up of intrusive sheets. Individual sheets are distinguished by conspicuous variations in mineral abundance, grain-size, magmatic textures and proportion of enclaves (Fig. 5.3a and 5.5c). The sheets are planar, parallel-sided and can, outcrop permitting, be traced for several meters to tens of meters along strike. Sheets range between 30 cm to several meters in thickness and are separated by either sharp or gradational boundaries. Some of the more gradational contacts are characterized by complex intermingling of Salem phases, for example between the biotite-rich and porphyritic phases. This intermingling is likely to have formed prior to the complete crystallization of the magma by hybridization between compositionally distinct, adjacent sheets (Fig. 5.6a) (Fernández et al., 1997). The continuity of magmatic crystal growth across sheet margins and the complex magma intermingling textures suggests that the sheets intruded into one another while the hosting sheets retained some melt (Blenkinsop and Treloar, 2001). The sheeted nature of the granite is particularly prominent along the southeastern margin of the pluton, becoming progressively diffuse further northwest, ca. 700 m away from the pluton periphery and into the centre of the pluton, where a more uniform, medium-grey, porphyritic phase of the Salem granite is developed.

Intrusive relationships between the different phases of the Salem granite illustrate multiple granite sheeting and a sequence of magmatic pulses. Based on cross-cutting relationships, the dark, biotite-rich granite represents the initial magmatic phase,





followed by the light-grey porphyritic granite and the leucocratic granite. These phases were ultimately intruded by pegmatites.

5.2.4 *Fabrics*

The Salem granite within the current study area preserves well-developed micro- and mesoscale fabrics. These are mainly planar and/or linear fabrics defined by the preferred orientation of minerals and/or mafic enclaves, variations in mineral proportions, micro-textures and/or variations in grain sizes. The main features that contribute to the composite fabrics within the Salem granite are discussed below.

1) Variation in grain sizes and mineral proportion within granitic sheets

Some sheets show a distinct internal layering recognized by variations in the relative proportion of minerals and their grain sizes (Fig. 5.3b and 5.6b and c). This layering trends northeast-southwest and exhibits an asymmetrical pattern along the width of the sheets. It is particularly prominent within the leucocratic-rich phases of the Salem granite.

2) Preferred Orientation of euhedral microcline phenocrysts

Microcline phenocrysts often define a planar and linear fabric within the Salem Granite (Fig. 5.3c). They form euhedral to subhedral, commonly compositionally zoned grains, interpreted to have crystallized directly from a magmatic phase. On a microscopic scale, the grain boundaries of the phenocrysts vary from being straight to highly irregular. The irregular grain boundaries are bound by microscopic intergranular aggregates of quartz and feldspar grains (<0.2 mm in diameter) that form lobate grain contacts with the phenocrysts (Fig. 5.7a). Myrmekitic intergrowths between quartz and feldspar are also common along these irregular grain boundaries (Fig. 5.7b).

The long axis of the tabular microcline phenocrysts is often preferentially aligned defining a prominent northeast-trending planar fabric and a moderate east- to northeast-plunging lineation along foliation planes (Fig 5.4b and d). The planar fabric defined by the phenocrysts is generally parallel to the northeast-trending granite margin and/or the

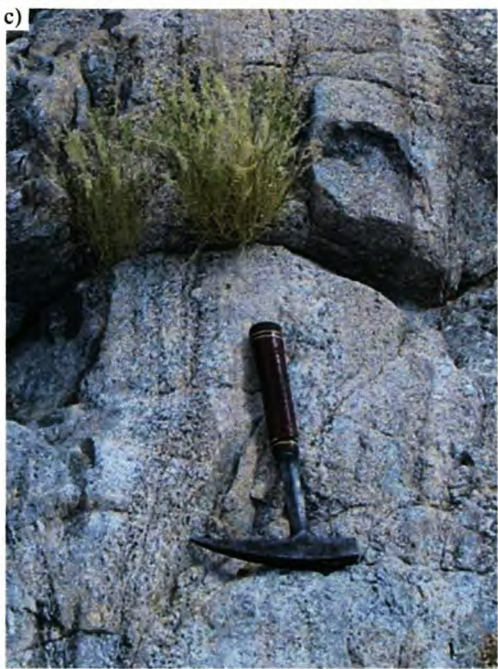
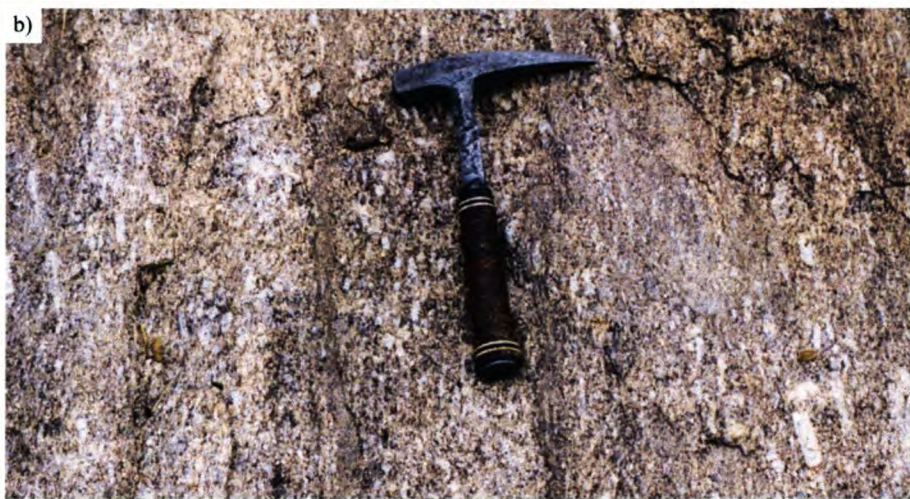


Figure 5.6a) Magmatic features within the Salem Granite characterized by Dark, biotite-rich clots of Salem Granite surrounded by, and, intermingling with microcline-rich pods of Salem Granite. This fabric appears magmatic in origin, formed by magma mingling. (b) Internal layering within a sheet of the Salem Granite. The dark-grey layers are defined by linear aggregates of biotite, forming a characteristic magmatic schlieren layering. The microcline phenocrysts show a strong preferential linear alignment, also defining a layering, parallel to the schlieren. (c) Internal magmatic layering within the Salem Granite, defined by variations in mineral abundance and grain sizes.

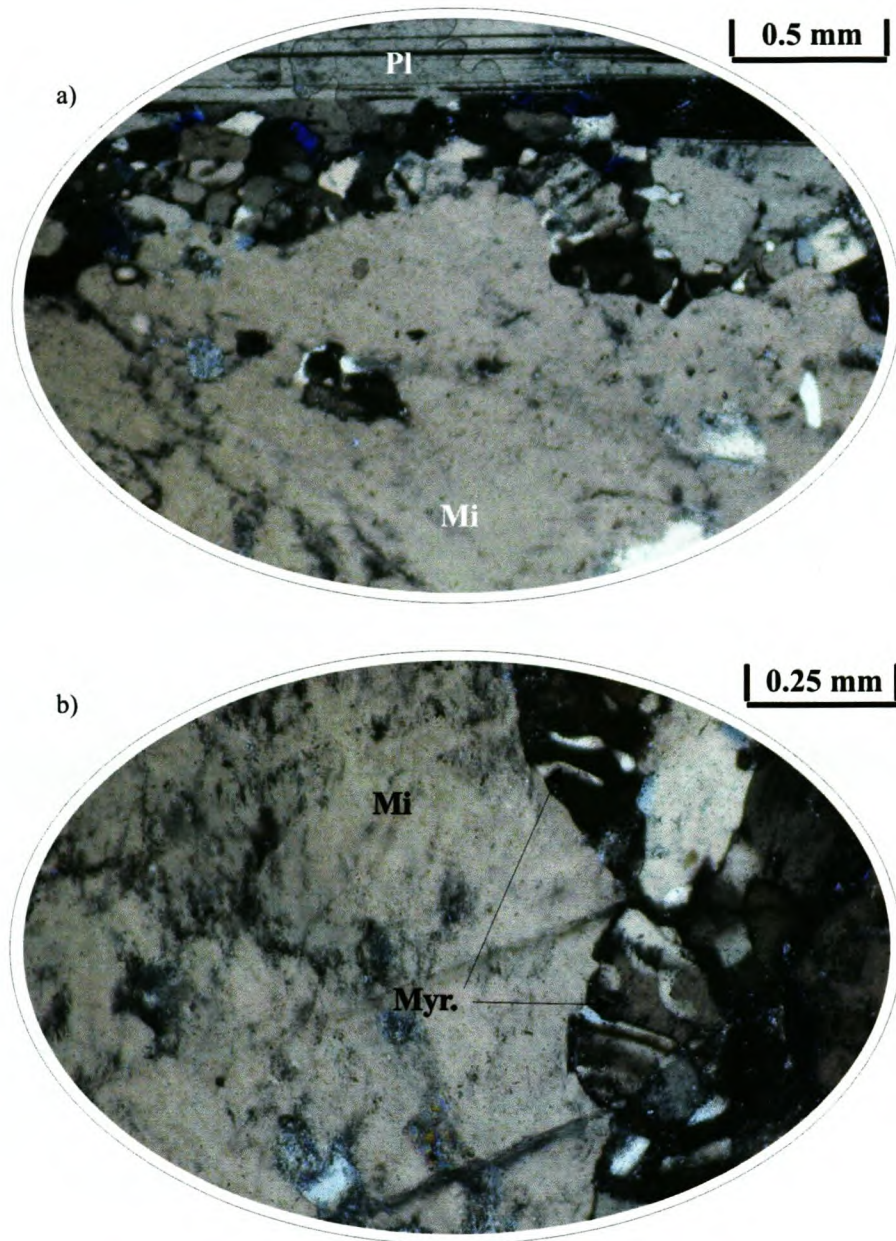


Figure 5.7 a) Photomicrograph (XPL) of the porphyritic phase of the Salem granite showing recrystallized myrmekites (comprising quartz and feldspar) along an irregular grain boundary between a microcline phenocryst (Mi) and plagioclase (Pl). (b) Photomicrograph (XPL) showing myrmekitic textures along an irregular grain boundary of a microcline phenocryst taken from the Salem granite.

internal sheeting of the granite, which in turn, is parallel to the early-S2 fabric in the wall rocks. The alignment of phenocrysts is particularly strongly-developed within thin subvertical sill-like sheets (<3 m in thickness). The alignment of phenocrysts becomes less prominent within the thicker granite sheets (>3 m in thickness) and a more random orientation is developed further away from the pluton boundary. Although the preferred orientation of these phenocrysts trends northeast-southwest, localized variations in the alignment also occur. For example, a subhorizontal planar fabric is developed along parts of the subhorizontal granite-host rock contact (S22° 04' 18"; E15° 32' 18") (see X in Fig. 5.4).

3) Biotite fabrics

The concentration of biotite varies significantly between and within alternating sheets of the Salem granite from biotite-rich phases to relatively biotite-poor, leucocratic phases. The preferred alignment of strain-free, basal sections of biotite grains imparts a moderate- to strong, penetrative planar fabric onto the granite. This subvertical, northeast-trending fabric is strongly developed within the biotite-rich phase of the Salem Granite, where it resembles a gneissosity. This gneissosity is parallel to the early-S2 in the wall rocks. Within the porphyritic phase of the Salem Granite biotite commonly occurs in aggregates that form bands. In places, these bands wrap around large grains such as feldspar. Tapering aggregates of biotite are also observed within the strain shadows of the phenocrysts, flanking the short crystal faces of feldspar phenocrysts (Fig. 5.8). Within leucocratic phases, isolated tabular grains of biotite are often aligned forming a northeast-southwest-trending foliation. In places, these biotite grains form elongate clusters, defining schlieren textures (Fig. 5.6b). These schlieren consistently trend northeast-southwest, parallel to most of the planar fabrics within the granite.

4) Quartz and Feldspar fabrics

Plagioclase forms elongate, subhedral grains that are commonly aligned, defining a northeast-trending fabric in plan view. Some plagioclase grains preserve primary optical zoning (Fig. 5.9a), while others contain deformation twins and kink bands (Fig. 5.9b and c).

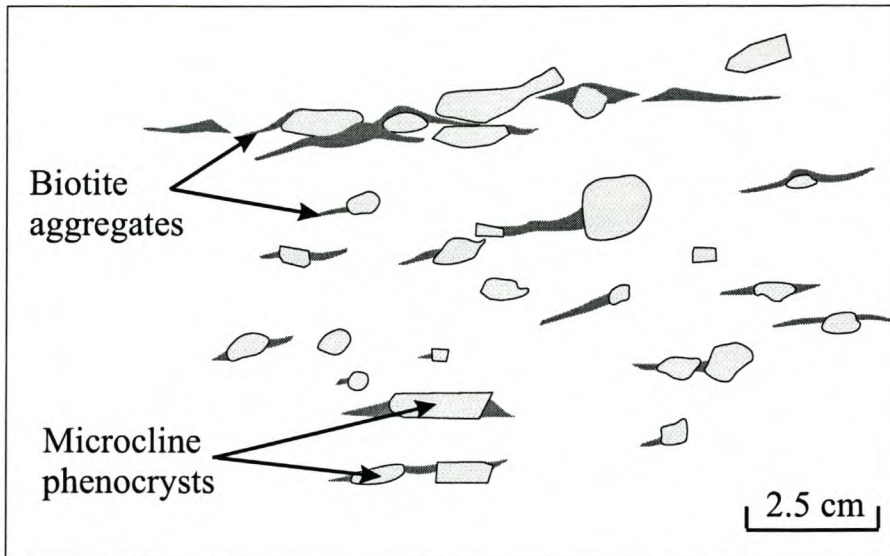


Figure 5.8 Sketch showing biotite aggregates concentrated along the strain shadows or short crystal faces of microcline phenocrysts within the Salem granite.

Perthitic textures within alkali-feldspar are common (Fig. 5.10a). Quartz within the matrix forms both equant, strain-free grains joining along triple junctions (Fig. 5.10b), as well as anhedral grains exhibiting undulose extinction and the development of irregular subgrain boundaries (Fig. 5.10c, d). The anhedral quartz grains are often elongate and oriented parallel to the fabric defined by biotite laths, microcline phenocrysts and plagioclase grains (Fig. 5.10c).

5) Enclaves

The marginal zone of the pluton contains abundant mafic enclaves, that show a preferred alignment, thus defining a planar fabric within individual sheets (Fig. 5.3a and 5.5c). They are typically elongate or sigmoidal in shape with drawn out, wispy tails containing an internal foliation parallel to the long axis of the enclave. Generally, the long axis of the enclaves trends northeast-southwest, parallel to the extent of the sheeting.

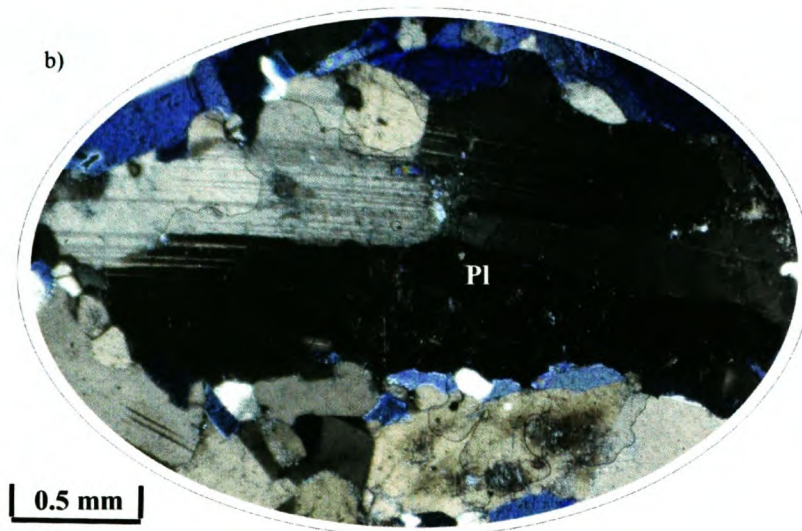
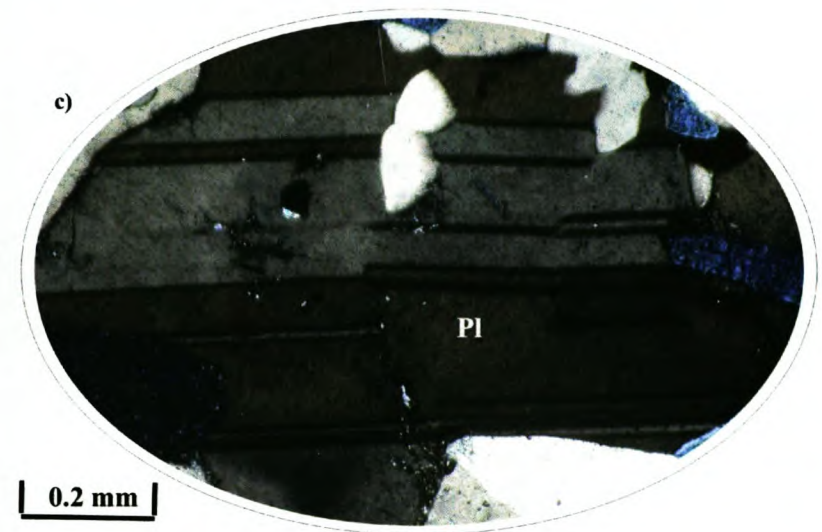
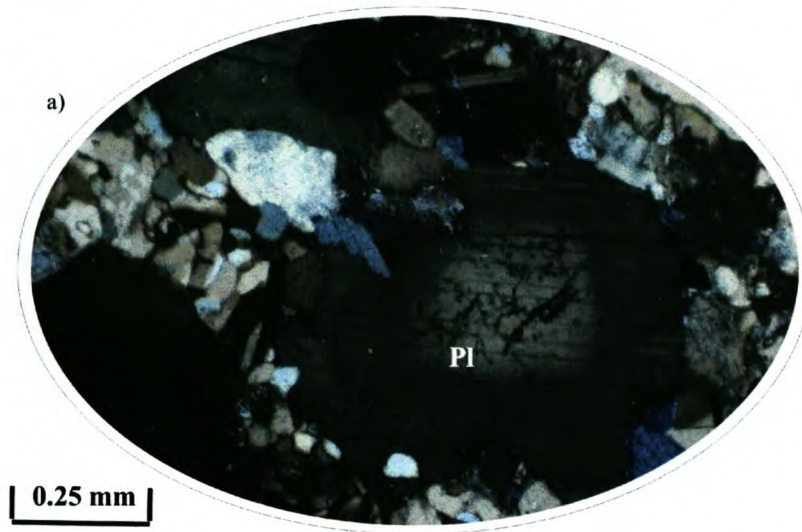


Figure 5.9 a) Photomicrograph (XPL) showing optical zoning within a plagioclase grain within the Salem granite.

(b) Photomicrograph (XPL) of a plagioclase grain from the Salem granite exhibiting subgrain boundaries and deformation twins.

(c) Photomicrograph (XPL) showing microfractures within a plagioclase grain from the Salem granite.

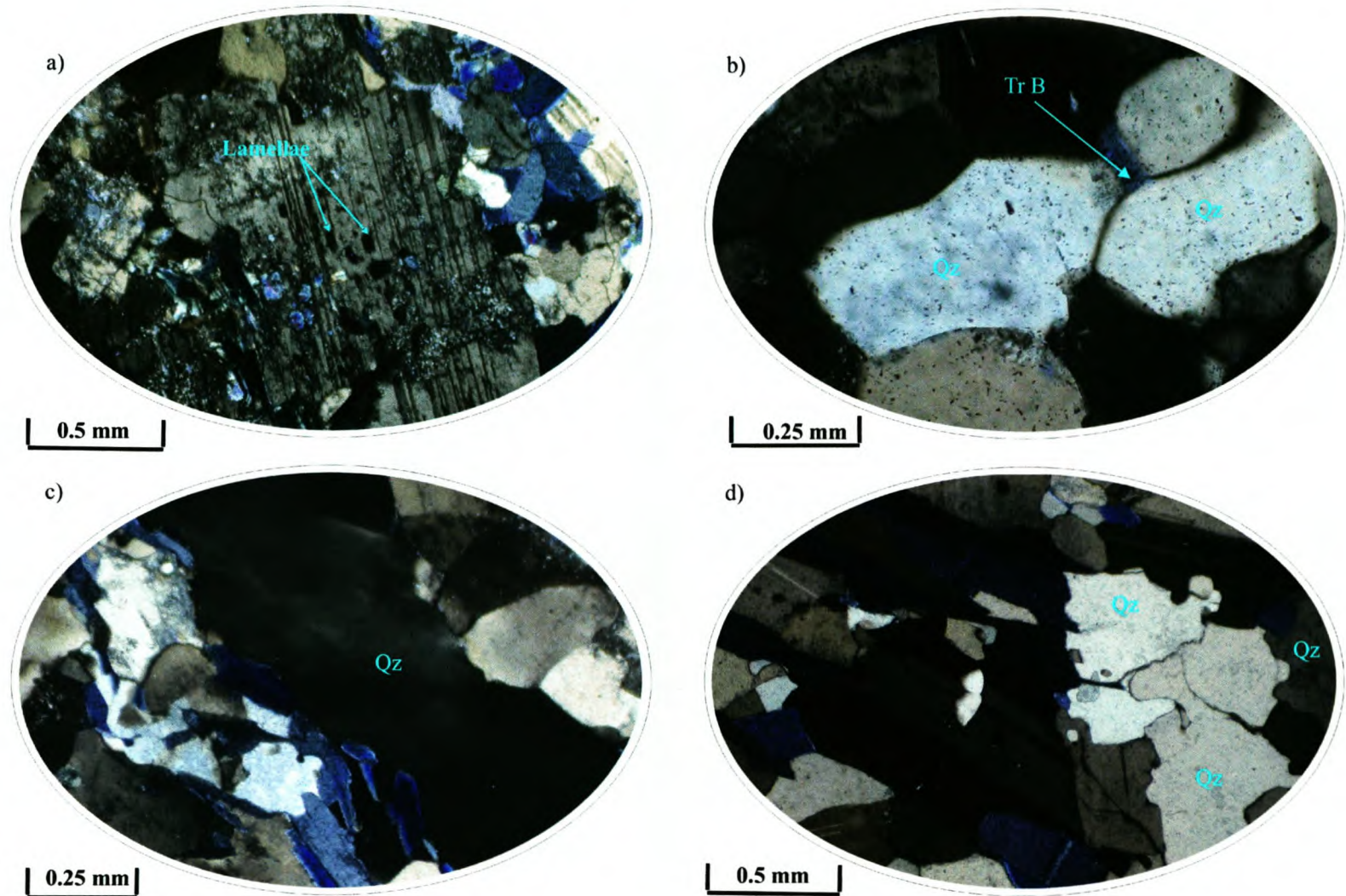


Figure 5.10 a) Photomicrograph (XPL) taken from the Salem granite, showing perthitic textures within K-feldspar. b) Photomicrograph (XPL) showing annealed quartz within the Salem granite. Note the triple junction between grains (Tr. B) and the relatively smooth grain boundaries. c) Photomicrograph (XPL) showing undulose extinction of quartz from the Salem granite. d) Photomicrograph (XPL) showing irregular grain boundaries of quartz from the Salem granite.

The enclaves vary in size from <1 cm to 30 cm in length and commonly show aspect ratios of, in plan view, between 2:1 and 6:1. In places, the enclaves are highly attenuated, defining a compositional layering that resembles schlieren. The relative abundance and grain size of minerals within individual enclaves appears to vary significantly and it is not uncommon to see several compositionally distinct enclaves within the same granitic sheet (Fig. 5.3a and 5.5c). The size, shape, density and composition of the enclaves may vary significantly from sheet to sheet (Fig. 5.5c). The origin of the enclaves within the Salem granite is uncertain. The majority of enclaves are biotite-rich granite. However, few enclaves near the granite margin can be correlated with calc-silicate felses from the surrounding country rock of the Karibib Formation. There is, therefore, likely to be a combination of magmatic and metasedimentary enclaves within the Salem granite. Enclaves comprising the Damara Sequence, however, lack the preferred orientation and elongate nature, characteristic of most enclaves.

5.3 Klein Aukas Granite

Medium- to coarse-grained leucogranites and pegmatites invade the metasedimentary rocks within the core of the southwestern portion of the Usakos dome. For the purpose of this study, these igneous rocks are referred to as the Klein Aukas granite, after the farm Klein Aukas 68 situated between E15°34' S22°3' and E15°38' S22°10'.

5.3.1 Occurrence and distribution

The Klein Aukas granite, for the most part, intrudes in to the lithostratigraphic units below the Karibib Formation and is only evident within the core of the southwestern portion of the Usakos dome (Fig. 5.1). The Klein Aukas granite incorporates a large central, granitic mass grading laterally into abundant leucocratic sills and dykes that inundate the Damara Sequence. The northeastern extent of the Klein Aukas granite occurs within the Tsawichas depression at S22°03'00", E15°38'50" while its northwestern, southeastern and southwestern extents generally coincide with the lower contact of the Karibib Formation.

5.3.2 Petrography and macroscopic appearance

The Klein Aukas granite is a garnet-bearing, two-mica leucogranite comprising mostly quartz, alkali-feldspar, muscovite, biotite and garnet with accessory apatite, beryl, schorl and zircon. The granite is generally an equigranular leucogranite, although grain size and relative proportion of minerals are distinctly heterogeneous throughout its extent. This heterogeneity is largely due to the fact that the Klein Aukas granite is built up of coalesced intrusive sheets distinguished by variations in mineral proportions and grain sizes (Fig. 5.11a) (see description of intrusive relationships in Chapter 5.3.3). The grain size of the granite varies from being medium-grained to pegmatitic.

Alkali feldspar and quartz are by far the most abundant minerals, forming euhedral to anhedral grains often intergrown to form graphic textures. Garnet is dark-red in colour and commonly forms euhedral, poikiloblastic grains ranging between 2 mm and 5 cm in diameter. Quartz and tourmaline form inclusions within the garnet. Garnet is, in places, relatively scarce, but it can also be concentrated within specific layers or pockets forming up to 60% of the rock. Garnet grains are, in places, surrounded by radiating, dendritic muscovite. Biotite and muscovite appear as random to well-oriented laths. They also vary in concentration between and within individual sheets, from being nearly absent to abundant.

5.3.3 Intrusive Relationships

The Klein Aukas granite consists of numerous intrusive sheets and can be broadly sub-divided into a marginal zone and a central body. The marginal zone along the limbs of the dome is characterized by lit-par-lit intrusive relationships between the Klein Aukas granite and the Damara Sequence (Fig. 5.11b). There is a clear preference for sheets to intrude the siliciclastic units of the Spes Bona and Oberwasser Formations, compared to the marble-rich units of the Okawayo and Karibib Formations where granite intrusions are scarce. It is not uncommon to find granitic sheets making up >75% of the rock volume within siliciclastic-rich host rocks, whereas, upon crossing a contact into a marble-rich horizon, granites are no longer observed (Fig. 5.12).

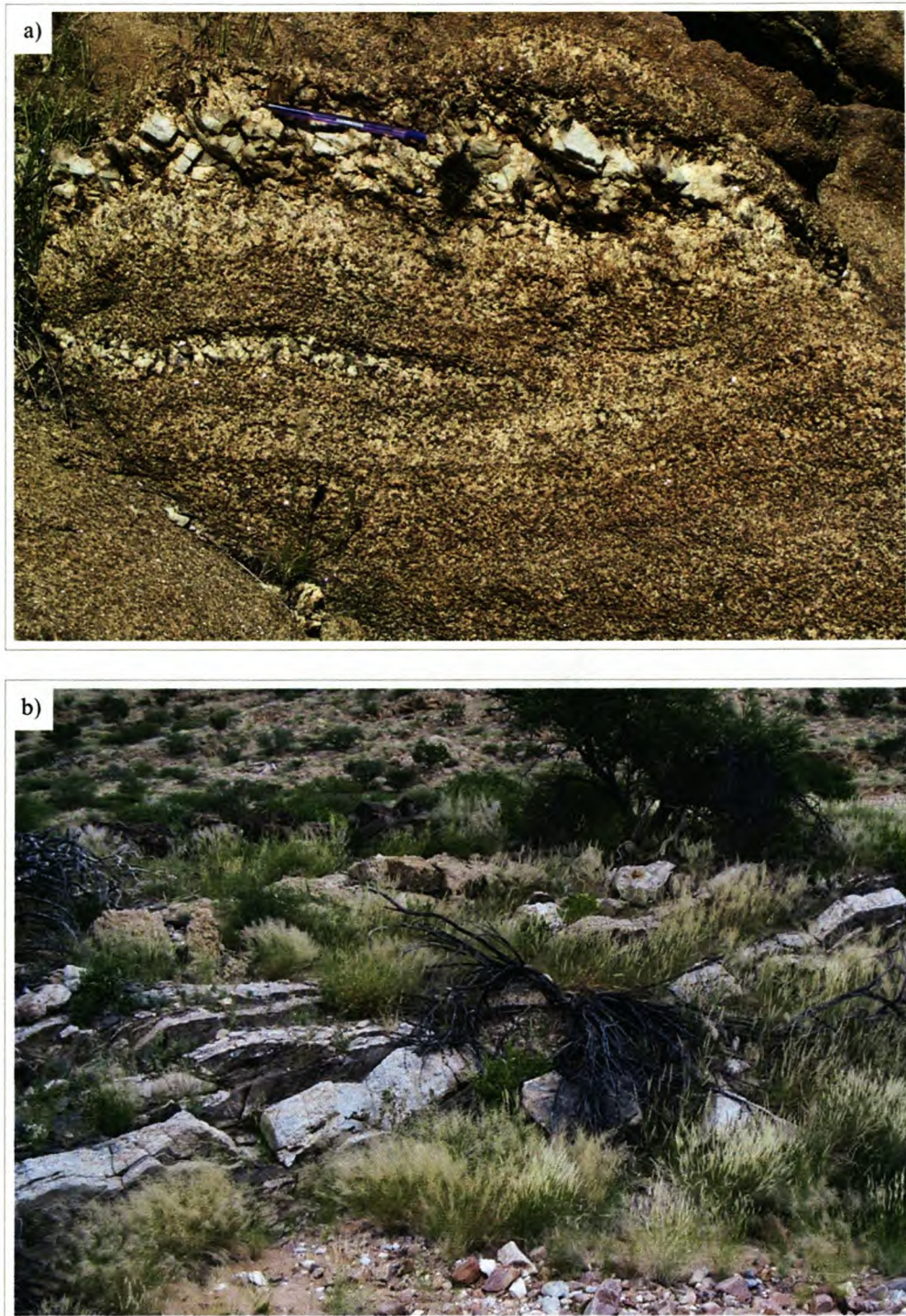


Figure 5.11 a) Variations in grain size and mineral abundance define an internal layering within the Klein Aukas granite. Pen for scale. (b) Steeply-dipping, white, leucocratic lit-par-lit intrusions characterize the marginal zones of the Klein Aukas granite. These sills, here intruding schists of the Oberwasser Formation, are particularly abundant within the siliciclastic-rich lithologies. The photograph is taken facing south.

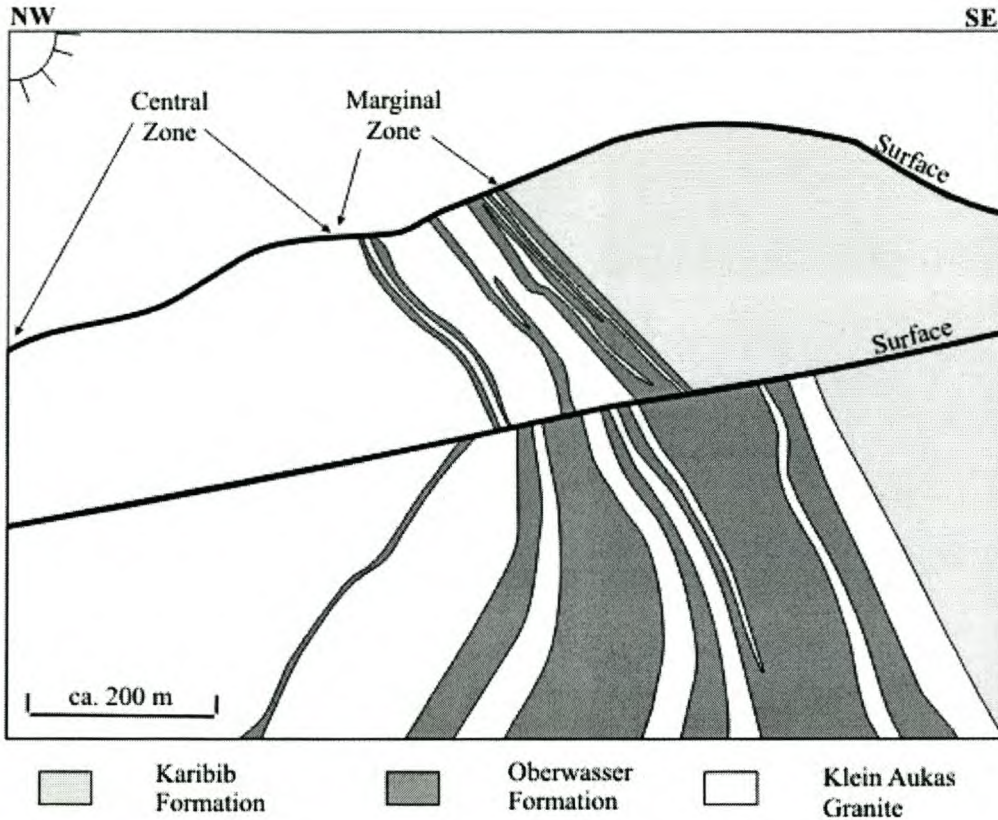


Figure 5.12 Sketch of a typical landscape observed along the southeastern limb of the dome, facing northeast. The steep, southeasterly-dipping Karibib Formation contains few if any granitic intrusions, whereas, within the adjacent schists of the Oberwasser Formation, numerous sills of the Klein Aukas granite inundate the sequence. Progressively closer to the core of the dome, the number and size of sheets increases, forming the central zone of the Klein Aukas granite, comprising amalgamated sheets with only isolated screens of supracrustals.

Granitic sheets within the siliciclastic units predominantly intrude as sills parallel to folded bedding of the host rocks (Fig. 5.13a, b). They vary in thickness from <1 cm to >15 m and can be traced from a few meters to several kilometers along strike. The sheets occasionally bifurcate and converge, forming horn and bridge structures before pinching out along strike (Fig. 5.13b). Some sills along the marginal zone of the Klein Aukas granite are strained, exhibiting chocolate-tablet boudins. Boudins are particularly evident along the steep to overturned northwestern limb of the dome (Fig. 5.14).

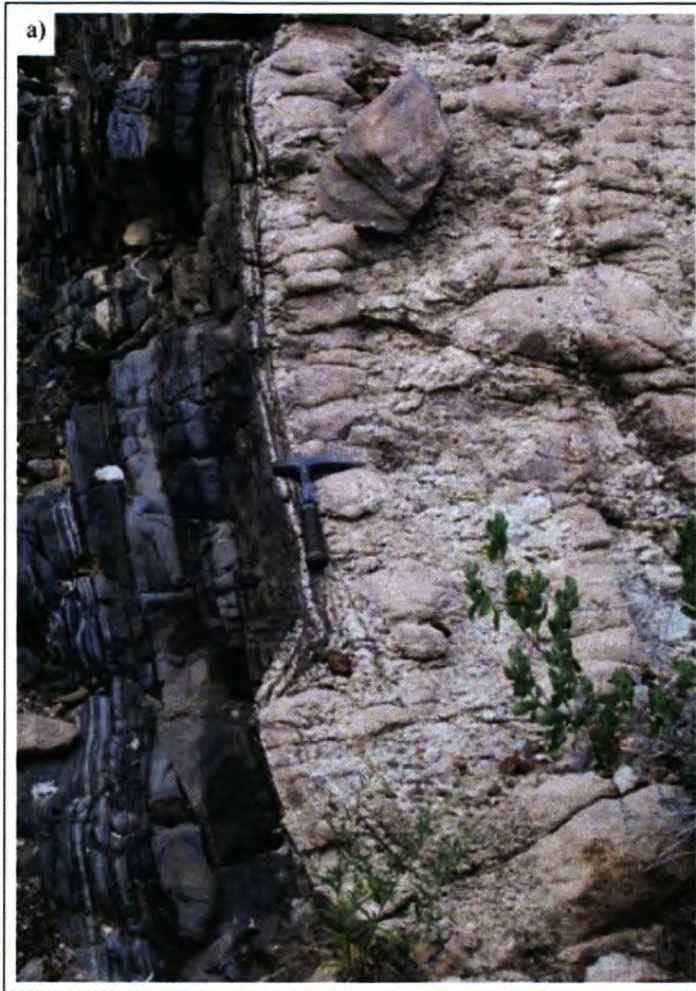


Figure 5.13 a) Photograph showing a plan view of a contact between a sill of Klein Aukus granite and the siliciclastic-rich lithologies of the Oberwasser Formation along the southeastern limb of the dome, facing northeast. Notice how the granite-host rock contact, the bedding of the Oberwasser Formation and the layering within the granite are sub-parallel. (b) Plan view of some horn and bridge structures observed along sills of the Klein Aukus granite intruding the Oberwasser Formation along the southeastern limb of the Usakos dome.





Figure 5.14 Quartz-rich pegmatite intruded into the Kuseb Formation along the northwestern limb of the dome has subsequently undergone boudinage.

In addition to the northeast-trending sheets along the marginal zones of the Klein Aukas granite, there are also volumetrically minor, irregularly-shaped, tens-of-meter-scale granitic pods commonly linking the sill-like intrusions. Examples of these are shown in Fig. 5.15 where the pod-like granites cross-cut the Okawayo Formation at high angles, linking the adjacent granitic sheets. Overall, this concordant and discordant relationship of the granite forms an interconnected network of granitic sheets inundating the metasedimentary sequence, particularly the siliciclastic units along the limbs of the dome.

Generally, the number and width of granitic bodies increases progressively, towards the core of the dome (Fig. 5.12). The transition between the marginal zone and the central zone of the Klein Aukas granites occurs where the subvertical sheets along the marginal zones branch into gently-dipping sheets towards the core of the dome. Fig. 5.16 illustrates this transition for the northeastern limb of the dome.

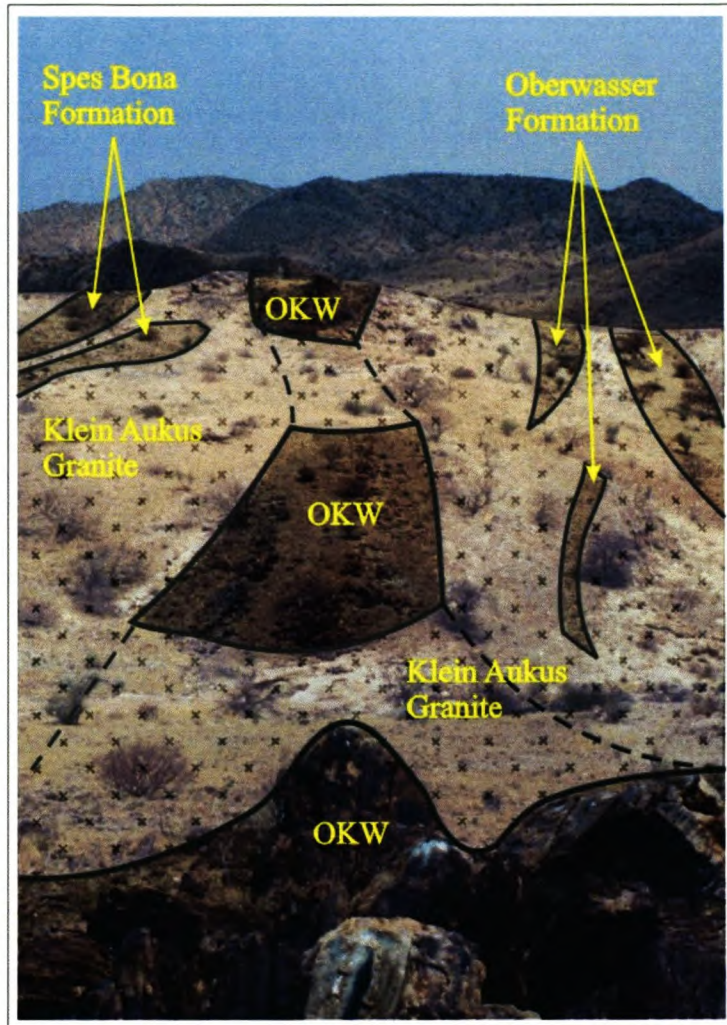


Figure 5.15 Photograph showing the ghost-stratigraphy preserved within the Klein Aukas Granite. The northeasterly trending Okawayo Formation (OKW) is disrupted along strike by dykes of Klein Aukas granite that link bedding-parallel sills. There is no apparent rotation of bedding within the isolated screens of the Damara Sequence between the granite sheets. The photo is taken along the northwestern limb of the dome, facing southwest. The granite exposure is highlighted with a hashed shading.

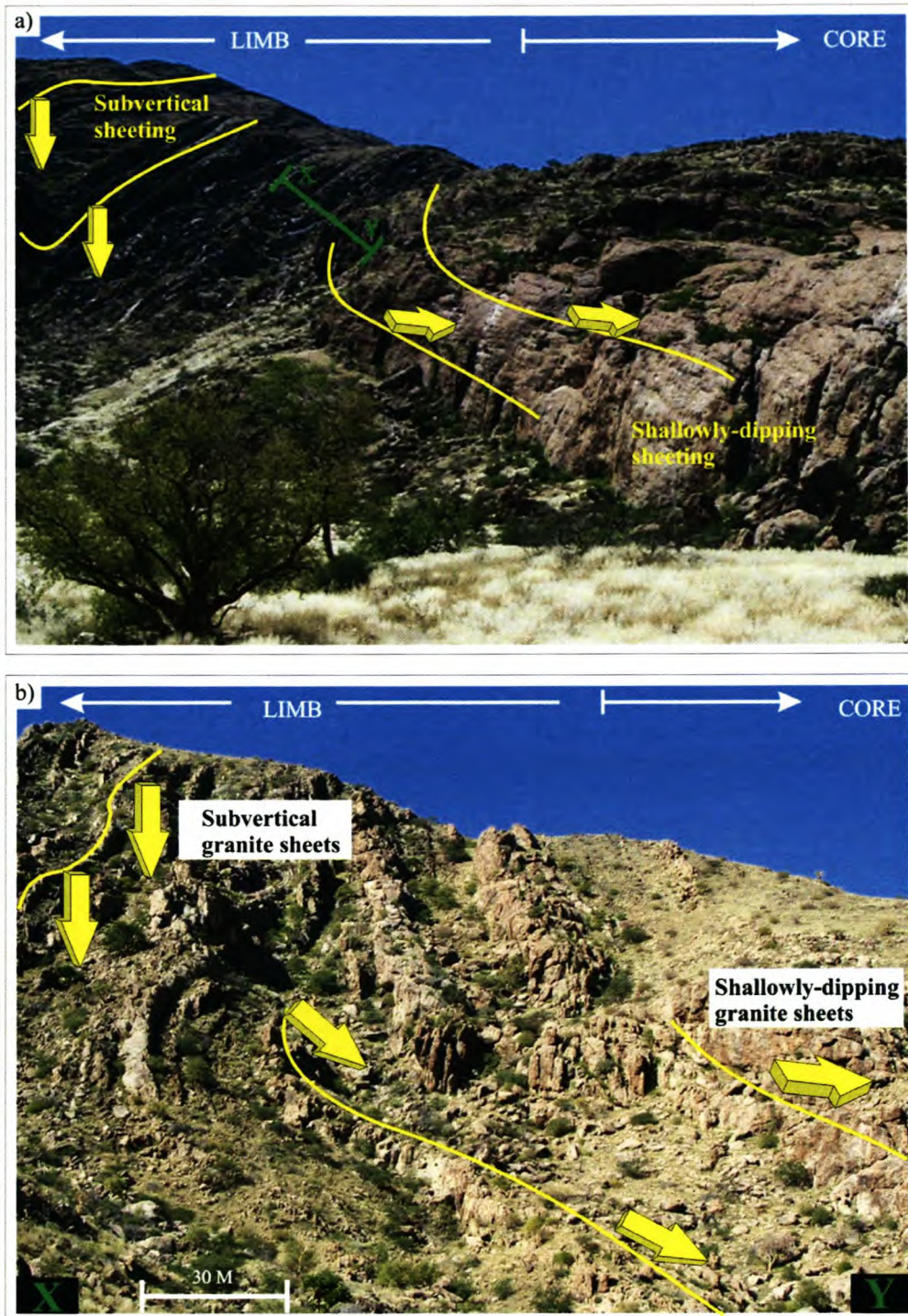


Figure 5.16 a) Photograph taken from within the core of the dome, facing north, showing the transition between the steeply-dipping granitic sheets characteristic of the marginal phase of the Klein Aukas granite and the shallowly-dipping sheets characteristic of the central granites. (b) Cross-sectional view through X-Y in a) showing the progression from steeply-dipping granitic sheets along the northwestern limb of the dome to shallowly-dipping sheets towards the core of the dome.

The central zone of the Klein Aukas granite forms a large, igneous body consisting of multiple, granitic sheets (Fig. 5.17a). These sheets give the granite a distinctive layered appearance on a decimeter- to meter-scale. Although undulating, the layering, dips for the most part, shallowly towards the dome center (Fig. 5.16a and 5.17a, b). Individual sheets can be distinguished by variations in grain size and/or amounts of quartz, feldspar, mica and garnet. They may be separated from one another by relatively unaltered screens of metapelitic host rock from the Oberwasser or Spes Bona Formations (Fig. 5.17c). Contacts between adjacent sheets are diffuse, where crystals in one sheet may intermingle with crystals from the adjacent sheet.

5.3.4 Fabrics

Apart from the sheeted nature of the granite, there are also systematic mineralogical and grain size variations within the sheets forming a prominent layering (Figs. 5.18a, b). This layering is often difficult to distinguish from the layering caused by sheeting of the granite (Fig. 5.17a). The internal layering is parallel to the sheet boundaries and commonly asymmetrical about the width of the sheet. Layering within the subvertical dykes along the marginal zones of the Klein Aukas granite is subvertical. Alternatively, layering within the central portion of the Klein Aukas granite is gently-dipping (between 0° and 45°) (Fig. 5.17a) and appears folded in places (and 5.19a). The folds vary in wavelength from decimeter- to meter-scales.

In places, there is a strong alignment of metasedimentary xenoliths and/or biotite schlieren. Xenoliths are common, particularly within the marginal zones of the Klein Aukas granite, and consist exclusively of elongate screens of siliciclastic country rock, commonly biotite-schists of Spes Bona of Oberwasser Formations wedged between adjacent granitic sheets. The orientation of these xenoliths is consistently parallel to the surrounding bedding of the host rocks and little if any internal deformation or rotation of the xenoliths is apparent.

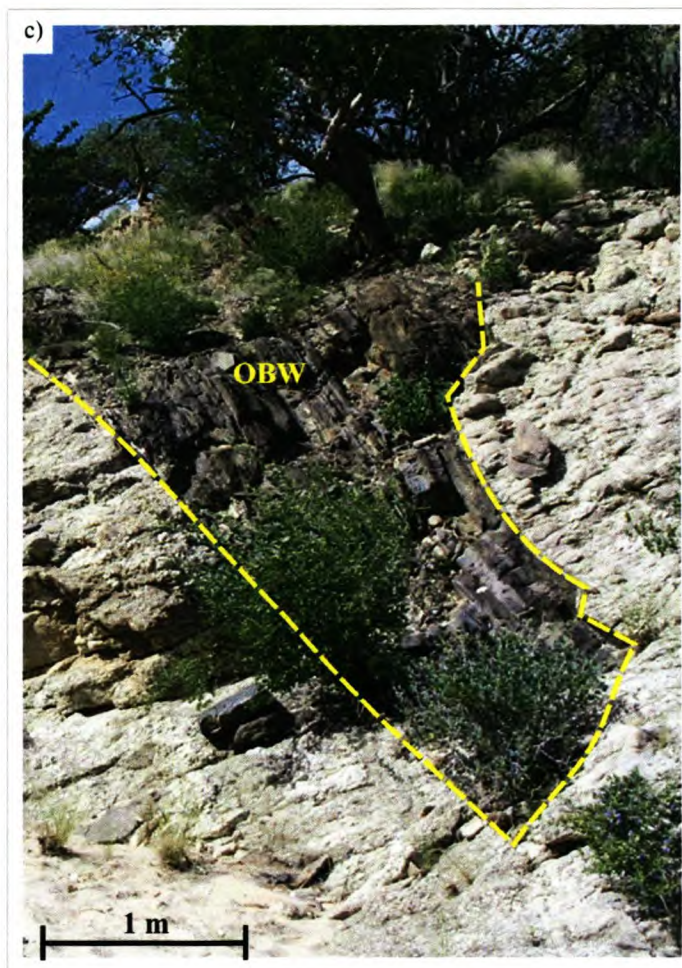
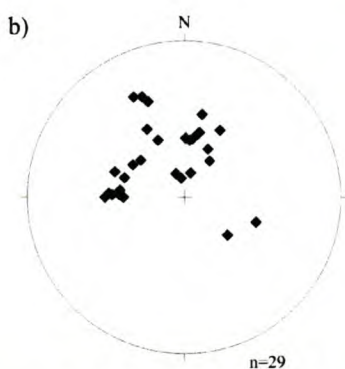


Figure 5.17 a) Cross-sectional view through the Klein Aukas granite showing its sheeted structure. Individual sheets dip towards the dome center (yellow arrows). Picture is taken facing northeast, person for scale. (b) Equal-area, lower-hemisphere stereographic projection showing poles to granite sheeting recorded from within the core of the dome. (c) Photograph showing an isolated screen of the Oberwasser Formation (OBW), surrounded by granitic sheets of the Klein Aukas granite. Taken facing northeast, along the southeastern limb of the dome.



Figure 5.18 a) Subhorizontal layering defined by compositional and grain size variations within the Klein Aukas granite exposed within the core of the dome. (b) Detail of the subhorizontal layering defined by grain size and compositional variations.

This relationship between granite sheets and in situ screens of host rock is comparable with the “ghost stratigraphy” described by Pitcher (1970) and Hutton (1992). Schlieren, defined by elongate concentrations of biotite are always developed parallel to the contacts of the sheets and therefore form a subvertical, northeast-trending fabric within the marginal, steeply-dipping sheets and a subhorizontal fabric within the central, gently undulating sheets (Fig. 5.19b).

The central portion of the Klein Aukas granite contains a heterogeneously developed, subhorizontal gneissosity. This gneissosity is defined by lensoid quartz aggregates separated by cleavage domains comprising anastomosing aggregates of white mica (Fig. 5.20a and b). The quartz lenses reach up to 1.5 cm in length and show length-to-width ratios ranging between 1:1 and 14:1. The gneissose fabric varies in intensity, but appears strongest within the medium-grained, quartz-rich layers within the granite. Textures within the quartz are highly variable. Some grains exhibit undulose extinction, while others are completely annealed into strain free, polygonal grains (Fig. 5.20b). Very fine-grained aggregates of white mica form cleavage domains that wrap around the lens-shaped quartz, anhedral feldspar and euhedral garnet grains. These cleavage domains appear to accommodate significant slip between grains, for example separating fractured portions of plagioclase grains (e.g. Fig. 5.21a). Feldspar occurs as anhedral grains, some of which exhibit undulose extinction and brittle fracturing (Fig. 5.21b).

Where intrusions of the Klein Aukas granite are discordant to the regional early-S2 foliation, the fabric leaves an imprint along the granite-host-rock contact, forming an intersection lineation (Fig. 5.22). Mineral lineations exposed within the host rocks are also preserved, defined by quartz along the granite-host rock contacts (e.g. Fig. 4.5b).

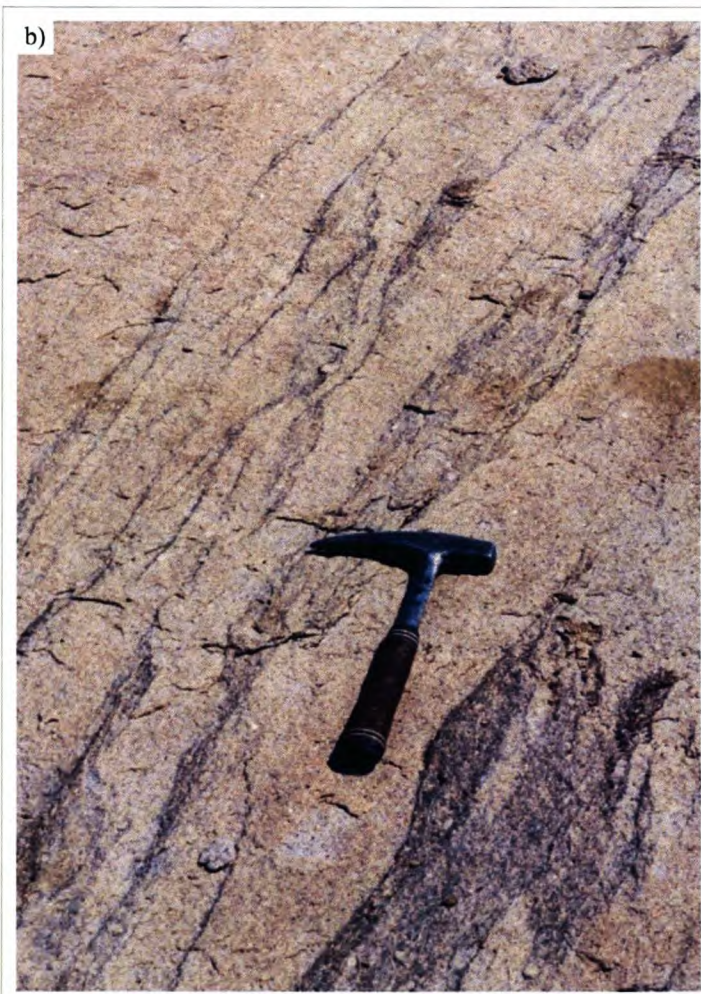
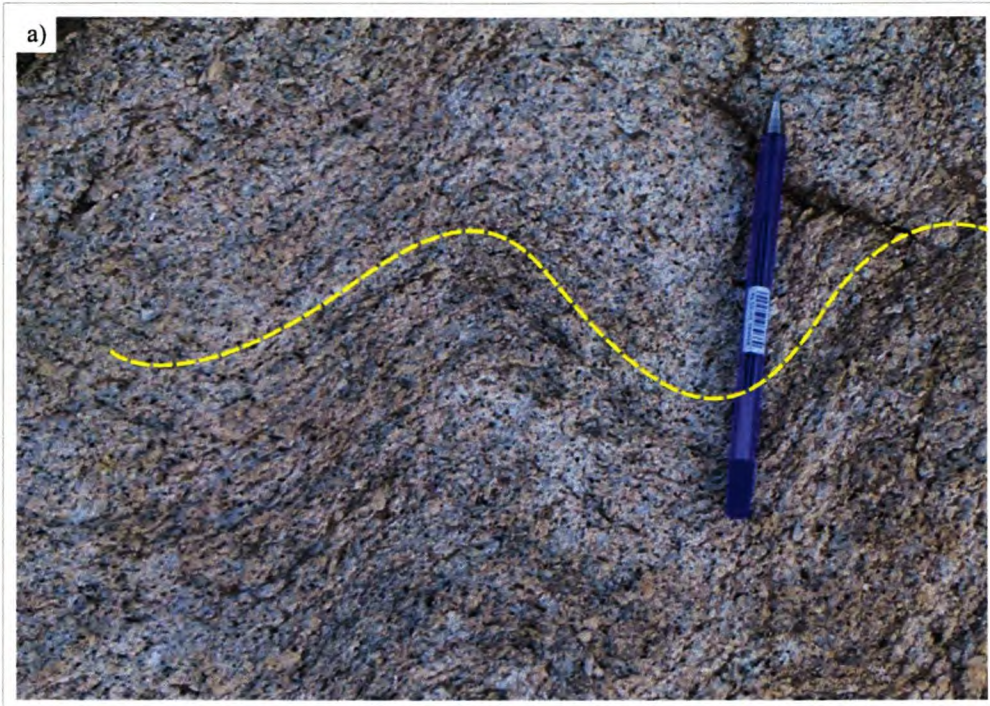


Figure 5.19 a) Centimeter-scale submagmatic layering within the Klein Aukas granite is folded within the core of the dome. (b) Plan view of northeast-trending schlieren defined by biotite aggregates within the Klein Aukas granite. The picture was taken close to the Spes Bona/Okawayo contact along the southeastern limb of the dome.

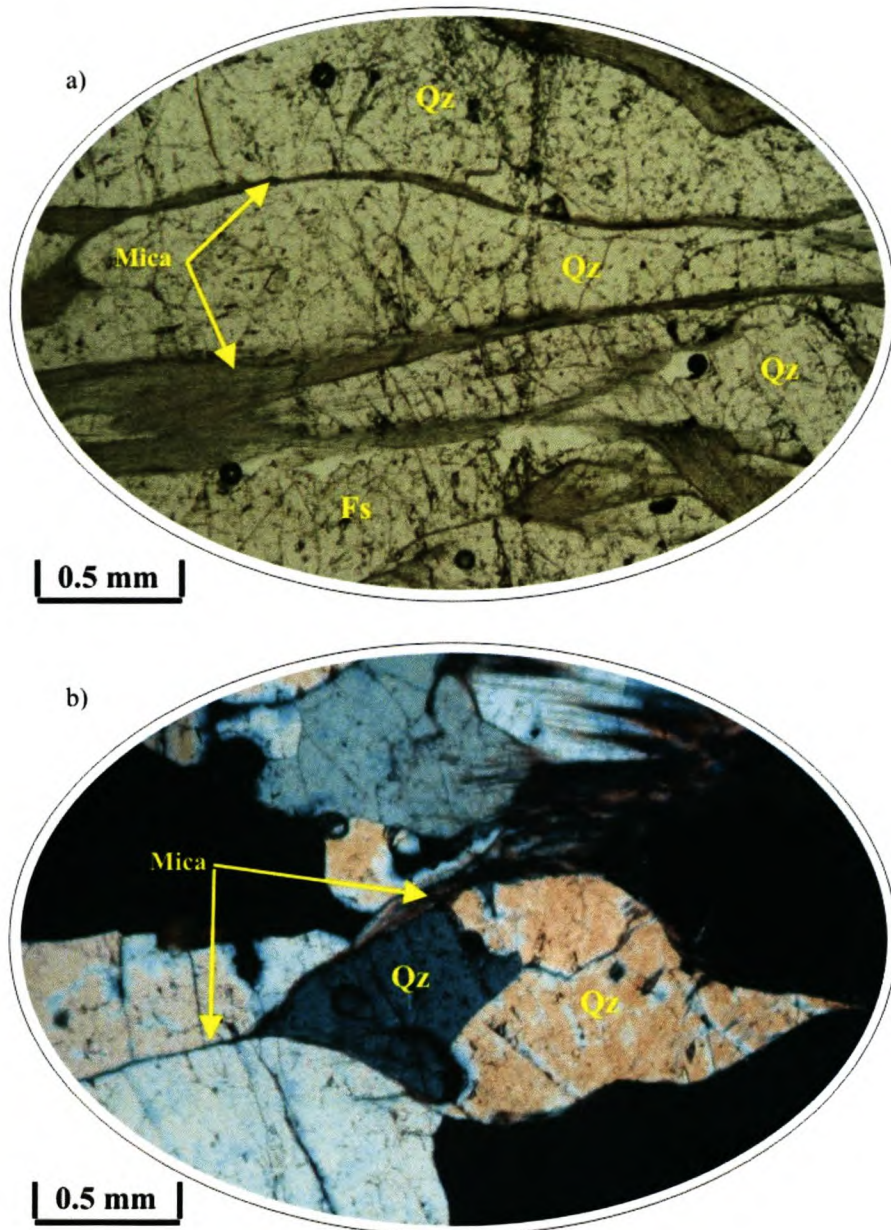


Figure 5.20 a) Photomicrograph (PPL) of the Klein Aukas granite comprising elongate grains of annealed quartz (Qz) and feldspar (Fs), separated by undulating aggregates of white mica (Mica). (b) Lens-shaped aggregates of unstrained quartz separated by thin, undulating bands of white mica within the Klein Aukas granite (shown in XPL).

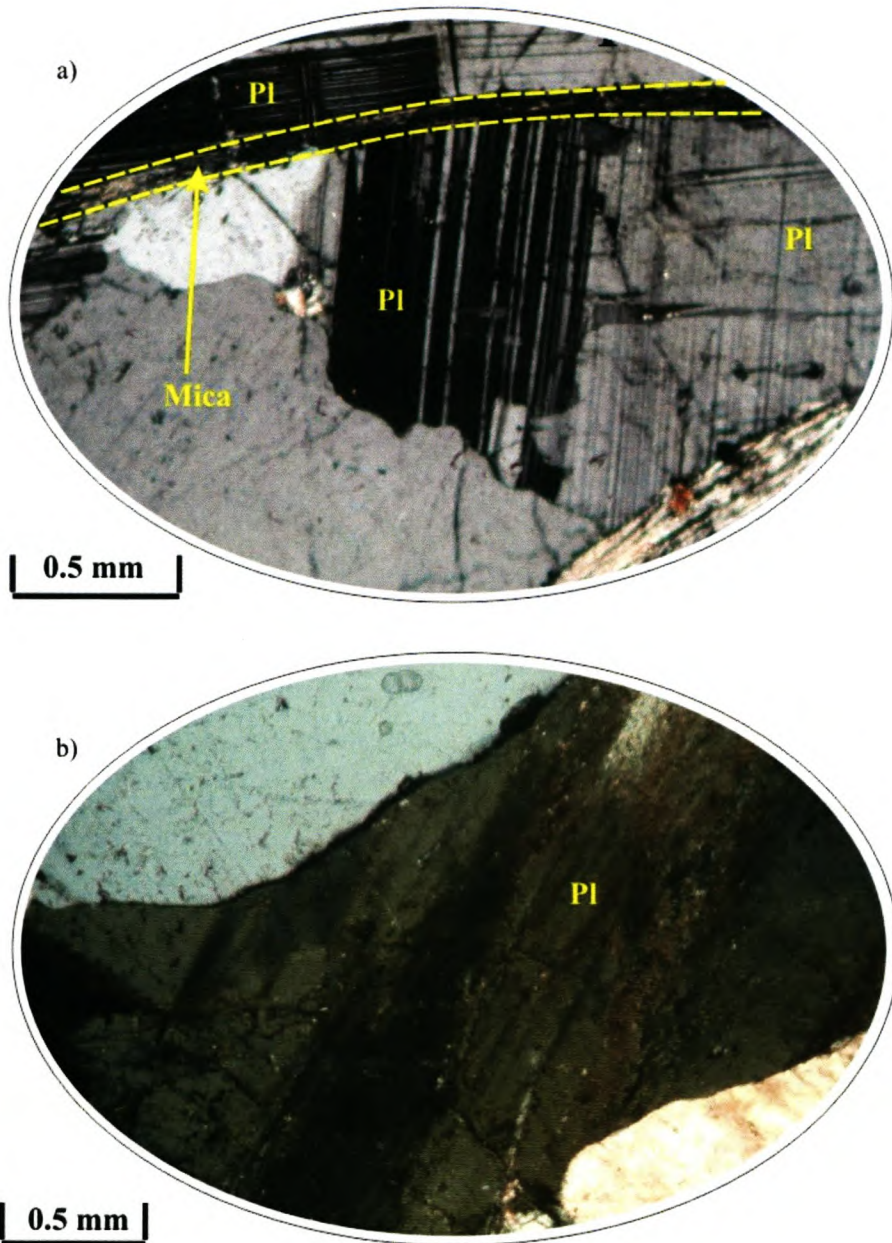


Figure 5.21 a) Photomicrograph (XPL) showing a mica-rich foliation plane truncating feldspar (Pl), within the Klein Aukas granite. (b) Undulose extinction of plagioclase within the Klein Aukas granite (XPL).

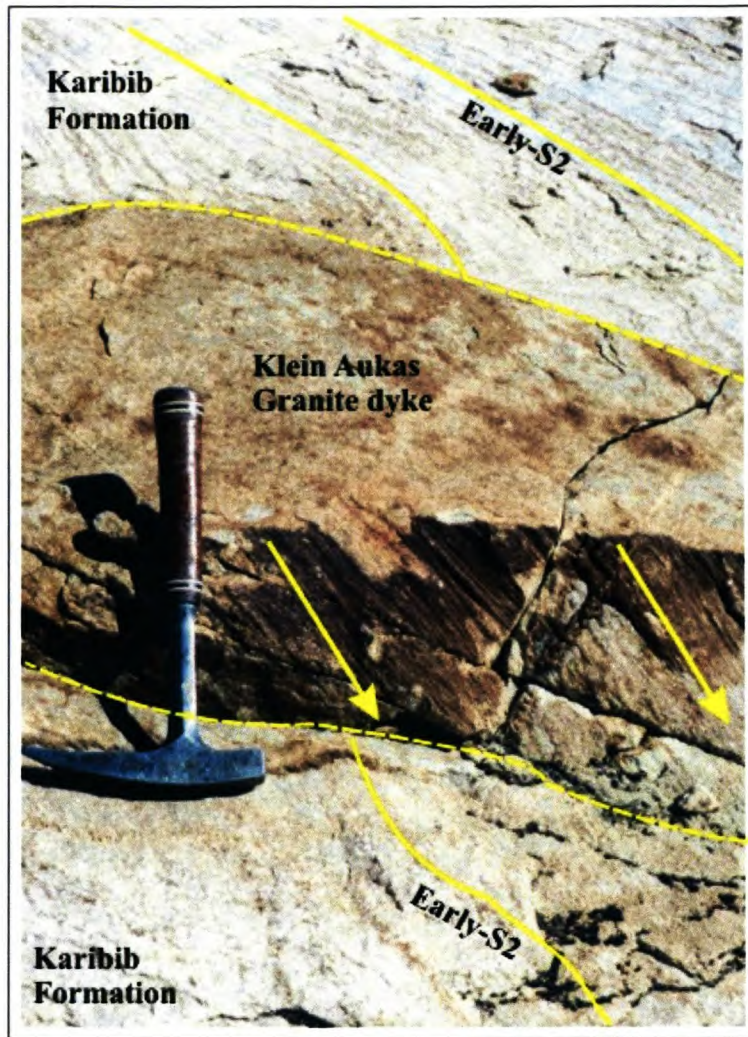


Figure 5.22 Photograph showing a discordant intrusion of the Klein Aukas granite within the Karibib Formation. Although the early-S2 foliation within the marbles is cross-cut by the dyke, the fabric is imprinted along the granite-host rock contact. The imprint defines an intersection lineation, shown by the yellow arrows.

5.4 Granite and Pegmatites along the northwestern limb of the dome

5.4.1 Occurrence and distribution

The Kuiseb Formation on the northwestern limb of the Usakos dome is intruded by numerous coarse-grained, leucocratic, granitic and pegmatitic sheets and/or pods. These intrusives are separated from the Klein Aukas granite in the core of the dome by the Karibib Formation and are mineralogically and texturally different from the Salem granite.

5.4.2 Macroscopic Appearance

The intrusions are dominated by coarse-grained leucocratic granites and pegmatites. The granites consist largely of quartz, white K-feldspar (often graphically intergrown with quartz), plagioclase, muscovite and biotite with accessory tourmaline, beryl and garnet. Some of the large intrusives are currently mined for gemstone-quality tourmaline. No petrographic analyses of these rocks have been undertaken during this study. Grain size and modal variations define a within-sheet layering along planar, sheeted intrusions. This layering appears asymmetrical about the width of the intrusions.

5.4.3 Intrusive Relationships

The pegmatitic and/or granitic intrusions form sheets and pods along the northwestern limb of the dome. The subvertical sheets trend in three main directions, namely towards the northeast, north-northwest and north-northeast. The northeast-trending sheets are concordant with bedding (S₀) and the regional northeast-trending early-S₂ foliation within the Damara Sequence. They range in thickness from <1 m up to 80 m and in length from a few meters up to 1 km. The north-northwest and north-northeast-trending sheets, on the other hand, are discordant, showing variable strike extents from being extremely linear to gently folded. The north-northeast trend is relatively well developed, with sheets ranging between 3 and 50 m in width and reaching > 1 km in length, while the north-northwesterly trending sheets are smaller and less abundant, ranging between 1 and 3 m in thickness and reaching 250 m in length. Leucocratic granitic and/or pegmatitic pods occur along this limb of the dome. These are massive intrusive bodies, with variable shapes and sizes, but often showing a preferred trend in a northeast-southwesterly direction. In places, the north-northeasterly-trending sheets branch into northeast-trending sheets suggesting a coeval relationship between the two dyke sets. Individual sheets pinch out along strike whereas the pod-like intrusives tend to terminate abruptly.

5.5 The Significance of Granitic Fabrics: A Discussion

5.5.1 Introduction

Fabrics within granite may develop during

- (1) the magmatic stage;
- (2) the transition from the magmatic to the solid-state phase, i.e. in the presence of crystals and melt;
- (3) the solid state, either as high-temperature or as low-temperature features.

Therefore, mechanisms responsible for producing the fabrics preserved within the Damaran granitoids may provide an insight into the temporal relationship between granite emplacement and Damaran tectonism. The term “magmatic flow” refers to the rotation of crystals by the displacement of melt, where the interaction between crystals is sufficiently low to prevent plastic deformation (Paterson et al., 1989). Within partially molten granite (>30 volume per cent melt), tabular objects such as mineral grains and enclaves, may undergo rigid-body rotation within the melt, aligning their planar surfaces parallel to the flow direction of the magma (Paterson et al., 1989). In this way, these planar minerals or enclaves define a magmatic flow fabric.

Paterson et al. (1989) have established a set of criteria that can be used to differentiate planar fabrics in granites formed by magmatic flow, tectonic (solid-state) processes and a combination of the two. These criteria can be applied to both the Salem and Klein Aukas granites.

5.5.2 Interpretation of Fabrics within the Salem Granite

The preferred alignment of magmatic minerals such as euhedral, tabular microcline and single platy grains of biotite, as well as elongate enclaves and the presence of schlieren within the Salem granite are indicative of magmatic flow fabrics.

Layering defined by variations in modal mineralogy and grain sizes of minerals is parallel to the sheeted geometry of the Salem granite. Such layering is interpreted to have formed during multiple intrusion of melt into partially crystallized sheets during

sheet-in-sheet emplacement. Similar examples of this type of layering are discussed by Blenkinsop and Treloar (2001) and Brown and Solar (1998). Compositional and grain size variations across sheets may also have formed during fractionation of the melt during cooling (e.g. Pawley et al., 2004). Some structures within the granite, such as those in Fig. 5.6a, are interpreted as having formed by the intermingling of different melt phases of granite prior to their complete crystallization (Fernández et al., 1997).

The process responsible for the alignment of the microcline phenocrysts in the Salem granite is somewhat enigmatic. The preferred alignment of euhedral phenocrysts within igneous rocks has been commonly attributed to flow within the magmatic phase (e.g. Paterson et al., 1989, 1998). However, in the case of the Salem granite, magmatic fabrics, defined by the preferred alignment of feldspars and tectonic fabrics in the host rocks, namely the northeast-trending early-S2 foliation are parallel. This suggests that feldspar alignment may have been influenced by the regional stress field during crystallization. Previous studies focusing on fabrics within granites describe similar concordant relationships between fabrics within plutons and their surrounding host rocks, (e.g. Paterson et al. (1998); Miller and Paterson (1994)). They suggest that prior to complete crystallization of the granite, the mixture of crystals and melt (crystal mush) possessed a sufficiently high viscosity to transmit a regional stress. In the case of the Salem granite, northeast-southwest-directed compression during the main D2 phase of deformation may have caused rotation of phenocrysts into parallelism so that their large crystal faces become oriented normal to the shortening direction. The presence of melt between the phenocrysts within the mush may have facilitated their rotation, allowing for rapid and relatively easy grain rotation during regional shortening (Ilfonse and Mancktelow, 1993). Despite the predominant northeast-southwest-trend of phenocrysts in the Salem granite, deviations from this trend do occur. This suggests that flow sorting plays some role in the localized alignment of the phenocrysts within the Salem granite. The preferred orientation of K-feldspar phenocrysts is therefore likely to have occurred by a combination of flow sorting and regional deformation.

Some fabrics within the Salem granite show evidence for solid-state deformation having affected the granite at some stage during its history. The subvertical, northeast-

trending fabric defined by the preferred orientation of biotite laths within the biotite-rich phases of the Salem granite resembles a gneissosity and is interpreted to have developed within the solid-state. Biotite within relatively leucocratic porphyritic phases often forms aggregates that bend around the microcline phenocrysts (for example Fig. 5.8). These resemble strain caps, which develop perpendicular to the shortening strain during regional deformation (Passchier and Trouw, 1996). In some places, biotite is observed to concentrate within the strain shadows of microcline phenocrysts. Although the exact mechanism for biotite concentration within these low strain sites is uncertain, their spatial relationship with the phenocrysts suggests a regional stress field was present at the time biotite crystallized/recrystallized.

All K-feldspars within the Salem granite show abundant microcline twinning. Irregular grain boundaries of microcline phenocrysts are rimmed by intergranular, fine-grained aggregates of quartz and feldspar. These aggregates are interpreted to have formed by dynamic recrystallization of the feldspar phenocrysts in response to an applied stress (Passchier and Trouw, 1996). The irregular grain boundaries and fine grained aggregates are normally associated with myrmekitic intergrowths of quartz and feldspar. The significance of myrmekites is ambiguous as they can be found in either metamorphic rocks formed in the solid state, or in igneous rocks (e.g. Hibbard, 1979; Hibbard, 1987; Simpson and Wintsch, 1989; Simpson, 1985). However, Vernon et al. (2004) suggest that the presence of myrmekites together with recrystallized quartz-feldspar aggregates indicates solid-state deformation at or close to the granite-solidus temperatures. The presence of brittle fractures, subgrain boundaries and perthitic exsolution within some feldspar grains is indicative of solid-state deformation (Paterson et al., 1989).

Quartz also shows evidence for dynamic recrystallization, for example forming elongate, preferentially aligned grains with undulose extinction and the development of subgrain boundaries (Passchier and Trouw, 1996; Vernon et al., 2004). Some quartz grains occur as strain free, well-annealed polygonal grains indicative of static recrystallization (Passchier and Trouw, 1996).

The features summarized below discuss several other lines of evidence to suggest that these granites were syn-tectonically emplaced:

- Fold structures within the Damara Sequence are truncated by the Salem granite (Fig. 5.4a). This indicates the host rock was folded during D2, prior to the emplacement of the Salem granite. However, at the same time, feldspar grains within the Salem granite have an axial planar orientation with respect to the early-F2 folds.
- On a regional scale, the Salem granite is observed to preferentially intrude synformal structures cored by the Kuiseb Formation (Miller, 1983). This suggests a strong structural and/or lithological control on the emplacement of the granite.
- The Salem granite displays a sheeted internal structure. Individual sheets are clearly magmatic features and therefore record the emplacement geometry of the granite. The sheets are concordant with the host rocks. This suggests the orientation of the sheeted intrusions was influenced either by the regional stress field or by the structural anisotropy of the host rocks. Small-scale concordant sills of Salem granite intruding into the Karibib Formation near the periphery of the main pluton are boudinaged along strike (Fig. 5.5b). The foliation of the marbles surrounding these boudins wraps around the boudin necks, which are commonly filled with quartz. The presence of boudinaged granitic sills provides evidence for the presence of a regional stress field subsequent to the emplacement of the Salem granite.
- The marginal zones of the Salem granite preserve well-aligned microcline phenocrysts forming a pervasive fabric. This alignment is less-developed towards the pluton interior in the northwest, where phenocrysts show a more random orientation. The preferred orientation of phenocrysts in the Salem granite is largely attributed to their rigid rotation in the presence of some melt in response to a regional stress field. The alignment of phenocrysts along the margins and not within the pluton center can be explained if the crystallization front within the pluton progressed from the margins towards the pluton interior and regional deformation ceased prior to the complete crystallization of the pluton. In this way, initial crystallization of the magma along the margins occurred during deformation, therefore preserving phenocryst alignment. As the crystallizing front progressed towards the pluton center,

during the waning stages of regional deformation, phenocrysts crystallized with a random orientation. The boundary between aligned phenocryst orientation and their random orientation within the pluton potentially freezes the final stages of the Damaran orogeny in its crystallization history.

- Microscopic solid-state deformation textures formed at contrasting temperature conditions (300-550° C) are observed within the same thin-section of granite. These solid-state fabrics are parallel to magmatic fabrics, suggesting deformation was likely to have continued throughout the cooling history of the granite.
- Magmatic and solid-state fabrics in the Salem granite are (sub-) parallel to the tectonic fabrics in the host rocks of the Damaran Sequence. For example, planar fabrics defined by magmatic sheeting, schlieren, the preferred orientation of magmatic minerals such as feldspar, biotite and elongate enclaves are parallel to the bedding (S0) and pervasive schistosity (early-S2) of the host rocks along the northwestern limb of the Usakos dome. Even lineations within the Salem granite, defined by easterly plunging microcline phenocrysts along foliation planes, are sub-parallel to the majority of mineral lineations recorded within the host rocks. Similarities in fabric orientations between plutons and their surrounding host lithologies have previously been recognized and are regarded as a common feature of plutons emplaced syn-tectonically (e.g. Miller and Paterson, 1994; Paterson et al., 1998).
- Flattened quartz grains formed during dynamic recrystallization are oriented parallel to the fabric defined by magmatic sorting, for example the preferred orientation of primary plagioclase crystals. This suggests that the direction of magmatic flow was parallel to, and possibly determined by the regional deformation.
- Evidence for solid-state deformation within individual minerals, for example undulose extinction, the development of subgrain boundaries, dynamic recrystallization, etc. indicates regional deformation took place subsequent to the crystallization of the granite within the marginal zones.

5.5.3 Interpretation of Fabrics within the Klein Aukas Granites

Elongate aggregates of biotite schlieren provide evidence for magmatic flow fabrics within the Klein Aukas granite. This fabric is subvertical, northeast-trending along the marginal zone of the Klein Aukas granite and subhorizontal within the central portion of the Klein Aukas granite. Apart from magmatic fabrics, the central portion of the granite shows variably developed solid-state fabrics including, flattened quartz grains and mica-rich foliae (Passchier and Trouw, 1996; Paterson et al., 1989). Some quartz grains exhibit undulose extinction and the development of subgrain boundaries, while others form strain free, polygonal grains, joining along triple junctions. Undulose extinction and the development of subgrain boundaries are characteristic microstructures indicating plastic deformation at temperatures of at least 300 and 400° C (Passchier and Trouw, 1996). Strain-free, polygonal grains, on the other hand, can develop in the absence of deformation during recovery at temperatures ca. 300° C (Passchier and Trouw, 1996). Some plagioclase crystals show deformation textures such as brittle fracturing, undulose extinction and perthitic exsolution, characteristic of deformation temperatures between 400 and 500 ° C during deformation. Microstructures of quartz and feldspar indicate deformation temperatures between 400 and 500° C and the presence of annealed fabrics indicate a post-deformation thermal overprint (Kruhl, 1996).

The features summarized below allow to discuss several, other observations that suggest these granites were syn-tectonically emplaced:

- On a regional scale, the intensity of sheeting of the Klein Aukas granite increases towards the center of the antiformal structure of the Usakos dome. This either suggests the sheets preferentially intrude the lowest-strain domain, i.e. the hinge of the F2a fold structure, and/or they preferentially intrude the siliciclastic units and pond beneath the thick, marble-rich horizon of the Karibib Formation.

- Granite sheets intruding all major rock types exposed in the study area are deformed to variable degrees. Where some intrusions appear relatively undeformed, others are boudinaged and folded. This suggests that granite emplacement occurred during and subsequent to the presence of a regional stress field. For example, subvertical, northeast-trending sheets along the marginal zone of the Klein Aukas granite are oriented parallel to bedding and the regional schistosity (S₂) along the limbs of the dome. Some bedding-parallel sheets are folded together with their host rocks, indicating emplacement prior to/or during folding, while other sheets oriented slightly oblique to bedding appear undeformed.
- Portions of the leucocratic granite within the core of the dome exhibit a strong schistose fabric. This fabric is sub-horizontal, orthogonal to the regionally-developed sub-vertical, north-east trending schistosity of the country rocks.
- Microstructures such as perthitic exsolution, undulose extinction and the development of subgrains within quartz and feldspar indicate deformation subsequent to crystallization of the Klein Aukas granite.
- The contacts of the granites with their metasedimentary host rocks show no discrete metamorphic aureole separable from the regional metamorphism. This indicates the granites intruded their host rocks during peak metamorphism, while the metasedimentary rocks were already significantly hot.

5.5.4 Interpretation of Fabrics within the Sills and Dykes along the northwestern limb of the dome

Many of the sheets occurring along the northwestern limb of the Usakos dome exhibit chocolate-tablet boudinage or are folded together with the bedding (Fig. 5.23), while others appear unaffected by regional deformation. The presence of folded dykes and sills as well as relatively undeformed and linear, discordant dykes suggests that these sheeted intrusions were emplaced syn- to post-tectonically.

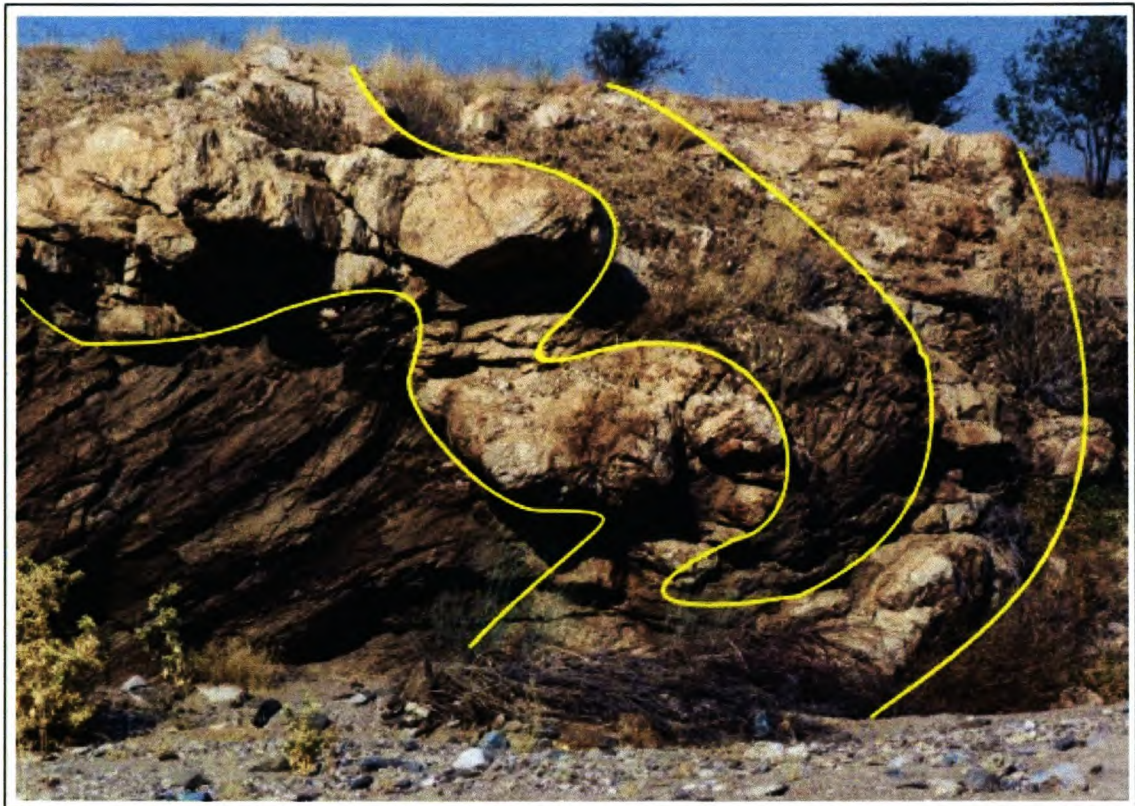


Figure 5.23 Photograph taken facing southwest, showing a northwest-vergent folded pegmatitic sheet within the Kuiseb Formation along the northwestern limb of the Usakos dome.

5.6 Granite emplacement

The Salem granite and the pegmatitic dykes and sills along the northwestern limb of the dome are confined to the Kuiseb Formation, while the sheeted granites of the Klein Aukas granite are confined to the Spes Bona and Oberwasser Formations within the core of the dome. There appears to be a rheological control on granite emplacement within the Usakos dome where granite sheets preferentially intrude siliciclastic units while avoiding marble-rich horizons such as the Karibib and Okawayo Formations. The Klein Aukas granite intrudes as subvertical, subparallel sheets within the moderate- to steeply-dipping Oberwasser and Spes Bona Formations forming the limbs of the F2a fold. These sheets become more numerous, closer-spaced and gently-dipping towards the core of the dome, ultimately forming large, subhorizontal or inward-dipping amalgamated sheeted bodies. The concentration of granite within low-strain domains such as cores of antiforms or domes is not uncommon (e.g. Soula, 1982; Holm et al., 1992; Faure et al., 1996; Roig and Faure, 1998). The subvertical sheets along the limbs appear to have formed by dyke propagation, exploiting pre-existing anisotropies such as bedding (S0), and foliation (S1 and possibly early-S2). Due to the antiformal shape of the dome, these dykes within the core of the dome may however, have intersected with the lower marble contact of the Karibib Formation. This intersection within the ductile marbles is likely to have provided an efficient stopping mechanism for dyke propagation (Corriveau et al., 1998). As a result, the ascending magma, unable to penetrate the ductile marbles, coalesced at the rheological interface forming subhorizontal amalgamated sheets within the core of the dome. In this way, the subvertical and subhorizontal sheets of the Klein Aukas granite, with their respective subvertical and subhorizontal magmatic fabrics intruded simultaneously within the Usakos dome during dome amplification. Similarly, the Salem granite shows characteristic subvertical sheeting as well as subhorizontal granite/host rock contacts (Fig. 5.4b, 5.5a). This may imply that the granite was fed by subvertical sheets, but was emplaced as a kilometer-scale subhorizontal sheet.

CHAPTER 6 DISCUSSION

Kilometer-scale, northeasterly-trending dome structures characterize the regional structural pattern of the sCZ for which several genetic models have been proposed in the literature (Chapter 2.3). However, none of these models appear to appropriately account for the formation of the Usakos dome.

An origin of the Usakos dome by vertical or gravity-driven processes whether magmatic or solid-state, is currently regarded as a mechanically and thermally improbable process during the emplacement of small-scale granitic plutons (ca. 10 km in diameter) (e.g. Clemens and Mawer, 1992; Petford, 1996) and thus, pose unlikely mechanisms for dome formation. The granites within the Usakos dome do not show any disruptive effect on the metasedimentary host rocks and wall-rock strains related to the emplacement of the Klein Aukas granite are almost entirely absent. Instead, an in-situ ghost-stratigraphy is locally preserved in the core of the dome. Therefore, magmatic diapirism and/or ballooning of the Klein Aukas granites are unlikely to have contributed to the formation of the Usakos dome. Similarly, the core complex model is also problematic. Oliver (1994) documented a tectonic contact between the basement and the Damaran cover in the high-grade terrane to the southwest as an extensional detachment. However, the tectonic contact between the basement and cover sequences in the study in the form of the MRTZ is a foreland-vergent thrust, and not a southwest-vergent extensional detachment. Field observations are also inconsistent with cross folding. Cross-folding produced by more than one deformational phase should produce widespread interference folds and orthogonal foliations. However, the cross-folding is only locally developed within the core-region of the Usakos dome and the orthogonal foliations developed within the Usakos dome do not overprint one another.

Recent studies in the high-grade, southwestern extent of the sCZ by Oliver (1994, 1995) and Poli and Oliver (2002) propose an episode involving orogen-parallel, top-to-the southwest tectonic transport within the laterally constricted middle crust as being responsible for the development of the dome structures. For the most part, the Usakos dome is, however, characterized by northeast-trending folds (early-F₂) and an associated axial

planar foliation (early-S2) and flattening-type strains, recording subhorizontal northwest-southeast-directed shortening strains, inconsistent with the orogen-parallel constrictional-type deformation described by Poli and Oliver (2001). Top-to-the northwest thrusting and northwest-vergent folding are described as a possible dome-forming mechanism in the northeastern portion of the Karibib District, where domes are tentatively related to large-scale tip-line folds located above blind thrusts (Kisters et al., 2004). This model for dome formation, however, can not explain the additional late-F2 folding observed within the southwestern portion of the Usakos dome.

6.1 Tectonic Evolution of the Usakos dome

There are a number of features observed within the Usakos dome that suggest the southwestern lobe of the dome was initially developed as a kilometer-scale northeast-trending, northwest-verging anticline resembling the regional-scale domes developed to the northeast, such as the Karibib dome and the northeastern lobe of the Uskaos dome. Firstly, second- and lower-order folds throughout the Usakos dome show ubiquitous northeasterly trends. Particularly in the northeast in Domain E, folds even verge towards the northwest. Secondly, the southeasterly-dipping, northeast-trending MRTZ along the southeastern limb of the dome, records top-to-the northwest kinematics, consistent with an origin within a foreland-vergent fold and thrust belt during collisional tectonics, as is recorded in the Karibib district (Kisters et al., 2004). Finally, the limbs of the Usakos dome contain a pervasive northeast-trending axial planar schistosity (early-S2). This schistosity is often associated with chocolate-tablet boudinage of competent layers and is indicative of northwest-southeast-directed, largely co-axial shortening strains.

Despite the similarities between the southwestern parts of the Usakos dome with northwest-vergent domes to the northeast, the Usakos dome shows some significant differences. These include:

1. Overturned stratigraphies towards the southwest

An important, yet subtle difference occurs within the core of the Usakos dome where the regional stratigraphy and fold structures become overturned along

strike. This deviates from the gentle, doubly-plunging geometry of domes to the northeast, i.e. the Karibib dome and northeastern portion of the Usakos dome. This inversion of the sequence is evident, for example, by the strike-parallel reversals in the polarity of the fold facing directions particularly in Domain A (Fig. 4.11; Chapter 4.5.2). The inverted stratigraphy suggests that the first-order fold structure defining the Usakos dome and its corresponding second-order folds originated as northeast-trending folds (early-F2) that were refolded about a shallow northeasterly-plunging, northwest-trending fold axis (late-F2) (Fig. 4.39). Studies of the Karibib dome and adjoining large-scale fold structures do not describe any evidence for this type of refolding (Kisters et al., 2004).

2. Radial fold hinges within the core of the fold

A periclinal geometry is typical for dome structures and mesoscale folds in the Karibib district (Kisters et al., 2004). In general, folds plunge shallow- to moderately towards the northeast or southwest, constituting the northeast trending structural grain of the sCZ. In the core of the southwestern portion of the Usakos dome, however, fold plunges and lineations (L2b) preserved within the ghost stratigraphy show marked deviations from this northeast-southwest trend. Fold plunges and their respective lineations (L2b) show a somewhat radial distribution, plunging away from the center of the dome core and towards the dome margins (Fig. 4.13a; Chapter 4.5.2).

3. Two sets of high-angle planar fabrics

The radial fold plunges and lineations (L2b) within the dome core are associated with a shallow-dipping schistosity (late-S2) confined to the siliciclastic and granitic rocks within the core of the dome (e.g. Figs. 4.3c; 4.13b). Other areas, namely the limbs of the dome and regions to the northeast lack this subhorizontal fabric and instead contain a subvertical, northeast-trending schistosity (early-S2). Thus the southwestern portion of the Usakos dome contains two sets of schistose fabrics oriented approximately orthogonally to one another.

The superposed folding, as well as the radial fold hinge lineations and subhorizontal foliations, all occur within the core of the dome, i.e. in the vicinity of the syntectonic Klein Aukas Granites (Chapter 5.5). Such a spatial and temporal relationship between

the geological structure and the occurrence of syntectonic granite suggests that D2 deformation was modified as a result of the emplacement of the granite.

The northeast-southwest-trending regional structural grain that characterizes the Central Zone is believed to have formed during the near-orthogonal (Coward, 1983; Miller, 1983) to slightly oblique (Poli and Oliver, 2001) collision between two relatively rigid bounding cratons, the Congo Craton to the north, and the Kalahari Craton to the south (Fig. 2.1a).

Kisters et al. (2004) recently mapped a portion of the Karibib District forming the northeastern extent of the sCZ. Here, dome structures generally show a northwest-vergence associated with top-to-the northwest thrusting, related to mid-crustal deformation in a foreland-vergent fold and thrust belt. The area ca. 100 km southwest of the Karibib District exhibits significantly higher metamorphic grades, leading to widespread migmatization and granite intrusions (Miller, 1983; Masberg, 2000; Nex et al., 2001; Jung and Mezger, 2003; Basson and Greenway, 2004). Shallow, northeasterly-plunging stretching lineations and southwest-closing sheath-like folds orthogonal to the Karibib District dominate the structural fabric (Kröner, 1984; Oliver, 1994, 1995; Poli and Oliver, 2001). This southwesterly-vergence is interpreted to have developed during constrictional deformation as a result of orogen-parallel extension at deep crustal levels (Oliver, 1994; Poli and Oliver, 2001). As pointed out by Kisters et al. (2004), no regional-scale detachment between these two structural domains along the length of the sCZ is indicated on regional maps. The timing of the D2 fabric preserved in the Karibib dome is constrained by SHRIMP U-Pb ages of the syn-D2 intrusion of the Mon Repos granodiorites and diorites and post-tectonic emplacement of the Rote Kuppe granite between ca. 550 and 540 Ma (Jacob et al., 2000). This age is indistinguishable from the U-Pb zircon ages of 542 ± 6 Ma (Tack et al., 2002) obtained from early, post-collisional granites cross-cutting extensional fabrics in the southwest. Thus, the two orthogonal fabric domains appear to have formed at the same time during the D2 orogenic event.

Significantly, the study area, straddled between two orthogonal vergence domains, preserves both a northwest- and a superposed southwest-directed vergence (early-F2

and late-F2 respectively) (Fig. 6.1). It exhibits a northwesterly-fold-and-thrust vergence along the limbs of the dome and a southwesterly-vergence within the granite-rich core of the dome. Thus, the Usakos dome contains a combination of features characteristic of both the northwest-vergent, thrust-dominated, upper crustal levels and the southwest-vergent, pure shear-dominated, deeper crustal levels.

In the study area, horizontal northwest-southeast directed shortening is manifest by northeast-trending, commonly northwest-verging folds, the upright- to southeast-dipping pervasive early-S2 axial planar foliation and a similarly trending and verging kilometer-scale thrust, namely, the MRTZ (See Phase 1, Fig. 6.2). Both folding and thrusting are mechanisms that thicken the crust. Crustal thickening by folding and thrusting is only possible where the crust is sufficiently rigid to sustain the increasing load. During crustal shortening and the formation of the northwest-vergent domes (early-D2), the core of the F2a Usakos dome became the preferential site for the syntectonic emplacement of the Klein Aukas granite (Chapter 5). Granitic melt was able to pond below the ductile marbles of the Karibib Formation (See Phase 2, Fig. 6.2). Several authors (e.g. Hollister and Crawford, 1986; Vanderhaeghe and Teyssier, 2001; Davis and Maiden, 2003) emphasize the importance syntectonic melt has on the rheology of the crust during orogenesis. They suggest that a combination of crustal overthickening, fluid-pressure weakening and crustal heating from the emplacement of magmatic bodies may initiate the gravitational collapse of thickened crust. It is suggested that, in the case of the Usakos dome, that the synkinematic granitic melts created a rheologically weak horizon decreasing the strength at the base of the F2a antiform that was undergoing fold amplification during ongoing shortening. As a consequence, fold amplification of the upright to northwest-vergent Usakos dome could no longer occur and the thickened pile, now too thick for its weakened substratum, collapsed (late-D2) (see Phase 3, Fig. 6.2).

Collapse and vertical shortening that took over are manifest by the radial fold plunges and the late-S2 observed within the core of the dome. In other words, the core records a switch from horizontal to vertical shortening. Within the Usakos dome, one, thus, observes the localized gravitational collapse confined to the granite-rich portion of the dome. Given that lateral shortening continued, the only available option for the overthickened section located above the rheologically weaker granites was to flow

laterally towards the southwest. This resulted in the hinge-parallel shearing and extrusion of the Usakos dome, which, on a regional scale, forms part of the orogen-parallel extrusion of rocks in the deeper parts of the sCZ. The low viscosity melts represented the catalyst for the localized collapse and also provided a surface along which the extrusion could take place.

The extruding granite-rich core of the dome is bounded by the highly transposed 'straightening zones' developed in the Karibib marbles on the limbs of the Usakos dome (Chapter 4.7). These straightening zones may have helped to maintain strain compatibility between the extruding core of the Usakos dome and its northwest-vergent surroundings. Differential flow within the marbles is certainly suggested by the sheath-folds and highly-variable fold plunges in these domains. However, non-coaxial shear fabrics are not preserved along these limbs, which may also be a function of the pervasive static recrystallization and annealing of the marbles.

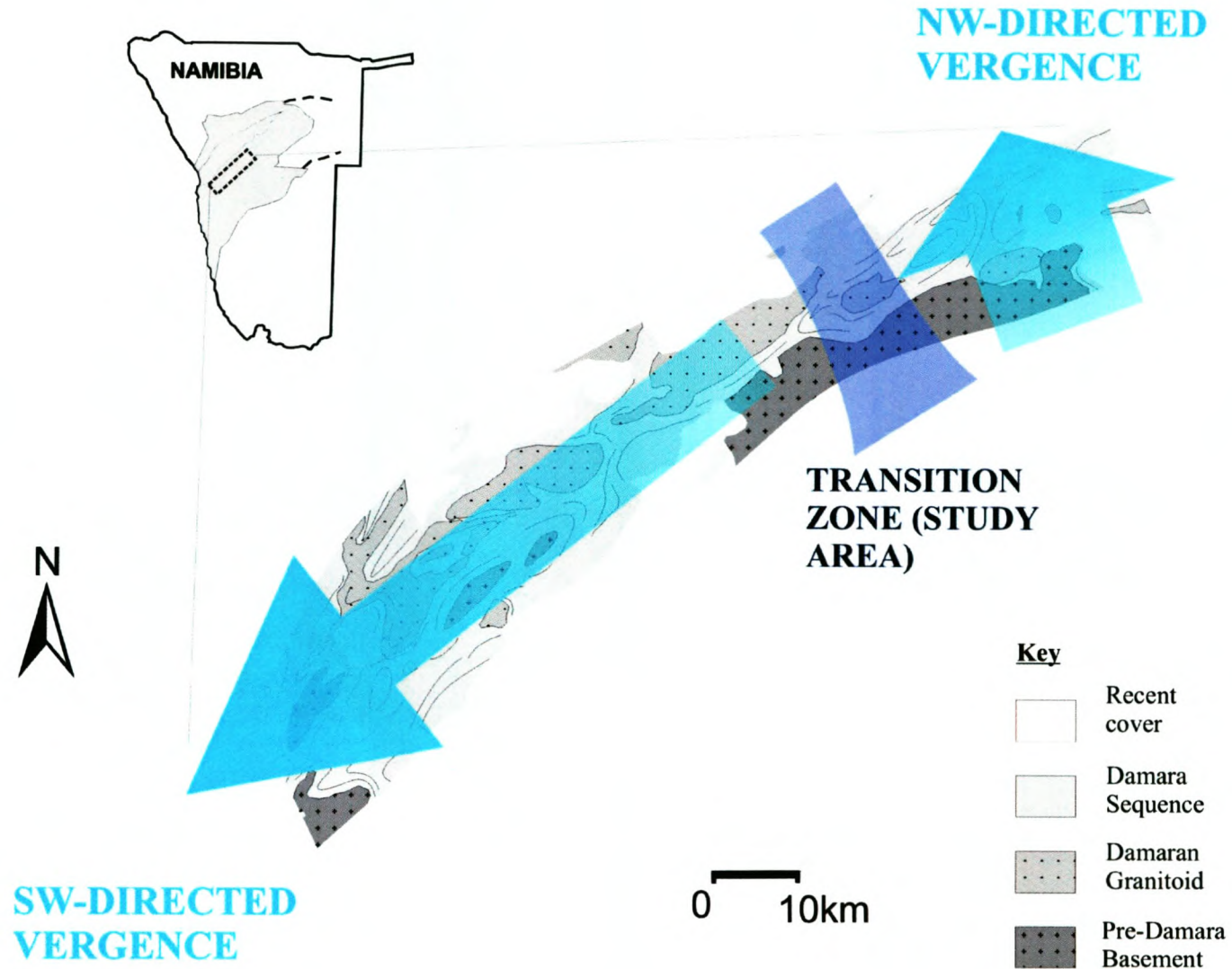
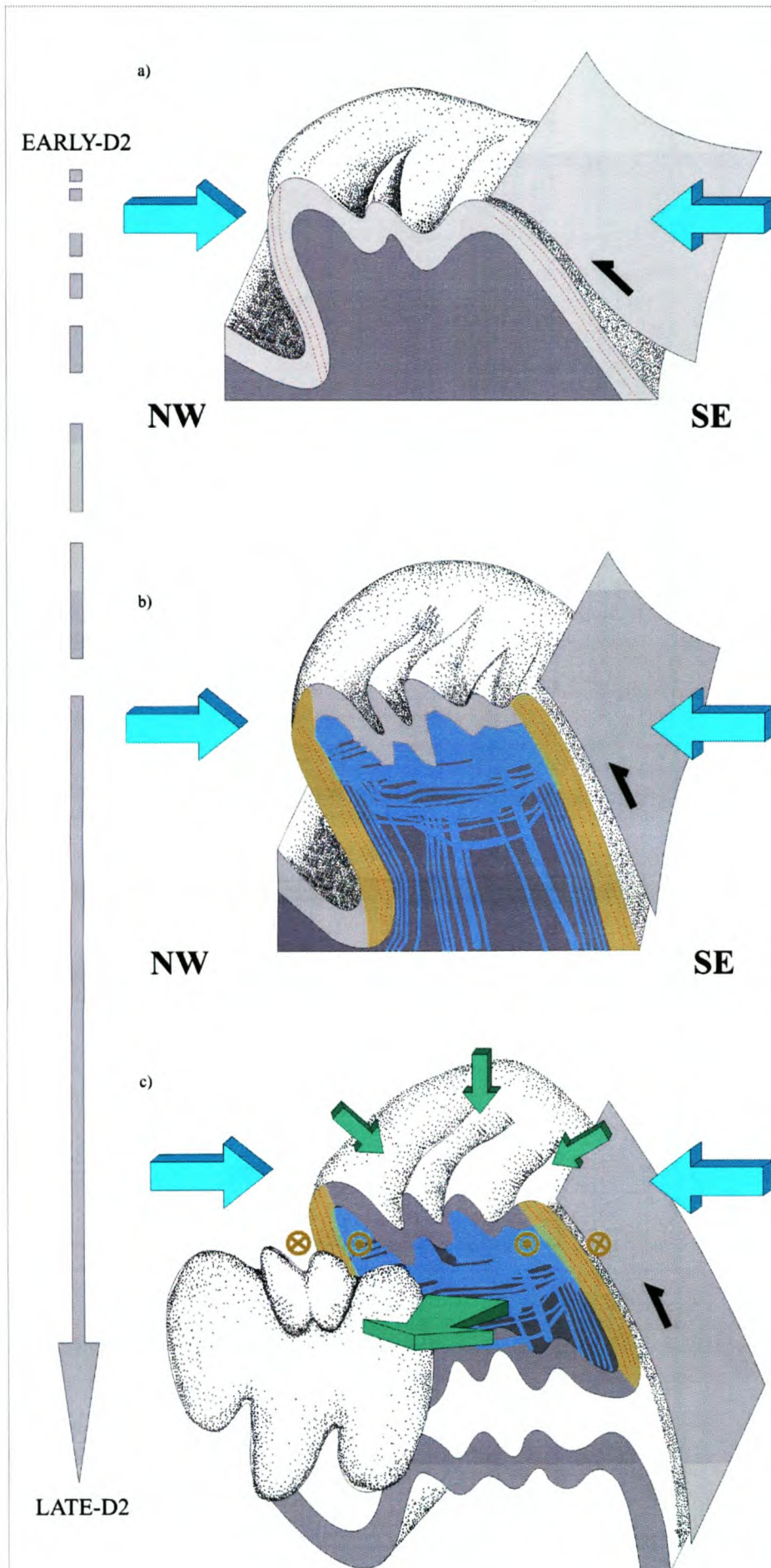


Figure 6.1 Schematic map of the sCZ showing the main vergence directions. The Usakos dome showing both vergence directions is situated between the northwest- and southwest-vergent domains.



Northwest-south
was accommodated
 • Northeast-trending
 • The formation of

Progressive contraction
 • Horizontal shortening
and steepening
 • The steeply dipping
subvertical transposition
development of
marble-rich
 • The low-strain
was inundated
subhorizontal

Progressive shortening
 • Oversteepening
weak melt-rich
 • Gravitational
of the melt-rich
southwest (later)
 • Lateral extrusion
strained strain
dome.

CHAPTER 7 CONCLUSIONS

The detailed structural mapping of the Usakos dome allows to describe the kilometer-scale structure as a composite fold, whose complex geometry reflects changing boundary conditions within the regional framework of the southern Central Zone in the Damara belt. The well-preserved relationships between localized granite emplacement and regional folding highlight the role of transient changes, for example, of wall-rock rheologies for the development of ductile structures in a mid-crustal section.

From this study, the following main conclusions can be drawn for the structural evolution of the Usakos dome:

For the most part, the Usakos dome shows a persistent northeasterly strike extent being developed as an antiformal anticline, associated with a steep southeasterly-dipping axial planar foliation (early-S2). In its southwestern core, the dome is intruded by syntectonic (D2) granites within which a ghost stratigraphy of the Damara Sequence can be followed. The stratigraphy of the Damara Sequence appears overturned in this granite-rich southwestern core of the dome. Here, the Usakos dome is developed as a synformal anticline. This is the result of the refolding of the northeast-trending first-order anticline about a subhorizontal, northwesterly-trending fold axis and gently-dipping fold axial plane trending at high angles to the original fold. Thus, the overall geometry of the Usakos dome is that of a kilometer-scale, southwest-vergent sheath-fold. Within the core of the Usakos dome, the hinges of the refolded second- and lower-order folds show a radial pattern of plunges, pointing away from the center of the dome, associated with a subhorizontal foliation (late-S2) developed within the siliciclastic and granitic rocks.

The spatial and temporal relationship between granite sheeting and fold amplification as well as the distinct fabric development in the core of the Usakos dome and orientation of lower-order structures provide clues about the origin of the refolding event. The sum of these features point to the rheological weakening and ensuing collapse of the developing first-order Usakos dome immediately above the synkinematic granites, i.e. a localized gravitational collapse. Hinge-parallel shearing,

refolding (late-F2) and orogen-parallel extrusion of the Usakos dome occurred in response to continued shortening of this weakened crustal portion that could not sustain vertical thickening through folding and thrusting.

The example of the Usakos dome illustrates that dramatic structural variations, i.e. orogen-normal folding and/or thrusting and orogen-parallel extrusion of rocks, may occur in immediate proximity to each other and at the same time. On a regional scale, the Usakos dome represents the link between the foreland-vergent folds and thrust of the lower-grade northeastern parts of the sCZ and the southwest-vergent, high-grade, partially migmatized southwestern parts of the sCZ.

REFERENCES

- Allsopp, H., Barton, E.S., Kröner, A., Welke, H.J. and Burger, A.J. (1983) Emplacement versus inherited isotopic age patterns: a Rb-Sr and U-Pb study of Salem-type granites in the central Damara belt. In: Miller, R.McG. (Ed), Evolution of the Damara Orogen of South West Africa. Special Publication of the Geological Society of South Africa, 11, 281-287
- Anderson, H. and Nash C. (1997) Intergrated lithostructural mapping of the Rössing Area, Namibia using high resolution aeromagnetic, radiometric, landsat and aerial photographs. *Exploration Geophysics*, 28, 185-191
- Badenhorst, F.P. (1987) Lithostratigraphy of the Damara Sequence in the Omaruru Area of the northern Central Zone of the Damaran Orogen and a proposed correlation across the Omaruru Lineament. *Communications of the Geological Survey of South West Africa*, 3, 3-8
- Badenhorst, F.P. (1988a) A note on stratiform tourmalinites in Late Precambrian Kuiseb Formation, Damara Sequence. *Communications of the Geological Survey of South West Africa*, 4, 67-70
- Badenhorst, F.P. (1988b) The lithostratigraphy of the Chuos mixtite in part of the southern Central Zone of the Damara Orogen, South West Africa. *Communications of the Geol. Survey of S.W.A./ Namibia*, 4, 103-110
- Badenhorst, F.P. (1992) The Lithostratigraphy of area 2115B and D in the Central Zone of the Damara Orogen in Namibia: with emphasis on facies changes and correlation. Unpublished MSc thesis, University of Port Elisabeth, pp 124
- Barnes, J.F.H. (1981) Some aspects of the tectonic history of the Khan-Swakop region of the Damara belt, Namibia. Unpublished. Ph.D thesis, Leeds University, pp 466
- Barnes, S.J. and Sawyer, E.W. (1980) An alternative model for continental convergence. *Precambrian Research*, 13, 297-336
- Barnes, J.F.H. and Downing K.N. (1979) Origin of domes in the central Damaran belt, South West Africa. *Revue de Geologie Dynamique et de Geographie Physique*, 21, 383-386
- Basson, I.J. and Greenway, G. (2004) The Rössing Uranium Deposit: a product of late-kinematic localization of uraniferous granites in the Central Zone of the Damara Orogen, Namibia. *Journal of African Earth Science*, 38, 413-435
- Blenkinsop, T.G. and Treloar P.J. (2001) Tabular intrusion and folding of the late Archaean Murehwa granite, Zimbabwe, during regional shortening. *Journal of the Geological Society of London*, 158, 653-664
- Blewett, R.S. (2002) Archaean tectonic processes: a case for horizontal shortening in the North Pilbara Granite-Greenstone Terrane, Western Australia. *Precambrian Research*, 36, 241-258

Botha P. J. (1978) Die geologie in die omgewing van die benede-Omarururivier, Suidwes-Afrika. Unpublished M.Sc. thesis, University of the Orange Free State, pp 157

Bowden, P., Herd, D., Kinnaird, J.A. (1995) The significance of Uranium and Thorium concentrations in pegmatitic leucogranites (alaskites), Rössing Mine, Swakopmund, Namibia. Communications of the Geological Survey, Namibia, 10, 43-49

Bowden, P., Tack, L., Williams, I.S. and Deblond, A. (1999) Transpressional and transtensional magmatism in the Central Damaran (Pan-African) orogenic belt, Western Namibia. Abstracts, GSA 11: Earth Resources for Africa. Journal of African Earth Sciences, 28, 13

Brandt, R. (1987) A revised stratigraphy for the Abbabis Complex in the Abbabis inlier Namibia. South African Journal of Geology, 90, 314-323

Briqueu, L., Lancelot, J.R., Valois, J.-P. and Walgenwitz, F. (1980) Géochronologie U-Pb et genese d'un type de mineralisation uranifère: les alaskite de Goanikontes (Namibia) et leur encaissant. Bullétin Centrale De Recherche Exploration-Production, Elf Aquitaine, 4, 759-811

Brown, M. and Solar, G.S. (1998) Granite ascent and emplacement during contractional deformation in convergent orogens. Journal of Structural Geology, 20, 1365-1393

Brun, J.P. and Van Den Driessche, J. (1994) Extensional gneiss domes and detachment faults- structure and kinematics. Bulletin de la Societé Geologique de France, 165, 519-530

Bühn, B. and Stanistreet, I.G. (1992) A correlation of structural patterns and lithostratigraphy at Otjosondu within the Damara Sequence of the southern Central Zone, Namibia. Communications of the Geological Survey of Namibia, 7, 15-19

Bühn, B., Okrusch, M., Woermann, E., Lehnert, K. and Hoernes, S. (1995) Metamorphic evolution of Neoproterozoic manganese formations and their country rocks at Otjosondu, Namibia. Journal of Petrology, 36, 519-528

Clemens, J.D. and Mawer, C.K. (1992) Granitic magma transport by fracture propagation. Tectonophysics, 204, 339-360

Corriveau, L. Rivard, B., van Breemen, O. (1998) Rheological controls on Grenvillian intrusive suites: implications for tectonic analysis. Journal of Structural Geology, 20, 1191-1204

Corner, B. (1982) An Interpretation of the Aeromagnetic data covering a portion of the Damara Orogenic Belt, with Special Reference to the Occurrence of Uraniferous Granite. Unpublished. D. Sc. thesis, University of the Witwatersrand, pp 108

- Corner, B. (2000) Crustal framework of Namibia derived from magnetic and gravity data. *Communications of the Geological Survey of Namibia*, 12, 13-20
- Coward, M.P. (1981) Diapirism and gravity tectonics: report of a Tectonic Studies Group conference held at Leeds University, 25-26 March 1980. *Journal Structural Geology*, 3, 89-90
- Coward, M.P. (1983) The tectonic history of the Damaran Belt. In: Miller, R.McG. (Ed), *Evolution of the Damara Orogen of South West Africa*. Special Publication of the Geological Society of South Africa, 11, 409-421
- Cuney, M. (1980) Preliminary results on the petrology and fluid inclusions of the Rössing uraniferous alaskites. *Transactions of the Geological Society of South Africa*, 83, 39-45
- Davis, G.H. and Reynolds, S.J. (1996) *Structural geology of rocks and regions*. 2nd Edition. John Wiley and Sons Inc. New York, pp 776
- De Kock, G.S. and Walraven, F. (1994) The age and geochemistry of some syndepositional and early tectonic magmatic rocks southeast of Karibib. Abstracts, *Proterozoic Crustal and Metallogenic Evolution*, Geological Society of Namibia, Windhoek, 13
- De Kock, G.S., Eglinton B., Armstrong R.A., Harmer, R.E. and Walraven, F. (2000) U-Pb and Pb-Pb ages on the Naupoort rhyolite, Kawakeup leptite and Okangava Diorite: implication for the onset of rifting and orogenesis in the Damara belt Namibia, *Communications of the Geological Survey of Namibia*, 12, 81-88
- Downing, K.N. and Coward, M.P. (1981) The Okahandja Linearment and its significance for Damaran Tectonics in South West Africa. *Geologische Rundschau*, 70, 972-1000
- Eberle, D., Andritzky, G. and Wackerle, R. (1995) The new magnetic data set of Namibia: its contributions to the understanding of crustal evolution and regional distribution of mineralization. *Communications of the Geological Survey of Namibia*, 10, 141-150
- England, P.C. and Thompson, A.A. (1984) Pressure-temperature-time paths of regional metamorphism, Part 1: Heat transfer during the evolution of regions of thickened continental crust: *Journal of Petrology*, 25, 894-928
- Eskola, P.E. (1949) The Problem of mantled gneiss domes. *Geological Society of London Quarterly Journal*, 104, 461-476
- Faure, M., Sun, Y., Shu, L. and Charvet, J. (1996) Extensional tectonics within a subduction-type orogen. The case study of the Wugongshan dome (Jiangxi Province, Southeastern China). *Tectonophysics*, 263, 77-106
- Fernández, C., Castro, A, De La Rosa, J.D. and Moreno-Ventas, I. (1997) Rheological aspects of magma transport inferred from rock structures. In: J.L. Bouchez, D.H.W.

Hutton, W.E. Stephens (Eds) Granite : from segregation of melt to emplacement fabrics. Kluwer Academic Publishers, 75-94

Freyer, E.E. and Haibich, I.W. (1994) Deformation history of the lower Ugab Belt. In: Niall, M. and McManus, C. (eds) Proterozoic Crustal and Metallogenic Evolution. Abstracts of the Geological Society and Geological Survey of Namibia Conference, Windhoek, 18

Frimmel, H. E. and Frank, W. (1998) Neoproterozoic tectono-thermal evolution of the Gariiep Belt and its basement, Namibia and South Africa. *Precambrian Research*, 90, 1-28

Gevers, T.W. (1931) Fundamental Complex of Western Damaraland, South West Africa- Unpublished. Doctor of Science thesis, University of Cape Town, pp 163

Goscombe, B., Hand M. and Gray, D. (2003) Structure of the Kaoko Belt , Namibia: Progressive evolution of a classic transpressional orogen. *Journal of Structural Geology*, 25, 1049-1081

Hartnady, C.J.H., Joubert, P. and Stowe, C.W. (1985) Proterozoic crustal evolution in South West Africa. *Episodes*, 8, 236-244

Hartmann, O., Hoffer, E. and Haak, U. (1983) Regional metamorphism in the Damaran Orogen: interaction of crustal motion and heat transfer. *Special Publication Geological Society of South Africa*, 11, 233-241

Henry, G., Stanistreet I.G. and Maiden, K.J. (1986) Preliminary results of a sedimentological study of the Chuos Formation in the Central Zone of the Damara Orogen: Evidence for mass flow processes and glacial activity. *Communications of the Geological Survey of South West Africa*, 2, 75-92

Henry, G., Stanistreet, I.G. and Maiden, K.J. (1988) Timing of continental breakup in the Damara Orogen: A review and discussion. *Extended Abstracts. Geocongress 88, Geological Society of South Africa, Durban*, 267-270

Henry, G., Clendenin, C.W., Stanistreet, I.G. and Maiden, K.J. (1990) A multiple detachment model for the early rifting stage of the Late Proterozoic Damara orogen in Namibia. *Geology*, 18, 67-71

Hibbard, M.J. (1979) Myrmekite as a marker between preaqueous and postaqueous phase saturation in granitic systems. *Geological Society of America Bulletin*, 90, 1047-1062

Hibbard, M.J. (1987) Deformation of incompletely crystallized magma systems: granitic gneisses and their tectonic implications. *Journal of Geology*, 95, 543-561

Hill, C.J., Baldwin, S.L. and Lister, G.S. (1992) Unroofing of active metamorphic core complexes in the d'Entrecasteaux region, Papua New Guinea. *Geology*, 20, 907-910

- Hoernes, S. and Hoffer, E. (1979) Equilibrium relations of prograde metamorphic mineral assemblages- a stable isotope study of rocks of the Damara orogen. *Contributions to Mineralogical and Petrology*, 68, 377-389
- Hoffer, E. (1978) On the 'late' formation of paragonite and its breakdown in pelitic rocks of the Southern Damara Orogen (South West Africa). *Contributions to Mineralogical and Petrology*, 67, 209-219
- Hoffman, P.F., Hawkins, D.P., Isachsen, C.E. and Bowring, S.A. (1996) Precise U-Pb zircon ages for early Damaran magmatism in the Summas Mountains and Welwitschia inlier, northern Damara belt, Namibia, *Communications of the Geological Survey of Namibia*, 11, 47-52
- Hoffmann, K.-H. (1983) Lithostratigraphy and facies of the Swakop Group of the southern Damara belt, SWA/ Namibia. In: Miller, R.McG. (Ed), *Evolution of the Damara Orogen of South West Africa*. Special Publication of the Geological Society of South Africa, 11, 43-63
- Hoffmann, K.-H. (1990) Sedimentary depositional history of the Damara Belt related to continental breakup, passive margin to active margin transition and foreland basin development. *Extended Abstracts. Geocongress 90*, Geological Society of South Africa, Cape Town, 250-253
- Hoffmann, K.-H., Condon, D.J., Bowring, S.A. and Crowley, J.L. (2004) U-Pb zircon date from the Neoproterozoic Ghaub Formation, Namibia: Constraints on Marinoan glaciation. *Geological Society of America*, (Data Repository Item).
- Holdsworth, R.E. (1988) The stereographic analysis of facing. *Journal of Structural Geology*, 10, 219-223
- Holm, D.K., Snow, J.K. and Lux, D.R. (1992) Thermal and barometric constraints on the intrusive and unroofing history of the Black Mountains: implications for timing, dip and kinematics of detachment faulting in the Death Valley region, California. *Tectonics*, 11, 507-522
- Holm, D.K. and Lux, D.R. (1996) Core complex model proposed for gneiss dome development during collapse of the Paleoproterozoic Penokean Orogen. *Geology*, 19, 343-346
- Hollister, L.S., and Crawford, M.L. (1986) Melt-enhanced deformation: A major tectonic process. *Geology*, 14, 558-561
- Hutton, D.H.W. (1992) Granite sheeted complexes: Evidence for the diking ascent mechanism. *Transactions of the Royal Society of Edinburgh Earth Sciences*, 83, 377-382
- Ildefonse, B. and Mancktelow, N.S. (1993) Deformation around rigid particles: the influence of slip at the particle/matrix interface. *Tectonophysics*, 221, 345-359

Jacob, R.E. (1974) Geology and metamorphic petrology of part of the Damaran Orogen along the lower Swakop River, South West Africa. *Bulletin of the Precambrian Research Unit, University of Cape Town*, 17, pp 201

Jacob, R.E., Snowden, P.A. and Bunting, F.J.L. (1983) Geology and structural development of the Tumas Basement Dome and its cover rocks. In: Miller, R.McG. (Ed), *Evolution of the Damara Orogen of South West Africa. Special Publication of the Geological Society of South Africa*, 11, 157-172

Jacob, R.E., Kröner, A. and Burger, A.J. (1978) Areal extent and first U-Pb age of Pre-Damara Abbabis Complex in the Central Damara belt of South West Africa. *Geologische Rundschau*, 67, 706-718

Jacob, R.E., Moore, J.M. and Armstrong, R.A. (2000) Zircon and titanite age determinations from igneous rocks in the Karibib District, Namibia: implications for Navachab vein-style gold mineralization. *Communications of the Geological Survey of Namibia*, 12, 157-166

Jung, S. and Mezger, K. (2003) Petrology of basement-dominated terranes: I Regional metamorphic T-t path from U-Pb monazite and Sm-Nd garnet geochronology (Central Damara Orogen, Namibia). *Chemical Geology*, 198, 223-247

Kasch, K.W. (1983a) Regional P-T variations in the Damara Orogen with particular reference to early high-pressure metamorphism along the Southern Margin. In: Miller, R.McG. (Ed.), *Evolution of the Damara Orogen of South West Africa, Geological Society of South Africa, Special Publication 11*, 243-254

Kasch, K.W. (1983b) Continental Collision, Suture Progradation and Thermal Relaxation: A Plate Tectonic Model for the Damara Orogen in Central Namibia. In: Miller, R.McG. (Ed.), *Evolution of the Damara Orogen of South West Africa, Geological Society of South Africa, Special Publication 11*, 423-429

Kaufmann, A.J., Knoll, A.H., and Narbonne, G.M. (1997) Isotopes, ice ages, and terminal Proterozoic Earth history: *Proceedings of the National Academy of Science*, 94, 600-605

Kisters, A.F.M., Smith Jordaan, L. and Neumaier, K. (2004) Thrust-related dome structures in the Karibib district and the origin of orthogonal fabric domains in the south Central Zone of the Pan-African Damara belt, Namibia. *Precambrian Research*, 133, 283-303

Kröner, A., Retief, E.A., Compston, W., Jacob, R.E. and Burger, A.J. (1991) Single-grain and conventional zircon dating of remobilized basement gneisses in the central Damara Belt of Namibia. *South African Journal of Geology*, 94, 279-387

Kröner, A. (1984) Dome structures and basement reactivation in the Pan-African Damara belt of Namibia. In: Kröner, A. and Greiling, R. (Eds.), *Precambrian Tectonics Illustrated*. E. Schweizerbart'sche Verlagbuchhandlung, Stuttgart, Germany, 191-206

Kruhl, J.H. (1996) Prism- and basal-plane parallel subgrain boundaries in quartz: a microstructural geothermobarometer. *Journal of Metamorphic Geology*, 14, 581-589

Kukla, C., Kramm, U., Kukla, P.A. and Okrusch, M. (1991) U-Pb monazite data relating to metamorphism and granite intrusion in the northwestern Khomas Trough, Damara Orogen, central Namibia. *Communications of the Geological Survey of Namibia*, 7, 49-54

Kukla, P. A. and Stanistreet, I. G. (1991) Record of the Damaran Khomas Hochland accretionary prism in central Namibia: refutation of an ensialic origin of a late Proterozoic orogenic belt. *Geology*, 19, 417-476.

Kukla, P.A., Opitz, C., Stanistreet, I. J. and Charlesworth, E.G. (1988) New aspects of the sedimentology and structure of the Kuiseb Formation in the western Khomas Trough, Damara Orogen of South West Africa, *Communications of the Geological Survey of South West Africa*, 4, 33-42

Lee, J., Hacker, B. and Wang, Y. (2004) Evolution of North Himalayan gneiss domes: structural and metamorphic studies in Mabja Dome, southern Tibet. *Journal of Structural Geology*, 26, 2297-2316

Lehtonen, M.I., Manninen, T.E.T. and Schreiber, U.M. (1996) Lithostratigraphy of the area between the Swakop, Khan and lower Omaruru Rivers, Namib Desert. *Communications of the Geological Survey of Namibia*, 11, 65-75

Maloof, A.C. (2000) Superposed folding at the junction of the inland and coastal belts, Damara Orogen, NW Namibia. *Communications of the Geological Survey of South West Africa*, 12, 89-98

Marlow, A.G. (1983) Geology and Rb-Sr geochronology of mineralized and radioactive granites. In: Miller, R.McG. (Ed.), *Evolution of the Damara Orogen of South West Africa*, Geological Society of South Africa, Special Publication, 11, 289-298

Martin, H. (1965) *The Precambrian geology of South West Africa and Namaqualand*. Precambrian Research Unit, University of Cape Town, pp 159

Martin, H. (1983) Overview of the geosynclinal, structural and metamorphic development of the intracontinental branch of the Damara Orogen. In: Martin, H., Eder, F.W. (Eds.), *Intracontinental Fold Belts*. Springer, Berlin, 473-502

Martin, H. and Porada, H. (1977) The Intracratonic branch of the Damara Orogen in South West Africa: Discussion of Geodynamic models. *Precambrian Research*, 5, 311-338

Masberg, H.P., Hoffer, E. and Hoernes, S. (1992) Microfabrics indicating granulite-facies metamorphism in the low-pressure central Damara Orogen, Namibia. *Precambrian Research*, 55, 243-257

- Masberg, H.P. (2003) Garnet growth in medium pressure granulite-facies metapelites from the central Damara Orogen: Igneous versus metamorphic history. *Communications of the Geological Survey of Namibia*, 12, 115-124
- Miller, H. and Hoffman, K.H. (1981) Guide to the excursion through the Damara Orogen. *Geocongress 81, Geological Society of Southern Africa, Windhoek, South West Africa*, pp 103
- Miller, R. McG. (1983) The Pan-African Damara Orogen of South West Africa/Namibia. In: Miller, R.McG. (Ed.), *Evolution of the Damara Orogen of South West Africa. Geological Society of South Africa, Special Publication*, 11, 431-515
- Miller, R.McG, Barnes, S. and Balkwill, G. (1983) Possible active margin deposits within the southern Damara orogen: The Kuiseb Formation between Okahandja and Windhoek. In: Miller, R.McG. (Ed.), *Evolution of the Damara Orogen of South West Africa. Geological Society of South Africa, Special Publication* 11, 73-88
- Miller, R.B. and Paterson, S.R. (1994) Transition from magmatic to high-temperature solid-state deformation, Mount Stuart batholith, Washington. *Journal of Structural Geology* 16, 853-865
- Miller, R. McG. (1988) *Geological Map of the Damara Orogen, South West Africa/Namibia. Geological Survey, Windhoek*
- Nelson, K.D., et al. (1996) Partially molten middle crust beneath southern Tibet: synthesis of project INDEPTH results. *Science*, 274, 1684-1688
- Neumaier, K. (2002) Structural and lithological mapping of the Usakso dome, central Namibia, Unpublished Diploma mapping project. *Ludwigs-Maximilians University*, pp 70
- Nex, P.A.M. (1997) Tectono-metamorphic setting and evolution of granitic sheets in the Goanikontes area, Namibia. Ph.D. thesis (Unpublished.). *National University of Ireland*, pp 322
- Nex P.A.M., Oliver, G.J.H. and Kinnaird, J. (2001) Spinel-bearing assemblages and P-T-t evolution of the Central Zone of the Damara Orogen, Namibia. *Journal of African Earth Sciences*, 32, 471-489
- Oliver, G.J.H. (1994) Mid-crustal detachment and domes in the central zone of the Damara orogen Namibia. *Journal of African Earth Sciences*, 19, 331-344
- Oliver, G.J.H. (1995) The Central Zone of the Damara Orogen, Namibia, as a deep metamorphic core complex. *Communications of the Geological Survey of Namibia*, 10, 33-41
- Passchier, C.W. and Trouw, R.A.J. (1996) *Microtectonics. Springer-Verlag, Berlin.* pp 283

- Passchier, C.W., Trouw, R.A.J., Ribeiro, A. and Paciullo, F.U. P. (2002) Tectonic evolution of the southern Kaoko belt, Namibia. *Journal of African Earth Sciences*, 35, 61-75
- Paterson, S.R., Vernon, R.H. and Tobisch, O.T. (1989) A review of criteria for the identification of magmatic and tectonic foliations in granitoids. *Journal of Structural Geology*, 11, 349-363
- Paterson, S.R., Fowler, T.K. Jr., Schmidt, K. L., Yoshinobu, A.S., Yuan, E.S. and Miller, R.B. (1998) Interpreting magmatic fabrics in plutons. *Lithos*, 44, 53-82
- Pawley, M.J., Van Kranendonk, M.J., and Collins, W.J. (2004) Interplay between deformation and magmatism during doming of the Archaean Shaw Granitoid Complex, Pilbara Craton, Western Australia. *Precambrian Research*, 131, 213-230
- Petford, N., (1996) Dykes or diapirs? *Transactions of the Royal Society of Edinburgh Earth Sciences*, 87, 105-114
- Pitcher, W.S. (1970) Ghost stratigraphy in intrusive granites: a review. In: Newall, G., and Rast, N., (eds), *Mechanisms of igneous intrusions*, Gallery Press, Liverpool, 123-140
- Poli, L.C. and Oliver, G.J.H. (2001) Constictional deformation in the Central Zone of the Damara Orogen, Namibia. *Journal of African Earth Sciences*, 33, 303-321
- Porada, H. (1989) Pan-African rifting and orogenesis in southern to equatorial Africa and eastern Brazil, *Precambrian Research*, 44, 103-138
- Puhan, D. (1983) Temperature and pressure of metamorphism in the Central Damara orogen. *Geological Society of South Africa. Special Publication*, 11, 219-223
- Prave, A.R. (1996) Tale of three cratons: Tectonostratigraphic anatomy of the Damara orogen in northwestern Namibia and the assembly of Gondwana. *Geology*, 24, 1115-1118
- Prave, A.R., and Hoffmann, K.H. (1995) Unequivocal evidence for two Neoproterozoic glaciations in the Damara succession of Namibia: *Geological Society of American Abstracts with Programs*, 27, 380
- Ramsay, J.G. (1967) Interference patterns produced by the superposition of folds of similar type. *Journal of Geology*, 70, 466-481
- Ramsay, J.G. (1980) Shear Zone Geometry: A review. *Journal of Structural Geology*, 2, 83-99
- Ramsay, J.G. and Huber, M., (1987) *Folds and Fractures*. In: *The Techniques of Modern Structural Geology*, vol. 2. Academic Press, London, pp 391
- Roig J. Y., Faure, M., and Truffet, C. (1998) Folding and granite emplacement inferred from structural, strain TEM and gravimetric analyses: the case study of the

Tulle antiform, Southwestern French Massif Central. *Journal of Structural Geology*, 20, 1169-1189

Sawyer, E.W. (1981) Damaran structural and metamorphic geology of an area southeast of Walvis Bay, South West Africa. *Memoirs for the Geological Survey of South West Africa*, 7, pp 94

Simpson, C. and Wintsch, R.P. (1989) Evidence of deformation-induced K-feldspar replacement by myrmekite. *Journal of Metamorphic Geology*, 7, 261-273

Simpson, C. (1985) Deformation of granitic rocks across the brittle-ductile transition. *Journal of Structural Geology*, 7, 503-511

Smith, D.A.M. (1965) The Geology of the Area Around the Khan and Swakop Rivers in South West Africa. *Memoirs of the Geological Survey of South West Africa*, 3, pp 113

Smith, D.A.M. (1966) Geological Map of area 2215B-Usakos, Geological Survey, Windhoek, South West Africa

Soula, J.C. (1982) Characteristics and mode of emplacement of gneiss domes and plutonic domes in central-eastern Pyrénées. *Journal of Structural Geology*, 4, 313-342

Stanistreet, I.G., Kukla, P.A. and Henry, G. (1991) Sedimentary basinal responses to a Late Precambrian Wilson Cycle: The Damara Orogen and Nama Foreland, Namibia. *Journal of African Earth Science*, 13, 141-156

Steven, N.M. (1993) A study of Epigenetic Mineralization in the Central Zone of the Damara Orogen, Namibia, with special reference to gold, tungsten, tin and rare elements. *Memoirs of the Geological Survey of Namibia*, 16, pp 166

Swart, R. (1992) The Sedimentology of the Zerrissene Turbidite System, Damara Orogen, Namibia. *Memoirs of the Geological Survey of Namibia*, 13, pp 54

Tack, L., Williams, I. and Bowden, P. (2002) SHRIMP constraints on granitoids in the Ida dome, Central Damara (Pan-African) belt, western Namibia. In: *Proceedings of the 11th IAGOD Quadrennial Symposium and GeoCongress*, Windhoek, Namibia. Geological Survey, Namibia, 1-5

Tack, L. and Bowden, P. (1999) Post-collisional granite magmatism in the Central Damara (Pan-African) Orogenic belt, western Namibia. *Journal of African Earth Sciences*, 28, 653-674

Teyssier, C. and Whitney, D.L. (2002) Gneiss domes and orogeny. *Geological Society of America*, 30, 1139-1142

Unrug, R. (1997) Rodinia to Gondwana: The Geodynamic Map of Gondwana Supercontinent Assembly. *Geological Society of Australia Today*, 7, 1-6

Vanderhaeghe, O. and Teyssier, C. (2001) Crustal-scale rheological transitions during late-orogenic collapse. *Tectonophysics*, 335, 211-228

Vernon, R.H., Johnson, S.E. and Melis, E.A. (2004) Emplacement-related microstructures in the margin of a deformed pluton: the San José tonalite, Baja California, México. *Journal of Structural Geology*, 26, 1867-1884